

JAERI-M

85-109

ROSA-III 50% BREAK INTEGRAL TEST RUN 916

(BREAK AREA PARAMETER TEST)

August 1985

Taisuke YONOMOTO, Kanji TASAKA, Yasuo KOIZUMI,
Yoshinari ANODA, Hiroshige KUMAMARU, Hideo NAKAMURA,
Mitsuhiko SUZUKI and Hideo MURATA

JAERI-M レポートは、日本原子力研究所が不定期に公刊している研究報告書です。

入手の問合せは、日本原子力研究所技術情報部情報資料課（〒319-11茨城県那珂郡東海村）
あて、お申しこしください。なお、このほかに財団法人原子力弘済会資料センター（〒319-11茨城
県那珂郡東海村日本原子力研究所内）で複写による実費頒布をおこなっております。

JAERI-M reports are issued irregularly.

Inquiries about availability of the reports should be addressed to Information Division, Department
of Technical Information, Japan Atomic Energy Research Institute, Tokai-mura, Naka-gun,
Ibaraki-ken 319-11, Japan.

© Japan Atomic Energy Research Institute, 1985

編集兼発行 日本原子力研究所
印 刷 日立高速印刷株式会社

JAERI-M 85-109

ROSA-III 50% BREAK INTEGRAL TEST RUN 916
(BREAK AREA PARAMETER TEST)

Taisuke YONOMOTO, Kanji TASAKA, Yasuo KOIZUMI,
Yoshinari ANODA, Hiroshige KUMAMARU, Hideo NAKAMURA,
Mitsuhiko SUZUKI and Hideo MURATA

Department of Reactor Safety Research,
Tokai Research Establishment, JAERI

(Received July 3, 1985)

This report presents the experimental data of RUN 916 conducted at the ROSA-III test facility. The facility is a volumetrically scaled (1/424) simulator for a BWR/6 with the electrically heated core, the break simulator and the scaled ECCS(emergency core cooling system). RUN 916 was a 50% split break test at the recirculation pump suction line with an assumption of HPCS diegel generator failure and conducted as one of the break area parameter tests. A peak cladding temperature (PCT) of 917 K was reached at 190 s after the break during the reflooding phase. Whole core was completely quenched by ECCS, and the effectiveness of ECCS was confermed.

The primary test results of RUN 916 are compared in this report with those of RUN 926, which was a 200 % double-ended break test. The initiation of core dryout in RUN 916 was later than that in RUN 926 because of the smaller discharge flow rate. Duration of core dryout was, however, longer in RUN 916 because of later actuation of ECCSs. PCT in RUN 916 was 133 K higher than that in RUN 926.

Keywords: BWR, LOCA, ECCS, Integral Test, the ROSA-III Program,
50% break, HPCS Failure, Break Area, Data Report

ROSA - III 50%破断総合実験 RUN 916 (破断面積パラメータ実験)

日本原子力研究所東海研究所原子炉安全工学部
与能本泰介・田坂 完二・小泉 安郎・安濃田良成
熊本 博滋・中村 秀夫・鈴木 光弘・村田 秀男

(1985年7月3日受理)

本報は、ROSA - III装置を用いて行われたRUN 916実験の結果について記述したものである。本実験装置は、BWR/6の体積比1/424の模擬装置であり電気加熱炉心、破断口及び緊急炉心冷却系(ECCS)を有している。RUN 916実験は、HPCSジーゼル発電機の故障を仮定した再循環ポンプ入口側配管における50%スプリット破断実験であり破断面積パラメータ実験のひとつとして行なわれた。被覆管最高温度(PCT)は、917Kであり破断後、190秒の再冠水期に記録された。全炉心は、ECCSにより完全にクエンチされ、ECCSの有効性が確認された。

本報では、主要なRUN 916実験結果と200%両端破断実験RUN 926の結果を比較している。RUN 916実験における炉心露出の開始はRUN 926実験の場合より破断流量が、少ないので遅くなった。しかし炉心露出の継続時間は、RUN 916実験の場合の方が、ECCSの作動が遅れるので長くなかった。RUN 916実験のPCTは、RUN 926実験の場合より133K高かった。

Contents

Abbreviations	(11)
1. Introduction	1
2. ROSA-III Test Facility	3
3. Instrumentation	5
4. Test Conditions and Procedure	7
5. Data Processing	9
6. Test Results and Comparison with those of RUN 926	15
7. Conclusions	19
Acknowledgments	20
References	20
Figures and Tables	21

目 次

略号	(11)
1. 序	1
2. ROSA-III実験装置	3
3. 計装	5
4. 実験条件および手順	7
5. 実験データ処理	9
6. 実験結果およびRUN 926との比較	15
7. 結論	19
謝辞	20
文献	20
図表	21

List of Tables

Table 2.1	Primary Characteristics of ROSA-III and BWR/6
Table 3.1	ROSA-III Instrumentation Summary List in RUN 916
Table 3.2	Measurement List for RUN 916
Table 3.3	Core Instrumentation Map
Table 4.1	Test Conditions of RUN 916
Table 4.2	Characteristics of Steam Discharge Line Valves
Table 4.3	Control Sequence for Steam Discharge Line Valves in RUN 916
Table 5.1	Sequence of Events in RUN 916
Table 5.2	Maximum Cladding Temperatures Distribution in the Core
Table 6.1	Comparison of Initial Conditions and Major Events in RUN 916 and RUN 926

List of Figures

Fig. 2.1	Schematic diagram of ROSA-III test facility
Fig. 2.2	Internal structure of pressure vessel of ROSA-III
Fig. 2.3	ROSA-III piping schematic
Fig. 2.4	Pressure vessel internals arrangement
Fig. 2.5	Simulated fuel rod of ROSA-III
Fig. 2.6	Axial power distribution of heater rod
Fig. 2.7	Radial power distribution of core
Fig. 2.8	Piping layout of recirculation loops and jet pumps
Fig. 3.1	Instrumentation location of ROSA-III test facility
Fig. 3.2	Instrumentation location in pressure vessel
Fig. 3.3	Upper plenum instrumentation
Fig. 3.4	Lower plenum instrumentation
Fig. 3.5	Core instrumentation (cf. Table 3.3)
Fig. 3.6	Upper tieplate instrumentations
Fig. 3.7	Beam directions of three-beam gamma densitometer
Fig. 3.8	Beam directions of two-beam gamma densitometer
Fig. 3.9	Arrangement and location of drag disks
Fig. 3.10	Location of two-phase flow measurement spool pieces
Fig. 4.1	Break configuration details
Fig. 4.2	Normalized power transient for ROSA-III test
Fig. 4.3	Main steam line schematic
Fig. 4.4	Feedwater line schematic
Fig. 4.5	Feedwater line between valve av-112 and pressure vessel
Fig. 5.1	Pressure in PV (pressure vessel)
Fig. 5.2	Pressure in broken loop JP (jet pump)
Fig. 5.3	Pressure near MRP (main recirculation pump)
Fig. 5.4	Pressure at MRP side of break
Fig. 5.5	Pressure at PV side of break
Fig. 5.6	Pressure in MSL (main steam line)
Fig. 5.7	Differential pressure between lower plenum and upper plenum
Fig. 5.8	Differential pressure between upper plenum and steam dome
Fig. 5.9	DC (downcomer) head
Fig. 5.10	Differential pressure between PV bottom and top
Fig. 5.11	Differential pressure between JP-1,2 discharge and suction
Fig. 5.12	Differential pressure between JP-1,2 drive and suction

- Fig. 5.13 Differential pressure between JP-3,4 discharge and suction
 Fig. 5.14 Differential pressure between JP-3,4 drive and suction
 Fig. 5.15 Differential pressure between MRP delivery and suction
 Fig. 5.16 Differential pressure between downcomer bottom and MRPl suction
 Fig. 5.17 Differential pressure between MRP delivery and JP-1,2 drive
 Fig. 5.18 Differential pressure between downcomer middle and JP-1,2 suction
 Fig. 5.19 Differential pressure between JP-1,2 discharge and lower plenum
 Fig. 5.20 Differential pressure between downcomer bottom and break B
 Fig. 5.21 Differential pressure between break A and MRP2 suction
 Fig. 5.22 Differential pressure between MRP dilivery and JP-3,4 drive
 Fig. 5.23 Differential pressure between downcomer middle and JP-3,4 suction
 Fig. 5.24 Differential pressure between JP-3,4 discharge and confluence
 Fig. 5.25 Differential pressure between JP-3,4 confluence in broken loop and lower plenum
 Fig. 5.26 Differential pressure between lower plenum and downcomer middle
 Fig. 5.27 Differential pressure between lower plenum and downcomer bottom
 Fig. 5.28 Differential pressure between downcomer bottom and downcomer middle
 Fig. 5.29 Differential pressure between downcomer middle and steam dome
 Fig. 5.30 Differential pressure between LP bottom and LP middle
 Fig. 5.31 Differential pressure across channel inlet orifice A
 Fig. 5.32 Differential pressure across channel inlet orifice B
 Fig. 5.33 Differential pressure across channel inlet orifice C
 Fig. 5.34 Differential pressure across channel inlet orifice D
 Fig. 5.35 Differential pressure across bypass hole
 Fig. 5.36 Liquid levels in ECCS tanks
 Fig. 5.37 Liquid levels in downcomer
 Fig. 5.38 Mass flow rate in MSL
 Fig. 5.39 ECC injection flow rate
 Fig. 5.40 Feedwater flow rate
 Fig. 5.41 JP-1,2 discharge flow rate (high range)
 Fig. 5.42 JP-3,4 discharge flow rate (high range)
 Fig. 5.43 JP-3,4 discharge flow rate (low range)
 Fig. 5.44 MRP discharge flow rate
 Fig. 5.45 Differential pressure across orifice flowmeter F-1
 Fig. 5.46 Differential pressure across orifice flowmeter F-2
 Fig. 5.47 Differential pressure across orifice flowmeter F-3
 Fig. 5.48 Differential pressure across venturi flowmeter F-17
 Fig. 5.49 Differential pressure across venturi flowmeter F-18
 Fig. 5.50 Differential pressure across orifice flowmeter F-19
 Fig. 5.51 Differential pressure across orifice flowmeter F-20
 Fig. 5.52 Differential pressure across orifice flowmeter F-21
 Fig. 5.53 Differential pressure across orifice flowmeter F-22
 Fig. 5.54 Differential pressure across venturi flowmeter F-27
 Fig. 5.55 Differential pressure across venturi flowmeter F-28
 Fig. 5.56 Electric core power

- Fig. 5.57 MRP revolution
 Fig. 5.58 Valve operation signal
 Fig. 5.59 ECCS operation signals
 Fig. 5.60 MRP operation signals
 Fig. 5.61 Fluid density at JP-1,2 outlet, beam A
 Fig. 5.62 Fluid density at JP-1,2 outlet, beam B
 Fig. 5.63 Fluid density at JP-1,2 outlet, beam C
 Fig. 5.64 Fluid density at JP-3,4 outlet, beam A
 Fig. 5.65 Fluid density at JP-3,4 outlet, beam B
 Fig. 5.66 Fluid density at JP-3,4 outlet, beam C
 Fig. 5.67 Fluid density at MRP side of break, beam A
 Fig. 5.68 Fluid density at MRP side of break, beam B
 Fig. 5.69 Fluid density at PV side of break, beam A
 Fig. 5.70 Fluid density at PV side of break, beam B
 Fig. 5.71 Momentum flux at break A spool piece (low range)
 Fig. 5.72 Momentum flux at break A spool piece (high range)
 Fig. 5.73 Momentum flux at break B spool piece (low range)
 Fig. 5.74 Momentum flux at break B spool piece (high range)
 Fig. 5.75 Fluid temperatures in lower plenum and upper plenum
 Fig. 5.76 Fluid temperatures in steam dome and MSL
 Fig. 5.77 Fluid temperatures in downcomer
 Fig. 5.78 Fluid temperatures in intact recirculation loop
 Fig. 5.79 Fluid temperatures in broken recirculation loop
 Fig. 5.80 Fluid temperatures at JP-1,2 outlet
 Fig. 5.81 Fluid temperatures at JP-3,4 outlet
 Fig. 5.82 Fluid temperatures near breaks A and B
 Fig. 5.83 Feedwater temperature
 Fig. 5.84 Fluid temperature at break orifice top
 Fig. 5.85 Fluid temperature at break orifice bottom
 Fig. 5.86 Surface temperatures of fuel rod A11
 Fig. 5.87 Surface temperatures of fuel rod A12
 Fig. 5.88 Surface temperatures of fuel rod A13
 Fig. 5.89 Surface temperatures of fuel rod A14
 Fig. 5.90 Surface temperatures of fuel rod A22
 Fig. 5.91 Surface temperatures of fuel rod A24
 Fig. 5.92 Surface temperatures of fuel rod A33
 Fig. 5.93 Surface temperatures of fuel rod A34
 Fig. 5.94 Surface temperatures of fuel rod A44
 Fig. 5.95 Surface temperatures of fuel rod A77
 Fig. 5.96 Surface temperatures of fuel rod A85
 Fig. 5.97 Surface temperatures of fuel rod A87
 Fig. 5.98 Surface temperatures of fuel rod A88
 Fig. 5.99 Surface temperatures of fuel rod B22
 Fig. 5.100 Surface temperatures of fuel rod C11
 Fig. 5.101 Surface temperatures of fuel rod C13
 Fig. 5.102 Surface temperatures of fuel rod C22
 Fig. 5.103 Surface temperatures of fuel rod C33
 Fig. 5.104 Surface temperatures of fuel rod C77
 Fig. 5.105 Surface temperatures of fuel rod D22
 Fig. 5.106 Surface temperatures of water rod simulator A45
 Fig. 5.107 Surface temperatures of water rod simulator C45
 Fig. 5.108 Inner Surface temperatures of channel box A,
 location A1
 Fig. 5.109 Inner Surface temperatures of channel box A,
 location A2
 Fig. 5.110 Inner Surface temperatures of channel box C
 (position 1)
 Fig. 5.111 Outer surface temperatures of channel box A

- Fig. 5.112 Outer Surface temperatures of channel box C
Fig. 5.113 Surface temperatures of fuel rod A15 at positions 1 and 4
Fig. 5.114 Surface temperatures of fuel rod A17 at positions 1 and 4
Fig. 5.115 Surface temperatures of fuel rod A26 at positions 1 and 4
Fig. 5.116 Surface temperatures of fuel rod A28 at positions 1 and 4
Fig. 5.117 Surface temperatures of fuel rod A31 at positions 1 and 4
Fig. 5.118 Surface temperatures of fuel rod A37 at positions 1 and 4
Fig. 5.119 Surface temperatures of fuel rod A42 at positions 1 and 4
Fig. 5.120 Surface temperatures of fuel rod A48 at positions 1 and 4
Fig. 5.121 Surface temperatures of fuel rod A51 at positions 1 and 4
Fig. 5.122 Surface temperatures of fuel rod A53 at positions 1 and 4
Fig. 5.123 Surface temperatures of fuel rod A57 at positions 1 and 4
Fig. 5.124 Surface temperatures of fuel rod A62 at positions 1 and 4
Fig. 5.125 Surface temperatures of fuel rod A66 at positions 1 and 4
Fig. 5.126 Surface temperatures of fuel rod A68 at positions 1 and 4
Fig. 5.127 Surface temperatures of fuel rod A71 at positions 1 and 4
Fig. 5.128 Surface temperatures of fuel rod A73 at positions 1 and 4
Fig. 5.129 Surface temperatures of fuel rod A75 at positions 1 and 4
Fig. 5.130 Surface temperature of fuel rod A82 at position 1
Fig. 5.131 Surface temperatures of fuel rod A84 at positions 1 and 4
Fig. 5.132 Surface temperatures of fuel rods B13,B31,B86 at position 4
Fig. 5.133 Surface temperatures of fuel rods B33,B53,B66 at position 4
Fig. 5.134 Surface temperatures of fuel rods B51,C15,D51,D77 at position 4
Fig. 5.135 Surface temperatures of fuel rods C31,C68 at position 4
Fig. 5.136 Surface temperatures of fuel rods C35,C66 at position 4
Fig. 5.137 Surface temperatures of fuel rods D11,D13,D31,D86 at position 4
Fig. 5.138 Surface temperatures of fuel rods D33,D53 at position 4
Fig. 5.139 Surface temperatures of fuel rods A11,A12,A13,A87,A88 at position 1
Fig. 5.140 Surface temperatures of fuel rods A11,A12,A13,A87,A88 at position 2
Fig. 5.141 Surface temperatures of fuel rods A11,A12,A13,A87,A88 at position 3
Fig. 5.142 Surface temperatures of fuel rods A11,A12,A13,A87,A88 at position 4

- Fig. 5.143 Surface temperatures of fuel rods A11,A12,A13,A87,A88 at position 5
Fig. 5.144 Surface temperatures of fuel rods A11,A12,A13,A87,A88 at position 6
Fig. 5.145 Surface temperatures of fuel rods A11,A12,A13,A87,A88 at position 7
Fig. 5.146 Surface temperatures of fuel rods A22,B22,C22,D22 at position 1
Fig. 5.147 Surface temperatures of fuel rods A22,B22,C22,D22 at position 2
Fig. 5.148 Surface temperatures of fuel rods A22,B22,C22,D22 at position 3
Fig. 5.149 Surface temperatures of fuel rods A22,B22,C22,D22 at position 4
Fig. 5.150 Surface temperatures of fuel rods A22,B22,C22,D22 at position 5
Fig. 5.151 Surface temperatures of fuel rods A22,B22,C22,D22 at position 6
Fig. 5.152 Surface temperatures of fuel rods A22,B22,C22,D22 at position 7
Fig. 5.153 Surface temperatures of fuel rods A77,C77 at position 1
Fig. 5.154 Surface temperatures of fuel rods A77,C77 at position 2
Fig. 5.155 Surface temperatures of fuel rods A77,C77 at position 3
Fig. 5.156 Surface temperatures of fuel rods A77,C77 at position 4
Fig. 5.157 Surface temperatures of fuel rods A77,C77 at position 5
Fig. 5.158 Surface temperatures of fuel rods A77,C77 at position 6
Fig. 5.159 Surface temperatures of fuel rods A77,C77 at position 7
Fig. 5.160 Fluid temperatures at channel inlet
Fig. 5.161 Fluid temperatures at channel A outlet
Fig. 5.162 Fluid temperatures at channel C outlet
Fig. 5.163 Fluid temperatures above UTP of channel A, openings 1,4,5
Fig. 5.164 Fluid temperatures above UTP of channel A, openings 8,10
Fig. 5.165 Fluid temperatures below UTP of channel A, openings 1,4,5
Fig. 5.166 Fluid temperatures below UTP of channel A, openings 8,10
Fig. 5.167 Fluid temperatures at UTP of channel A, opening 1
Fig. 5.168 Fluid temperatures at UTP of channel A, opening 4
Fig. 5.169 Fluid temperatures at UTP of channel A, opening 5
Fig. 5.170 Fluid temperatures at UTP of channel A, opening 8
Fig. 5.171 Fluid temperatures at UTP of channel A, opening 10
Fig. 5.172 Inner and outer surface temperatures of channel box at pos.1
Fig. 5.173 Inner and outer surface temperatures of channel box at pos.2
Fig. 5.174 Inner and outer surface temperatures of channel box at pos.3
Fig. 5.175 Inner and outer surface temperatures of channel box at pos.4
Fig. 5.176 Inner and outer surface temperatures of channel box at pos.5
Fig. 5.177 Inner and outer surface temperatures of channel box at pos.6

- Fig. 5.178 Inner and outer surface temperatures of channel box at pos.7
- Fig. 5.179 Fluid temperatures in lower plenum center
- Fig. 5.180 Fluid temperatures in lower plenum north
- Fig. 5.181 Liquid level signals in channel box A, location A1
- Fig. 5.182 Liquid level signals in channel box A, location A2
- Fig. 5.183 Liquid level signals in channel box B
- Fig. 5.184 Liquid level signals in channel box C
- Fig. 5.185 Liquid level signals in channel box D
- Fig. 5.186 Liquid level signals in channel A outlet, location A1
- Fig. 5.187 Liquid level signals in channel A outlet, location A2
- Fig. 5.188 Liquid level signals in channel A outlet, center
- Fig. 5.189 Liquid level signals in channel C outlet, location C1
- Fig. 5.190 Liquid level signals in channel C outlet, location C2
- Fig. 5.191 Liquid level signals in channel C outlet, center
- Fig. 5.192 Liquid level signals in channel A inlet
- Fig. 5.193 Liquid level signals in channel B inlet
- Fig. 5.194 Liquid level signals in channel C inlet
- Fig. 5.195 Liquid level signals in channel D inlet
- Fig. 5.196 Liquid level signals in lower plenum, north
- Fig. 5.197 Liquid level signals in lower plenum, south
- Fig. 5.198 Liquid level signals in guide tube, north
- Fig. 5.199 Liquid level signals in guide tube, south
- Fig. 5.200 Liquid level signals in downcomer, D side
- Fig. 5.201 Liquid level signals in downcomer, B side
- Fig. 5.202 Estimated liquid level in pressure vessel
- Fig. 5.203 Dryout and quench transients in channel A
- Fig. 5.204 Dryout and quench transients in channel C
- Fig. 5.205 Average density at MRP side of break
- Fig. 5.206 Average density at PV side of break
- Fig. 5.207 Flow rate at MRP side of break (based on low range drag disk data)
- Fig. 5.208 Flow rate at PV side of break (based on low range drag disk data)
- Fig. 5.209 Flow rate at MRP side of break (based on high range drag disk data)
- Fig. 5.210 Flow rate at PV side of break (based on high range drag disk data)
- Fig. 5.211 Total discharge flow rate from break (based on low range drag disk data)
- Fig. 5.212 Total discharge flow rate from break (based on high range drag disk data)
- Fig. 5.213 Steam discharge flow rate through MSL
- Fig. 5.214 Flow rate at channel A inlet
- Fig. 5.215 Flow rate at channel B inlet
- Fig. 5.216 Flow rate at channel C inlet
- Fig. 5.217 Flow rate at channel D inlet
- Fig. 5.218 Flow rate at bypass hole
- Fig. 5.219 Total channel inlet flow rate
- Fig. 5.220 Flow rate at JP-1,2 outlet (high range)
- Fig. 5.221 Flow rate at JP-3,4 outlet (high range)
- Fig. 5.222 Flow rate at JP-3,4 outlet (low range)
- Fig. 5.223 Total JP outlet flow rate (high range)
- Fig. 5.224 Collapsed liquid level in downcomer
- Fig. 5.225 Collapsed liquid level inside core shroud
- Fig. 5.226 Fluid inventory in downcomer
- Fig. 5.227 Fluid inventory inside core shroud
- Fig. 5.228 Total fluid inventory in pressure vessel

- Fig. 5.229 Fluid mass increase by ECCS and FW and decrease by steam discharge flow
- Fig. 5.230 Discharged fluid mass from break
- Fig. 5.231 Discharge flow rate from break
- Fig. 6.1 Lower plenum pressures
- Fig. 6.2 Differential pressures between top and bottom of pressure vessel
- Fig. 6.3 Collapsed liquid levels in downcomer
- Fig. 6.4 Total flow rates through channel inlet orifice
- Fig. 6.5 ECCS flow rates
- Fig. 6.6 Liquid levels in the core
- Fig. 6.7 Peak cladding temperatures

ABBREVIATIONS

ADS	Automatic Depressurization System
AT	Air Tank
AV	Air Actuation Valve
(2)B	(2) inches pipe of Schedule 80
BN	Boron Nitride
BWR	Boiling Water Reactor
CA	Chromel-Alumel
CCFL	Counter Current Flow Limiting
CHV	Check Valve
CP	Conductivity Probe
CV	Control Valve
CWT	Cooling Water Tank
D	Differential Pressure
d	Diameter
DF	Density of Fluid
DL(+100)	Elevation (+100 mm) from the bottom of PV
ECCS	Emergency Core Cooling System
ESF	Engineered Safety Features
EX	Heat Exchanger
F	Flow Rate
Fig.	Figure
FS	Full Scale
FW	Feedwater
FWLF	Feedwater Line Flashing
FWP	Feedwater Pump
FWT	Feedwater Tank
HPCS	High Pressure Core Spray
HPCSP	High Pressure Core Spray Pump
HPCST	High Pressure Core Spary Tank

HFWP	High Pressure Water Pump
ID	Inner diameter
INC 600	Inconel 600
JP	Jet Pump
K	Kelvin
kg	Kilogram
kPa	Kilopascal
kW	Kilowatt
L	Liter
LB	Liquid Level in Channel Box
LBWR	Large Boiling Water Reactor
LL	Liquid Level
LOCA	Loss-of-Coolant Accident
LOCE	Loss-of-Coolant Experiment
LP	Lower Plenum
LPCI	Low Pressure Coolant Injection
LPCIP	Low Pressure Coolant Injection Pump
LPCIT	Low Pressure Coolant Injection Tank
LPCS	Low Pressure Core Spray
LPCSP	Low Pressure Core Spary Pump
LPCST	Low Pressure Core Spary Tank
LPF	Lower Plenum Flashing
LTP	Lower Tie Plate
M	Momentum Flux
m	Meter
mm	Milimeter
MLHR	Maximum Linear Heat Rate
MPa	Megapascal
MRP	Main Recirculation Pump
MSIV	Main Steam Isolation Valve
MSL	Main Steam Line

MW	Megawatt
N	Rotation Speed
OR	Orifice
P	Pressure
	Power
PCT	Peak Cladding Temperature
PV	Pressure Vessel
PWT	Pure Water Tank
QOBV	Quick Opening Blowdown Valve
QSV	Quick Shut-off Valve
RCN	Rapid Condenser
ROSA	Rig of Safety Assessment
rpm	Revolution per Minute
S	Signal
s	Second
Sch	Schedule
SUS	Stainless Steel
T	Temperature
T/C	Thermocouple
TC	Temperature of Fluid
TF	Temperature of Fuel
TS	Temperature of Structure Material
UTP	Upper Tie Plate
V	Valve
VF	Void Fraction
W	Watt
WL	Water Level
WSP	Water Supply Pump

1. Introduction

The Rig of Safety Assessment (ROSA)-III program was initiated in 1976 to study the thermal-hydraulic behavior of a Boiling Water Reactor (BWR) during a postulated Loss of Coolant Accident (LOCA) with the Emergency Core Cooling System (ECCS) actuation and to obtain the data base to evaluate the predictability of computer codes developed for reactor safety analysis. The ROSA-III test facility was fabricated in 1978 and consisted of the volumetrically scaled (1/424) primary system of a 3800 MW BWR/6-251 with the electrically heated core, the break simulator and the scaled ECCS⁽¹⁾.

Special emphasis is made on the following objectives in the ROSA-III program :

- (1) To provide the system data required to improve and evaluate the analytical methods currently used to predict the LOCA response of large BWRs. The performance of the Engineered Safety Features (ESFs), with particular emphasis on ECCSs, and the quantitative margins of safety inherent in performance of the ESFs are of primary interest.
- (2) To identify and investigate any unexpected event(s) or threshold(s) in the response of either the plant or the ESFs and develop analytical techniques that adequately describe and account for such unexpected behavior.

The information acquired from Loss of Coolant Experiments (LOCEs) is thus used for evaluation and development of LOCA analytical methods and assessment for the qualitative margins of safety of ESFs in response to a LOCA.

RUN 916 was conducted on June 18, 1981, as one of the break area parameter series tests, and was simulated a 50 % split break at the recirculation pump suction line with the assumption of HPCS diegel generator failure.

The specific objectives of RUN 916 are as follows :

- (1) To obtain test data of a 50% break test at the recirculation pump suction line without HPCS actuation
- (2) To study the effect of the break area difference on the system thermal-hydraulic behavior comparing with the results obtained in the tests using the other size of break area

In this report, all the data obtained in RUN 916 are presented. The processed data like mass inventory in the pressure vessel are also given.

2. ROSA-III Test Facility

The ROSA-III test facility is a volumetrically scaled (1/424) BWR system with an electrically heated core designed to study the response of the primary system, the core and the ECCS during the postulated LOCA. The test facility is instrumented such that various thermal-hydraulic parameters are measured and recorded during the test. Details of the instrumentation are described in section 3.

The test facility consists of four subsystems. These subsystems are : (a) the pressure vessel, (b) the steam line and the feedwater line, (c) the recirculation loops and (d) the ECCS. Figures 2.1 through 2.3 illustrate configuration of the test facility, the pressure vessel internals and the piping schematics, respectively. Table 2.1 compares the major dimensions of the ROSA-III test facility to the corresponding dimensions of the reference BWR system.

The ROSA-III pressure vessel includes various components in it simulating the internal structures of the reactor vessel in the BWR system as shown in Fig. 2.4. The interior of the vessel is divided into the core, the lower plenum, the upper plenum, the downcomer annulus, the steam separator, the steam dome and the steam dryer. The core is consisted of four model fuel assemblies of half length and a control rod simulator. Each fuel assembly contains 62 heater rods (Fig. 2.5) and 2 water rods spaced in a 8 x 8 square array and supported by spacers and upper and lower tie plates. The heater rod is heated electrically with chopped cosine power distribution along the axis as shown in Fig. 2.6. The effective heated length is 1880 mm, one half of the active length of a BWR fuel rod. The electric power supplied to the model fuel assembly "A" is 1.4 times larger than the power supplied to each of the other assemblies. The heater rods in each assembly are divided into three groups in terms of heat generation rate as shown in Fig. 2.7. The relative power generation rate of a heater rod in each group is 1.1, 1.0, and 0.875 respectively. The orifice plates are inserted at the core inlet to control the core inlet flow⁽¹⁾.

The steam line is connected to the steam dome of the pressure vessel. A control valve is installed in the steam line to control the steam dome pressure in steady state before the initiation of the tests. The steam line has a branch in which the Automatic Depressurization System (ADS) is installed. The operation of valves in the steam line is described in Sec.

4. The feedwater is supplied from the feedwater tank (FWT) through the feedwater line and the feedwater sparger below the steam separator.

Figure 2.8 shows the recirculation lines consisted of two loops. Each line is furnished with a pump and two jet pumps. The jet pumps are installed outside the pressure vessel to simulte the relative volume and the relative height to the core. Two break simulators and a Quick Shut-off Valve (QSV) are installed in one of these loops to simulate the various break conditions. Each break simulator consists of a nozzle or an orifice to determine the break size and a Quick Opening Blowdown Valve (QOBV) to initiate the test. The break mode (double-ended or split), the break size and the break location can be changed. The diameter of the largest nozzle and orifice available is 26.2 mm. Figure 2.8 shows two QOBVs, a QSV and flow nozzles installed upstream of the QOBVs. Several flow nozzles and orifices of different size are prepared to vary the break size.

The ROSA-III test facility is furnished with all kinds of the ECCS available in the BWR system, i.e., the High Pressure Core Spray (HPCS), the Low Pressure Core Spray (LPCS), the Low Pressure Coolant Injection (LPCI), and the Automatic Depressurization System (ADS). The HPCS and the LPCS provide the cooling water from the top of the core. The LPCI injects the cooling water into the core bypass. Each ECCS consists of a pump, a tank, pipings, and a control system.

Reference (1) serves more detailed information on the facility.

3. Instrumentation

The instrumentation of the ROSA-III is designed to obtain thermal-hydraulic data during the simulated BWR LOCA. The data obtained from the experiments will contribute to the assessment of the analytical computer code. Table 3.1 summarizes instrumentation used in RUN 916.

Table 3.2 shows the measurement list of RUN 916. Table 3.3 shows the core instrumentation list. Instrumentation locations are shown in Figs. 3.1 through 3.7.

Typical measured parameters in the ROSA-III are pressure, differential pressure, flow rate, electric power, pump speed, fluid and metal temperature, collapsed liquid level, two-phase mixture level, coolant fluid density, on-off type signals and so on.

Pressure and differential pressure transducers are two-wire, direct-current type which convert diaphragm displacement to electric capacitance. The pressure lead pipes are either the standard single, cylindrical pipes used in conjunction with condensate pots, or dual concentric cylinders capable of the circulation of cooling water to prevent flashing of the fluid.

The flow rate is measured either by an orifice or a venturi type flow meter depending on the fluid condition and measurement location.

The temperatures of the fluid, structural material and fuel rod cladding are measured with chromel-alumel thermocouples (CA T/C) of 1.6 or 0.5 mm ϕ .

Liquid levels are measured by either differential pressure transducers, described above or needle type electrical conductivity probes (CP) developed in the ROSA-III program. The probes are distributed along the vessel height to detect the existence of water or vapor at different levels.

The electric power supplied to the simulated fuel rods is controlled to follow the predetermined function of time and measured by a fast response electric power meter.

Pump speed is measured by a pulse generator integral of the pump. On-off signals such as selected valve positions, decay heat and pump coast-down simulation initiations and so on are detected in order to record the exact actuation time.

Fluid density in the pipe is measured by means of gamma densitometers. Preliminary studies indicate that a three-beam densitometer should be used to determine the flow regime. Figures 3.7 and 3.8 show the beam directions of the three-beam and the two-beam gamma densitometers, respectively. The

gamma-ray source is ^{137}Cs and the detector is a water cooled NaI(Tl) scintillation counter.

Momentum flux is measured by a drag disk as shown in Fig. 3.9. The combination of signals from a drag disk and a gamma densitometer is used to determine the two-phase flow rate as shown in Fig. 3.10.

The data acquisition system (DATAAC 2000B, Iwasaki Tsushinki Co.) scans all the 700 channels of signals with the frequency up to 30 Hz. The data recorded on magnetic tape are processed by the FACOM M200 system computer at JAERI by off-line control. After evaluation, for example by comparing the initial and final pressure values with standard values, the data is reprocessed using the correct conversion factors as determined from the consistency examination.

More detailed information on the instrumentation and the data processing procedure are available in reference (2).

4. Test Conditions and Procedure

RUN 916 was a 50% break test at the recirculation pump suction in the recirculation line. A sharp-edged orifice was used in RUN916 as a break plane. The break area is determined by inserting an orifice or a nozzle upstream of the QOBV as shown in Figs. 4.1 and 3.9. Blowdown is initiated by opening the blowdown valve B. The initial conditions of RUN 916 are as follows: the steam dome pressure is 7.32 MPa, the lower plenum temperature is 551 K giving the subcooling of 11.2 K, the core inlet flow rate is 16.5 kg/s. the core heat generating rate is 3.967 MW. The estimated quality at the core outlet is 14.2%. The detailed conditions are summarized in Table 4.1

To conduct the test, makeup water (pure water) is pumped into the primary system of the test facility and electric power is supplied to the core to heat the water in the system and to achieve the saturation condition in the upper portion of the pressure vessel. The core power is 3.967 MW in RUN 916 before the break initiation and is 44% of the steady state power 9 MW based on the conservation of the power to volume ratio in the reference BWR. The core power is changed during the transient after the break initiation as shown in Fig. 4.2. The power is kept constant for the first 9.0 seconds and reduced along the curve shown in the figure which simulated the total heat transfer rate in the core of the reference BWR (the delayed neutron fission power, the decay power of fission products and actinides and the stored heat in the nuclear fuel) neglecting the stored heat of ROSA-III heater rod(3). The maximum linear heat rates of the peak power rod are 16.7 kW/m in RUN 916 before the break initiation.

The schematics of the main steam line and the feedwater line are shown in Figs. 4.3 and 4.4. The main steam line of the ROSA-III has three branches: (1) steady flow branch, (2) ADS branch and (3) transient branch. the transient branch was not used in RUN 916. Before the break initiation CV-130 in the steady flow branch controls the steam flow to maintain the steam dome pressure constant and CV-1 and CV-2 are opened to provide steam to the heat exchanger to heat the feedwater. At the break initiation, CV-1 and CV-2 are closed completely, and CV-130 is fully opened manually. Then the MSIV is simulated by CV-130 in the steady flow branch. The steam flow before MSIV closure is limited by an orifice OR-3 of 18.0 mm ID (inner diameter) installed upstream of CV-130. Tables 4.2 and 4.3 show the characteristics and the control sequence of steam discharge line valves in

the present test, respectively.

The details of the feedwater line is shown in Fig. 4.5. The feedwater is terminated at 2 s after the break by closing AV-112 in the feedwater line. However, the feedwater remained in the piping between the valve AV-112 and the feedwater sparger below the steam separator in the pressure vessel.

The coolant recirculation pumps are tripped to start coasting down at the break initiation.

The liquid level signals in the downcomer are used to actuate the ECCS and to close the MSIV. The downcomer level in the steady state operation is set at the scram level L3 (5.00 meters above the bottom of the pressure vessel) and L1 and L2 levels are 4.25 meters and 4.76 meters, respectively. The L2 level signal is used to close the MSIV with a time delay of 3 s and to actuate HPCS with time delay of 27 s. The L1 level signal is used to actuate LPCS, LPCI and ADS with time delay of 40 s, 40 s and 120 s, respectively. The above lag times of 3 s, 27 s, 40 s and 120 s are used in a safety analysis of the reference BWR⁽⁴⁾. LPCS and LPCI could inject cooling water after the primary system pressure is reduced below 2.16 MPa and 1.57 MPa, respectively. Specified system pressures for actuating LPCS and LPCI were decided from the pump characteristics used in the safety analysis of the reference BWR⁽⁵⁾. The test was terminated after the whole core was quenched at 255 s after the break initiation.

5. Data Processing

The data acquisition by DATAC 2000B was started 157 s in RUN 916 before the break initiation and terminated 801 s after the break initiation. The data acquisition frequency was 10 Hz. The test data were processed and reduced to 1000 data points for computer plotting. The time span and frequency of the reduced data for plotting were 500 s and 2.0 Hz in RUN 916. The test data are shown in Figs. 5.1 through 5.201 for RUN 916. In these figures, the measured quantity is identified by the channel number and the alphabetic characters (Ref. Tables 3.2)

The major test sequences and events observed in RUN 916 are summarized in Table 5.1.

Figures 5.1 through 5.6 show the pressure data in the pressure vessel and in the recirculation loop in RUN 916. Figures 5.7 through 5.35 show differential pressure data between various positions in the pressure vessel and the recirculation loop. Figures 5.36 and 5.37 show the liquid levels in the pressure vessel and in the tanks. Figures 5.38 through 5.44 show the flow rates. Differential pressures across orifices and venturies shown in Figs. 5.45 through 5.55 are useful to check out the flow rate instrumentation. Figure 5.56 shows the power supplies to the core with the maximum capacities of 2100 and 3150 kW. The revolution speeds of the recirculation pumps are shown in Fig. 5.57. On-off signals such as the break initiation signal and the valve positioning signals are shown in Figs. 5.58 through 5.60. Figures 5.61 through 5.70 show the fluid densities measured by the gamma densitometer. Figures 5.71 through 5.74 show momentum fluxes measured by drag disks. Figures 5.75 through 5.85 show the fluid temperatures at various positions in the loops. The fuel rod cladding temperature and the surface temperatures of the water rods and the channel boxes measured at positions 1 through 7 are given in Figs. 5.86 through 5.112. Figures 5.113 through 5.159 show the fuel rod cladding temperatures in a different manner. Figures 5.160 through 5.162 show the fluid temperatures at the inlet and outlet of the channel box. The fluid temperatures at upper tieplate of Channel A are shown in Figs. 5.163 through 5.171. The surface temperatures of the channel box are shown in Figs. 5.172 through 5.178, comparing the data at the same elevation. The fluid temperature in the lower plenum are given in Figs. 5.179 and 5.180. The liquid level signals in the core, the upper and lower plena, the guide tube and the downcomer are shown in Fig. 5.181 through 5.201. The Peak Cladding Tempera-

ture (PCT) distributions in the core are given in Table 5.2 for RUN 916.

Quantities obtained from reduction of the test data are shown in Fig. 5.202 through 5.231. Figures 5.202 shows the estimated liquid level in the pressure vessel obtained by reducing the conductivity probe signals in Figs. 5.181 through 5.201. Figures 5.203 and 5.204 show transients of the dryout front and the quenching front. Figures 5.205 and 5.206 show the average density calculated from the data measured by the three-beam or two-beam gamma densitometers. The beam configurations of gamma densitometers installed in the ROSA-III facility are shown in Figs. 3.7 and 3.8. The average density is calculated as an arithmetic mean of the densities in multi directions with the weight of the cord length.

For the three beam densitometer at the jet pump outlet spool piece,

$$\rho_{av} = 0.3221\rho_A + 0.43\rho_B + 0.2479\rho_C \quad (5.1)$$

where,

ρ_{av} : average density obtained from the three-beam gamma densitometer,

ρ_A : density measured by beam A (bottom),

ρ_B : density measured by beam B (middle),

ρ_C : density measured by beam C (top).

For the two-beam densitometer at the break spool piece,

$$\rho_{av} = 0.5863\rho_A + 0.4137\rho_B \quad (5.2)$$

where,

ρ_{av} : average density obtained from the two-beam gamma densitometer,

ρ_A : density measured by beam A (bottom),

ρ_B : density measured by beam B (top).

Figures 5.207 through 5.210 show the flow rates at upstream sides of the break in the recirculation loop. The flow rate is computed from the drag disk data and the gamma densitometer data using the following equation,

$$G = C_D \cdot A \cdot \sqrt{\rho_{av} \cdot \rho v^2} \quad (5.3)$$

where,

G : mass flow rate,
 C_D : drag coefficient ($= 1.13$),
 A : flow area ($= 1.923 \times 10^{-3} \text{ m}^2$),
 ρ_{av} : average density from gamma densitometer,
 ρv^2 : momentum flux from drag disk.

The break flow is derived from the flow rate in the recirculation loop as follows.

$$G_B = G_P - G_V \quad (5.4)$$

where,

G_B : break flow,
 G_P : flow rate at the pump side of the break,
 G_V : flow rate at the vessel side of the break,

The break flow rates are shown in Figs. 5.211 and 5.212. Figures 5.213 through 5.223 show the fluid flow rates at the main steam line, the channel inlet orifices, the bypass hole and the jet pump outlets. The fluid flow rates are calculated from the test data which are the pressure drop across the orifices or venturi flow meters and the liquid density obtained from the temperature and the pressure condition. The equation used for the calculation is as follows :

$$G = C_D \cdot A \cdot \sqrt{2g \cdot \rho_l \cdot \Delta P} \quad (5.5)$$

where,

G : flow rate,
 ΔP : pressure drop across the orifice,
 C_D : discharge coefficient,
 $= 0.6552$ (the orifice to measure the steam discharge flow rate)
 $= 0.4761$ (the channel inlet orifice)
 $= 0.8032$ (the bypass hole)
 $= 0.7383$ (the orifice to measure the jet pump outlet flow rate)
 $= 1.1260$ (the venturi tube to measure the jet pump outlet flow rate)

A : flow area (m^2)
 $= 2.875 \times 10^{-3}$ (the orifice to measure the steam discharge flow rate)
 $= 1.521 \times 10^{-3}$ (the channel inlet orifice)
 $= 1.758 \times 10^{-4}$ (the bypass hole)
 $= 1.133 \times 10^{-3}$ (the orifice to measure the jet pump outlet flow rate)
 $= 9.095 \times 10^{-4}$ (the venturi tube to measure the jet pump outlet flow rate)
 g : gravitational acceleration ($= 9.807 \text{ m/s}^2$),
 ρ_l : density of the single-phase liquid (kg/m^3),

This calculation method is not applicable for two-phase flow condition after the LPF initiation at the channel inlet orifice, the bypass hole and the jet pump outlet. The calculated value shows only a trend in two-phase flow condition. Total channel inlet flow rate presents the sum of four channel inlet flow rates.

Figure 5.224 and 5.225 show the collapsed water level outside and inside the shroud. The collapsed water level is obtained from the differential pressure in the pressure vessel. The differential pressure may include the flow resistance effect, however, the flow resistance becomes negligible after completion of the recirculation pump coastdown.

Figures 5.226 through 5.228 show the fluid mass inventories in the pressure vessel. The fluid mass inventory is determined from the density and the volumes of liquid outside and inside the shroud,

$$M = \rho_l \cdot Q \quad (5.6)$$

where,

M : fluid inventory,
 ρ_l : liquid density estimated from the saturation temperature and/or pressure.
 Q : liquid volume calculated from the liquid level.

The volume Q (m^3) outside the shroud is given below as a function of height.

$$Q = 0.0 \quad (L \leq 0.494)$$

$Q = 0.0225L - 0.0111$	$(0.494 < L \leq 1.384)$	
$Q = 0.0697L - 0.0769$	$(1.384 < L \leq 1.519)$	
$Q = 0.0225L - 0.0048$	$(1.519 < L \leq 3.355)$	
$Q = 0.0801L - 0.1980$	$(3.355 < L \leq 4.250)$	
$Q = 0.2443L - 0.8959$	$(4.250 < L \leq 4.413)$	
$Q = 0.2611L - 0.9700$	$(4.413 < L \leq 4.578)$	
$Q = 0.2504L - 0.9211$	$(4.578 < L \leq 4.654)$	(5.7)
$Q = 0.2375L - 0.8610$	$(4.654 < L \leq 4.815)$	
$Q = 0.2866L - 1.0974$	$(4.815 < L \leq 4.915)$	
$Q = 0.3396L - 1.3580$	$(4.915 < L \leq 5.143)$	
$Q = 0.3607L - 1.4665$	$(5.143 < L \leq 5.365)$	
$Q = 0.3848L - 1.5960$	$(5.365 < L \leq 5.955)$	
$Q = 0.7111$	$(5.955 < L)$	

The volume Q (m^3) inside the shroud is given below as a function of height.

$Q = 0.0$	$(L \leq 0.0)$	
$Q = 0.2350L$	$(0.0 < L \leq 0.497)$	
$Q = 0.1245L + 0.0549$	$(0.497 < L \leq 1.354)$	
$Q = 0.0698L + 0.1290$	$(1.354 < L \leq 3.589)$	
$Q = 0.1648L - 0.2120$	$(3.589 < L \leq 3.744)$	
$Q = 0.1933L - 0.3299$	$(3.744 < L \leq 4.243)$	(5.8)
$Q = 0.0196L + 0.4199$	$(4.243 < L \leq 4.578)$	
$Q = 0.0186L + 0.4244$	$(4.578 < L \leq 4.654)$	
$Q = 0.0410L + 0.3201$	$(4.654 < L \leq 5.099)$	
$Q = 0.0196L + 0.4292$	$(5.099 < L \leq 5.365)$	
$Q = 0.5344$	$(5.365 < L)$	

The total fluid mass inventory in the pressure vessel is obtained as the summation of the mass inventory outside and inside the shroud.

Figure 5.229 show the mass decrease by the fluid discharge from the break and the fluid mass recovery by the ECCS water and the feedwater injections. The variation of fluid mass inventory with time is calculated by the following equation.

$$M = \int_0^t \{ G + \rho_1 \cdot (W_H + W_L + W_I) + \rho_2 \cdot W_F \} dt \quad (5.9)$$

where,

M : mass accumulation,

G : steam discharge flow rate,

ρ_1 : density of saturated liquid at 315 K,

ρ_2 : density of saturated liquid at 489 K,

W_H : volumetric flow rate of the HPCS,

W_L : volumetric flow rate of the LPCS,

W_I : volumetric flow rate of the LPCI,

W_F : volumetric flow rate of the feedwater.

Figure 5.230 show the fluid mass discharged from the break. The fluid mass discharge M_B is calculated as follows neglecting the change of the fluid mass inventory in the loops,

$$M_B = (M_P)_i - M_P + M_F \quad (5.10)$$

where,

M_B : fluid mass discharged from the break,

$(M_P)_i$: fluid mass inventory in the pressure vessel ($= 640 \text{ kg}$),

M_P : fluid mass inventory in the pressure vessel,

M_F : net fluid mass increase by the ECCS, the feedwater flow and the steam discharge flow.

Figures 5.231 show the break flow calculated from the fluid mass inventory in the pressure vessel. The break flow is estimated from the mass inventory as follows,

$$G_B = \frac{d}{dt} M_B \quad (5-11)$$

where,

G_B : break flow,

M_B : fluid mass discharged from the break.

6. Test Results and Comparison with those of RUN 926

This section presents interpretation of RUN 916 test data, as well as comparison of RUN 926⁽⁶⁾. RUN 926 was the test with a 200% break at MRP suction line and HPCS failure logic. The effect of break area difference can be evaluated by comparing with the results of these two tests.

6.1 Test Conditions

Table 6.1 compares the initial test conditions and major events in the two tests. The test conditions of the two tests were nearly the same except for break area.

6.2 System Pressure

The lower plenum pressures in RUNs 916 and 926 are compared in Fig. 6.1. The pressures represent typical system pressure responses in the two tests, respectively. The pressure transients in the two tests show very similar trends: After the initial decrease, the pressure began to recover when MSIV was closed, and to decrease again as the recirculation line was uncovered. The MSIV initiated to close at 7.5 s in RUN 916, 2.1 s later than in RUN 926. The temporary pressure increase after the MSIV closure was larger in RUN 916 than in RUN 926 because of the break flow difference. The lower plenum flashing (LPF) started at 38 s and 17 s in RUNs 916 and 926, respectively, as the system depressurized to the saturation pressure corresponding to the lower plenum fluid temperature. The pressure in RUN 926 decreased faster than that in RUN 916 because the break flow rate in RUN 926 was larger than that in RUN 916. Therefore, the feedwater line flashing (FWLF) in RUN 916 occurred later than in RUN 926 as shown in Fig. 6.1. After the FWLF initiation the system pressure decrease rates were decreased in both tests. LPCI and ADS affected the pressure transient little.

6.3 Differential Pressure

The differential pressures between the top and bottom of the pressure vessel in the two tests are compared in Fig. 6.2. The differential pressures in the two tests showed the similar trend. The differential pressures decreased rapidly after the break, and kept nearly constant value before the LPF. Temporary differential pressure increase occurred when LPF began, which

occurred more significantly in RUN 926. That indicates an upward flow in the shroud occurred due to LPF. After LPF, the differential pressure decrease rate was larger in RUN 926 than in RUN 916 because of larger mass discharge rate. The decrease rates were increased when FWLF occurred. The differential pressure increase after LPCI actuation indicates the water accumulation in the pressure vessel. The collapsed liquid levels in the downcover calculated from the downcomer differential pressure are shown in Fig.6.3. Measured range is separated as ECC spray line nozzle elevation (3900mm as shown in Fig.3.2). The collapsed liquid levels in the two tests showed very similar behaviors, but the decrease rate was larger in RUN 926 because of larger mass discharge. Since the liquid level in the upper downcomer is used for tripping ADS. ADS actuation timing was earlier in RUN 926 than that in RUN 916. Considerable influence of fluid acceleration and flow friction loss on the lower downcomer differential pressure was observed immediately after the break in both tests: the downward flow of the downcomer fluid reduced the measured differential pressure.

6.4 Coolant Flow Rate

The coolant flow rate through the channel inlet orifices and the bypass hole are calculated from the differential pressures across these flow paths as mentioned in section 5. The total channel inlet flow rate in Run 916, shown in Fig.5.223, is compared with that in RUN 926 in Fig.6.4. The flow rates in the two tests decreased rapidly after break and kept nearly constant value. The flow rate decreased again to nearly zero after the liquid level in the downcomer decreased to the jet pump suction level. After the LPF initiation the flow rate increased temporarily. However, when the flow through the orifice became two phase, the calculated flow rate became incorrect giving only the trend. The flow rate in RUN 916 showed the downward flow with oscillation after LPF until core inlet dryout, but that in RUN 926 showed the upward flow until FWLF. This indicates that CCFL at core inlet was promoted more considerably in RUN 926 because of larger steam flow caused by larger pressure decreasing rate. When the liquid level above the channel inlet orifice disappeared, the core inlet flow turned to upward direction. After the FWLF initiation the core flow was reversed to the downward direction temporarily. This is because the rapid steam generation in the feedwater line reduced the system depressurization rate, and reduce the steam generation in the lower plenum. Oscillatory downward flow after 200 s

in RUN 916 and 120 s in RUN 926 were caused by LPCI actuation.

Figure 6.5 shows the ECCS flow rates in RUNs 916 and 926. The LPCI flow rate was four times as large as the LPCS flow rates. LPCS and LPCI actuated later in RUN 916 than in RUN 926 because of the slower depressurization in RUN 916 than in RUN 926.

6.5 Liquie Level

Liquid levels in the core in RUNs 916 and 926 are compared in Fig.6.6. These liquid levels are estimated from signals obtained from the conductivity probes installed in the fuel assembly.

The liquied level behaviours showed the same trend between RUNs 916 and 926. Temporary mixture level falls before LPF occurred in both tests. The core liquid levels in the two tests began to drop again at 61 s in RUN 916 and at 40 s in RUN 926 from the upper tieplate as LPF moderated. The whole core dryout occurred in both tests. When LPCI was actuated, the core reflooding started. The core uncovery time was longer in RUN 916 than that in RUN 926.

CCFL was observed at both of the upper tieplate and the channel inlet orifice. The CCFL at core inlet orifice affected the core mixture level behavior. The core mixture level began to rize before the lower plenum was completely filled with water in both tests.

6.6 Fuel Rod Surface Temperature

Dryout and quenching behaviors in channels A and C in RUN 916 are shown in Figs.5.203 and 5.204. These behaviors were estimated from the fuel rod surface temperature histories. The mixture levels in channels A and C are also presented in Figs.5.203 and 5.204,respectively. The dryout behaviors corresponded closely to the mixture level in the channel box. The dryout front followed the falling liquid level. The quench occured from core top by LPCS actuation and from core bottom by core mixture level rize.They are called top-down quench and bottom-up quench,respectivly.

In RUN 916 the peak cladding temperature (PCT) was 917 K and was occured at 190 s at midplane of A82 rod in the peak power channel A as shown in Fig.6.7. The PCT in RUN 926 was 784 K and occured at 119 s at midplane of the fuel rod A71 in the peak power channel A. The PCT in RUN 916 was 133 K higher than that in RUN 926 because of the longer duration of core dryout.

6.7 Density, Momentum Flux and Discharge Flow

Density, momentum flux and discharge flow rate from the break obtained in RUN 916 showed nearly the same tendency as those obtained in RUN 926. The area-averaged fluid densities measured at upstream of the MRP side break and PV side break are shown in Figs.5.205 and 5.206.

The density at the MRP side break stayed at the single phase after break and decreased at 35 s due to the mass inventory decrease in the piping. The density at the PV side break also stayed at the single phase liquid value until the recirculation pump suction line was uncovered at 16 s. After 210 s the density at the PV side of the break began to increase gradually as the coolant flowing out from the core shroud reached to the break.

Figs. 5.71 through 5.74 show the momentum flux at the break measured by drag disks. The low range drag disks saturated during the initial blowdown phase. Since the break flow rates shown in Figs.5.207 through 5.212 were calculated from the measured momentum flux, the calculated break flow rate is incorrect when the drag disks were saturated. The steady state flow directions were defined as negative at the MRP side of the break and as positive at the PV side of the break. The flow direction at the MRP side of the break was reversed immediately after the break initiation.

These total flow rates obtained from the measurements with the dragdisks and gamma densitometers include an error of at least $\pm 20\%$ in the two phase condition. The total break flow rate was also calculated by differentiating the mass inventory with respect to time as shown in Fig.5.231. This estimated flow rate includes the error caused by the mass inventory calculation from the differential pressure because the differential pressure includes not only the water head but also frictional loss and acceleration loss.

7. Conclusions

In this report, all the available test data obtained in a 50% break LOCA test RUN 916 were presented with information on the ROSA-III test facility, instrumentation and the test procedure. The explanations of the test results were also given.

RUN 916 was a 50 % break LOCA test at the recirculation pump suction line without HPCS actuation. From evaluation of the test results of RUN 916 and comparison between the test results of RUN 916 and RUN 926 which was a 200% double-ended break test, the following conclusions were obtained :

- (1) The fundamental thermal-hydraulic phenomena during a 50% break LOCA at a recirculation pump suction line have been clarified.
- (2) The PCT in RUN 916 was 917 k and observed at midplane of the A82 rod in the high power channel at 190 s after break. All fuel rods were quenched after the LPCI actuation and the effectiveness of ECCS for core cooling has been confirmed.
- (3) There were strong correlations between the mixture level transients in the core and the fuel rod surface temperature transients.
- (4) Top-down and bottom-up quenchings were observed at the same time after LPCI actuation.
- (5) The innitiation timing of core mixture level fall was later than that in RUN 926 because of the smaller break flow rate in RUN 916. But the core dryout duration was longer in RUN 916 because of later actuation of ECCSs.
- (6) The PCT in RUN 916 of 50% break test was 133 k higher than that in RUN 926 of 200 % break test because of the longer druation of core dryout.

Acknowledgment

The authors are grateful to Mr.M.Shiba for discussions and suggestions and H. Asahi, T. Odaira, T. Takayasu, S. Sekiguchi, Y. Kitano and T. Numata of Nuclear Engineering Corporation for their assistance in conducting the experiment and K. Yamano, H. Gotoh, Y.Hirano and K. Hiyama of Information System Laboratory Corporation for preparing the data.

References

- (1) ANODA, Y., et. al., "ROSA-III System Descripiton for Fuel Assembly No. 4", JAERI-M 9363 (1981).
- (2) SOBAJIMA, M., et. al., "Instrumentation and Data Processing for ROSA-III Test" (in japanese), JAERI-M 8499 (1979).
- (3) ABE, N., et. al., "Electric Power Transient Curve for ROSA-III Tests", JAERI-M 8728 (1980).
- (4) "General Electric Standard Safety Analysis Report, BWR/6", DOCKET-STN-50531-22, General Electric Company.
- (5) "BWR Blowdown Emergency Core Cooling Program, Preliminary Facility Description Report for the BT/ECCIA Test Phase", GEAP-23592, NRC-2 (1977).
- (6) Nakamura, H., et. al., "ROSA-III Double-ended Break Integral Test RUN 926 (HPCS Failure)", JAERI-M 84-008 (1984).

Acknowledgment

The authors are grateful to Mr.M.Shiba for discussions and suggestions and H. Asahi, T. Odaira, T. Takayasu, S. Sekiguchi, Y. Kitano and T. Numata of Nuclear Engineering Corporation for their assistance in conducting the experiment and K. Yamano, H. Gotoh, Y.Hirano and K. Hiyama of Information System Laboratory Corporation for preparing the data.

References

- (1) ANODA, Y., et. al., "ROSA-III System Descripiton for Fuel Assembly No. 4", JAERI-M 9363 (1981).
- (2) SOBAJIMA, M., et. al., "Instrumentation and Data Processing for ROSA-III Test" (in japanese), JAERI-M 8499 (1979).
- (3) ABE, N., et. al., "Electric Power Transient Curve for ROSA-III Tests", JAERI-M 8728 (1980).
- (4) "General Electric Standard Safety Analysis Report, BWR/6", DOCKET-STN-50531-22, General Electric Company.
- (5) "BWR Blowdown Emergency Core Cooling Program, Preliminary Facility Description Report for the BT/ECCIA Test Phase", GEAP-23592, NRC-2 (1977).
- (6) Nakamura, H., et. al., "ROSA-III Double-ended Break Integral Test RUN 926 (HPCS Failure)", JAERI-M 84-008 (1984).

Table 2.1 Primary Characteristics of ROSA-III and BWR/6

	BWR *	ROSA-III	BWR/ROSA-III
Number of Recirc. Loops	2	2	1
Number of Jet Pumps	24	4	6
Number of Separators	251	1	251
Number of Fuel Assemblies	848	4	212
Active Fuel Length (m)	3.76	1.88	2
Total Volume (m^3)	621	1.42	437
Power (MW)	3,800	4.40	864
Pressure (MPa)	7.23	7.23	1
Core Flow (kg/s)	1.54×10^4	36.4	424
Recirculation Flow (l/s)	2,970	7.01	424
Feedwater Flow (kg/s)	2,060	4.86	424
Feedwater Temp. (K)	489	489	1

* BWR/6-251

Table 3.1 ROSA-III Instrumentation Summary List

ITEM	SENSOR	NUMBER	NOTE
Pressure	Pressure Transducer	20	
Differential Pressure	DP Cell	60	PV and Loop 44 Level Measurement 5 Flow Meter 11
Fluid Temperature	CA Thermocouple	129	Primary Loop 23 DTT 4 Tie Rod 28 Upper Plenum 10 Lower Plenum 10 Tie Plate 40 Bypass 14
Fuel Rod Temperature	CA Thermocouple	213	
Slab Surface Temperature	CA Thermocouple	70	Core Barrel 24 Pressure Vessel 3 Channel Box 35 Shroud Support 8
Slab Inner Temperature	CA Thermocouple	9	JP Diffuser 4 PV Wall 5
Volumetric Flow Rate	Turbine Flow Meter Venturi Flow Meter Orifice Flow Meter	3 4 6	ECCS Loop 3 Primary Loop 10
Mass Flow Rate	Turbine Flow Meter Orifice Flow Meter	4 3	Recirculation Loop 4 Main Steam Line 3
Liquid Level	Conductivity Probe Capacitance Probe	138 2	
Density	Gamma Densitometer	10	2 Beam GD 2 3 Beam GD 2
Momentum Flux	Drag Disk	4	JP Spool Piece 2 Break Spool Piece 4 Break Orifice 1
Signal	ON/OFF Switch	14	
Pump Speed	Revolution Counter	2	
Electric Core Power	VA Meter	2	
TOTAL		693	

Table 3.2 Measurement List for RUN 916

Ch.	Item	Symbol	ID.	Location	Fig.No.	Range	Unit	Accuracy
1	Press.	P-	1	PA	Fig.5. 1	0.100	MPa	1.08%FS
2	Press.	P-	2	PA	Fig.5. 1	0.100	MPa	1.08%FS
3	Press.	P-	3	PA	Fig.5. 1	0.100	MPa	1.08%FS
4	Press.	P-	4	PA	Fig.5. 1	0.100	MPa	1.08%FS
5	Press.	P-	5	PA	Fig.5. 2	0.100	MPa	1.08%FS
6	Press.	P-	6	PA	Fig.5. 2	0.100	MPa	1.08%FS
7	Press.	P-	7	PA	Fig.5. 2	0.100	MPa	1.08%FS
8	Press.	P-	8	PA	Fig.5. 2	0.100	MPa	1.08%FS
9	Press.	P-	9	PA	Fig.5. 3	0.100	MPa	1.08%FS
10	Press.	P-	10	PA	Fig.5. 3	0.100	MPa	1.08%FS
11	Press.	P-	11	PA	Fig.5. 3	0.100	MPa	1.08%FS
12	Press.	P-	12	PA	Fig.5. 4	0.100	MPa	1.08%FS
13	Press.	P-	13	PA	Fig.5. 4	0.100	MPa	1.08%FS
14	Press.	P-	14	PA	Fig.5. 4	0.100	MPa	1.08%FS
15	Press.	P-	15	PA	Fig.5. 5	0.100	MPa	1.08%FS
16	Press.	P-	16	PA	Fig.5. 5	0.100	MPa	1.08%FS
17	Press.	P-	17	PA	Fig.5. 6	0.100	MPa	1.08%FS
18	Press.	P-	18	PA	Not Measured	0.100	MPa	1.08%FS
19	Press.	P-	19	PA	Not Measured	0.100	MPa	1.08%FS
20	Press.	P-	20	PA	Fig.5. 4	0.100	MPa	1.08%FS
21	Diff.P.	D-	1	PD	Fig.5. 5	0.100	MPa	1.08%FS
22	Diff.P.	D-	2	PD	Fig.5. 7	-50.0	kPa	0.63%FS
23	Diff.P.	D-	3	PD	Fig.5. 8	-10.0	kPa	0.63%FS
24	Diff.P.	D-	4	PD	Not Measured	0.0	MPa	1.08%FS
25	Diff.P.	D-	5	PD	Fig.5. 9	-100.	kPa	0.63%FS
26	Diff.P.	D-	6	PD	Fig.5. 10	-100.	kPa	0.63%FS
27	Diff.P.	D-	7	PD	Fig.5. 11	-100.	kPa	0.63%FS
28	Diff.P.	D-	8	PD	Fig.5. 12	0.0	MPa	0.63%FS
29	Diff.P.	D-	9	PD	Fig.5. 12	-100.	MPa	0.63%FS
30	Diff.P.	D-	10	PD	Fig.5. 12	0.0	MPa	0.63%FS
31	Diff.P.	D-	11	PD	Fig.5. 13	-100.	MPa	0.63%FS
32	Diff.P.	D-	12	PD	Fig.5. 14	-4.00	MPa	0.63%FS
33	Diff.P.	D-	13	PD	Fig.5. 14	-100.	MPa	0.63%FS
34	Diff.P.	D-	14	PD	Fig.5. 14	-4.00	MPa	0.63%FS
35	Diff.P.	D-	15	PD	Fig.5. 15	-100.	MPa	0.63%FS
36	Diff.P.	D-	16	PD	Fig.5. 15	-50.0	MPa	0.63%FS
37	Diff.P.	D-	17	PD	Fig.5. 16	0.0	MPa	0.63%FS
38	Diff.P.	D-	18	PD	Fig.5. 17	0.0	MPa	0.63%FS
39	Diff.P.	D-	19	PD	DC Middle-JP1 Suction	Fig.5. 18	0.0	MPa
40	Diff.P.	D-	20	PD	DC Middle-JP2 Suction	Fig.5. 18	0.0	MPa
41	Diff.P.	D-	21	PD	JP1 Disch.-Lower Pl.	Fig.5. 19	-100.	MPa
42	Diff.P.	D-	22	PD	JP2 Disch.-Lower Pl.	Fig.5. 19	-100.	MPa
43	Diff.P.	D-	23	PD	DC Bottom-Break B	Fig.5. 20	-60.0	MPa
44	Diff.P.	D-	24	PD	Break B-Break A	Not Measured	0.0	MPa
45	Diff.P.	D-	25	PD	Break A-MRP2 Suction	Fig.5. 21	-500.	MPa
46	Diff.P.	D-	26	PD	MRP2 Deliv.-JP3 Drive	Fig.5. 22	-500.	MPa
47	Diff.P.	D-	27	PD	MRP2 Deliv.-JP4 Drive	Fig.5. 22	-500.	MPa
48	Diff.P.	D-	28	PD	DC Middle-JP3 Suction	Fig.5. 23	-250.	MPa
49	Diff.P.	D-	29	PD	DC Middle-JP4 Suction	Fig.5. 23	-250.	MPa
50	Diff.P.	D-	30	PD	JP3 Disch.-Confluence	Fig.5. 24	-100.	MPa

Table 3-2 Measurement List for RUN 916 (Continued)

Ch.	Item	Symbol	ID.	Location	Fig.-No.	Range	Unit	Accuracy
51	Diff.P.	D-31	PD	S1 JPA Disch.-Confluence	Fig.5.24	-100.	kPa	0.63%FS
52	Diff.P.	D-32	PD	S2 Confluence-Lower Pl.	Fig.5.25	-50.0	kPa	0.63%FS
53	Diff.P.	D-33	PD	S3 Lower Pl.-DC Middle	Fig.5.26	-250.	kPa	0.63%FS
54	Diff.P.	D-34	PD	S4 Lower Pl.-DC Bottom	Fig.5.27	-250.	kPa	0.63%FS
55	Diff.P.	D-35	PD	S5 DC Bottom-DC Middle	Fig.5.28	-50.0	kPa	0.63%FS
56	Diff.P.	D-36	PD	S6 DC Middle-Steam Dome	Fig.5.29	-50.0	kPa	0.63%FS
57	Diff.P.	D-37	PD	S7 Lower Pl.-Mid-Upper Pl.	Not Measured	50.0	kPa	0.63%FS
58	Diff.P.	D-38	PD	S8 Lower Pl.-Bottom-Mid.	Fig.5.30	0.0	kPa	0.63%FS
59	Diff.P.	D-39	PD	S9 Upper Plenum Head	Not Used	-20.0	kPa	0.63%FS
60	Diff.P.	D-40	PD	S10 Channel Orifice A	Fig.5.31	-50.0	kPa	0.63%FS
61	Diff.P.	D-41	PD	S11 Channel Orifice B	Fig.5.32	-50.0	kPa	0.63%FS
62	Diff.P.	D-42	PD	S12 Channel Orifice C	Fig.5.33	-25.0	kPa	0.63%FS
63	Diff.P.	D-43	PD	S13 Channel Orifice D	Fig.5.34	-50.0	kPa	0.63%FS
64	Diff.P.	D-44	PD	S14 Lower Plenum Head	Fig.5.35	-100.	kPa	0.63%FS
65	Level	WL-1	LM	S15 HPCS Tank	Not Used	0.0	m	1.00%FS
66	Level	WL-2	LM	S16 LPCS Tank	Fig.5.36	2.30	m	1.00%FS
67	Level	WL-3	LM	S17 LPCI Tank	Fig.5.36	0.0	m	1.00%FS
68	Level	WL-4	LM	S18 Upper Downcomer	Fig.5.37	0.0	m	1.00%FS
69	Level	WL-5	LM	S19 Lower Downcomer	Fig.5.37	3.90	m	1.00%FS
70	Mass.F.	F-1	FM	S20 Steam Line (Low Range)	Fig.5.38	0.938	m	1.00%FS
71	Mass.F.	F-2	FM	S21 Steam Line (High Range)	Fig.5.38	0.0	kg/s	0.92%FS
72	Mass.F.	F-3	FM	S22 Steam Line (Mid Range)	Fig.5.38	0.0	kg/s	0.92%FS
73	Vol.F.	F-7	FV	S23 HPCS (Upper Plenum)	Not Used	0.0	m ³ /s	1.40%FS
74	Vol.F.	F-9	FV	S24 LPCS (Upper Plenum)	Fig.5.39	0.0	m ³ /s	0.79%FS
75	Vol.F.	F-11	FV	S25 LPCI (Core Bypass)	Fig.5.39	0.0	m ³ /s	0.79%FS
76	Vol.F.	F-15	FV	S26 Feedwater	Fig.5.40	0.0	m ³ /s	0.79%FS
77	Vol.F.	F-16	FV	S27 HPWP Suction Flow	Not Used	0.0	m ³ /s	0.79%FS
78	Vol.F.	F-17	FV	S28 JP1 Discharge	Fig.5.41	0.0	m ³ /s	0.79%FS
79	Vol.F.	F-18	FV	S29 JP2 Discharge	Fig.5.41	0.0	m ³ /s	0.88%FS
80	Vol.F.	F-19	FV	S30 JP3 Disch. Positive	Fig.5.42	0.0	m ³ /s	0.88%FS
81	Vol.F.	F-20	FV	S31 JP3 Disch. Negative	Fig.5.43	0.0	m ³ /s	0.92%FS
82	Vol.F.	F-21	FV	S32 JP4 Disch. Positive	Fig.5.42	0.0	m ³ /s	0.92%FS
83	Vol.F.	F-22	FV	S33 JP4 Disch. Negative	Fig.5.43	0.0	m ³ /s	0.92%FS
84	Mass.F.	F-23	FM	S34 JP1/2 Outlet Spool	Not Measured	0.0	m ³ /s	1.40%FS
85	Mass.F.	F-24	FM	S35 JP3/4 Outlet Spool	Not Measured	0.0	m ³ /s	1.40%FS
86	Mass.F.	F-25	FM	S36 Break A Spool Piece	Not Measured	0.0	m ³ /s	1.40%FS
87	Mass.F.	F-26	FM	S37 Break B Spool Piece	Not Measured	0.0	m ³ /s	1.40%FS
88	Vol.F.	F-27	FV	S38 MRP-1	Fig.5.44	0.0	m ³ /s	0.88%FS
89	Vol.F.	F-28	FV	S39 MRP-2	Fig.5.44	0.0	m ³ /s	0.63%FS
90	Diff.P.	D-F1	PD	S40 F1 Orifice	Fig.5.45	0.0	m ³ /s	0.63%FS
91	Diff.P.	D-F2	PD	S41 F2 Orifice	Fig.5.46	0.0	m ³ /s	0.63%FS
92	Diff.P.	D-F3	PD	S42 F3 Orifice	Fig.5.47	0.0	m ³ /s	0.63%FS
93	Diff.P.	D-F17	PD	S43 F17 Venturi	Fig.5.48	0.0	m ³ /s	0.63%FS
94	Diff.P.	D-F18	PD	S44 F18 Venturi	Fig.5.49	0.0	m ³ /s	0.63%FS
95	Diff.P.	D-F19	PD	S45 F19 Orifice	Fig.5.50	0.0	m ³ /s	0.63%FS
96	Diff.P.	D-F20	PD	S46 F20 Orifice	Fig.5.51	0.0	m ³ /s	0.63%FS
97	Diff.P.	D-F21	PD	S47 F21 Orifice	Fig.5.52	13.2	kPa	0.63%FS
98	Diff.P.	D-F22	PD	S48 F22 Orifice	Fig.5.53	14.7	kPa	0.63%FS
99	Diff.P.	D-F27	PD	S49 F27 Venturi	Fig.5.54	13.2	kPa	0.63%FS
100	Diff.P.	D-F28	PD	S50 F28 Venturi	Fig.5.55	200.	kPa	0.63%FS

Table 3.2 Measurement List for RUN 916 (Continued)

Ch.	Item	Symbol	ID.	Location	Fig.-No.	Range	Unit	Accuracy
101	Power Power	W- 1 W- 2	WE WE	101 102	2100 kW Power Supplier 3150 kW Power Supplier	Fig.5.56 Fig.5.56	0.0 0.0	- 0.210E+04 kW - 0.315E+04 kW
102	Rev.	N- 1	SR	104	MRP-1 Revolution	Fig.5.57	0.0	- 1.00%FS
103	Rev.	N- 2	SR	105	MRP-2 Revolution	Fig.5.57	0.0	- 1.00%FS
104	Signal	S- 1	EV	106	Break Signal A	Fig.5.58	-	- 1.08%FS
105	Signal	S- 2	EV	107	Break Signal B	Fig.5.58	-	- 1.08%FS
106	Signal	S- 3	EV	108	QSV Signal	Fig.5.58	-	-
107	Signal	S- 4	EV	109	HPCS Valve	Fig.5.59	-	-
108	Signal	S- 5	EV	110	LPCS Valve	Fig.5.59	-	-
109	Signal	S- 6	EV	110	LPCI Valve	Fig.5.59	-	-
110	Signal	S- 7	EV	111	Feedwater Control	Fig.5.58	-	-
111	Signal	S- 8	EV	112	MSIV Signal	Fig.5.58	-	-
112	Signal	S- 9	EV	113	Steam Line Valve	Fig.5.58	-	-
113	Signal	S-10	EV	114	ADS Valve	Fig.5.59	-	-
114	Signal	S-11	EV	115	MRP-1 Power OFF	Fig.5.60	-	-
115	Signal	S-12	EV	116	MRP-2 Power OFF	Fig.5.60	-	-
116	Signal	S-13	EV	117	MRP-1 Rev. Direction Failure	Fig.5.61	-	- 0.100E+04 kg/m ³
117	Signal	S-14	EV	118	MRP-2 Rev. Direction Failure	Fig.5.61	-	- 0.100E+04 kg/m ³
118	Signal	RD- 1	EV	119	JP1/2 Rev. Beam A	Fig.5.62	0.0	- 1.00%FS
119	Signal	RD- 2	EV	120	JP1/2 Outlet Beam A	Fig.5.62	0.0	- 1.00%FS
120	Density	DF- 1	DE	120	JP1/2 Outlet Beam B	Fig.5.62	0.0	- 1.00%FS
121	Density	DF- 2	DE	121	JP1/2 Outlet Beam C	Fig.5.63	0.0	- 1.00%FS
122	Density	DF- 3	DE	122	JP1/2 Outlet Beam D	Fig.5.63	0.0	- 1.00%FS
123	Density	DF- 4	DE	123	JP3/4 Outlet Beam A	Fig.5.64	0.0	- 1.00%FS
124	Density	DF- 5	DE	124	JP3/4 Outlet Beam B	Fig.5.65	0.0	- 1.00%FS
125	Density	DF- 6	DE	125	JP3/4 Outlet Beam C	Fig.5.66	0.0	- 1.00%FS
126	Density	DF- 7	DE	126	Break A Beam A	Fig.5.67	0.0	- 1.00%FS
127	Density	DF- 8	DE	127	Break A Beam B	Fig.5.68	0.0	- 1.00%FS
128	Density	DF- 9	DE	128	Break B Beam A	Fig.5.69	0.0	- 1.00%FS
129	Density	DF-10	DE	129	Break B Beam B	Fig.5.70	0.0	- 1.00%FS
130	Mo.Flux	M- 1	MF	130	JP1/2 Outlet Spool	Not Measured	0.0	- 0.220E+05 kg/ms ²
131	Mo.Flux	M- 2	MF	131	JP3/4 Outlet Spool	Not Measured	0.0	- 0.220E+05 kg/ms ²
132	Mo.Flux	M- 3	MF	132	Break A (Low Range)	Fig.5.71	0.0	- 0.220E+05 kg/ms ²
133	Mo.Flux	M- 4	MF	133	Break B (Low Range)	Fig.5.72	0.0	- 0.220E+05 kg/ms ²
134	Mo.Flux	M- 5	MF	134	Break A (High Range)	Fig.5.73	0.0	- 0.220E+06 kg/ms ²
135	Mo.Flux	M- 6	MF	135	Break B (High Range)	Fig.5.74	0.0	- 0.220E+06 kg/ms ²
136	Mo.Flux	M- 7	MF	136	Break Orifice	Not Measured	0.0	- 0.220E+05 kg/ms ²
137	Fluid T.	T- 1	TE	138	Lower Plenum	Fig.5.75	-	- 0.64%FS
138	Fluid T.	T- 2	TE	139	Upper Plenum	Fig.5.75	-	- 0.64%FS
139	Fluid T.	T- 3	TE	140	Steam Dome	Fig.5.76	-	- 0.64%FS
140	Fluid T.	T- 4	TE	141	Upper Downcomer	Fig.5.77	-	- 0.64%FS
141	Fluid T.	T- 5	TE	142	Lower Downcomer	Fig.5.77	-	- 0.64%FS
142	Fluid T.	T- 6	TE	143	JP-1 Drive	Fig.5.78	-	- 0.64%FS
143	Fluid T.	T- 7	TE	144	JP-2 Drive	Fig.5.78	-	- 0.64%FS
144	Fluid T.	T- 8	TE	145	JP-3 Drive	Fig.5.79	-	- 0.64%FS
145	Fluid T.	T- 9	TE	146	JP-4 Drive	Fig.5.79	-	- 0.64%FS
146	Fluid T.	T-10	TE	147	JP-1 Discharge	Fig.5.80	-	- 0.64%FS
147	Fluid T.	T-11	TE	148	JP-2 Discharge	Fig.5.80	-	- 0.64%FS
148	Fluid T.	T-12	TE	149	JP-3 Discharge	Fig.5.81	-	- 0.64%FS
149	Fluid T.	T-13	TE	150	JP-4 Discharge	Fig.5.81	-	- 0.64%FS

Table 3.2 Measurement List for RUN 916 (Continued)

Ch.	Item	Symbol	ID.	Location	Fig. No.	Range	Unit	Accuracy
151	Fluid T.	T-14	TE 151	MRP-1 Suction	Fig.5.78	273.	K	0.64%FS
152	Fluid T.	T-15	TE 152	MRP-1 Delivery	Fig.5.78	273.	K	0.64%FS
153	Fluid T.	T-16	TE 153	MRP-2 Suction	Fig.5.79	273.	K	0.64%FS
154	Fluid T.	T-17	TE 154	MRP-2 Delivery	Fig.5.79	273.	K	0.64%FS
155	Fluid T.	T-18	TE 155	Break A Upstream	Fig.5.82	273.	K	0.64%FS
156	Fluid T.	T-19	TE 156	Break B Upstream	Fig.5.82	273.	K	0.64%FS
157	Fluid T.	T-20	TE 157	RCN A Condensed Water	Not Used	273.	K	0.64%FS
158	Fluid T.	T-21	TE 158	RCN B Condensed Water	Not Used	273.	K	0.64%FS
159	Fluid T.	T-22	TE 159	Discharged Steam	Fig.5.76	273.	K	0.64%FS
160	Fluid T.	T-24	TE 160	JP-1/2 Outlet Spool	Fig.5.80	273.	K	0.64%FS
161	Fluid T.	T-25	TE 161	JP-3/4 Outlet Spool	Fig.5.81	273.	K	0.64%FS
162	Fluid T.	T-26	TE 162	Break A Spool Piece	Fig.5.82	273.	K	0.64%FS
163	Fluid T.	T-37	TE 163	Break B Spool Piece	Fig.5.82	273.	K	0.64%FS
164	Fluid T.	T-38	TE 164	Feedwater	Fig.5.83	273.	K	0.64%FS
165	Slab T.	TS-1	TE 165	Break Orifice Top	Fig.5.84	273.	K	0.64%FS
166	Slab T.	TS-2	TE 166	Break Orifice Bottom	Fig.5.85	273.	K	0.64%FS
167	Slab T.	TS-3	TE 167	Core Barrel C Pos.3	Not Measured	273.	K	0.64%FS
168	Slab T.	TS-4	TE 168	Core Barrel C Pos.4	Not Measured	273.	K	0.64%FS
169	Slab T.	TS-5	TE 169	Core Barrel C Pos.5	Not Measured	273.	K	0.64%FS
170	Slab T.	TS-6	TE 170	Core Barrel C Pos.6	Not Measured	273.	K	0.64%FS
171	Slab T.	TS-7	TE 171	Core Barrel A Pos.1	Not Measured	273.	K	0.64%FS
172	Slab T.	TS-8	TE 172	Core Barrel A Pos.2	Not Measured	273.	K	0.64%FS
173	Slab T.	TS-9	TE 173	Core Barrel A Pos.3	Not Measured	273.	K	0.64%FS
174	Slab T.	TS-10	TE 174	Core Barrel A Pos.4	Not Measured	273.	K	0.64%FS
175	Slab T.	TS-11	TE 175	Core Barrel A Pos.5	Not Measured	273.	K	0.64%FS
176	Slab T.	TS-12	TE 176	Core Barrel A Pos.6	Not Measured	273.	K	0.64%FS
177	Slab T.	TS-13	TE 177	Filler Block C Pos.1	Not Measured	273.	K	0.64%FS
178	Slab T.	TS-14	TE 178	Filler Block C Pos.2	Not Measured	273.	K	0.64%FS
179	Slab T.	TS-15	TE 179	Filler Block C Pos.3	Not Measured	273.	K	0.64%FS
180	Slab T.	TS-16	TE 180	Filler Block C Pos.4	Not Measured	273.	K	0.64%FS
181	Slab T.	TS-17	TE 181	Filler Block C Pos.5	Not Measured	273.	K	0.64%FS
182	Slab T.	TS-18	TE 182	Filler Block C Pos.6	Not Measured	273.	K	0.64%FS
183	Slab T.	TS-19	TE 183	Filler Block A Pos.1	Not Measured	273.	K	0.64%FS
184	Slab T.	TS-20	TE 184	Filler Block A Pos.2	Not Measured	273.	K	0.64%FS
185	Slab T.	TS-21	TE 185	Filler Block A Pos.3	Not Measured	273.	K	0.64%FS
186	Slab T.	TS-22	TE 186	Filler Block A Pos.4	Not Measured	273.	K	0.64%FS
187	Slab T.	TS-23	TE 187	Filler Block A Pos.5	Not Measured	273.	K	0.64%FS
188	Slab T.	TS-24	TE 188	Filler Block A Pos.6	Not Measured	273.	K	0.64%FS
189	Slab T.	TS-25	TE 189	JP-1 Diffuser Wall	Not Measured	273.	K	0.64%FS
190	Slab T.	TS-26	TE 190	JP-2 Diffuser Wall	Not Measured	273.	K	0.64%FS
191	Slab T.	TS-27	TE 191	JP-3 Diffuser Wall	Not Measured	273.	K	0.64%FS
192	Slab T.	TS-28	TE 192	JP-4 Diffuser Wall	Not Measured	273.	K	0.64%FS
193	Slab T.	TS-29	TE 193	PV Wall Inside 1-1	Not Measured	273.	K	0.64%FS
194	Slab T.	TS-30	TE 194	PV Inner Surface 1-2	Not Measured	273.	K	0.64%FS
195	Slab T.	TS-31	TE 195	PV Inner Surface 1-3	Not Measured	273.	K	0.64%FS
196	Slab T.	TS-32	TE 196	PV Wall Inside 2	Not Measured	273.	K	0.64%FS
197	Slab T.	TS-33	TE 197	PV Wall Inside 3	Not Measured	273.	K	0.64%FS
198	Slab T.	TS-34	TE 198	PV Wall Inside 4	Not Measured	273.	K	0.64%FS
199	Slab T.	TS-35	TE 199	L.P. Inner Surface	Not Measured	273.	K	0.64%FS
200	Slab T.	TS-36	TE 200	L.P. Wall Inside	Not Measured	273.	K	0.64%FS

Table 3.2 Measurement List for RUN 916 (Continued)

Ch.	Item	Symbol	ID.	Location	Fig. No.	Range	Unit	Accuracy
201	Temp.	TF-	1	TE	201	A11 Fuel Rod Pos.1	0.147E+04 K	0.64%FS
202	Temp.	TF-	2	TE	202	A11 Fuel Rod Pos.2	0.147E+04 K	0.64%FS
203	Temp.	TF-	3	TE	203	A11 Fuel Rod Pos.3	0.147E+04 K	0.64%FS
204	Temp.	TF-	4	TE	204	A11 Fuel Rod Pos.4	0.147E+04 K	0.64%FS
205	Temp.	TF-	5	TE	205	A11 Fuel Rod Pos.5	0.147E+04 K	0.64%FS
206	Temp.	TF-	6	TE	206	A11 Fuel Rod Pos.6	0.147E+04 K	0.64%FS
207	Temp.	TF-	7	TE	207	A11 Fuel Rod Pos.7	0.147E+04 K	0.64%FS
208	Temp.	TF-	8	TE	208	A12 Fuel Rod Pos.1	0.147E+04 K	0.64%FS
209	Temp.	TF-	9	TE	209	A12 Fuel Rod Pos.2	0.147E+04 K	0.64%FS
210	Temp.	TF-	10	TE	210	A12 Fuel Rod Pos.3	0.147E+04 K	0.64%FS
211	Temp.	TF-	11	TE	211	A12 Fuel Rod Pos.4	0.147E+04 K	0.64%FS
212	Temp.	TF-	12	TE	212	A12 Fuel Rod Pos.5	0.147E+04 K	0.64%FS
213	Temp.	TF-	13	TE	213	A12 Fuel Rod Pos.6	0.147E+04 K	0.64%FS
214	Temp.	TF-	14	TE	214	A12 Fuel Rod Pos.7	0.147E+04 K	0.64%FS
215	Temp.	TF-	15	TE	215	A13 Fuel Rod Pos.1	0.147E+04 K	0.64%FS
216	Temp.	TF-	16	TE	216	A13 Fuel Rod Pos.2	0.147E+04 K	0.64%FS
217	Temp.	TF-	17	TE	217	A13 Fuel Rod Pos.3	0.147E+04 K	0.64%FS
218	Temp.	TF-	18	TE	218	A13 Fuel Rod Pos.4	0.147E+04 K	0.64%FS
219	Temp.	TF-	19	TE	219	A13 Fuel Rod Pos.5	0.147E+04 K	0.64%FS
220	Temp.	TF-	20	TE	220	A13 Fuel Rod Pos.6	0.147E+04 K	0.64%FS
221	Temp.	TF-	21	TE	221	A13 Fuel Rod Pos.7	0.147E+04 K	0.64%FS
222	Temp.	TF-	22	TE	222	A14 Fuel Rod Pos.1	0.147E+04 K	0.64%FS
223	Temp.	TF-	23	TE	223	A14 Fuel Rod Pos.2	0.147E+04 K	0.64%FS
224	Temp.	TF-	24	TE	224	A14 Fuel Rod Pos.3	0.147E+04 K	0.64%FS
225	Temp.	TF-	25	TE	225	A14 Fuel Rod Pos.4	0.147E+04 K	0.64%FS
226	Temp.	TF-	26	TE	226	A14 Fuel Rod Pos.5	0.147E+04 K	0.64%FS
227	Temp.	TF-	27	TE	227	A14 Fuel Rod Pos.6	0.147E+04 K	0.64%FS
228	Temp.	TF-	28	TE	228	A14 Fuel Rod Pos.7	0.147E+04 K	0.64%FS
229	Temp.	TF-	29	TE	229	A15 Fuel Rod Pos.1	0.147E+04 K	0.64%FS
230	Temp.	TF-	30	TE	230	A15 Fuel Rod Pos.2	0.147E+04 K	0.64%FS
231	Temp.	TF-	31	TE	231	A17 Fuel Rod Pos.1	0.147E+04 K	0.64%FS
232	Temp.	TF-	32	TE	232	A17 Fuel Rod Pos.2	0.147E+04 K	0.64%FS
233	Temp.	TF-	33	TE	233	A22 Fuel Rod Pos.1	0.147E+04 K	0.64%FS
234	Temp.	TF-	34	TE	234	A22 Fuel Rod Pos.2	0.147E+04 K	0.64%FS
235	Temp.	TF-	35	TE	235	A22 Fuel Rod Pos.3	0.147E+04 K	0.64%FS
236	Temp.	TF-	36	TE	236	A22 Fuel Rod Pos.4	0.147E+04 K	0.64%FS
237	Temp.	TF-	37	TE	237	A22 Fuel Rod Pos.5	0.147E+04 K	0.64%FS
238	Temp.	TF-	38	TE	238	A22 Fuel Rod Pos.6	0.147E+04 K	0.64%FS
239	Temp.	TF-	39	TE	239	A22 Fuel Rod Pos.7	0.147E+04 K	0.64%FS
240	Temp.	TF-	40	TE	240	A24 Fuel Rod Pos.1	0.125E+04 K	0.64%FS
241	Temp.	TF-	41	TE	241	A24 Fuel Rod Pos.2	0.125E+04 K	0.64%FS
242	Temp.	TF-	42	TE	242	A24 Fuel Rod Pos.3	0.125E+04 K	0.64%FS
243	Temp.	TF-	43	TE	243	A24 Fuel Rod Pos.4	0.125E+04 K	0.64%FS
244	Temp.	TF-	44	TE	244	A24 Fuel Rod Pos.5	0.125E+04 K	0.64%FS
245	Temp.	TF-	45	TE	245	A24 Fuel Rod Pos.6	0.125E+04 K	0.64%FS
246	Temp.	TF-	46	TE	246	A24 Fuel Rod Pos.7	0.125E+04 K	0.64%FS
247	Temp.	TF-	47	TE	247	A26 Fuel Rod Pos.1	0.125E+04 K	0.64%FS
248	Temp.	TF-	48	TE	248	A26 Fuel Rod Pos.2	0.125E+04 K	0.64%FS
249	Temp.	TF-	49	TE	249	A28 Fuel Rod Pos.1	0.125E+04 K	0.64%FS
250	Temp.	TF-	50	TE	250	A28 Fuel Rod Pos.4	0.125E+04 K	0.64%FS

Table 3.2 Measurement List for RUN 916 (Continued)

Ch.	Item	Symbol	ID.	Location	Fig.No.	Range	Unit	Accuracy
251	Temp.	TF-	51	TE	251	A31	Fuel Rod Pos.1	0.64%FS
252	Temp.	TF-	52	TE	252	A31	Fuel Rod Pos.4	0.64%FS
253	Temp.	TF-	53	TE	253	A33	Fuel Rod Pos.1	0.64%FS
254	Temp.	TF-	54	TE	254	A33	Fuel Rod Pos.2	0.64%FS
255	Temp.	TF-	55	TE	255	A33	Fuel Rod Pos.3	0.64%FS
256	Temp.	TF-	56	TE	256	A33	Fuel Rod Pos.4	0.64%FS
257	Temp.	TF-	57	TE	257	A33	Fuel Rod Pos.5	0.64%FS
258	Temp.	TF-	58	TE	258	A33	Fuel Rod Pos.6	0.64%FS
259	Temp.	TF-	59	TE	259	A33	Fuel Rod Pos.7	0.64%FS
260	Temp.	TF-	60	TE	260	A34	Fuel Rod Pos.1	0.64%FS
261	Temp.	TF-	61	TE	261	A34	Fuel Rod Pos.2	0.64%FS
262	Temp.	TF-	62	TE	262	A34	Fuel Rod Pos.3	0.64%FS
263	Temp.	TF-	63	TE	263	A34	Fuel Rod Pos.4	0.64%FS
264	Temp.	TF-	64	TE	264	A34	Fuel Rod Pos.5	0.64%FS
265	Temp.	TF-	65	TE	265	A34	Fuel Rod Pos.6	0.64%FS
266	Temp.	TF-	66	TE	266	A34	Fuel Rod Pos.7	0.64%FS
267	Temp.	TF-	67	TE	267	A37	Fuel Rod Pos.1	0.64%FS
268	Temp.	TF-	68	TE	268	A37	Fuel Rod Pos.4	0.64%FS
269	Temp.	TF-	69	TE	269	A42	Fuel Rod Pos.1	0.64%FS
270	Temp.	TF-	70	TE	270	A42	Fuel Rod Pos.4	0.64%FS
271	Temp.	TF-	71	TE	271	A44	Fuel Rod Pos.1	0.64%FS
272	Temp.	TF-	72	TE	272	A44	Fuel Rod Pos.2	0.64%FS
273	Temp.	TF-	73	TE	273	A44	Fuel Rod Pos.3	0.64%FS
274	Temp.	TF-	74	TE	274	A44	Fuel Rod Pos.4	0.64%FS
275	Temp.	TF-	75	TE	275	A44	Fuel Rod Pos.5	0.64%FS
276	Temp.	TF-	76	TE	276	A44	Fuel Rod Pos.6	0.64%FS
277	Temp.	TF-	77	TE	277	A44	Fuel Rod Pos.7	0.64%FS
278	Temp.	TF-	78	TE	278	A48	Fuel Rod Pos.1	0.64%FS
279	Temp.	TF-	79	TE	279	A48	Fuel Rod Pos.4	0.64%FS
280	Temp.	TF-	80	TE	280	A51	Fuel Rod Pos.1	0.64%FS
281	Temp.	TF-	81	TE	281	A51	Fuel Rod Pos.4	0.64%FS
282	Temp.	TF-	82	TE	282	A53	Fuel Rod Pos.1	0.64%FS
283	Temp.	TF-	83	TE	283	A53	Fuel Rod Pos.4	0.64%FS
284	Temp.	TF-	84	TE	284	A57	Fuel Rod Pos.1	0.64%FS
285	Temp.	TF-	85	TE	285	A57	Fuel Rod Pos.4	0.64%FS
286	Temp.	TF-	86	TE	286	A62	Fuel Rod Pos.1	0.64%FS
287	Temp.	TF-	87	TE	287	A62	Fuel Rod Pos.4	0.64%FS
288	Temp.	TF-	88	TE	288	A66	Fuel Rod Pos.1	0.64%FS
289	Temp.	TF-	89	TE	289	A66	Fuel Rod Pos.4	0.64%FS
290	Temp.	TF-	90	TE	290	A68	Fuel Rod Pos.1	0.64%FS
291	Temp.	TF-	91	TE	291	A68	Fuel Rod Pos.4	0.64%FS
292	Temp.	TF-	92	TE	292	A71	Fuel Rod Pos.1	0.64%FS
293	Temp.	TF-	93	TE	293	A71	Fuel Rod Pos.4	0.64%FS
294	Temp.	TF-	94	TE	294	A73	Fuel Rod Pos.1	0.64%FS
295	Temp.	TF-	95	TE	295	A73	Fuel Rod Pos.4	0.64%FS
296	Temp.	TF-	96	TE	296	A75	Fuel Rod Pos.1	0.64%FS
297	Temp.	TF-	97	TE	297	A75	Fuel Rod Pos.4	0.64%FS
298	Temp.	TF-	98	TE	298	A77	Fuel Rod Pos.1	0.64%FS
299	Temp.	TF-	99	TE	299	A77	Fuel Rod Pos.2	0.64%FS
300	Temp.	TF-100	TE	300	A77	Fuel Rod Pos.3	0.64%FS	

Table 3.2 Measurement List for RUN 916 (Continued)

Ch.	Item	Symbol	ID.	Location	Fig. No.	Range	Unit	Accuracy
301	Temp.	TF-101	TE 301	A77 Fuel Rod Pos.4	Fig.5.95, 156	273.	-	0.64%FS
302	Temp.	TF-102	TE 302	A77 Fuel Rod Pos.5	Fig.5.95,	273.	-	0.64%FS
303	Temp.	TF-103	TE 303	A77 Fuel Rod Pos.6	Fig.5.95,	273.	-	0.64%FS
304	Temp.	TF-104	TE 304	A77 Fuel Rod Pos.7	Failure	273.	-	0.64%FS
305	Temp.	TF-105	TE 305	A82 Fuel Rod Pos.1	Fig.5.130	273.	-	0.64%FS
306	Temp.	TF-106	TE 306	A82 Fuel Rod Pos.4	Fig.5.130	273.	-	0.64%FS
307	Temp.	TF-107	TE 307	A84 Fuel Rod Pos.1	Fig.5.131	273.	-	0.64%FS
308	Temp.	TF-108	TE 308	A84 Fuel Rod Pos.4	Fig.5.131	273.	-	0.64%FS
309	Temp.	TF-109	TE 309	A85 Fuel Rod Pos.1	Fig.5.96	273.	-	0.64%FS
310	Temp.	TF-110	TE 310	A85 Fuel Rod Pos.2	Fig.5.96	273.	-	0.64%FS
311	Temp.	TF-111	TE 311	A85 Fuel Rod Pos.3	Fig.5.96	273.	-	0.64%FS
312	Temp.	TF-112	TE 312	A85 Fuel Rod Pos.4	Fig.5.96	273.	-	0.64%FS
313	Temp.	TF-113	TE 313	A85 Fuel Rod Pos.5	Fig.5.96	273.	-	0.64%FS
314	Temp.	TF-114	TE 314	A85 Fuel Rod Pos.6	Fig.5.96	273.	-	0.64%FS
315	Temp.	TF-115	TE 315	A85 Fuel Rod Pos.7	Fig.5.96	273.	-	0.64%FS
316	Temp.	TF-116	TE 316	A87 Fuel Rod Pos.1	Fig.5.97,	273.	-	0.64%FS
317	Temp.	TF-117	TE 317	A87 Fuel Rod Pos.2	Fig.5.97,	273.	-	0.64%FS
318	Temp.	TF-118	TE 318	A87 Fuel Rod Pos.3	Fig.5.97,	273.	-	0.64%FS
319	Temp.	TF-119	TE 319	A87 Fuel Rod Pos.4	Fig.5.97,	273.	-	0.64%FS
320	Temp.	TF-120	TE 320	A87 Fuel Rod Pos.5	Fig.5.97,	273.	-	0.64%FS
321	Temp.	TF-121	TE 321	A87 Fuel Rod Pos.6	Fig.5.97,	273.	-	0.64%FS
322	Temp.	TF-122	TE 322	A87 Fuel Rod Pos.7	Fig.5.97,	273.	-	0.64%FS
323	Temp.	TF-123	TE 323	A88 Fuel Rod Pos.1	Fig.5.98,	273.	-	0.64%FS
324	Temp.	TF-124	TE 324	A88 Fuel Rod Pos.2	Fig.5.98,	273.	-	0.64%FS
325	Temp.	TF-125	TE 325	A88 Fuel Rod Pos.3	Fig.5.98,	273.	-	0.64%FS
326	Temp.	TF-126	TE 326	A88 Fuel Rod Pos.4	Fig.5.98,	273.	-	0.64%FS
327	Temp.	TF-127	TE 327	A88 Fuel Rod Pos.5	Fig.5.98,	273.	-	0.64%FS
328	Temp.	TF-128	TE 328	A88 Fuel Rod Pos.6	Fig.5.98,	273.	-	0.64%FS
329	Temp.	TF-129	TE 329	A88 Fuel Rod Pos.7	Fig.5.98,	273.	-	0.64%FS
330	Temp.	TF-130	TE 330	B11 Fuel Rod Pos.1	Not Measured	273.	-	0.64%FS
331	Temp.	TF-131	TE 331	B11 Fuel Rod Pos.2	Not Measured	273.	-	0.64%FS
332	Temp.	TF-132	TE 332	B11 Fuel Rod Pos.3	Not Measured	273.	-	0.64%FS
333	Temp.	TF-133	TE 333	B11 Fuel Rod Pos.4	Not Measured	273.	-	0.64%FS
334	Temp.	TF-134	TE 334	B11 Fuel Rod Pos.5	Not Measured	273.	-	0.64%FS
335	Temp.	TF-135	TE 335	B11 Fuel Rod Pos.6	Not Measured	273.	-	0.64%FS
336	Temp.	TF-136	TE 336	B11 Fuel Rod Pos.7	Not Measured	273.	-	0.64%FS
337	Temp.	TF-137	TE 337	B13 Fuel Rod Pos.4	Fig.5.132	273.	-	0.64%FS
338	Temp.	TF-138	TE 338	B22 Fuel Rod Pos.1	Fig.5.99,	273.	-	0.64%FS
339	Temp.	TF-139	TE 339	B22 Fuel Rod Pos.2	Fig.5.99,	273.	-	0.64%FS
340	Temp.	TF-140	TE 340	B22 Fuel Rod Pos.3	Fig.5.99,	273.	-	0.64%FS
341	Temp.	TF-141	TE 341	B22 Fuel Rod Pos.4	Fig.5.99,	273.	-	0.64%FS
342	Temp.	TF-142	TE 342	B22 Fuel Rod Pos.5	Fig.5.99,	273.	-	0.64%FS
343	Temp.	TF-143	TE 343	B22 Fuel Rod Pos.6	Fig.5.99,	273.	-	0.64%FS
344	Temp.	TF-144	TE 344	B22 Fuel Rod Pos.7	Fig.5.99,	273.	-	0.64%FS
345	Temp.	TF-145	TE 345	B31 Fuel Rod Pos.4	Fig.5.132	273.	-	0.64%FS
346	Temp.	TF-146	TE 346	B33 Fuel Rod Pos.4	Fig.5.133	273.	-	0.64%FS
347	Temp.	TF-147	TE 347	B51 Fuel Rod Pos.4	Fig.5.134	273.	-	0.64%FS
348	Temp.	TF-148	TE 348	B53 Fuel Rod Pos.4	Fig.5.133	273.	-	0.64%FS
349	Temp.	TF-149	TE 349	B66 Fuel Rod Pos.4	Fig.5.133	273.	-	0.64%FS
350	Temp.	TF-150	TE 350	B77 Fuel Rod Pos.1	Not Measured	273.	-	0.64%FS

Table 3-2 Measurement List for RUN 916 (Continued)

Ch.	Item	Symbol	ID.	Location	Fig.No.	Range	Unit	Accuracy
351	Temp.	TF-151	TE	351	B77	Fuel Rod Pos.2	273.	0.64%FS
352	Temp.	TF-152	TE	352	B77	Fuel Rod Pos.3	273.	0.64%FS
353	Temp.	TF-153	TE	353	B77	Fuel Rod Pos.4	273.	0.64%FS
354	Temp.	TF-154	TE	354	B77	Fuel Rod Pos.5	273.	0.64%FS
355	Temp.	TF-155	TE	355	B77	Fuel Rod Pos.6	273.	0.64%FS
356	Temp.	TF-156	TE	356	B77	Fuel Rod Pos.7	273.	0.64%FS
357	Temp.	TF-157	TE	357	B86	Fuel Rod Pos.4	Fig.5.132	0.64%FS
358	Temp.	TF-158	TE	358	C11	Fuel Rod Pos.1	Fig.5.100	0.64%FS
359	Temp.	TF-159	TE	359	C11	Fuel Rod Pos.2	Fig.5.100	0.64%FS
360	Temp.	TF-160	TE	360	C11	Fuel Rod Pos.3	Fig.5.100	0.64%FS
361	Temp.	TF-161	TE	361	C11	Fuel Rod Pos.4	Fig.5.100	0.64%FS
362	Temp.	TF-162	TE	362	C11	Fuel Rod Pos.5	Fig.5.100	0.64%FS
363	Temp.	TF-163	TE	363	C11	Fuel Rod Pos.6	Fig.5.100	0.64%FS
364	Temp.	TF-164	TE	364	C11	Fuel Rod Pos.7	Fig.5.100	0.64%FS
365	Temp.	TF-165	TE	365	C13	Fuel Rod Pos.1	Fig.5.101	0.64%FS
366	Temp.	TF-166	TE	366	C13	Fuel Rod Pos.2	Fig.5.101	0.64%FS
367	Temp.	TF-167	TE	367	C13	Fuel Rod Pos.3	Fig.5.101	0.64%FS
368	Temp.	TF-168	TE	368	C13	Fuel Rod Pos.4	Fig.5.101	0.64%FS
369	Temp.	TF-169	TE	369	C13	Fuel Rod Pos.5	Fig.5.101	0.64%FS
370	Temp.	TF-170	TE	370	C13	Fuel Rod Pos.6	Fig.5.101	0.64%FS
371	Temp.	TF-171	TE	371	C13	Fuel Rod Pos.7	Fig.5.101	0.64%FS
372	Temp.	TF-172	TE	372	C13	Fuel Rod Pos.4	Fig.5.133	0.64%FS
373	Temp.	TF-173	TE	373	C22	Fuel Rod Pos.1	Fig.5.102,	0.64%FS
374	Temp.	TF-174	TE	374	C22	Fuel Rod Pos.2	Fig.5.102,	0.64%FS
375	Temp.	TF-175	TE	375	C22	Fuel Rod Pos.3	Fig.5.102,	0.64%FS
376	Temp.	TF-176	TE	376	C22	Fuel Rod Pos.4	Fig.5.102,	0.64%FS
377	Temp.	TF-177	TE	377	C22	Fuel Rod Pos.5	Fig.5.102,	0.64%FS
378	Temp.	TF-178	TE	378	C22	Fuel Rod Pos.6	Fig.5.102,	0.64%FS
379	Temp.	TF-179	TE	379	C22	Fuel Rod Pos.7	Fig.5.102,	0.64%FS
380	Temp.	TF-180	TE	380	C31	Fuel Rod Pos.4	Fig.5.135	0.64%FS
381	Temp.	TF-181	TE	381	C33	Fuel Rod Pos.1	Fig.5.103	0.64%FS
382	Temp.	TF-182	TE	382	C33	Fuel Rod Pos.2	Fig.5.103	0.64%FS
383	Temp.	TF-183	TE	383	C33	Fuel Rod Pos.3	Fig.5.103	0.64%FS
384	Temp.	TF-184	TE	384	C33	Fuel Rod Pos.4	Fig.5.103	0.64%FS
385	Temp.	TF-185	TE	385	C33	Fuel Rod Pos.5	Fig.5.103	0.64%FS
386	Temp.	TF-186	TE	386	C33	Fuel Rod Pos.6	Fig.5.103	0.64%FS
387	Temp.	TF-187	TE	387	C33	Fuel Rod Pos.7	Fig.5.103	0.64%FS
388	Temp.	TF-188	TE	388	C35	Fuel Rod Pos.4	Fig.5.136	0.64%FS
389	Temp.	TF-189	TE	389	C66	Fuel Rod Pos.4	Fig.5.104,	0.64%FS
390	Temp.	TF-190	TE	390	C68	Fuel Rod Pos.4	Fig.5.135	0.64%FS
391	Temp.	TF-191	TE	391	C77	Fuel Rod Pos.1	Fig.5.104,	0.64%FS
392	Temp.	TF-192	TE	392	C77	Fuel Rod Pos.2	Fig.5.104,	0.64%FS
393	Temp.	TF-193	TE	393	C77	Fuel Rod Pos.3	Fig.5.104,	0.64%FS
394	Temp.	TF-194	TE	394	C77	Fuel Rod Pos.4	Fig.5.104,	0.64%FS
395	Temp.	TF-195	TE	395	C77	Fuel Rod Pos.5	Fig.5.104,	0.64%FS
396	Temp.	TF-196	TE	396	C77	Fuel Rod Pos.6	Fig.5.104,	0.64%FS
397	Temp.	TF-197	TE	397	C77	Fuel Rod Pos.7	Fig.5.104,	0.64%FS
398	Temp.	TF-198	TE	398	D11	Fuel Rod Pos.4	Fig.5.137	0.64%FS
399	Temp.	TF-199	TE	399	D13	Fuel Rod Pos.4	Fig.5.137	0.64%FS
400	Temp.	TF-200	TE	400	D22	Fuel Rod Pos.1	Fig.5.105,	0.64%FS

Table 3.2 Measurement List for RUN 916 (Continued)

Ch.	Item	Symbol	ID.	Location	F19.No.	Range	Unit	Accuracy
401	Temp.	TF-201	TE 401	D22 Fuel Rod Pos.2	Fig.5.105,	147	273.	-0.64%FS
402	Temp.	TF-202	TE 402	D22 Fuel Rod Pos.3	Fig.5.105,	148	273.	-0.125E+04 K
403	Temp.	TF-203	TE 403	D22 Fuel Rod Pos.4	Fig.5.105,	149	273.	-0.64%FS
404	Temp.	TF-204	TE 404	D22 Fuel Rod Pos.5	Fig.5.105,	150	273.	-0.125E+04 K
405	Temp.	TF-205	TE 405	D22 Fuel Rod Pos.6	Fig.5.105,	151	273.	-0.125E+04 K
406	Temp.	TF-206	TE 406	D22 Fuel Rod Pos.7	Fig.5.109,	152	273.	-0.125E+04 K
407	Temp.	TF-207	TE 407	D31 Fuel Rod Pos.4	Fig.5.137		273.	-0.64%FS
408	Temp.	TF-208	TE 408	D33 Fuel Rod Pos.4	Fig.5.138		273.	-0.125E+04 K
409	Temp.	TF-209	TE 409	D51 Fuel Rod Pos.4	Fig.5.134		273.	-0.64%FS
410	Temp.	TF-210	TE 410	D53 Fuel Rod Pos.4	Fig.5.138		273.	-0.125E+04 K
411	Temp.	TF-211	TE 411	D66 Fuel Rod Pos.4	Not measured		273.	-0.64%FS
412	Temp.	TF-212	TE 412	D77 Fuel Rod Pos.4	Fig.5.134		273.	-0.125E+04 K
413	Temp.	TF-213	TE 413	D86 Fuel Rod Pos.4	Fig.5.137		273.	-0.64%FS
414	Fluid T.	TW-1	TE 414	A45 Tie Rod Pos.1	Fig.5.106		273.	-0.125E+04 K
415	Fluid T.	TW-2	TE 415	A45 Tie Rod Pos.2	Fig.5.106		273.	-0.64%FS
416	Fluid T.	TW-3	TE 416	A45 Tie Rod Pos.3	Fig.5.106		273.	-0.125E+04 K
417	Fluid T.	TW-4	TE 417	A45 Tie Rod Pos.4	Fig.5.106		273.	-0.64%FS
418	Fluid T.	TW-5	TE 418	A45 Tie Rod Pos.5	Fig.5.106		273.	-0.64%FS
419	Fluid T.	TW-6	TE 419	A45 Tie Rod Pos.6	Fig.5.106		273.	-0.64%FS
420	Fluid T.	TW-7	TE 420	A45 Tie Rod Pos.7	Fig.5.106		273.	-0.64%FS
421	Fluid T.	TW-8	TE 421	B45 Tie Rod Pos.1	Not measured		273.	-0.125E+04 K
422	Fluid T.	TW-9	TE 422	B45 Tie Rod Pos.2	Not measured		273.	-0.125E+04 K
423	Fluid T.	TW-10	TE 423	B45 Tie Rod Pos.3	Not measured		273.	-0.125E+04 K
424	Fluid T.	TW-11	TE 424	B45 Tie Rod Pos.4	Not measured		273.	-0.125E+04 K
425	Fluid T.	TW-12	TE 425	B45 Tie Rod Pos.5	Not measured		273.	-0.125E+04 K
426	Fluid T.	TW-13	TE 426	B45 Tie Rod Pos.6	Not measured		273.	-0.125E+04 K
427	Fluid T.	TW-14	TE 427	B45 Tie Rod Pos.7	Not measured		273.	-0.125E+04 K
428	Fluid T.	TW-15	TE 428	C45 Tie Rod Pos.1	Fig.5.107		273.	-0.64%FS
429	Fluid T.	TW-16	TE 429	C45 Tie Rod Pos.2	Fig.5.107		273.	-0.64%FS
430	Fluid T.	TW-17	TE 430	C45 Tie Rod Pos.3	Fig.5.107		273.	-0.64%FS
431	Fluid T.	TW-18	TE 431	C45 Tie Rod Pos.4	Fig.5.107		273.	-0.64%FS
432	Fluid T.	TW-19	TE 432	C45 Tie Rod Pos.5	Fig.5.107		273.	-0.64%FS
433	Fluid T.	TW-20	TE 433	C45 Tie Rod Pos.6	Fig.5.107		273.	-0.64%FS
434	Fluid T.	TW-21	TE 434	C45 Tie Rod Pos.7	Fig.5.107		273.	-0.125E+04 K
435	Fluid T.	TW-22	TE 435	D45 Tie Rod Pos.1	Not measured		273.	-0.125E+04 K
436	Fluid T.	TW-23	TE 436	D45 Tie Rod Pos.2	Not measured		273.	-0.125E+04 K
437	Fluid T.	TW-24	TE 437	D45 Tie Rod Pos.3	Not measured		273.	-0.125E+04 K
438	Fluid T.	TW-25	TE 438	D45 Tie Rod Pos.4	Not measured		273.	-0.64%FS
439	Fluid T.	TW-26	TE 439	D45 Tie Rod Pos.5	Not measured		273.	-0.64%FS
440	Fluid T.	TW-27	TE 440	D45 Tie Rod Pos.6	Not measured		273.	-0.64%FS
441	Fluid T.	TW-28	TE 441	D45 Tie Rod Pos.7	Not measured		273.	-0.125E+04 K
442	Fluid T.	TC-1	TE 442	Channel Box A Inlet	Fig.5.160		273.	-0.64%FS
443	Fluid T.	TC-2	TE 443	Channel Box B Inlet	Fig.5.160		273.	-0.125E+04 K
444	Fluid T.	TC-3	TE 444	Channel Box C Inlet	Fig.5.160		273.	-0.125E+04 K
445	Fluid T.	TC-4	TE 445	Channel Box D Inlet	Fig.5.160		273.	-0.64%FS
446	Fluid T.	TC-5	TE 446	Channel Box Outlet A-1	Fig.5.161		273.	-0.125E+04 K
447	Fluid T.	TC-6	TE 447	Channel Box Outlet A-2	Fig.5.161		273.	-0.125E+04 K
448	Fluid T.	TC-7	TE 448	Channel Box Outlet A-3	Fig.5.161		273.	-0.64%FS
449	Fluid T.	TC-8	TE 449	Channel Box Outlet A-4	Fig.5.161		273.	-0.125E+04 K
450	Fluid T.	TC-9	TE 450	Channel Box Outlet A-6	Fig.5.161		273.	-0.125E+04 K

Table 3.2 Measurement List for RUN 916 (Continued)

Ch.	Item	Symbol	ID.	Location	Fig.No.	Range	Unit	Accuracy
451	Fluid T.	TC-10	TE 451	Channel Box Outlet C-1	Fig.5.162	273.	0.125E+04 K	0.64%FS
452	Fluid T.	TC-11	TE 452	Channel Box Outlet C-2	Fig.5.162	273.	0.125E+04 K	0.64%FS
453	Fluid T.	TC-12	TE 453	Channel Box Outlet C-3	Fig.5.162	273.	0.125E+04 K	0.64%FS
454	Fluid T.	TC-13	TE 454	Channel Box Outlet C-4	Fig.5.162	273.	0.125E+04 K	0.64%FS
455	Fluid T.	TC-14	TE 455	Channel Box Outlet C-6	Fig.5.162	273.	0.125E+04 K	0.64%FS
456	Fluid T.	TG-1	TE 456	Upper Tieplate A Up-1	Fig.5.163, 167	273.	0.125E+04 K	0.64%FS
457	Fluid T.	TG-2	TE 457	Upper Tieplate A Up-2	Not Measured	273.	0.125E+04 K	0.64%FS
458	Fluid T.	TG-3	TE 458	Upper Tieplate A Up-3	Not Measured	273.	0.125E+04 K	0.64%FS
459	Fluid T.	TG-4	TE 459	Upper Tieplate A Up-4	Fig.5.163, 168	273.	0.125E+04 K	0.64%FS
460	Fluid T.	TG-5	TE 460	Upper Tieplate A Up-5	Fig.5.163, 169	273.	0.125E+04 K	0.64%FS
461	Fluid T.	TG-6	TE 461	Upper Tieplate A Up-6	Not Measured	273.	0.125E+04 K	0.64%FS
462	Fluid T.	TG-7	TE 462	Upper Tieplate A Up-7	Not Measured	273.	0.125E+04 K	0.64%FS
463	Fluid T.	TG-8	TE 463	Upper Tieplate A Up-8	Fig.5.164, 170	273.	0.125E+04 K	0.64%FS
464	Fluid T.	TG-9	TE 464	Upper Tieplate A Up-9	Not Measured	273.	0.125E+04 K	0.64%FS
465	Fluid T.	TG-10	TE 465	Upper Tieplate A Up-10	Fig.5.164, 171	273.	0.125E+04 K	0.64%FS
466	Fluid T.	TG-11	TE 466	Upper Tieplate A Lo-1	Fig.5.165, 167	273.	0.125E+04 K	0.64%FS
467	Fluid T.	TG-12	TE 467	Upper Tieplate A Lo-2	Not Measured	273.	0.125E+04 K	0.64%FS
468	Fluid T.	TG-13	TE 468	Upper Tieplate A Lo-3	Not Measured	273.	0.125E+04 K	0.64%FS
469	Fluid T.	TG-14	TE 469	Upper Tieplate A Lo-4	Fig.5.165, 168	273.	0.125E+04 K	0.64%FS
470	Fluid T.	TG-15	TE 470	Upper Tieplate A Lo-5	Fig.5.165, 169	273.	0.125E+04 K	0.64%FS
471	Fluid T.	TG-16	TE 471	Upper Tieplate A Lo-6	Not Measured	273.	0.125E+04 K	0.64%FS
472	Fluid T.	TG-17	TE 472	Upper Tieplate A Lo-7	Not Measured	273.	0.125E+04 K	0.64%FS
473	Fluid T.	TG-18	TE 473	Upper Tieplate A Lo-8	Fig.5.166, 170	273.	0.125E+04 K	0.64%FS
474	Fluid T.	TG-19	TE 474	Upper Tieplate A Lo-9	Not Measured	273.	0.125E+04 K	0.64%FS
475	Fluid T.	TG-20	TE 475	Upper Tieplate A Lo-10	Fig.5.166, 171	273.	0.125E+04 K	0.64%FS
476	Fluid T.	TG-21	TE 476	Upper Tieplate C Up-1	Not Measured	273.	0.125E+04 K	0.64%FS
477	Fluid T.	TG-22	TE 477	Upper Tieplate C Up-2	Not Measured	273.	0.125E+04 K	0.64%FS
478	Fluid T.	TG-23	TE 478	Upper Tieplate C Up-3	Not Measured	273.	0.125E+04 K	0.64%FS
479	Fluid T.	TG-24	TE 479	Upper Tieplate C Up-4	Not Measured	273.	0.125E+04 K	0.64%FS
480	Fluid T.	TG-25	TE 480	Upper Tieplate C Up-5	Not Measured	273.	0.125E+04 K	0.64%FS
481	Fluid T.	TG-26	TE 481	Upper Tieplate C Up-6	Not Measured	273.	0.125E+04 K	0.64%FS
482	Fluid T.	TG-27	TE 482	Upper Tieplate C Up-7	Not Measured	273.	0.125E+04 K	0.64%FS
483	Fluid T.	TG-28	TE 483	Upper Tieplate C Up-8	Not Measured	273.	0.125E+04 K	0.64%FS
484	Fluid T.	TG-29	TE 484	Upper Tieplate C Up-9	Not Measured	273.	0.125E+04 K	0.64%FS
485	Fluid T.	TG-30	TE 485	Upper Tieplate C Up-10	Not Measured	273.	0.125E+04 K	0.64%FS
486	Fluid T.	TG-31	TE 486	Upper Tieplate C Lo-1	Not Measured	273.	0.125E+04 K	0.64%FS
487	Fluid T.	TG-32	TE 487	Upper Tieplate C Lo-2	Not Measured	273.	0.125E+04 K	0.64%FS
488	Fluid T.	TG-33	TE 488	Upper Tieplate C Lo-3	Not Measured	273.	0.125E+04 K	0.64%FS
489	Fluid T.	TG-34	TE 489	Upper Tieplate C Lo-4	Not Measured	273.	0.125E+04 K	0.64%FS
490	Fluid T.	TG-35	TE 490	Upper Tieplate C Lo-5	Not Measured	273.	0.125E+04 K	0.64%FS
491	Fluid T.	TG-36	TE 491	Upper Tieplate C Lo-6	Not Measured	273.	0.125E+04 K	0.64%FS
492	Fluid T.	TB-1	TE 492	Upper Tieplate C Lo-7	Not Measured	273.	0.125E+04 K	0.64%FS
493	Fluid T.	TB-2	TE 493	Upper Tieplate C Lo-8	Not Measured	273.	0.125E+04 K	0.64%FS
494	Fluid T.	TB-3	TE 494	Upper Tieplate C Lo-9	Not Measured	273.	0.125E+04 K	0.64%FS
495	Fluid T.	TB-4	TE 495	Upper Tieplate C Lo-10	Not Measured	273.	0.125E+04 K	0.64%FS
496	Slab T.	TB-5	TE 496	C.B. A1 Inner ,Pos.1	Fig.5.108, 172	273.	0.125E+04 K	0.64%FS
497	Slab T.	TB-6	TE 497	C-B. A1 Inner ,Pos.2	Fig.5.108, 173	273.	0.125E+04 K	0.64%FS
498	Slab T.	TB-7	TE 498	C-B. A1 Inner ,Pos.3	Fig.5.108, 174	273.	0.125E+04 K	0.64%FS
499	Slab T.	TB-8	TE 499	C-B. A1 Inner ,Pos.4	Fig.5.108, 175	273.	0.125E+04 K	0.64%FS
500	Slab T.	TB-9	TE 500	C-B. A1 Inner ,Pos.5	Fig.5.108, 176	273.	0.125E+04 K	0.64%FS

Table 3.2 Measurement List for RUN 916 (Continued)

Ch.	Item	Symbol	ID.	Location	Fig.-No.	Range	Unit	Accuracy
501	Slab T.	TB- 6	TE 501	C.B. A1 Inner /Pos. 6	Fig. 5-108,	177	-	0.64%FS
502	Slab T.	TB- 7	TE 502	C.B. A1 Inner /Pos. 7	Fig. 5-108,	178	-	0.64%FS
503	Slab T.	TB- 8	TE 503	C.B. A2 Inner /Pos. 1	Fig. 5-109,	172	273.	0.64%FS
504	Slab T.	TB- 9	TE 504	C.B. A2 Inner /Pos. 2	Fig. 5-109,	173	273.	0.64%FS
505	Slab T.	TB-10	TE 505	C.B. A2 Inner /Pos. 3	Fig. 5-109,	174	273.	0.64%FS
506	Slab T.	TB-11	TE 506	C.B. A2 Inner /Pos. 4	Fig. 5-109,	175	273.	0.64%FS
507	Slab T.	TB-12	TE 507	C.B. A2 Inner /Pos. 5	Fig. 5-109,	176	273.	0.64%FS
508	Slab T.	TB-13	TE 508	C.B. A2 Inner /Pos. 6	Fig. 5-109,	177	273.	0.64%FS
509	Slab T.	TB-14	TE 509	C.B. A2 Inner /Pos. 7	Fig. 5-109,	178	273.	0.64%FS
510	Slab T.	TB-15	TE 510	C.B. B Inner /Pos. 1	Not Measured	-	273.	0.64%FS
511	Slab T.	TB-16	TE 511	C.B. B Inner /Pos. 2	Not Measured	-	273.	0.64%FS
512	Slab T.	TB-17	TE 512	C.B. B Inner /Pos. 3	Not Measured	-	273.	0.64%FS
513	Slab T.	TB-18	TE 513	C.B. B Inner /Pos. 4	Not Measured	-	273.	0.64%FS
514	Slab T.	TB-19	TE 514	C.B. B Inner /Pos. 5	Not Measured	-	273.	0.64%FS
515	Slab T.	TB-20	TE 515	C.B. B Inner /Pos. 6	Not Measured	-	273.	0.64%FS
516	Slab T.	TB-21	TE 516	C.B. B Inner /Pos. 7	Not Measured	-	273.	0.64%FS
517	Slab T.	TB-22	TE 517	C.B. C Inner /Pos. 1	Fig. 5-110,	172	273.	0.64%FS
518	Slab T.	TB-23	TE 518	C.B. C Inner /Pos. 2	Fig. 5-110,	173	273.	0.64%FS
519	Slab T.	TB-24	TE 519	C.B. C Inner /Pos. 3	Fig. 5-110,	174	273.	0.64%FS
520	Slab T.	TB-25	TE 520	C.B. C Inner /Pos. 4	Fig. 5-110,	175	273.	0.64%FS
521	Slab T.	TB-26	TE 521	C.B. C Inner /Pos. 5	Fig. 5-110,	176	273.	0.64%FS
522	Slab T.	TB-27	TE 522	C.B. C Inner /Pos. 6	Fig. 5-110,	177	273.	0.64%FS
523	Slab T.	TB-28	TE 523	C.B. C Inner /Pos. 7	Fig. 5-110,	178	273.	0.64%FS
524	Slab T.	TB-29	TE 524	C.B. D Inner /Pos. 1	Not Measured	-	273.	0.64%FS
525	Slab T.	TB-30	TE 525	C.B. D Inner /Pos. 2	Not Measured	-	273.	0.64%FS
526	Slab T.	TB-31	TE 526	C.B. D Inner /Pos. 3	Not Measured	-	273.	0.64%FS
527	Slab T.	TB-32	TE 527	C.B. D Inner /Pos. 4	Not Measured	-	273.	0.64%FS
528	Slab T.	TB-33	TE 528	C.B. D Inner /Pos. 5	Not Measured	-	273.	0.64%FS
529	Slab T.	TB-34	TE 529	C.B. D Inner /Pos. 6	Not Measured	-	273.	0.64%FS
530	Slab T.	TB-35	TE 530	C.B. D Inner /Pos. 7	Not Measured	-	273.	0.64%FS
531	Fluid T.	TB-36	TE 531	C.B. A Outer /Pos. 1	Fig. 5-111,	172	273.	0.64%FS
532	Fluid T.	TB-37	TE 532	C.B. A Outer /Pos. 2	Fig. 5-111,	173	273.	0.64%FS
533	Fluid T.	TB-38	TE 533	C.B. A Outer /Pos. 3	Fig. 5-111,	174	273.	0.64%FS
534	Fluid T.	TB-39	TE 534	C.B. A Outer /Pos. 4	Fig. 5-111,	175	273.	0.64%FS
535	Fluid T.	TB-40	TE 535	C.B. A Outer /Pos. 5	Fig. 5-111,	176	273.	0.64%FS
536	Fluid T.	TB-41	TE 536	C.B. A Outer /Pos. 6	Fig. 5-111,	177	273.	0.64%FS
537	Fluid T.	TB-42	TE 537	C.B. A Outer /Pos. 7	Fig. 5-111,	178	273.	0.64%FS
538	Fluid T.	TB-43	TE 538	C.B. C Outer /Pos. 1	Fig. 5-112,	172	273.	0.64%FS
539	Fluid T.	TB-44	TE 539	C.B. C Outer /Pos. 2	Fig. 5-112,	173	273.	0.64%FS
540	Fluid T.	TB-45	TE 540	C.B. C Outer /Pos. 3	Fig. 5-112,	174	273.	0.64%FS
541	Fluid T.	TB-46	TE 541	C.B. C Outer /Pos. 4	Fig. 5-112,	175	273.	0.64%FS
542	Fluid T.	TB-47	TE 542	C.B. C Outer /Pos. 5	Fig. 5-112,	176	273.	0.64%FS
543	Fluid T.	TP- 48	TE 543	C.B. C Outer /Pos. 6	Fig. 5-112,	177	273.	0.64%FS
544	Fluid T.	TP- 49	TE 544	C.B. C Outer /Pos. 7	Fig. 5-112,	178	273.	0.64%FS
545	Fluid T.	TP- 50	TE 545	Lower PL. Center 1	Fig. 5-119	-	273.	0.64%FS
546	Fluid T.	TP- 51	TE 546	Lower PL. Center 2	Fig. 5-119	-	273.	0.64%FS
547	Fluid T.	TP- 52	TE 547	Lower PL. Center 3	Fig. 5-119	-	273.	0.64%FS
548	Fluid T.	TP- 53	TE 548	Lower PL. Center 4	Fig. 5-119	-	273.	0.64%FS
549	Fluid T.	TP- 54	TE 549	Lower PL. Center 5	Fig. 5-119	-	273.	0.64%FS
550	Fluid T.	TP- 55	TE 550	Lower PL. Center 7	Fig. 5-119	-	273.	0.64%FS

Table 3.2 Measurement List for RUN 916 (Continued)

Ch.	Item	Symbol	ID.	Location	Fig.-No.	Range	Unit	Accuracy
551	Slab T.	TP- 7	TE	551 Lower Pl. North	Fig.5.180	- 0.125E+04	K	0.64%FS
552	Slab T.	TP- 8	TE	552 Lower Pl. North	Not Measured	273.	-	0.64%FS
553	Slab T.	TP- 9	TE	553 Lower Pl. North	Not Measured	273.	-	0.64%FS
554	Slab T.	TP-10	TE	554 Lower Pl. North	Not Measured	273.	-	0.64%FS
555	Slab T.	TP-11	TE	555 Lower Pl. South	Not Measured	273.	-	0.64%FS
556	Slab T.	TP-12	TE	556 Lower Pl. South	Not Measured	273.	-	0.64%FS
557	Slab T.	TP-13	TE	557 Lower Pl. South	Not Measured	273.	-	0.64%FS
558	Slab T.	TP-14	TE	558 Lower Pl. South	Not Measured	273.	-	0.64%FS
559	Level	LB- 1	LM	559 C.B.Liquid Level	Fig.5.181	A1-1	-	
560	Level	LB- 2	LM	560 C.B.Liquid Level	Fig.5.181	A1-2	-	
561	Level	LB- 3	LM	561 C.B.Liquid Level	Fig.5.181	A1-3	-	
562	Level	LB- 4	LM	562 C.B.Liquid Level	Fig.5.181	A1-4	-	
563	Level	LB- 5	LM	563 C.B.Liquid Level	Fig.5.181	A1-5	-	
564	Level	LB- 6	LM	564 C.B.Liquid Level	Fig.5.181	A1-6	-	
565	Level	LB- 7	LM	565 C.B.Liquid Level	Fig.5.181	A1-7	-	
566	Level	LB- 8	LM	566 C.B.Liquid Level	Fig.5.182	A2-1	-	
567	Level	LB- 9	LM	567 C.B.Liquid Level	Fig.5.182	A2-2	-	
568	Level	LB-10	LM	568 C.B.Liquid Level	Fig.5.182	A2-3	-	
569	Level	LB-11	LM	569 C.B.Liquid Level	Fig.5.182	A2-4	-	
570	Level	LB-12	LM	570 C.B.Liquid Level	Fig.5.182	A2-5	-	
571	Level	LB-13	LM	571 C.B.Liquid Level	Fig.5.182	A2-6	-	
572	Level	LB-14	LM	572 C.B.Liquid Level	Fig.5.182	A2-7	-	
573	Level	LB-15	LM	573 C.B.Liquid Level	Fig.5.183	B-1	-	
574	Level	LB-16	LM	574 C.B.Liquid Level	Fig.5.183	B-2	-	
575	Level	LB-17	LM	575 C.B.Liquid Level	Fig.5.183	B-3	-	
576	Level	LB-18	LM	576 C.B.Liquid Level	Fig.5.183	B-4	-	
577	Level	LB-19	LM	577 C.B.Liquid Level	Fig.5.183	B-5	-	
578	Level	LB-20	LM	578 C.B.Liquid Level	Fig.5.183	B-6	-	
579	Level	LB-21	LM	579 C.B.Liquid Level	Fig.5.183	B-7	-	
580	Level	LB-22	LM	580 C.B.Liquid Level	Fig.5.184	C-1	-	
581	Level	LB-23	LM	581 C.B.Liquid Level	Fig.5.184	C-2	-	
582	Level	LB-24	LM	582 C.B.Liquid Level	Fig.5.184	C-3	-	
583	Level	LB-25	LM	583 C.B.Liquid Level	Fig.5.184	C-4	-	
584	Level	LB-26	LM	584 C.B.Liquid Level	Fig.5.184	C-5	-	
585	Level	LB-27	LM	585 C.B.Liquid Level	Fig.5.184	C-6	-	
586	Level	LB-28	LM	586 C.B.Liquid Level	Fig.5.184	C-7	-	
587	Level	LB-29	LM	587 C.B.Liquid Level	Fig.5.185	D-1	-	
588	Level	LB-30	LM	588 C.B.Liquid Level	Fig.5.185	D-2	-	
589	Level	LB-31	LM	589 C.B.Liquid Level	Fig.5.185	D-3	-	
590	Level	LB-32	LM	590 C.B.Liquid Level	Fig.5.185	D-4	-	
591	Level	LB-33	LM	591 C.B.Liquid Level	Failure	D-5	-	
592	Level	LB-34	LM	592 C.B.Liquid Level	Fig.5.185	D-6	-	
593	Level	LB-35	LM	593 C.B.Liquid Level	Fig.5.185	D-7	-	
594	Level	LL- 1	LM	594 Ch.Box Outlet A1-5	Fig.5.186		-	
595	Level	LL- 2	LM	595 Ch.Box Outlet A1-6	Fig.5.186		-	
596	Level	LL- 3	LM	596 Ch.Box Outlet A1-7	Failure		-	
597	Level	LL- 4	LM	597 Ch.Box Outlet A2-5	Fig.5.187		-	
598	Level	LL- 5	LM	598 Ch.Box Outlet A2-6	Fig.5.187		-	
599	Level	LL- 6	LM	599 Ch.Box Outlet A2-7	Fig.5.187		-	
600	Level	LL- 7	LM	600 Ch.Box Outlet A-1	Failure		-	

Table 3.2 Measurement List for RUN 916 (Continued)

Ch.	Item	Symbol	ID.	Location	Fig.No.	Range	Unit	Accuracy
601	Level	LL-8	LM	601	Ch.-Box	Outlet A-2		
602	Level	LL-9	LM	602	Ch.-Box	Outlet A-3		Failure Fig.5.188
603	Level	LL-10	LM	603	Ch.-Box	Outlet A-4		Fig.5.188
604	Level	LL-11	LM	604	Ch.-Box	Outlet A-6		Fig.5.188
605	Level	LL-12	LM	605	Ch.-Box	Outlet C1-5		Fig.5.189
606	Level	LL-13	LM	606	Ch.-Box	Outlet C1-6		Fig.5.189
607	Level	LL-14	LM	607	Ch.-Box	Outlet C1-7		Fig.5.189
608	Level	LL-15	LM	608	Ch.-Box	Outlet C2-5		Fig.5.190
609	Level	LL-16	LM	609	Ch.-Box	Outlet C2-6		Fig.5.190
610	Level	LL-17	LM	610	Ch.-Box	Outlet C2-7		Fig.5.190
611	Level	LL-18	LM	611	Ch.-Box	Outlet C-1		Fig.5.191
612	Level	LL-19	LM	612	Ch.-Box	Outlet C-2		Fig.5.191
613	Level	LL-20	LM	613	Ch.-Box	Outlet C-3		Fig.5.191
614	Level	LL-21	LM	614	Ch.-Box	Outlet C-4		Fig.5.191
615	Level	LL-22	LM	615	Ch.-Box	Outlet C-6		Fig.5.191
616	Level	LL-23	LM	616	Ch.-Box	Inlet A-1		Fig.5.192
617	Level	LL-24	LM	617	Ch.-Box	Inlet A-2		Fig.5.192
618	Level	LL-25	LM	618	Ch.-Box	Inlet B-1		Fig.5.193
619	Level	LL-26	LM	619	Ch.-Box	Inlet B-2		Fig.5.193
620	Level	LL-27	LM	620	Ch.-Box	Inlet C-1		Fig.5.194
621	Level	LL-28	LM	621	Ch.-Box	Inlet C-2		Fig.5.194
622	Level	LL-29	LM	622	Ch.-Box	Inlet D-1		Fig.5.195
623	Level	LL-30	LM	623	Ch.-Box	Inlet D-2		Fig.5.195
624	Level	LL-31	LM	624	Lower Pl.	North 1		Fig.5.196
625	Level	LL-32	LM	625	Lower Pl.	North 2		Fig.5.196
626	Level	LL-33	LM	626	Lower Pl.	North 3		Fig.5.196
627	Level	LL-34	LM	627	Lower Pl.	North 4		Fig.5.196
628	Level	LL-35	LM	628	Lower Pl.	North 5		Fig.5.196
629	Level	LL-36	LM	629	Lower Pl.	North 6		Fig.5.196
630	Level	LL-37	LM	630	Lower Pl.	South 1		Fig.5.197
631	Level	LL-38	LM	631	Lower Pl.	South 2		Fig.5.197
632	Level	LL-39	LM	632	Lower Pl.	South 3		Fig.5.197
633	Level	LL-40	LM	633	Lower Pl.	South 4		Fig.5.197
634	Level	LL-41	LM	634	Lower Pl.	South 5		Fig.5.197
635	Level	LL-42	LM	635	Lower Pl.	South 6		Fig.5.197
636	Level	LL-43	LM	636	Guide Tube	North 0		Fig.5.198
637	Level	LL-44	LM	637	Guide Tube	North 1		Fig.5.198
638	Level	LL-45	LM	638	Guide Tube	North 3		Fig.5.198
639	Level	LL-46	LM	639	Guide Tube	North 6		Fig.5.198
640	Level	LL-47	LM	640	Guide Tube	South 0		Fig.5.199
641	Level	LL-48	LM	641	Guide Tube	South 1		Failure
642	Level	LL-49	LM	642	Guide Tube	South 3		Fig.5.199
643	Level	LL-50	LM	643	Guide Tube	South 6		Fig.5.199
644	Level	L-1	LM	644	Downcomer	D-Side	1	Fig.5.200
645	Level	L-2	LM	645	Downcomer	D-Side	2	Fig.5.200
646	Level	L-3	LM	646	Downcomer	D-Side	3	Fig.5.200
647	Level	L-4	LM	647	Downcomer	D-Side	4	Fig.5.200
648	Level	L-5	LM	648	Downcomer	D-Side	5	Failure
649	Level	L-6	LM	649	Downcomer	B-Side	1	Fig.5.201
650	Level	L-7	LM	650	Downcomer	B-Side	2	Fig.5.201

Table 3.2 Measurement List for RUN 916 (Continued)

Ch.	Item	Symbol	ID.	Location	Fig. No.	Range	Unit	Accuracy
651	Level	L-	8	LM	651	Downcomer	B-Side	3
652	Level	L-	9	LM	652	Downcomer	B-Side	4
653	Level	L-	10	LM	653	Downcomer	B-Side	5
654	Void	VF-	1	VD	654	A54 Tie Rod	Pos.1	Not Measured
655	Void	VF-	2	VD	655	A54 Tie Rod	Pos.2	Not Measured
656	Void	VF-	3	VD	656	A54 Tie Rod	Pos.3	Not Measured
657	Void	VF-	4	VD	657	A54 Tie Rod	Pos.4	Not Measured
658	Void	VF-	5	VD	658	A54 Tie Rod	Pos.5	Not Measured
659	Void	VF-	6	VD	659	A54 Tie Rod	Pos.6	Not Measured
660	Void	VF-	7	VD	660	A54 Tie Rod	Pos.7	Not Measured
661	Void	VF-	8	VD	661	B54 Tie Rod	Pos.1	Not Measured
662	Void	VF-	9	VD	662	B54 Tie Rod	Pos.2	Not Measured
663	Void	VF-	10	VD	663	B54 Tie Rod	Pos.3	Not Measured
664	Void	VF-	11	VD	664	B54 Tie Rod	Pos.4	Not Measured
665	Void	VF-	12	VD	665	B54 Tie Rod	Pos.5	Not Measured
666	Void	VF-	13	VD	666	B54 Tie Rod	Pos.6	Not Measured
667	Void	VF-	14	VD	667	B54 Tie Rod	Pos.7	Not Measured
668	Void	VF-	15	VD	668	C54 Tie Rod	Pos.1	Not Measured
669	Void	VF-	16	VD	669	C54 Tie Rod	Pos.2	Not Measured
670	Void	VF-	17	VD	670	C54 Tie Rod	Pos.3	Not Measured
671	Void	VF-	18	VD	671	C54 Tie Rod	Pos.4	Not Measured
672	Void	VF-	19	VD	672	C54 Tie Rod	Pos.5	Not Measured
673	Void	VF-	20	VD	673	C54 Tie Rod	Pos.6	Not Measured
674	Void	VF-	21	VD	674	C54 Tie Rod	Pos.7	Not Measured
675	Void	VF-	22	VD	675	D54 Tie Rod	Pos.3	Not Measured
676	Void	VF-	23	VD	676	D54 Tie Rod	Pos.4	Not Measured
677	Void	VF-	24	VD	677	D54 Tie Rod	Pos.5	Not Measured
678	Void	VF-	25	VD	678	D54 Tie Rod	Pos.6	Not Measured
679	Void	VF-	26	VD	679	D54 Tie Rod	Pos.7	Not Measured
680	Void	VF-	27	VD	680	D54 Tie Rod	Pos.7	Not Measured
681	Void	VF-	28	VD	681	D54 Tie Rod	Pos.7	Not Measured
682	Void	VE-	1	VD	682	Channel A	Outlet 1	Not Measured
683	Void	VE-	2	VD	683	Channel A	Outlet 2	Not Measured
684	Void	VE-	3	VD	684	Channel A	Outlet 3	Not Measured
685	Void	VE-	4	VD	685	Channel B	Outlet 1	Not Measured
686	Void	VE-	5	VD	686	Channel B	Outlet 2	Not Measured
687	Void	VE-	6	VD	687	Channel B	Outlet 3	Not Measured
688	Void	VE-	7	VD	688	Channel C	Outlet 1	Not Measured
689	Void	VE-	8	VD	689	Channel C	Outlet 2	Not Measured
690	Void	VE-	9	VD	690	Channel C	Outlet 3	Not Measured
691	Void	VE-	10	VD	691	Channel D	Outlet 1	Not Measured
692	Void	VE-	11	VD	692	Channel D	Outlet 2	Not Measured
693	Void	VE-	12	VD	693	Channel D	Outlet 3	Not Measured
694	Void	VE-	13	VD	694	Lower Plenum	Bottom 1	Not Measured
695	Void	VE-	14	VD	695	Lower Plenum	Bottom 2	Not Measured
696	Void	VE-	15	VD	696	Lower Plenum	Bottom 3	Not Measured
697	Void	VP-	1	VD	697	Lower Plenum	Inlet	Not Measured
698	Void	VP-	2	VD	698	Lower Plenum	Inlet	Not Measured

Table 3.3 Core Instrumentation Map

Item	Pos. DL Rod NO.	Core Outlet	Pos.1	Pos.2	Pos.3	Pos.4	Pos.5	Pos.6	Pos.7	Core Inlet
		3660	3417	3114.5	2879.5	2527	2174.5	1939.5	1637	1454
Surface Temp.	A11		TF 1	TF 2	TF 3	TF 4	TF 5	TF 6	TF 7	
	A12		TF 8	TF 9	TF 10	TF 11	TF 12	TF 13	TF 14	
	A13		TF 15	TF 16	TF 17	TF 18	TF 19	TF 20	TF 21	
	A14		TF 22	TF 23	TF 24	TF 25	TF 26	TF 27	TF 28	
	A15		TF 29			TF 30				
	A17		TF 31			TF 32				
	A22		TF 33	TF 34	TF 35	TF 36	TF 37	TF 38	TF 39	
	A23		TF 40	TF 41	TF 42	TF 43	TF 44	TF 45	TF 46	
	A24		TF 47	TF 48	TF 49	TF 50	TF 51	TF 52	TF 53	
	A26		TF 54			TF 55				
	A28		TF 56			TF 57				
	A31		TF 58			TF 59				
	A33		TF 60	TF 61	TF 62	TF 63	TF 64	TF 65	TF 66	
	A34		TF 67	TF 68	TF 69	TF 70	TF 71	TF 72	TF 73	
	A35		TF 74			TF 75				
	A37		TF 76			TF 77				
	A42		TF 78			TF 79				
Fluid Temp.	A44	TC 1	TF180	TF181	TF182	TF183	TF184	TF185	TF186	TC 2
Surface Temp.	A45		TF 80			TF 81				
	A46		TF 82			TF 83				
	A48		TF 84			TF 85				
	A51		TF 86			TF 87				
	A53		TF 88			TF 89				
	A54		TF 90							
	A57		TF 91			TF 92				
	A62		TF 93			TF 94				
	A64		TF 95			TF 96				
	A66		TF 97			TF 98				
	A68		TF 99			TF100				
	A71		TF101			TF102				
	A73		TF103			TF104				
	A75		TF105			TF106				
	A77		TF107			TF108				

Table 3.3 Core Instrumentation Map (Continued)

Item	Pos. Rod NO.	Core Outlet	Pos.1	Pos.2	Pos.3	Pos.4	Pos.5	Pos.6	Pos.7	Core Inlet
			DL	3660	3417	3114.5	2879.5	2527	2174.5	1939.5
Surface Temp.	A82			TF109			TF110			
	A84			TF111			TF112			
	A86			TF113			TF114			
	A88			TF115			TF116			
	B11						TF117			
	B13						TF118			
	B15			TF119	TF120	TF121	TF122	TF123	TF124	TF125
	B31						TF126			
	B33						TF127			
	B35						TF128			
Fluid Temp.	B44	TC 3	TF187	TF188	TF189	TF190	TF191	TF192	TF193	TC 4
Surface Temp.	B51						TF129			
	B53						TF130			
	B85		TF131	TF132	TF133	TF134	TF135	TF136	TF137	
	C11						TF138			
	C13						TF139			
	C15						TF140			
	C31						TF141			
	C33		TF142	TF143	TF144	TF145	TF146	TF147	TF148	
	C35						TF149			
Fluid Temp.	C44	TC 5	TF194	TF195	TF196	TF197	TF198	TF199	TF200	TC 6
Surface Temp.	C51						TF150			
	C53						TF151			
	C77		TF152	TF153	TF154	TF155	TF156	TF157	TF158	
	D11						TF159			
	D13						TF160			
	D27		TF161	TF162	TF163	TF164	TF165	TF166	TF167	
	D31						TF168			
	D33						TF169			
	D35						TF170			
Fluid Temp.	D44	TC 7	TF201	TF202	TF203	TF204	TF205	TF206	TF207	TC 8
Surface Temp.	D51						TF171			
	D53						TF172			
	D88		TF173	TF174	TF175	TF176	TF177	TF178	TF179	

Table 3.3 Core Instrumentation Map (Continued)

Item	Pos. Rod NO.	Core Outlet DL	Pos.1	Pos.2	Pos.3	Pos.4	Pos.5	Pos.6	Pos.7	Core Inlet
			3660	3417	3114.5	2879.5	2527	2174.5	1939.5	1454
Void	A55		VF 1	VF 2	VF 3	VF 4	VF 5	VF 6	VF 7	
	B55		VF 8	VF 9	VF 10	VF 11	VF 12	VF 13	VF 14	
	C55		VF 15	VF 16	VF 17	VF 18	VF 19	VF 20	VF 21	
	D55		VF 22	VF 23	VF 24	VF 25	VF 26	VF 27	VF 28	
Channel Box Surface Temp.	A1*		TB 1	TB 2	TB 3	TB 4	TB 5	TB 6	TB 7	
	A2*		TB 8	TB 9	TB 10	TB 11	TB 12	TB 13	TB 14	
	B*		TB 15	TB 16	TB 17	TB 18	TB 19	TB 20	TB 21	
	C*		TB 22	TB 23	TB 24	TB 25	TB 26	TB 27	TB 28	
	D*		TB 29	TB 30	TB 31	TB 32	TB 33	TB 34	TB 35	
Liquid Level in the Channel Box	A1*		LB 1	LB 2	LB 3	LB 4	LB 5	LB 6	LB 7	
	A2*		LB 8	LB 9	LB 10	LB 11	LB 12	LB 13	LB 14	
	B*		LB 15	LB 16	LB 17	LB 18	LB 19	LB 20	LB 21	
	C*		LB 22	LB 23	LB 24	LB 25	LB 26	LB 27	LB 28	
	D*		LB 29	LB 30	LB 31	LB 32	LB 33	LB 34	LB 35	

Table 4.1 Test Conditions of RUN 916

Parameter	I	Specified Value	I	Measured Value
Break Conditions	I		I	
Location	I	MRP Suction	I	MRP Suction
Type	I	Split	I	Split
Break Orifice Dia. (mm)	I	18.5	I	18.5
Initial System Conditions	I		I	
Steam Dome Press. (MPa)	I	7.36	I	7.32
Lower Plenum Temperature (k)	I	551.7	I	550.8
Lower Plenum Subcooling (K)	I	10.5	I	11.2
Core Inlet Flow Rate (kg/s)	I	16.0	I	16.5
Core Outlet Quality	I	13.8	I	14.2
Power Level (kw)	I	1260 + 2700	I	1263 + 2700
Maximum Linear Heat Rate(kW/m)	I		I	
Channel A P.F.=1.1	I	16.65	I	16.67
P.F.=1.0	I	15.13	I	15.16
P.F.=0.875	I	13.24	I	13.26
Channel B-D P.F.=1.1	I	11.89	I	11.92
P.F.=1.0	I	10.81	I	10.84
P.F.=0.875	I	9.46	I	9.48
Water Level in PV (m)	I	5.0	I	5.0
Feedwater Conditions	I		I	
Temperature (K)	I	489.0	I	489.0
Flow Rate (kg/s)	I	2.39	I	Fig.5.1.40
Initiation of Line Closure (s)	I	2.0	I	0.5 - 3.2 s

note L3 Level for Scram : 5.0 m from PV Bottom

not include core bypass flow
core bypass flow is assumed to be 1.6kg/s

Table 4.1 Test Conditions of RUN 916 (contd.)

Parameter	I	Specified Value	I	Measured Value
Steam Discharge Conditions	I		I	
Steady State Flow Rate(kg/s)	I	2.39	I	2.03
Transient Flow Rate (kg/s)	I	keep steady value	I	Fig.5.38
Orifice Diameter (mm)	I	18.0	I	18.0
Initiation of Line Closure(s)	I	L2 +3 (s)	I	7.5
Safety Relief Valve	I	$8.24 \leq P \leq 8.34$	I	not-used
Setting Pressure (MPa)	I		I	
ECCS Conditions	I		I	
HPCS	I	not-used	I	not-used
LPCS	I		I	
Injection Location	I	Upper Plenum	I	Upper Plenum
Initial Conditions	I	L1 +40(s) and $\leq 2.16(\text{MPa})$	I	143(s) at PV Press. 2.18(MPa)
Coolant Temperature (K)	I	313	I	313
Injection Flow Rate (m^3/s)	I	1.13×10^{-3}	I	Fig.5.39
LPCI	I		I	
Injection Location	I	Core Bypass Top	I	Core Bypass Top
Initiation Conditions	I	L1 +40 (s) and $< 1.57 (\text{MPa})$	I	183 (s) at PV Press. 1.58(MPa)
Coolant Temperature (K)	I	313	I	313
Injection Flow Rate (m^3/s)	I	3.50×10^{-3}	I	Fig.5.39
ADS Conditions	I		I	
Initiation Time (s)	I	L1 +120 (s)	I	131 (s)
Flow Rate	I	BWR Scaled Flow	I	Fig.5.38
Orifice Diameter	I	15.5	I	15.5

note : Each trip level is as follows;

L3 Level for Scram : 5.0 m from PV Bottom

L2 Level for MSIV and HPCS : 4.76 m from PV Bottom

L1 Level for LPCS,LPCI and ADS : 4.25 from PV Bottom

Table 4.2 Characteristics of Steam Discharge Line Valves

Valve	Close to Open (sec)	Open to Close (sec)
AV165	Not Used	Not Used
AV168	-	0.1
AV169	0.3	2.0

Orifice	Diameter (mm)	Area (mm ²)
OR3	18.0	254.5
OR4	15.5	188.7
OR5	Not Used (Blind)	Not Used (Blind)

Table 4.3 Control Sequence for Steam Discharge Line Valves

Time	$t < 0$ s	$t = 0$ s (Break)	$P \leq 6.67\text{MPa}$	$L2 + 3$ s	$P \geq 8.14\text{MPa}$	\dots	$L1 + 120$ s
CV-1	Open	Close (Manual)	Closed	Closed	Closed	Closed	Closed
CV-2 (see Fig. 2.3)	Open	Close (Manual)	Closed	Closed	Closed	Closed	Closed
CV-130	Control to maintain steady state pressure	Open (Manual)	Control to maintain system pressure at 6.67MPa (Auto)	Close (Manual)	Control to maintain system pressure at 8.14MPa (Auto)	Control to maintain system pressure at 8.14MPa (Auto)	Control to maintain system pressure at 8.14MPa (Auto)
AV-168	Open	Open	Open	Open	Open	Open	Close (Auto)
AV-169 (ADS Line)	Closed	Closed	Closed	Closed	Closed	Closed	Open (Auto)

 $t = 0$ s : Break $t = L2 + 3$ s : MSIV closure $t = L1 + 120$ s : ADS valve opening

Table 5.1 Sequence of Events in RUN 916

Time after break (s)	I	Events
0.0	I	
	I	Break
	I	
	I	Initiation of core power control
	I	Termination of MRP power input
	I	
1.6	I	Initiation of FW line valve closure
	I	
3.2	I	Closure of FW line valve
	I	
5.6	I	L2 level trip signal
	I	
10.3	I	L1 level trip signal
	I	
7.5-12.2	I	Main steam line valve closure
	I	
9.0	I	Initiation of core power reduction
	I	
13.4	I	Jet pump suction nozzle uncovery
	I	
17.6	I	Recirculation line nozzle uncovery
	I	
22.5	I	Dryout at the top of the core
	I	
38.3	I	Initiation of lower plenum flashing
	I	
105	I	Whole core uncovery
	I	
131	I	ADS actuation
	I	
142	I	Initiation of FW line flashing
	I	
143	I	LPCS initiation (at system pressure 2.26 MPa)
	I	
183	I	LPCI initiation (at system pressure 1.68 MPa)
	I	
210	I	Completion of core reflooding
	I	
255	I	Whole core quench

Table 5.2 Maximum Cladding Temperature Distribution in the Core

	Pos.1	Pos.2	Pos.3	Pos.4	Pos.5	Pos.6	Pos.7
A-11 rod	TE 201	TE 202	TE 203	TE 204	TE 205	TE 206	TE 207
PCT (K)	610.3	736.3	855.1	900.7	840.7	731.5	587.0
Time (s)	12.0	151.2	156.8	192.0	190.4	188.8	166.4
A-12 rod	TE 208	TE 209	TE 210	TE 211	TE 212	TE 213	TE 214
PCT (K)	583.9	767.5	843.1	883.9	814.3	717.1	570.7
Time (s)	88.0	156.0	156.0	192.8	190.4	185.6	156.8
A-13 rod	TE 215	TE 216	TE 217	TE 218	TE 219	TE 220	TE 221
PCT (K)	587.5	768.7	843.1	881.5	816.7	715.9	571.9
Time (s)	89.6	156.0	157.6	190.4	192.8	184.8	152.8
A-14 rod	TE 222	TE 223	TE 224	TE 225	TE 226	TE 227	TE 228
PCT (K)	589.9	759.1	835.9	867.1	796.3	697.9	571.9
Time (s)	93.6	156.8	182.4	191.2	192.8	190.4	157.6
A-15 rod	TE 229			TE 230			
PCT (K)	593.5			867.1			
Time (s)	96.8			191.2			
A-17 rod	TE 231			TE 232			
PCT (K)	662.6			863.4			
Time (s)	147.2			195.2			
A-22 rod	TE 233	TE 234	TE 235	TE 236	TE 237	TE 238	TE 239
PCT (K)	660.9	790.3	850.3	889.6	821.0	721.4	571.0
Time (s)	145.6	157.6	164.8	192.8	191.2	188.0	155.2
A-24 rod	TE 240	TE 241	TE 242	TE 243	TE 244	TE 245	TE 246
PCT (K)	584.5	774.1	845.4	871.7	801.3	704.5	570.1
Time (s)	24.0	156.0	183.2	191.2	192.8	189.6	158.4

Table 5.2 Maximum Cladding Temperature Distribution in the Core (Continued)

	Pos.1	Pos.2	Pos.3	Pos.4	Pos.5	Pos.6	Pos.7
A-26 rod	TE 247			TE 248			
PCT (K)	674.2			882.0			
Time (s)	212.8			189.6			
A-28 rod	TE 249			TE 250			
PCT (K)	690.3			899.0			
Time (s)	151.2			192.8			
A-31 rod	TE 251			TE 252			
PCT (K)	616.7			916.2			
Time (s)	99.2			192.8			
A-33 rod	TE 253	TE 254	TE 255	TE 256	TE 257	TE 258	TE 259
PCT (K)	578.8	752.5	809.7	844.5	768.5	681.8	567.2
Time (s)	89.6	156.8	167.2	193.6	189.6	179.2	13.6
A-34 rod	TE 260	TE 261	TE 262	TE 263	TE 264	TE 265	TE 266
PCT (K)	587.4	752.5	817.2	843.5	768.5	680.8	567.2
Time (s)	95.2	159.2	192.8	191.2	189.6	178.4	16.8
A-37 rod	TE 267			TE 268			
PCT (K)	594.1			890.5			
Time (s)	96.0			190.4			
A-42 rod	TE 269			TE 270			
PCT (K)	743.1			899.0			
Time (s)	201.6			193.6			
A-44 rod	TE 271	TE 272	TE 273	TE 274	TE 275	TE 276	TE 277
PCT (K)	582.6	764.7	820.1	831.3	758.1	669.5	565.3
Time (s)	147.2	190.4	192.8	190.4	189.6	176.8	14.4

Table 5.2 Maximum Cladding Temperature Distribution in the Core (Continued)

	Pos.1	Pos.2	Pos.3	Pos.4	Pos.5	Pos.6	Pos.7
A-48 rod	TE 278			TE 279			
PCT (K)	734.6			875.5			
Time (s)	199.2			191.2			
A-51 rod	TE 280			TE 281			
PCT (K)	651.4			890.5			
Time (s)	146.4			191.2			
A-53 rod	TE 282			TE 283			
PCT (K)	620.9			842.6			
Time (s)	148.0			192.0			
A-57 rod	TE 284			TE 285			
PCT (K)	759.5			892.4			
Time (s)	202.4			191.2			
A-62 rod	TE 286			TE 287			
PCT (K)	689.3			900.9			
Time (s)	148.8			192.8			
A-66 rod	TE 288			TE 289			
PCT (K)	725.2			851.0			
Time (s)	204.0			189.6			
A-68 rod	TE 290			TE 291			
PCT (K)	737.4			908.4			
Time (s)	184.0			190.4			
A-71 rod	TE 292			TE 293			
PCT (K)	698.8			914.1			
Time (s)	163.2			194.4			

Table 5.2 Maximum Cladding Temperature Distribution in the Core (Continued)

	Pos.1	Pos.2	Pos.3	Pos.4	Pos.5	Pos.6	Pos.7
A-73 rod	TE 294			TE 295			
PCT (K)	702.6			896.2			
Time (s)	156.0			192.0			
A-75 rod	TE 296			TE 297			
PCT (K)	721.4			888.6			
Time (s)	204.8			190.4			
A-77 rod	TE 298	TE 299	TE 300	TE 301	TE 302	TE 303	TE 304
PCT (K)	764.7	852.9	889.6	888.6	817.2	703.5	-----
Time (s)	203.2	200.0	198.4	188.8	190.4	193.6	-----
A-82 rod	TE 305			TE 306			
PCT (K)	706.4			917.0			
Time (s)	156.0			190.4			
A-84 rod	TE 307			TE 308			
PCT (K)	696.9			894.3			
Time (s)	156.0			192.8			
A-85 rod	TE 309	TE 310	TE 311	TE 312	TE 313	TE 314	TE 315
PCT (K)	698.8	826.6	878.3	894.3	821.0	714.8	580.7
Time (s)	163.2	199.2	192.0	190.4	191.2	190.4	178.4
A-87 rod	TE 316	TE 317	TE 318	TE 319	TE 320	TE 321	TE 322
PCT (K)	742.1	842.6	897.1	909.4	835.1	725.2	583.6
Time (s)	200.0	198.4	191.2	189.6	191.2	190.4	169.6
A-88 rod	TE 323	TE 324	TE 325	TE 326	TE 327	TE 328	TE 329
PCT (K)	696.9	833.2	891.5	912.2	837.9	728.0	584.5
Time (s)	157.6	190.4	191.2	192.0	192.8	191.2	165.6

Table 5.2 Maximum Cladding Temperature Distribution in the Core (Continued)

	Pos.1	Pos.2	Pos.3	Pos.4	Pos.5	Pos.6	Pos.7
B-11 rod	TE 330	TE 331	TE 332	TE 333	TE 334	TE 335	TE 336
PCT (K)	-----	-----	-----	-----	-----	-----	-----
Time (s)	-----	-----	-----	-----	-----	-----	-----
B-13 rod				TE 337			
PCT (K)				807.9			
Time (s)				192.0			
B-22 rod	TE 338	TE 339	TE 340	TE 341	TE 342	TE 343	TE 344
PCT (K)	626.7	725.2	781.6	808.8	735.5	658.1	566.2
Time (s)	144.0	145.6	161.6	189.6	191.2	184.8	13.6
B-31 rod				TE 345			
PCT (K)				806.9			
Time (s)				192.0			
B-33 rod				TE 346			
PCT (K)				756.2			
Time (s)				180.0			
B-51 rod				TE 347			
PCT (K)				786.3			
Time (s)				192.0			
B-53 rod				TE 348			
PCT (K)				759.1			
Time (s)				188.8			
B-66 rod				TE 349			
PCT (K)				766.6			
Time (s)				188.8			

Table 5.2 Maximum Cladding Temperature Distribution in the Core (Continued)

	Pos.1	Pos.2	Pos.3	Pos.4	Pos.5	Pos.6	Pos.7
B-77 rod	TE 350	TE 351	TE 352	TE 353	TE 354	TE 355	TE 356
PCT (K)	404.0	460.7	-----	-----	-----	-----	-----
Time (s)	232.0	218.4	-----	-----	-----	-----	-----
B-86 rod				TE 357			
PCT (K)				829.4			
Time (s)				188.8			
C-11 rod	TE 358	TE 359	TE 360	TE 361	TE 362	TE 363	TE 364
PCT (K)	610.4	656.2	783.5	808.8	745.9	667.6	568.1
Time (s)	41.6	105.6	155.2	195.2	192.0	185.6	16.0
C-13 rod	TE 365	TE 366	TE 367	TE 368	TE 369	TE 370	TE 371
PCT (K)	622.9	728.0	785.4	806.0	743.1	666.6	567.2
Time (s)	40.8	147.2	154.4	188.8	191.2	179.2	13.6
C-15 rod				TE 372			
PCT (K)				804.1			
Time (s)				191.2			
C-22 rod	TE 373	TE 374	TE 375	TE 376	TE 377	TE 378	TE 379
PCT (K)	620.9	724.3	776.9	791.9	732.7	662.8	567.2
Time (s)	146.4	145.6	153.6	178.4	193.6	190.4	13.6
C-31 rod				TE 380			
PCT (K)				809.7			
Time (s)				184.8			
C-33 rod	TE 381	TE 382	TE 383	TE 384	TE 385	TE 386	TE 387
PCT (K)	601.8	698.8	743.1	744.0	696.0	640.0	565.3
Time (s)	40.8	147.2	155.2	164.0	181.6	186.4	15.2

Table 5.2 Maximum Cladding Temperature Distribution in the Core (Continued)

	Pos.1	Pos.2	Pos.3	Pos.4	Pos.5	Pos.6	Pos.7
C-35 rod				TE 388			
PCT (K)				776.0			
Time (s)				192.8			
C-66 rod				TE 389			
PCT (K)				764.7			
Time (s)				188.0			
C-68 rod				TE 390			
PCT (K)				833.2			
Time (s)				188.8			
C-77 rod	TE 391	TE 392	TE 393	TE 394	TE 395	TE 396	TE 397
PCT (K)	719.5	794.7	821.0	815.4	741.2	652.4	567.2
Time (s)	200.8	200.0	189.6	189.6	188.8	186.4	16.8
D-11 rod				TE 398			
PCT (K)				822.9			
Time (s)				188.8			
D-13 rod				TE 399			
PCT (K)				813.5			
Time (s)				192.8			
D-22 rod	TE 400	TE 401	TE 402	TE 403	TE 404	TE 405	TE 406
PCT (K)	641.9	738.4	791.0	807.9	742.1	664.7	567.2
Time (s)	144.0	148.8	156.0	189.6	188.0	187.2	17.6
D-31 rod				TE 407			
PCT (K)				823.8			
Time (s)				192.0			

Table 5.2 Maximum Cladding Temperature Distribution in the Core (Continued)

	Pos.1	Pos.2	Pos.3	Pos.4	Pos.5	Pos.6	Pos.7
D-33 rod				TE 408			
PCT (K)				752.5			
Time (s)				175.2			
D-51 rod				TE 409			
PCT (K)				800.4			
Time (s)				192.0			
D-53 rod				TE 410			
PCT (K)				775.0			
Time (s)				193.6			
D-66 rod				TE 411			
PCT (K)				674.2			
Time (s)				187.2			
D-77 rod				TE 412			
PCT (K)				814.3			
Time (s)				190.4			
D-86 rod				TE 413			
PCT (K)				822.9			
Time (s)				186.4			

Table 5.2 Maximum Cladding Temperature Distribution in the Core (Continued)

** Order of PCT **

No. 1	A-82 rod	Pos. 4	PCT = 917.0 (K)	Time = 190.4 (s)
No. 2	A-31 rod	Pos. 4	PCT = 916.2 (K)	Time = 192.8 (s)
No. 3	A-71 rod	Pos. 4	PCT = 914.1 (K)	Time = 194.4 (s)
No. 4	A-88 rod	Pos. 4	PCT = 912.2 (K)	Time = 192.0 (s)
No. 5	A-87 rod	Pos. 4	PCT = 909.4 (K)	Time = 189.6 (s)
No. 6	A-68 rod	Pos. 4	PCT = 908.4 (K)	Time = 190.4 (s)
No. 7	A-62 rod	Pos. 4	PCT = 900.9 (K)	Time = 192.8 (s)
No. 8	A-11 rod	Pos. 4	PCT = 900.7 (K)	Time = 192.0 (s)
No. 9	A-28 rod	Pos. 4	PCT = 899.0 (K)	Time = 192.8 (s)
No. 10	A-42 rod	Pos. 4	PCT = 899.0 (K)	Time = 193.6 (s)

Table 6.1 Comparison of Initial Conditions and
Major Events in RUN 916 and RUN 926

Parameter	I	RUN 916	I	RUN 926
Break Diameter	I	18.5 mm	I	26.2/26.2 mm
ECCS Condition	I	HPCS Failure	I	HPCS Failure
Core Power	I	3.963 MW	I	3.967 MW
Steam Dome Pressure	I	7.32 MPa	I	7.37 MPa
Core Inlet Flow	I	16.5 kg/s	I	16.3 kg/s
Lower Plenum Subcooling	I	11.2 K	I	10.0 K
PCT	I	917 K	I	784 K
	I	(A82 Pos.4 190s)	I	(A71 Pos.4 119s)
Events	I	Time after break	s	
Feedwater Stop	I	1.6 - 3.2	I	1.5 - 4.0
MSIV Closure	I	7.5 - 12.2	I	5.4 - 9.2
LPF initiation	I	38	I	17
ADS Actuation	I	131	I	130
FWLF Initiation	I	142	I	68
LPCS Actuation	I	143	I	71
LPCI Actuation	I	183	I	96
Whole core quench	I	255	I	188

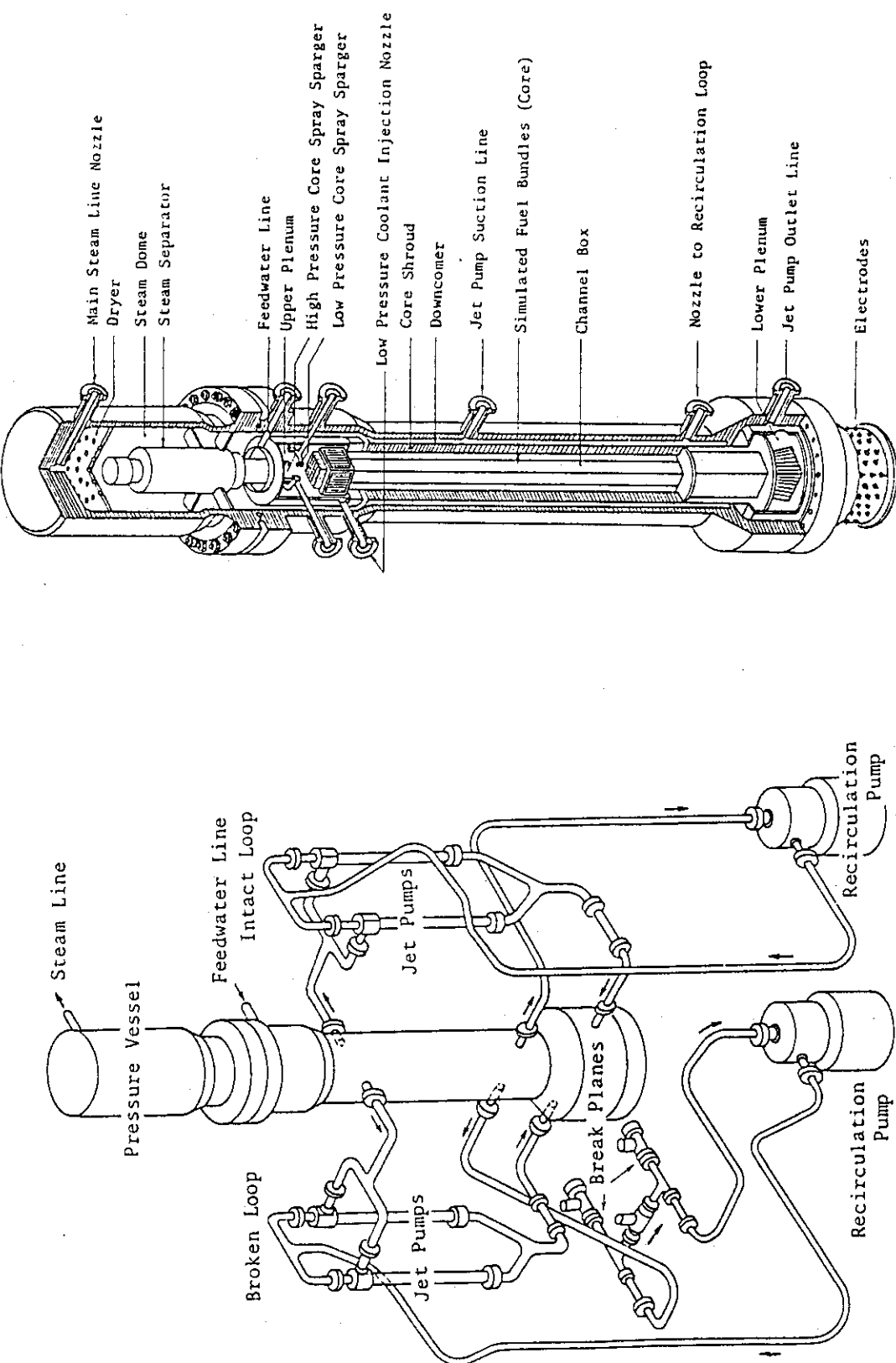


Fig. 2.1

Schematic Diagram of ROSA-III Test Facility

Internal Structure of Pressure Vessel of ROSA-III

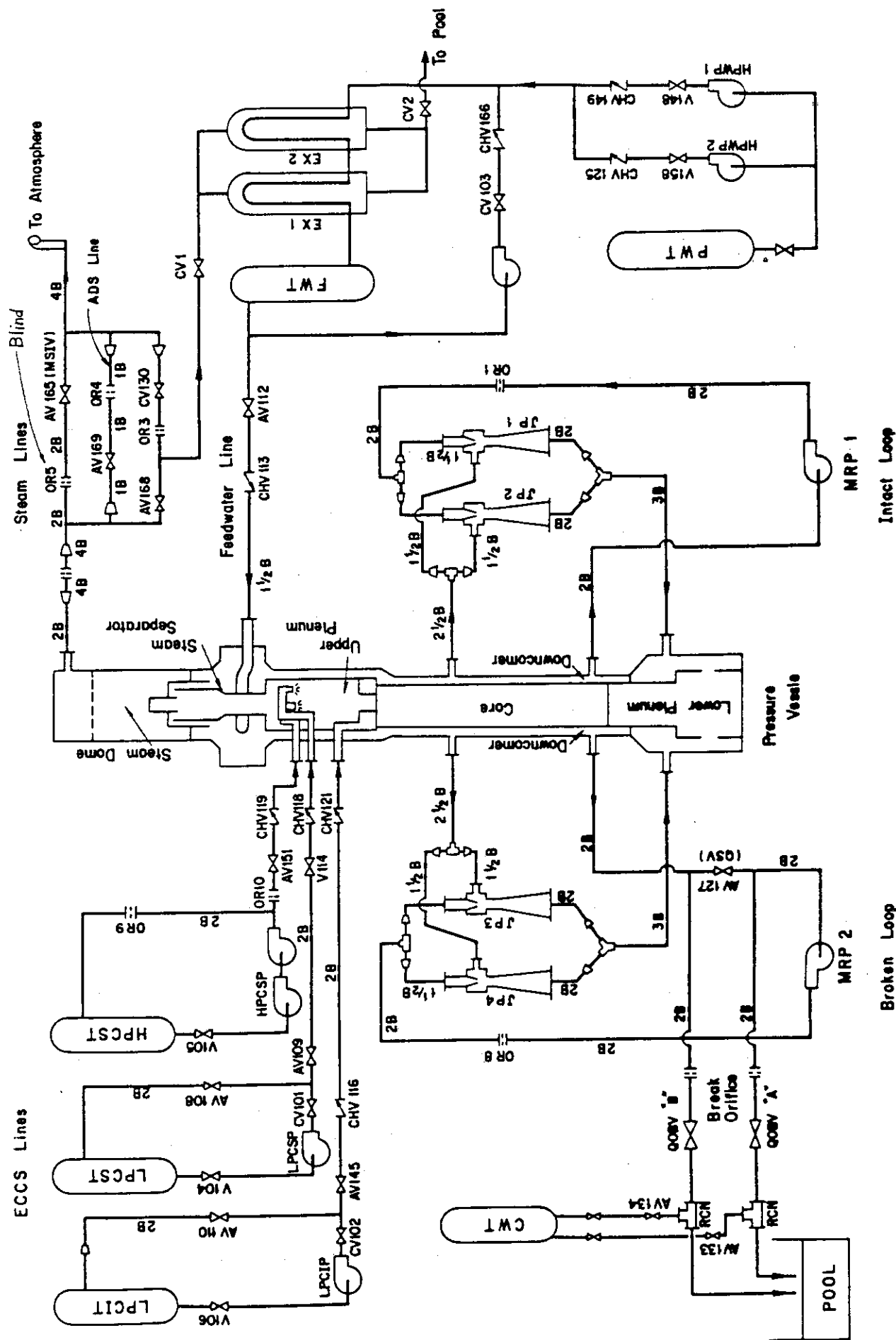


Fig. 2.3 ROSA-III Piping Schematics

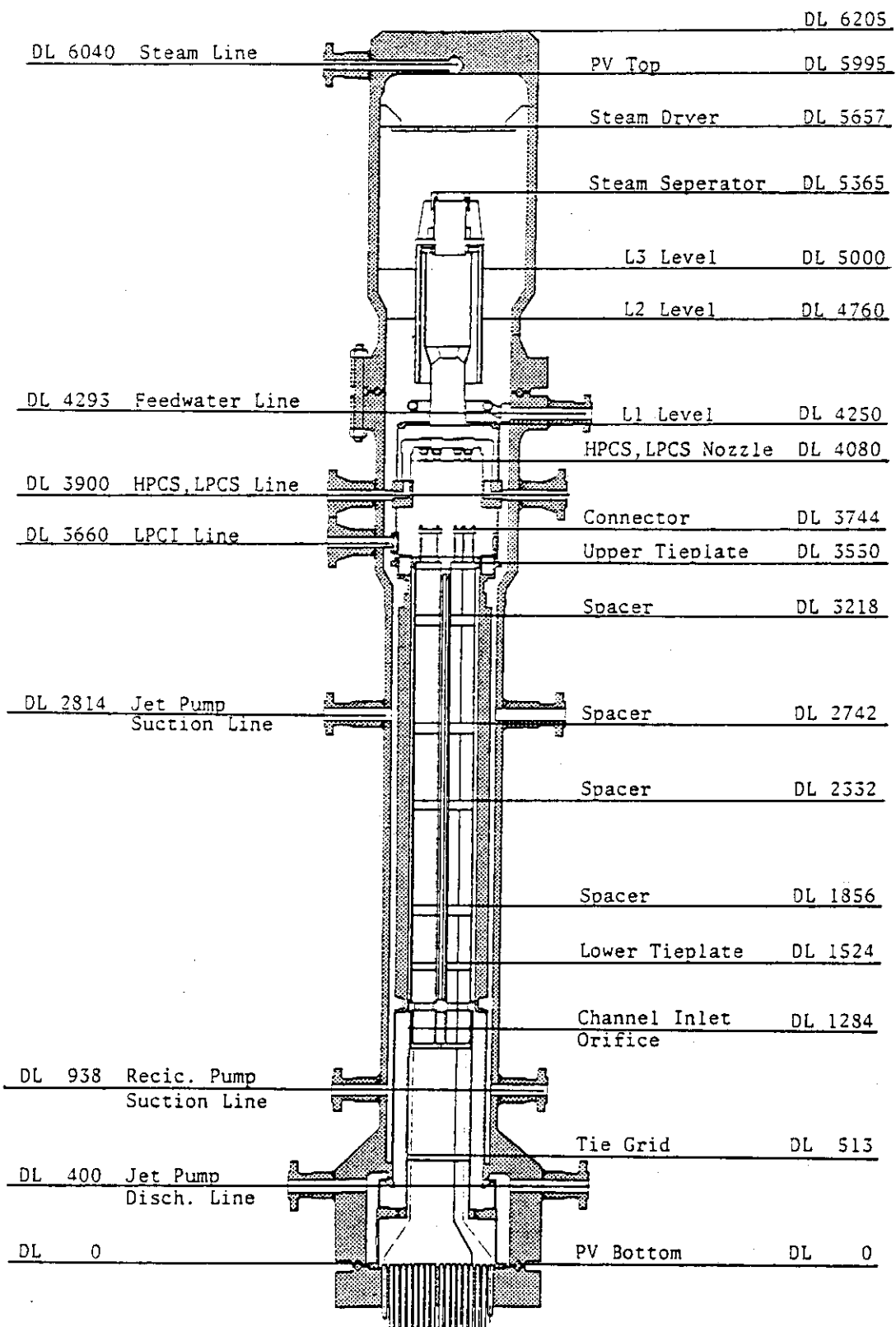
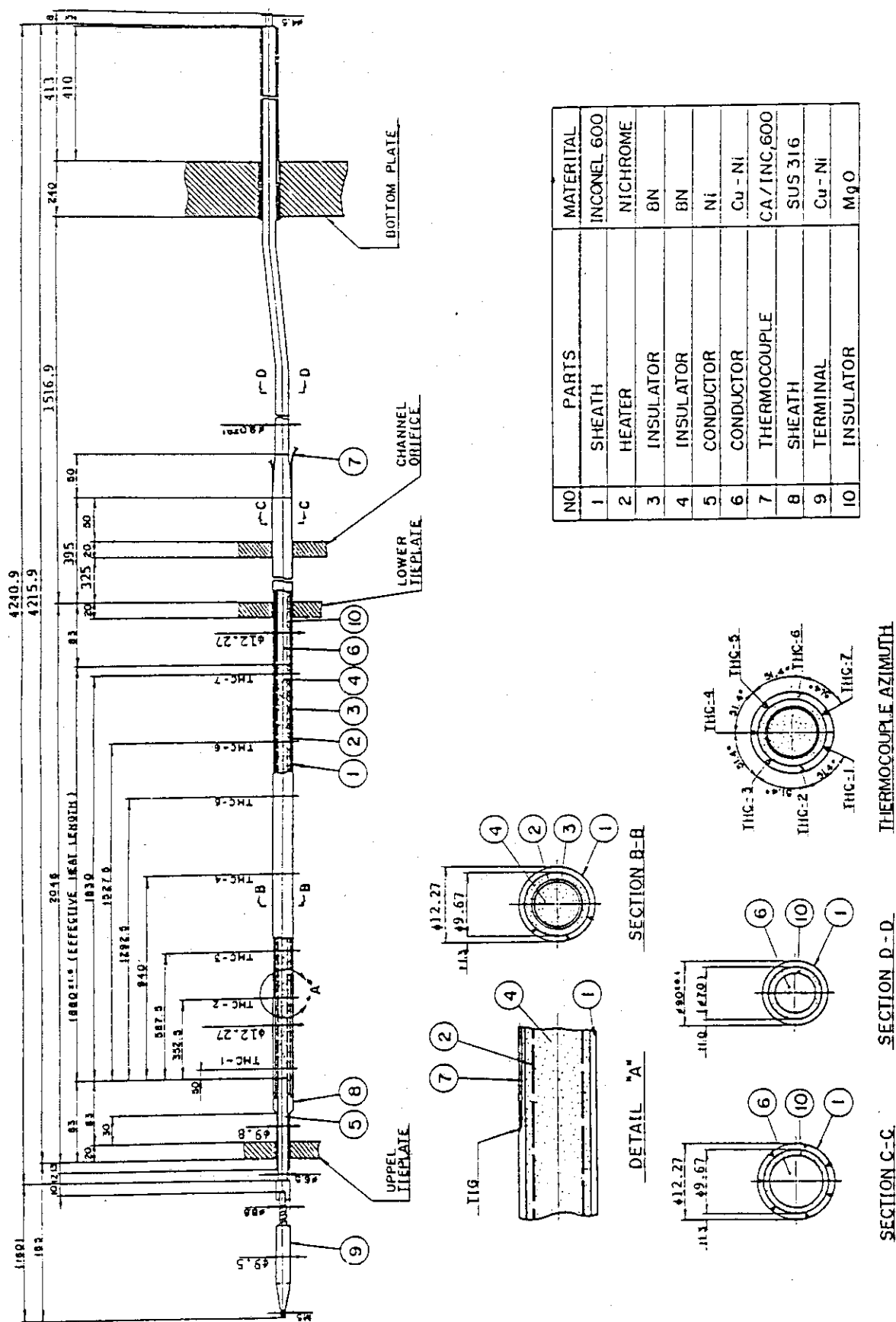
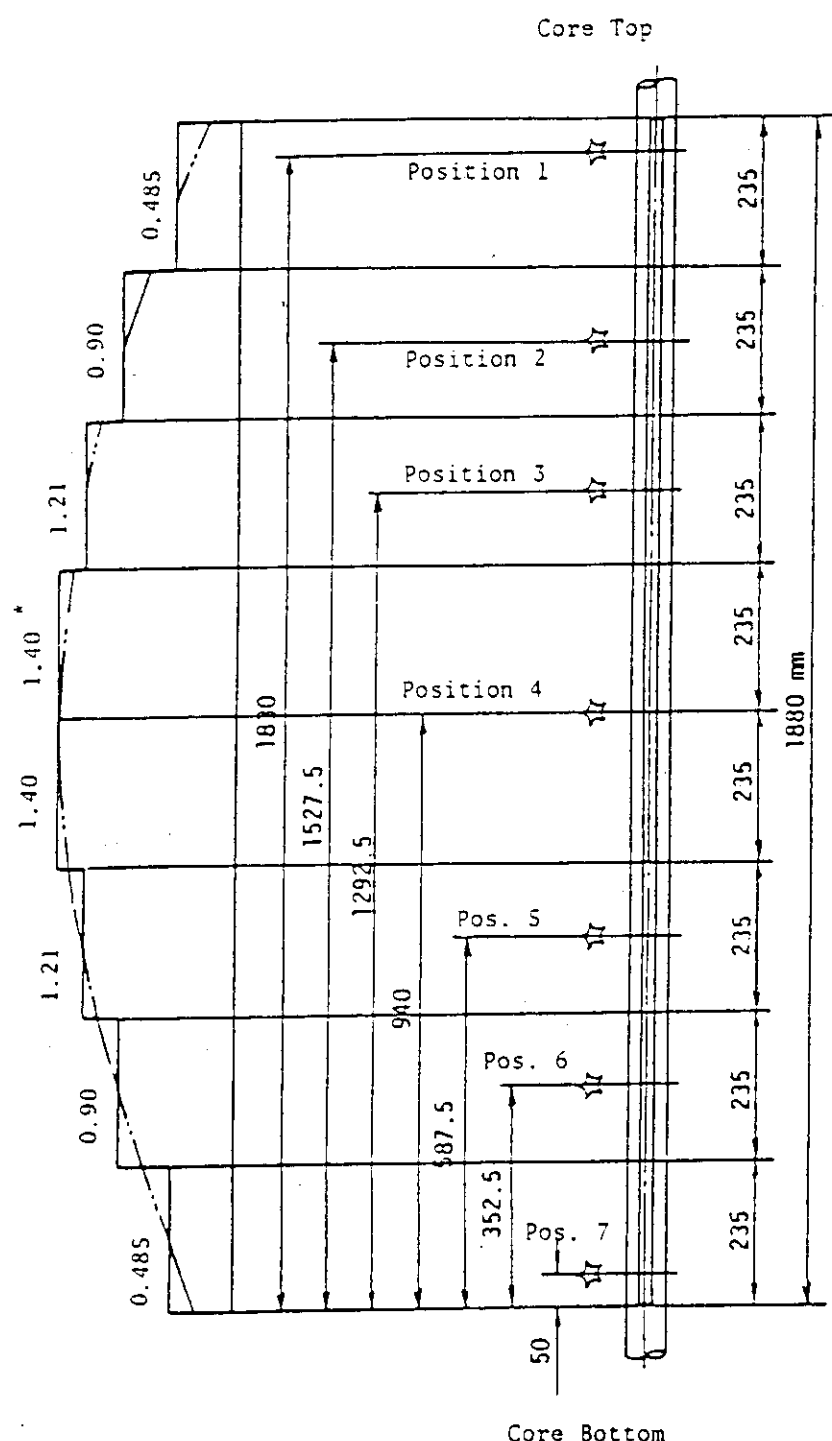


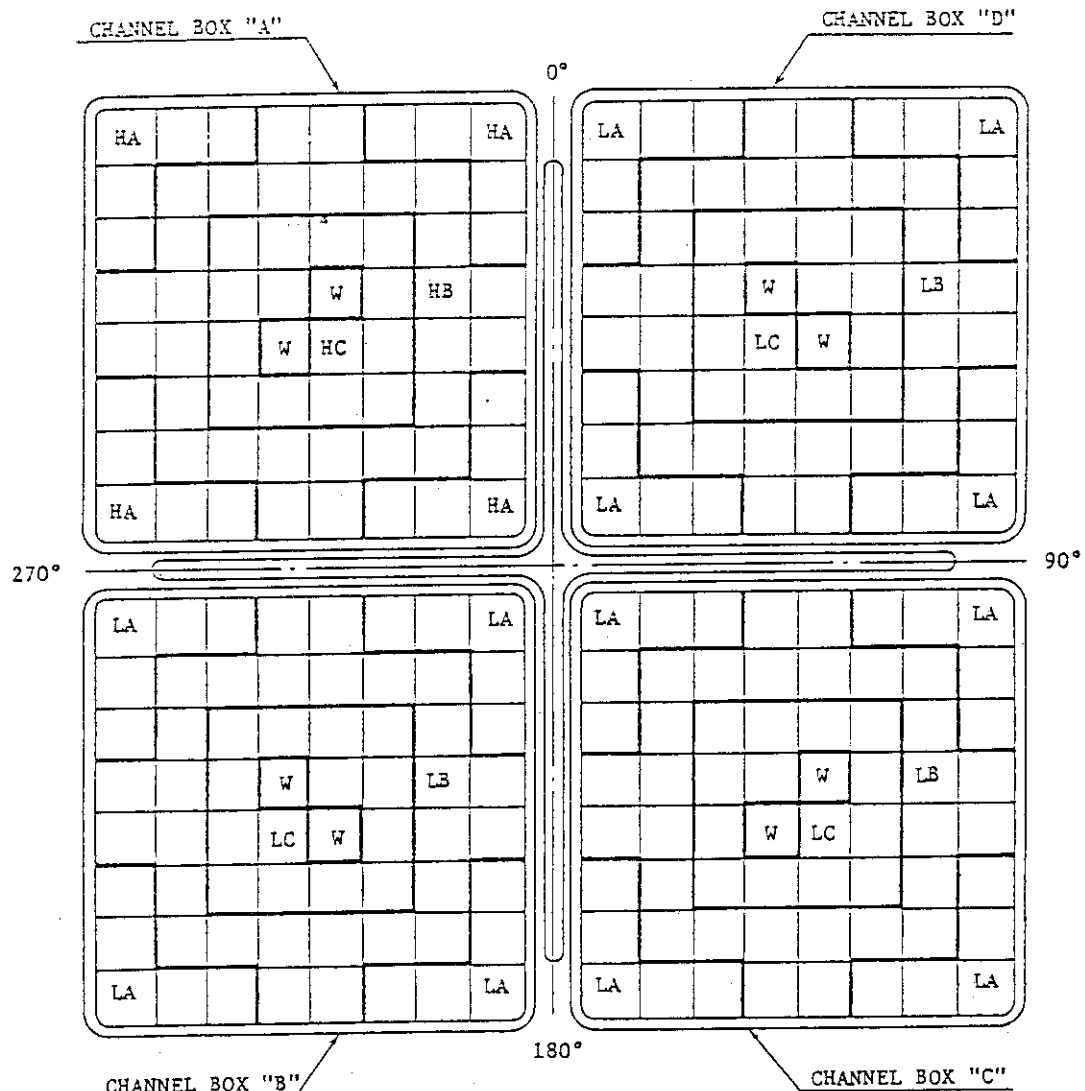
Fig. 2.4 Pressure Vessel Internals Arrangement





☆ Indicates position of thermocouple. * Axial Peaking Factor

Fig.2.6 Axial Power Distribution of Heater Rod



Region	HA	HB	HC	LA	LB	LC	W
Linear Heat Rate (kW/m)	18.5	16.81	14.41	13.21	12.01	10.29	0.0
Local peaking factor	1.1	1.0	0.875	1.1	1.0	0.875	0.0
No. of Rods	20	28	14	60	84	42	8

* note : Radial peaking factor is 1.4

Fig. 2.7 Radial Power Distribution of Core

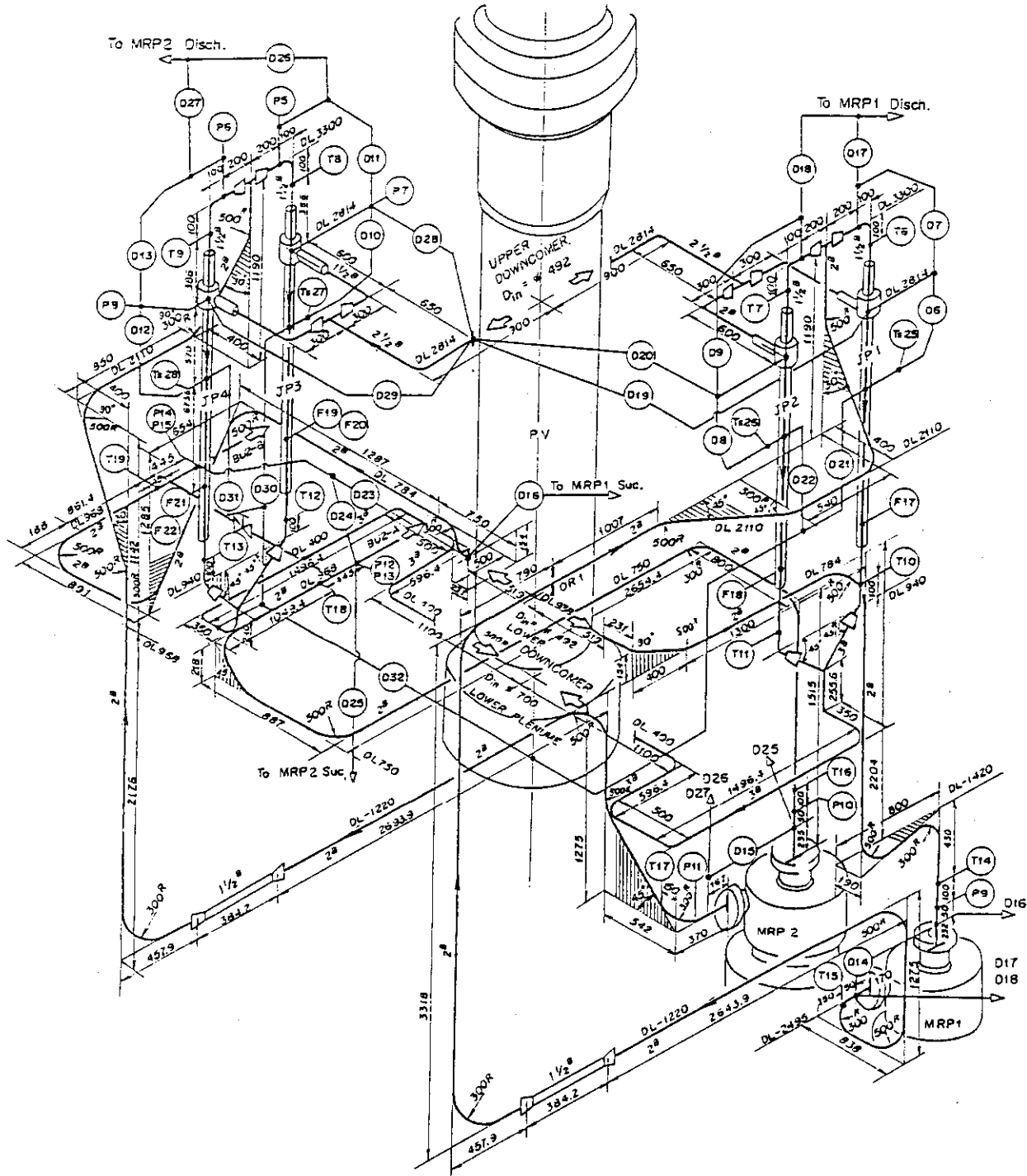


Fig. 2.8 Piping Layout of Recirculation Loops and Jet Pumps

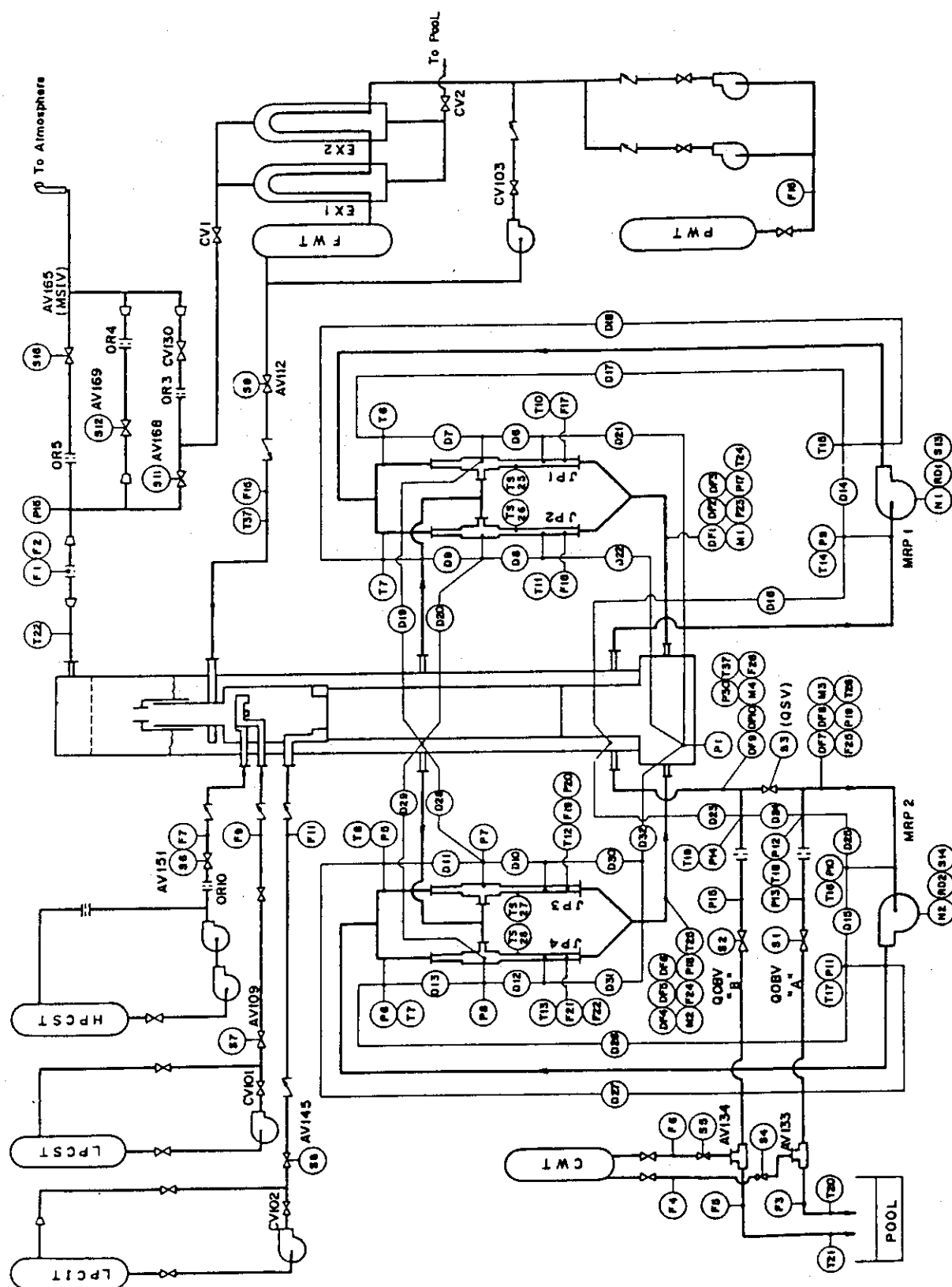


Fig. 3.1 Instrumentation Location of ROSA-III Test Facility

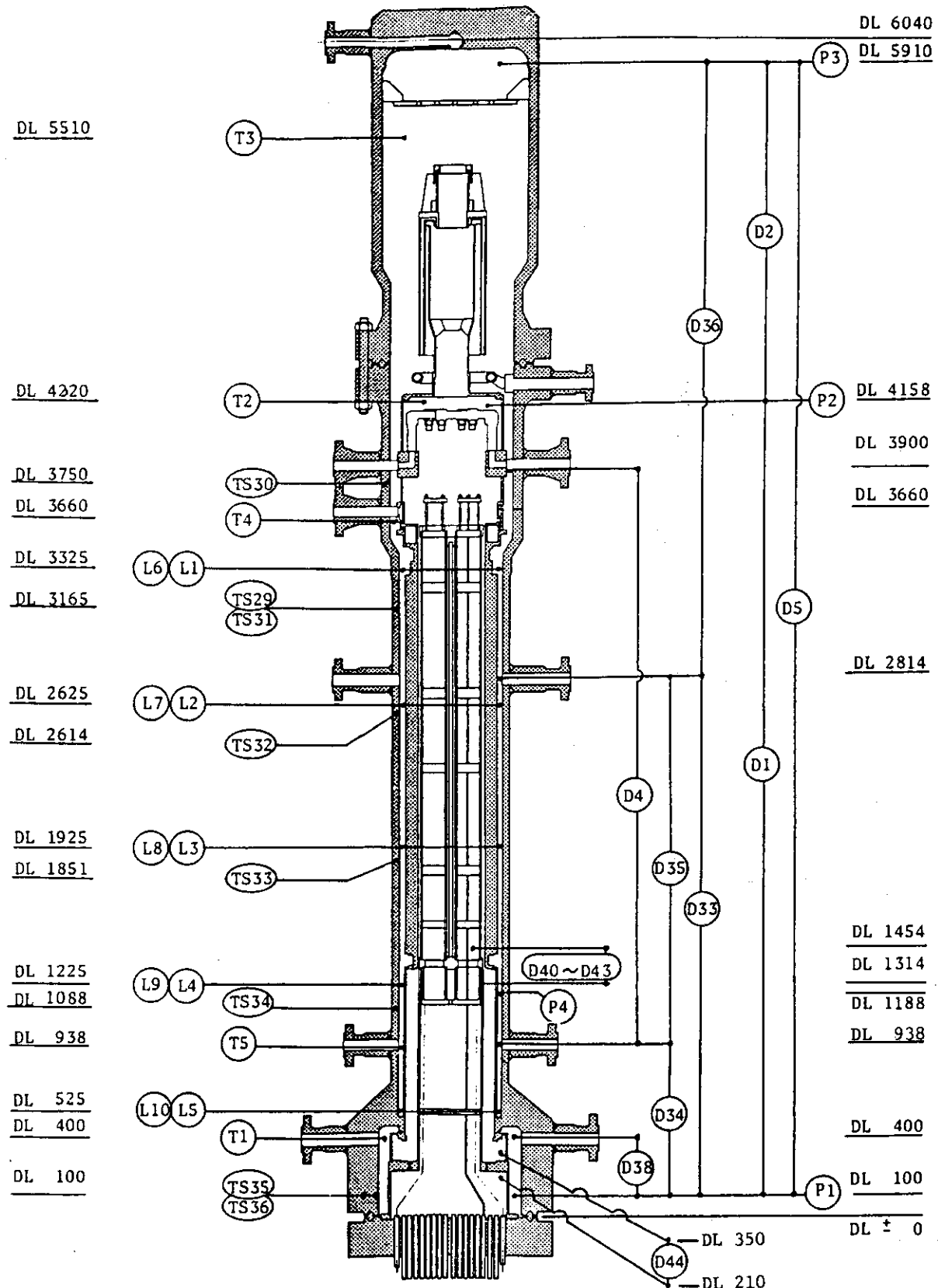


Fig. 3.2 Instrumentation Location in Pressure Vessel

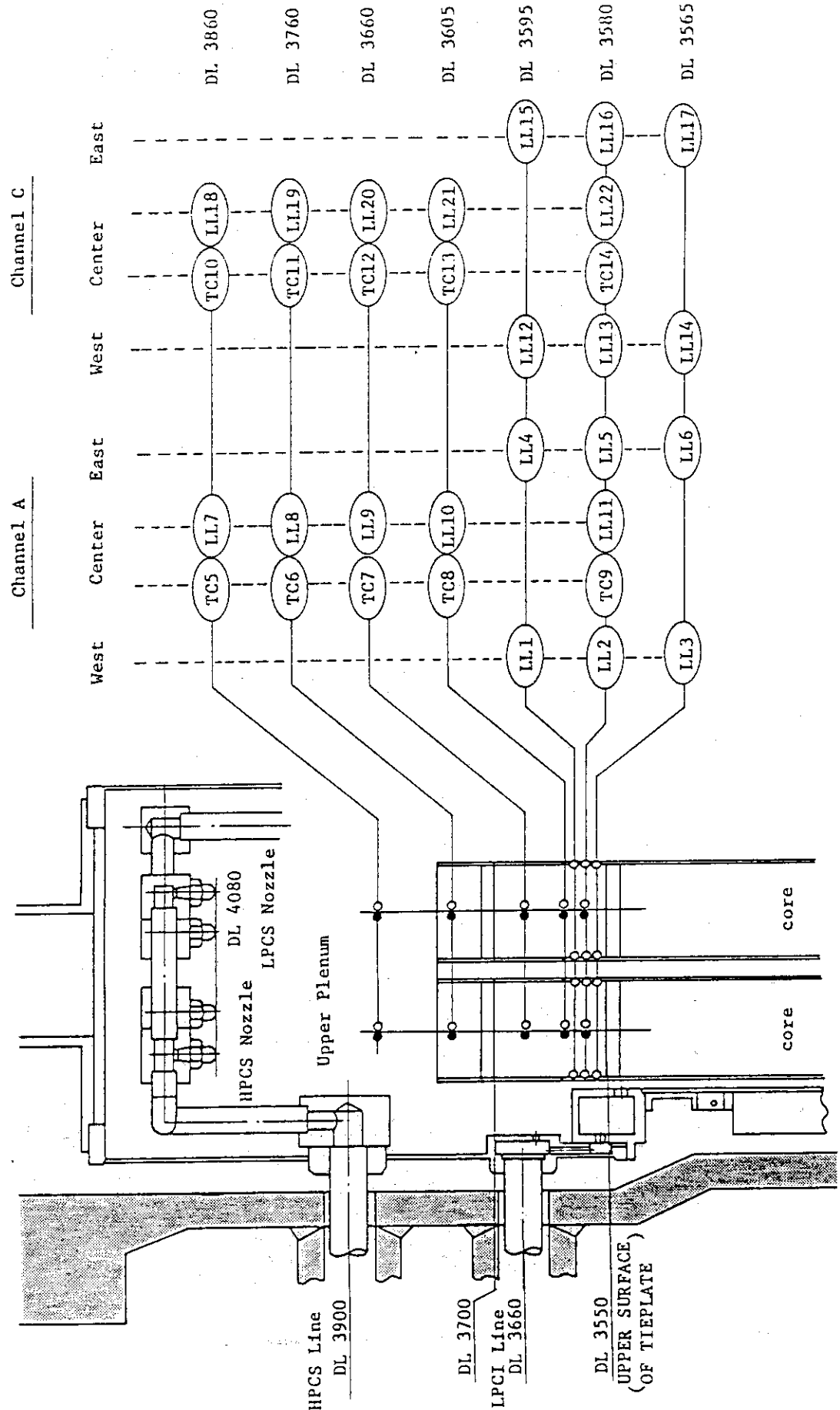


Fig. 3.3 Upper Plenum Instrumentation

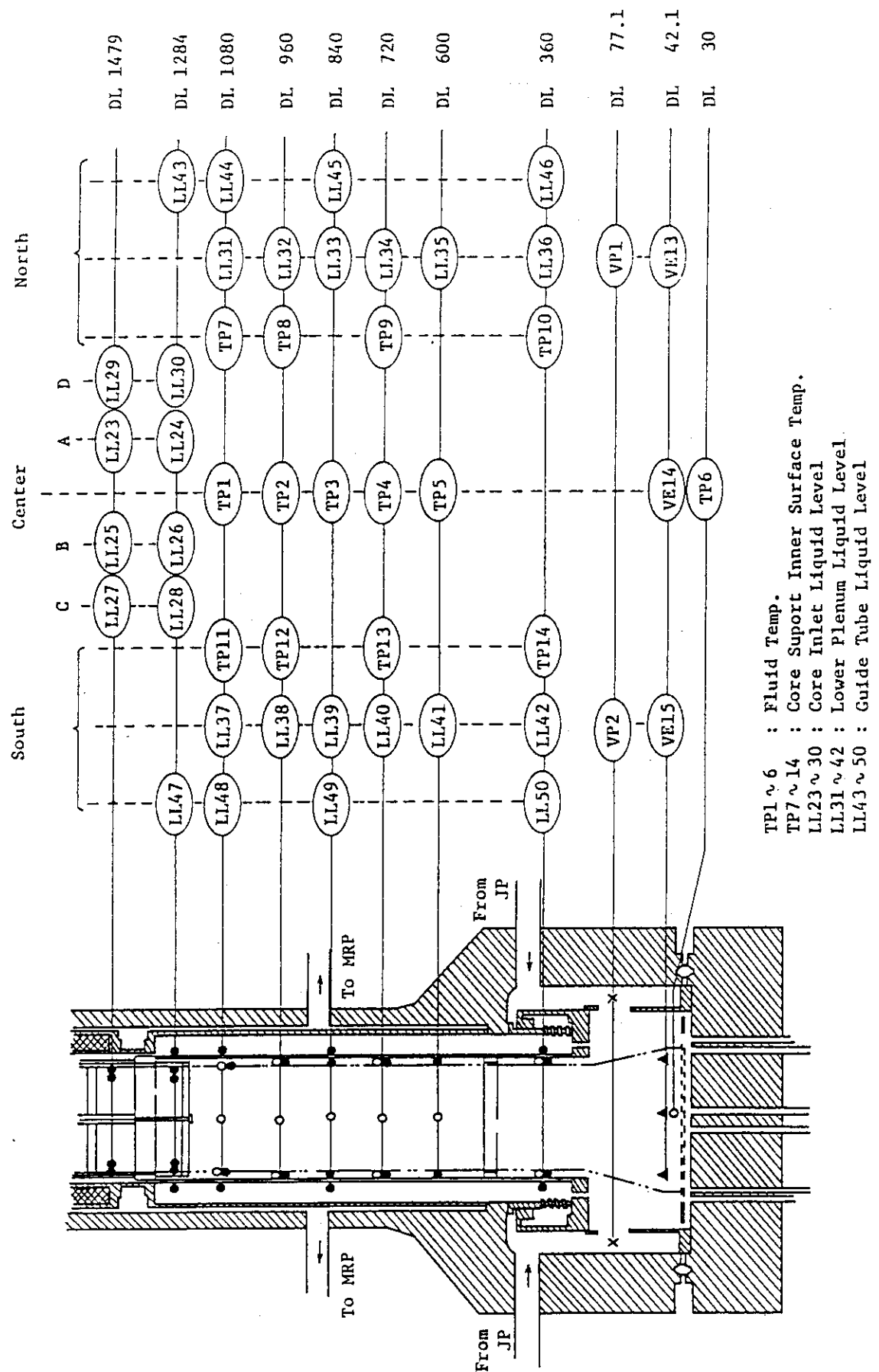
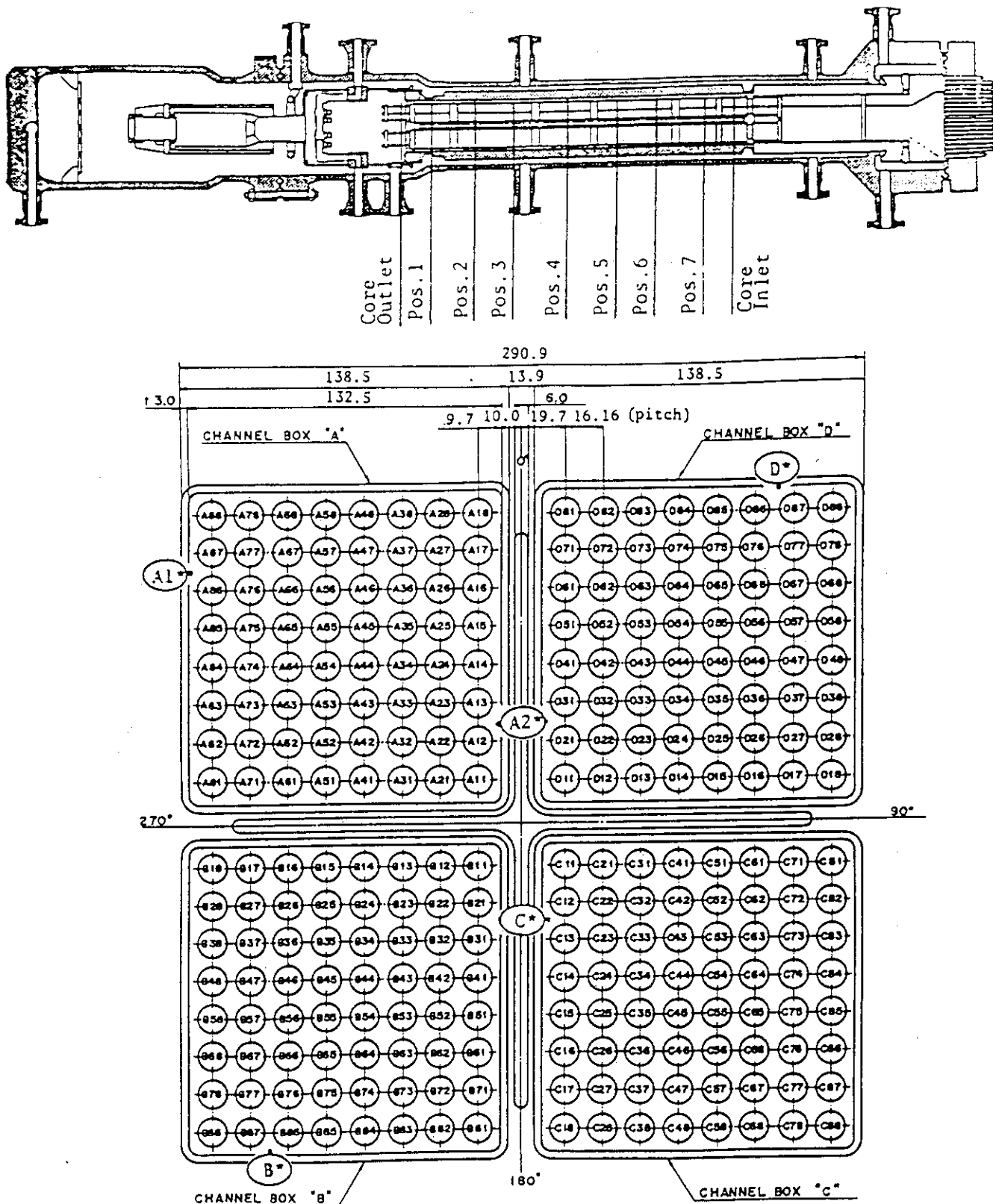


Fig. 3.4 Lower Plenum Instrumentation

TP₁ ~ 6 : Fluid Temp.
 TP₇ ~ 14 : Core Support Inner Surface Temp.
 LL₂₃ ~ 30 : Core Inlet Liquid Level
 LL₃₁ ~ 42 : Lower Plenum Liquid Level
 LL₄₃ ~ 50 : Guide Tube Liquid Level



Heater rod O.D. is 12.27mm

A54, B54, C54 and D54 are water rod simulators with void probes,
O.D. = 15.01mm

A45, B45, C45 and D45 are water rod simulators with thermocouples,
O.D. = 15.01mm

Fig. 3.5 Core Instrumentation (cf. Table 3.3)

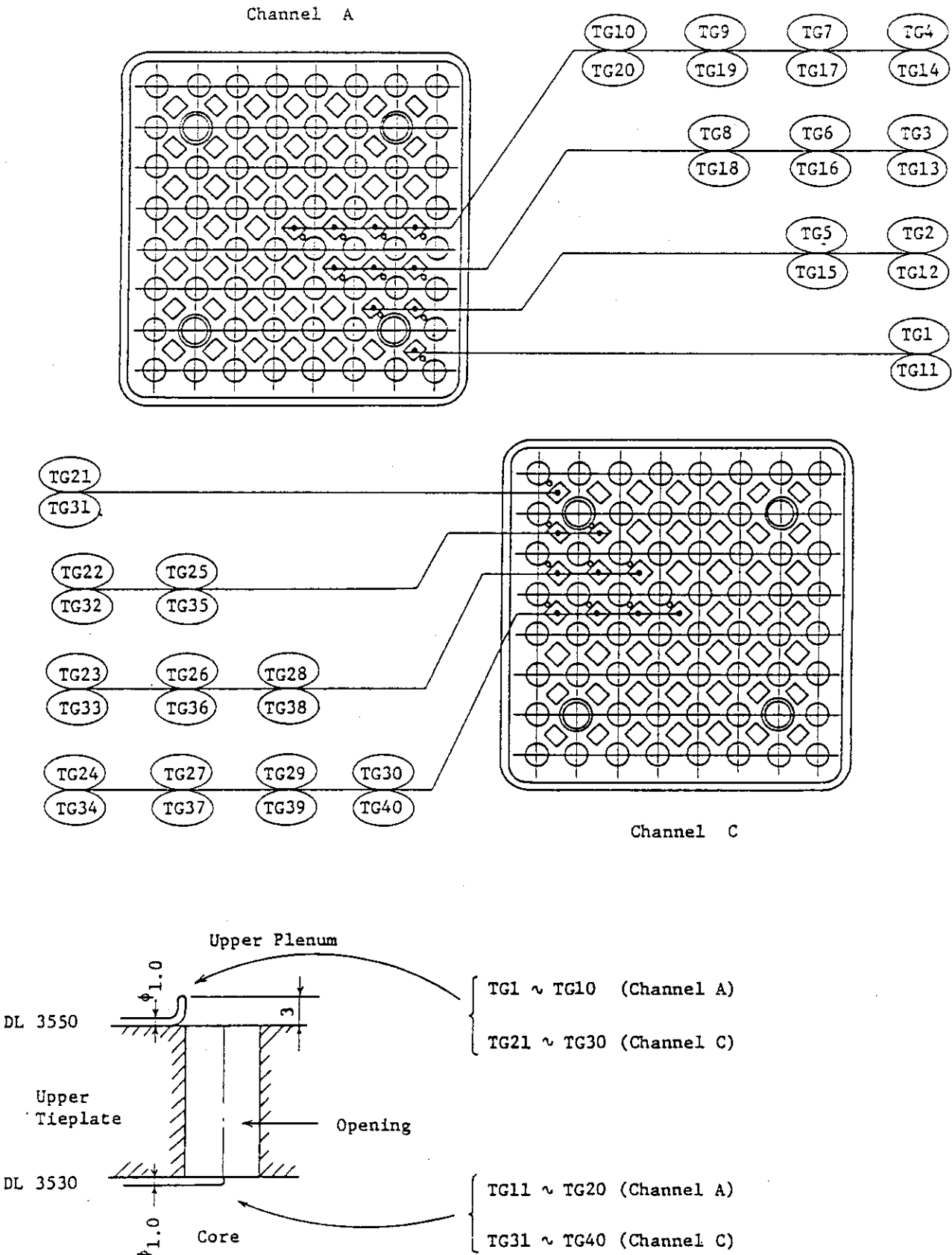


Fig. 3.6 Upper Tieplate Instrumentation

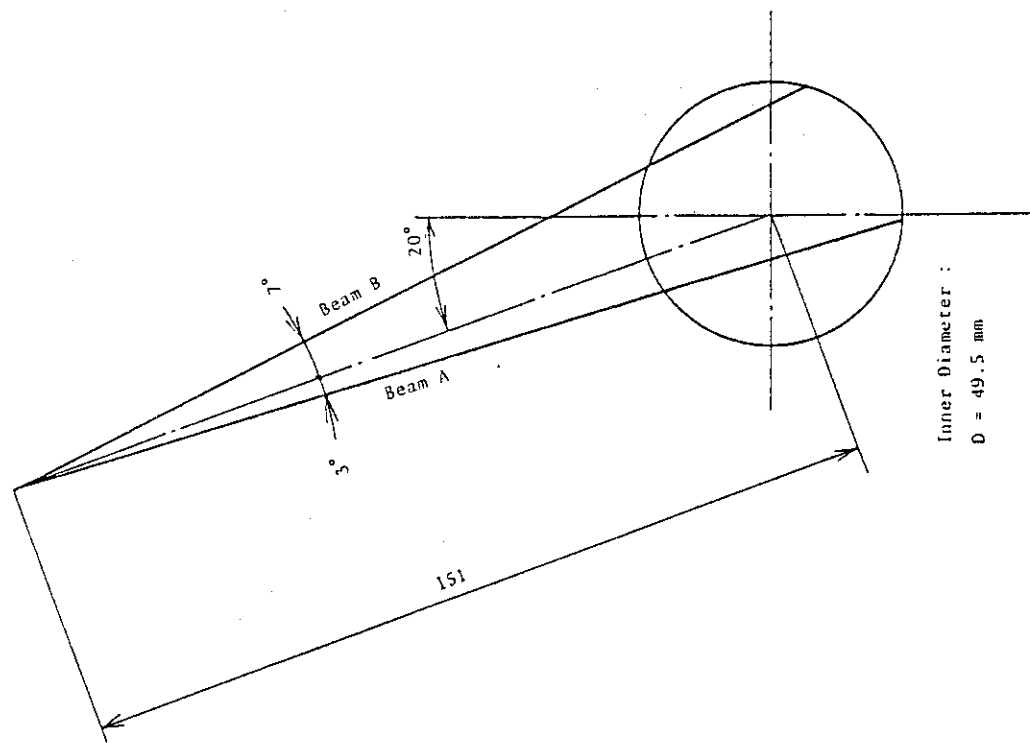


Fig. 3.8 Beam Directions of Two-Beam
Gamma Densitometer

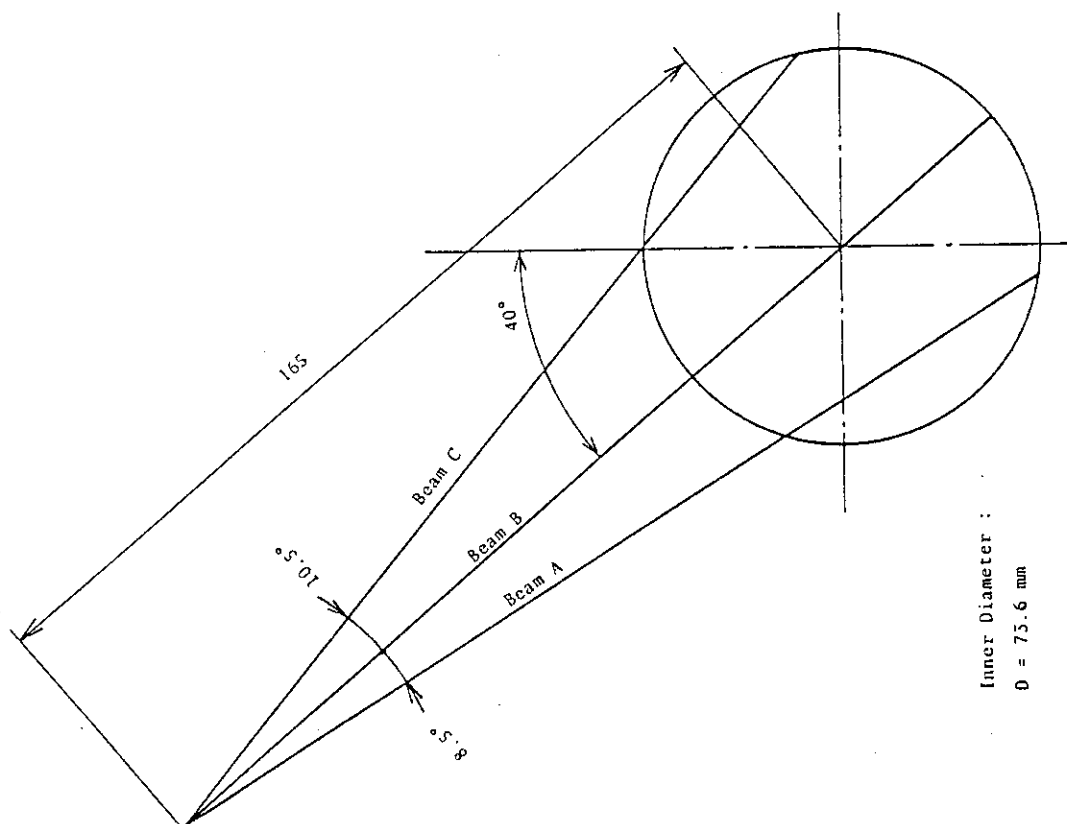
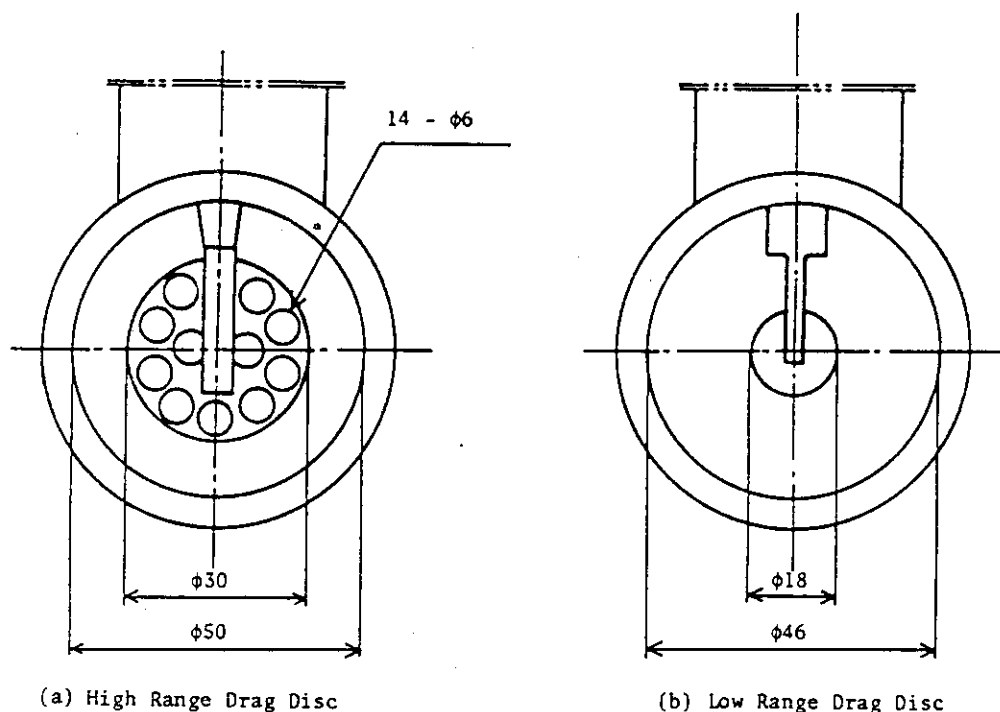
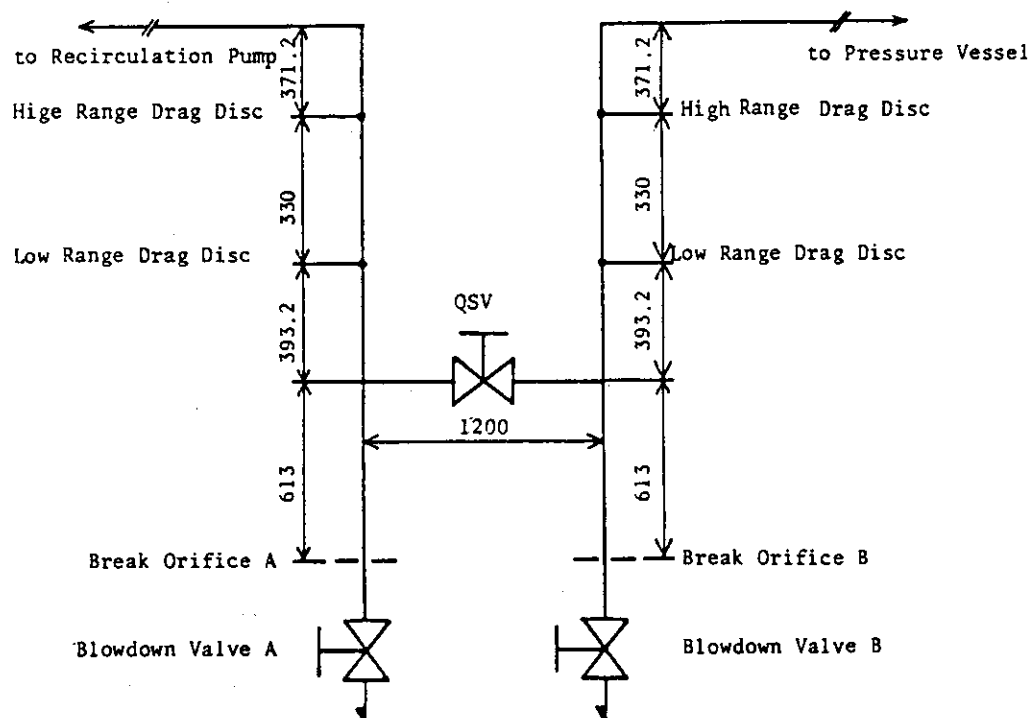


Fig. 3.7 Beam Directions of Three-Beam
Gamma Densitometer



(a) High Range Drag Disc

(b) Low Range Drag Disc



(c) Location of Drag Discs

Fig. 3.9 Arrangement and Location of Drag Disks

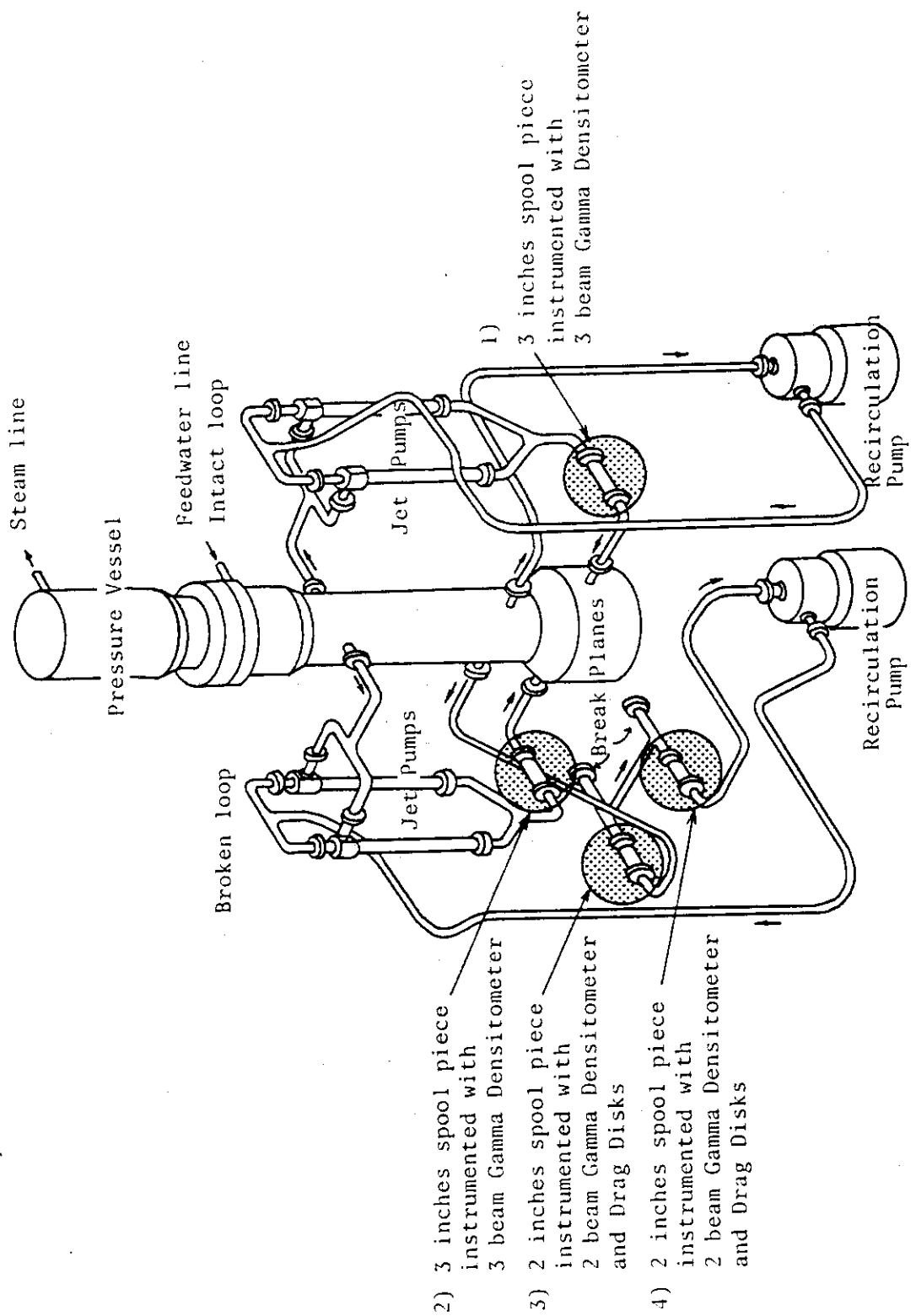


Fig. 3.10 Location of Two-Phase Flow Measurement Spool Pieces

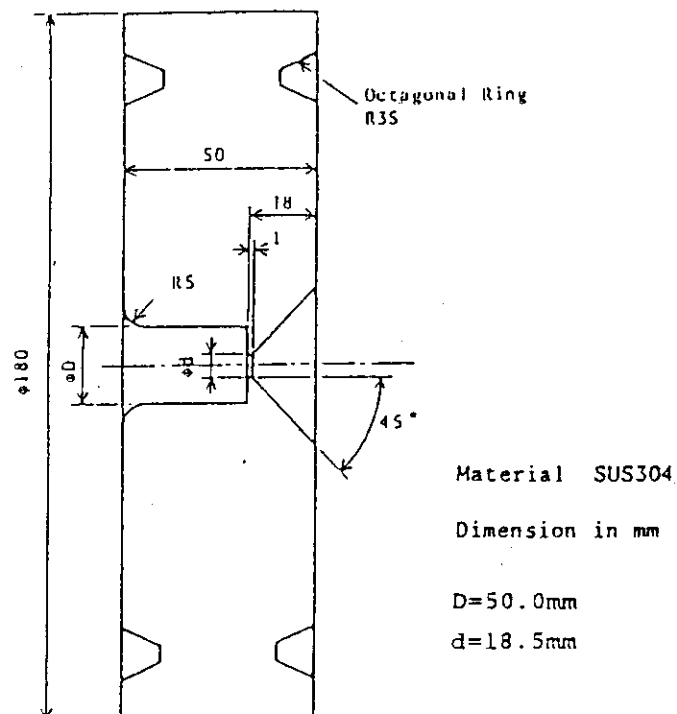


Fig. 4.1 Break configuration details

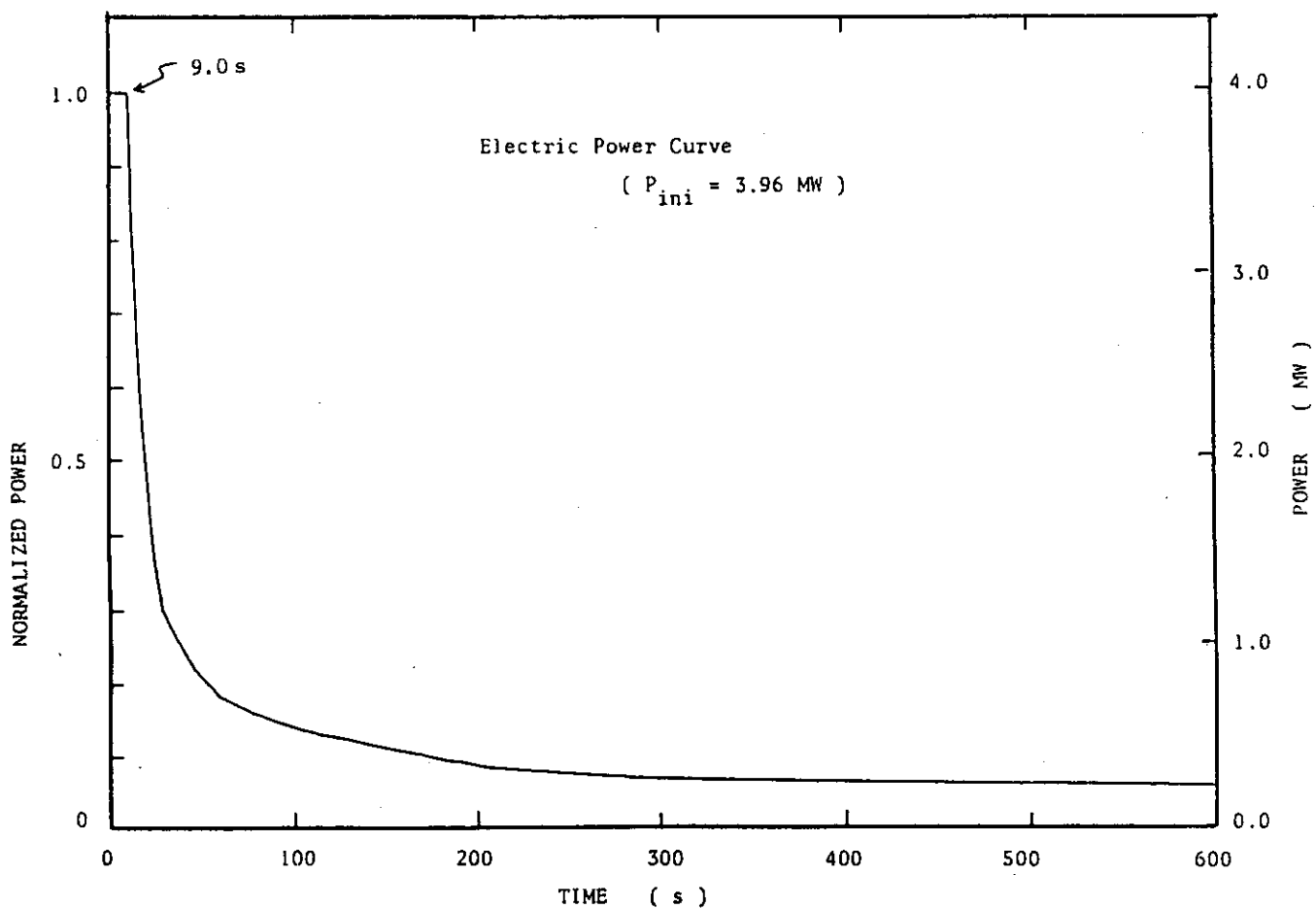


Fig. 4.2 Normalized Poewr Transient for ROSA-III Test

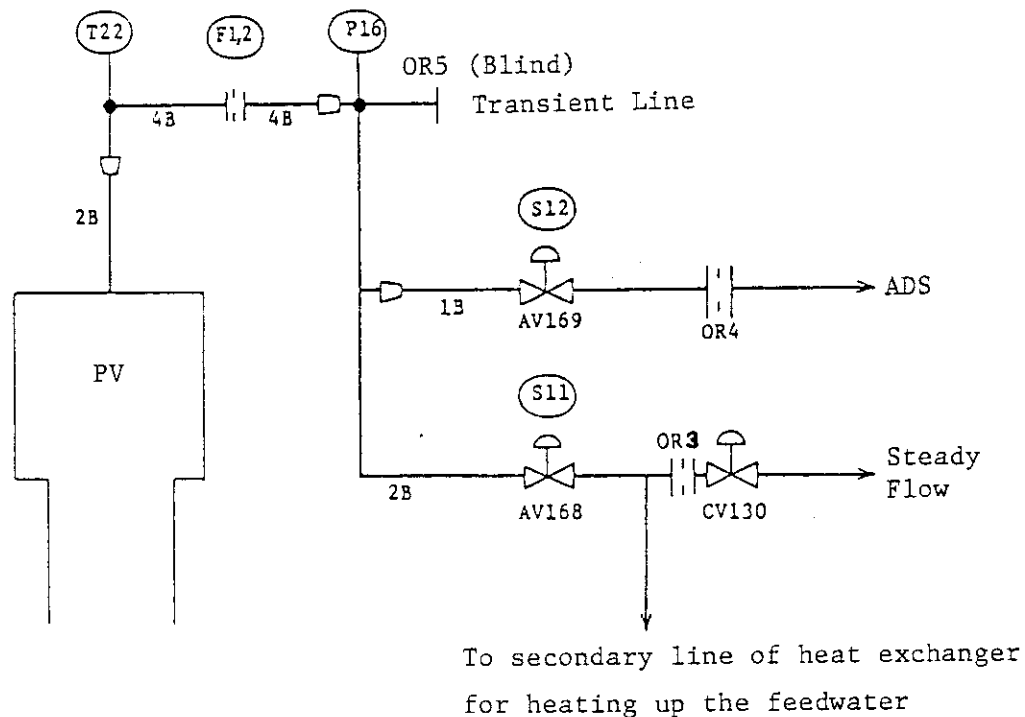


Fig. 4.3 Main Steam Line Schematic

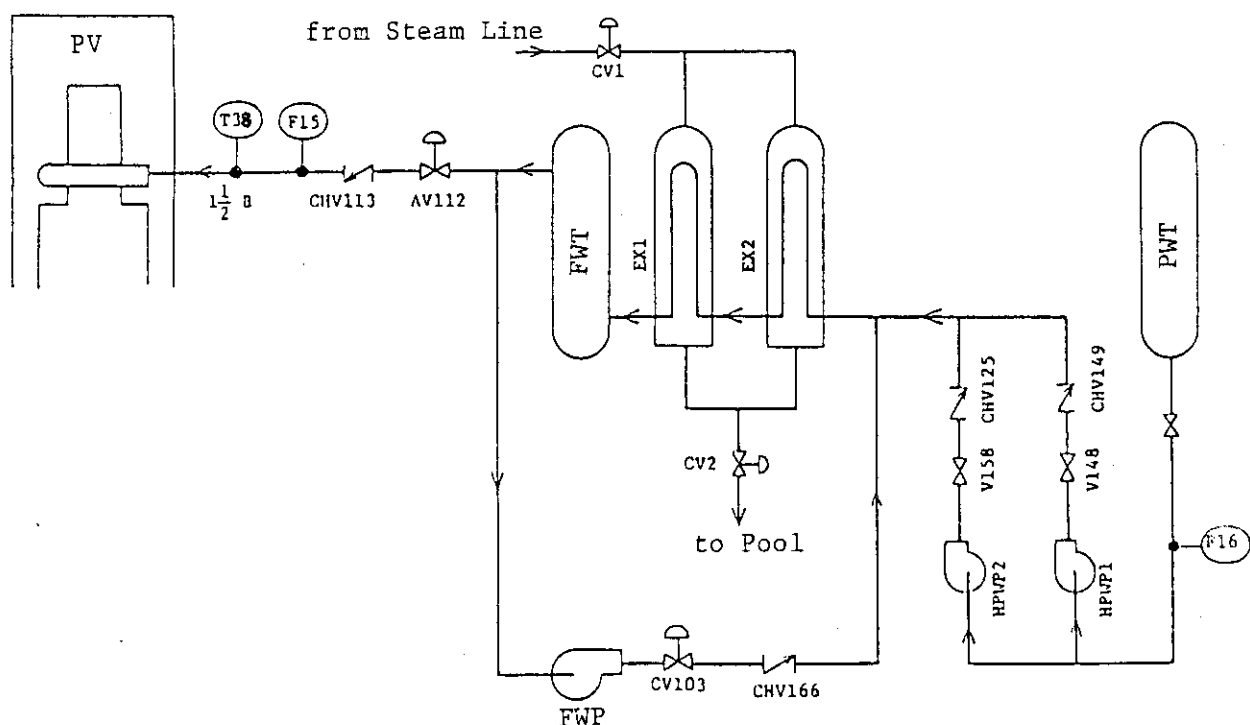


Fig. 4.4 Feedwater Line Schematic

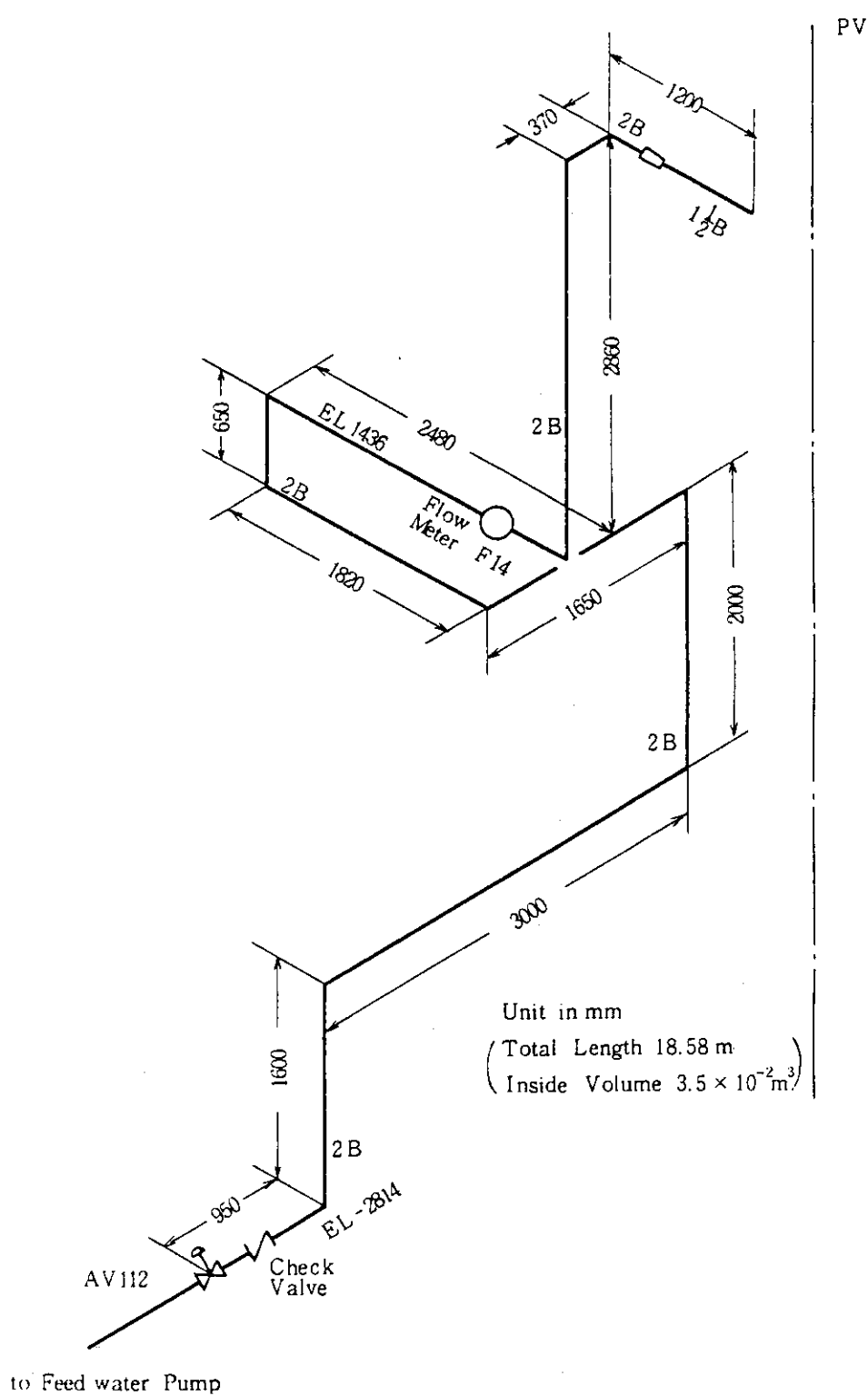


Fig. 4.5 Feedwater Line between Valve AV-112 and Pressure Vessel

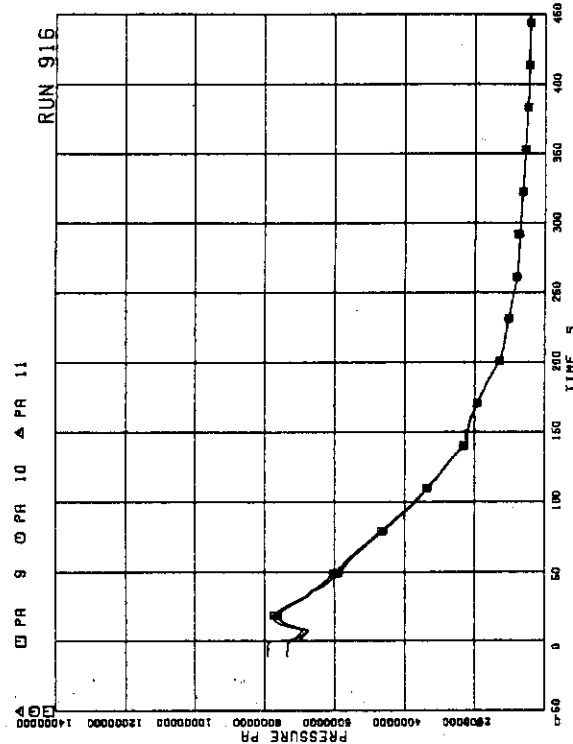


FIG. 5. 1 PRESSURE IN PV (PRESSURE VESSEL)

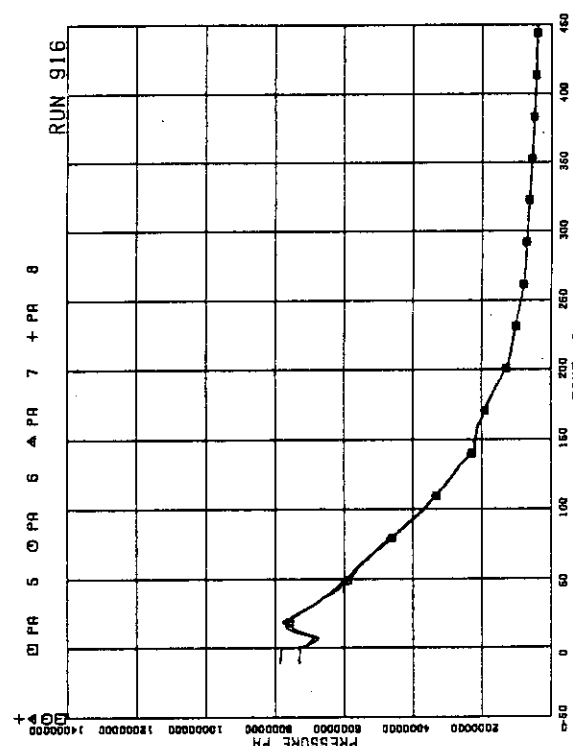


FIG. 5. 2 PRESSURE IN BROKEN LOOP JP (JET PUMP)

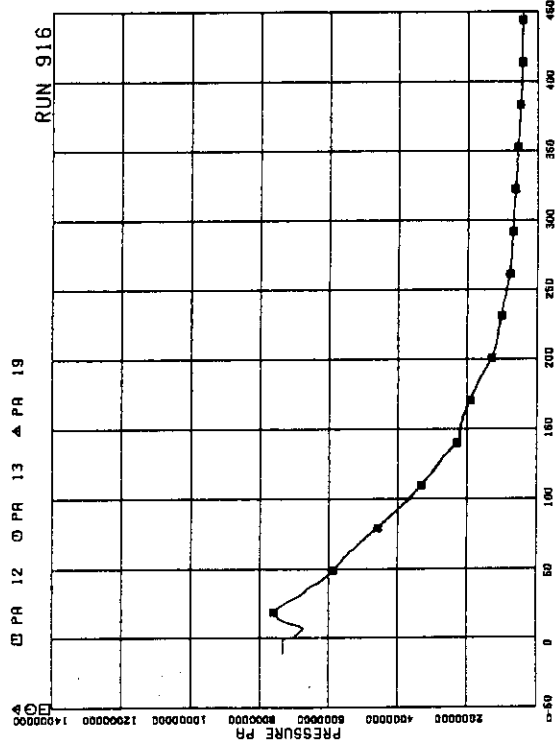


FIG. 5. 3 PRESSURE NEAR MRP
(MAIN RECIRCULATION PUMP)

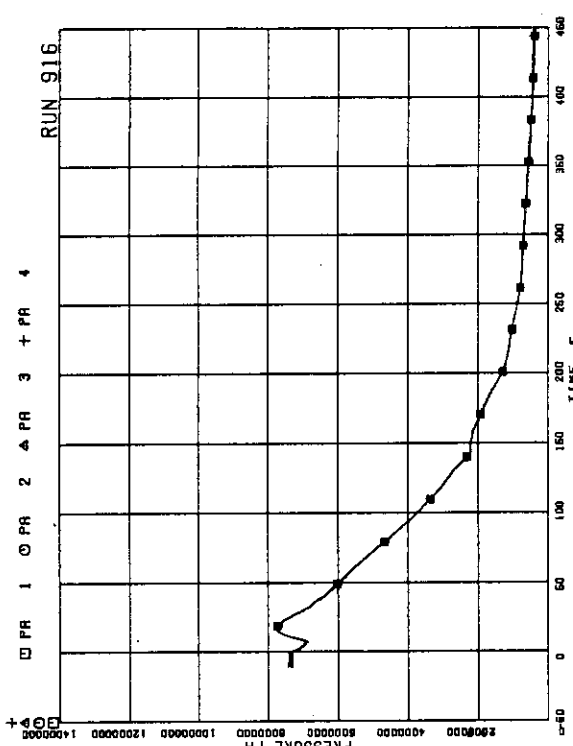


FIG. 5. 4 PRESSURE AT MRP SIDE OF BREAK

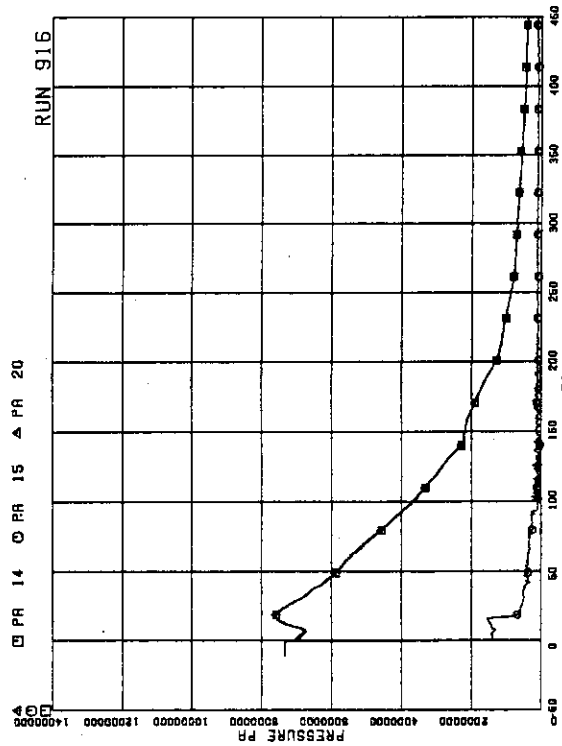


FIG. 5. PRESSURE AT PV SIDE OF BREAK

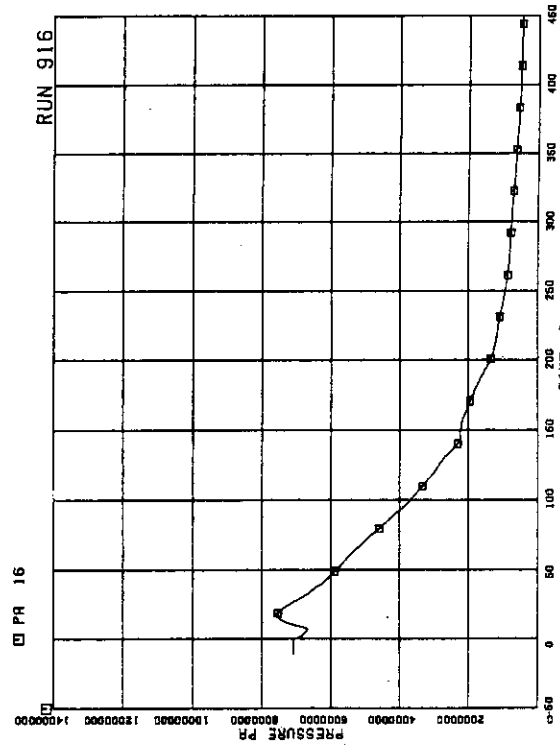


FIG. 5. 6. PRESSURE IN MSL (MAIN STEAM LINE)

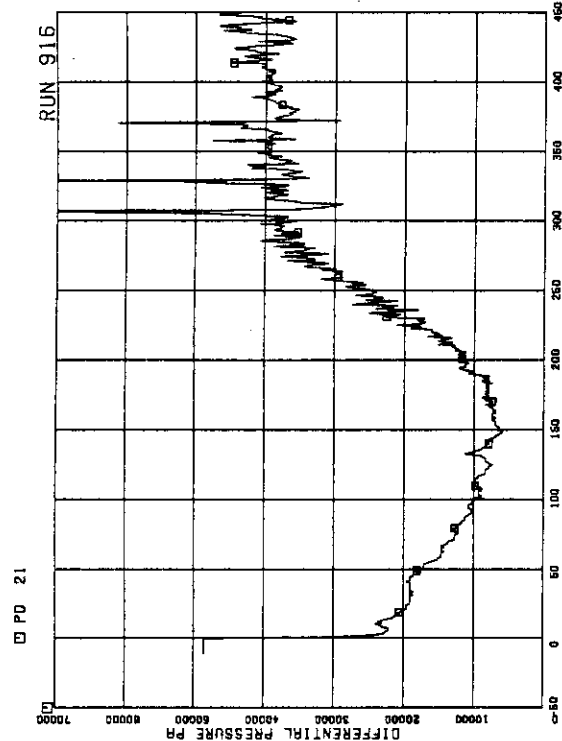


FIG. 5. 7. DIFFERENTIAL PRESSURE BETWEEN LOWER PLENUM AND UPPER PLENUM

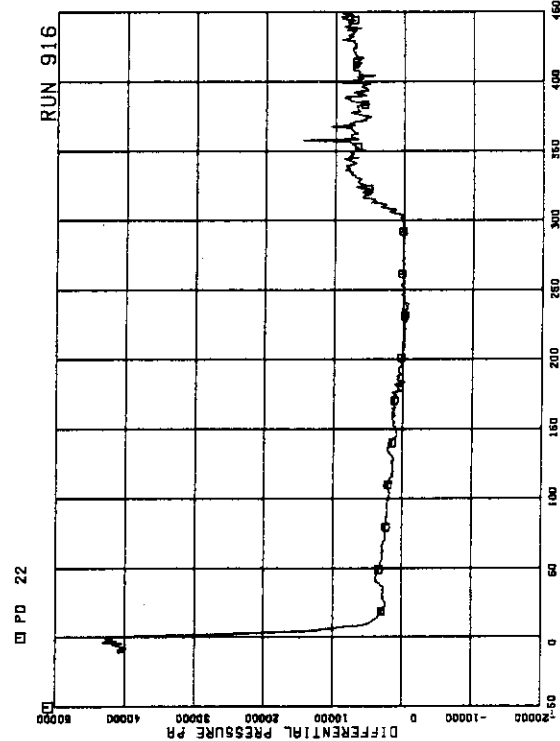


FIG. 5. 8. DIFFERENTIAL PRESSURE BETWEEN UPPER PLENUM AND STEAM DOME

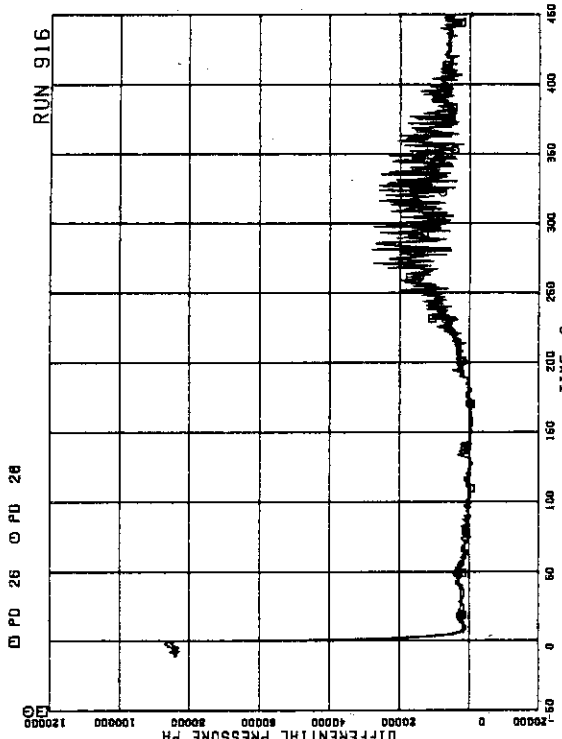


FIG. 5. 11 DIFFERENTIAL PRESSURE BETWEEN
JP-1,2 DISCHARGE AND SUCTION

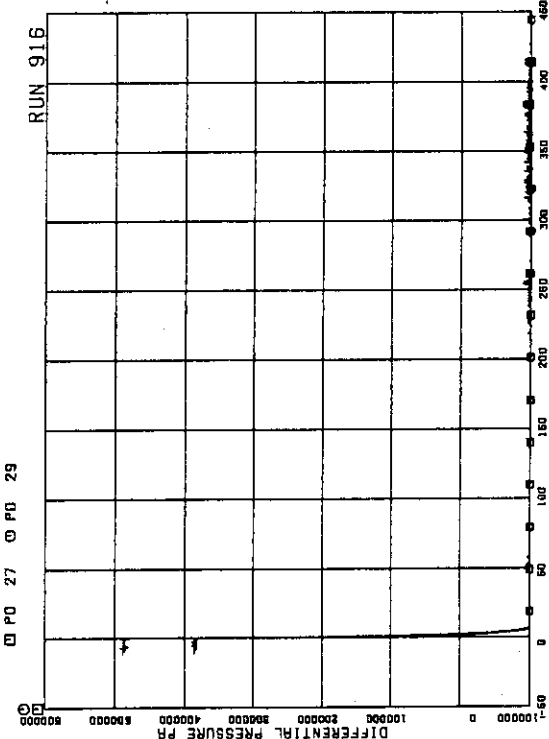


FIG. 5. 12 DIFFERENTIAL PRESSURE BETWEEN
JP-1,2 DRIVE AND SUCTION

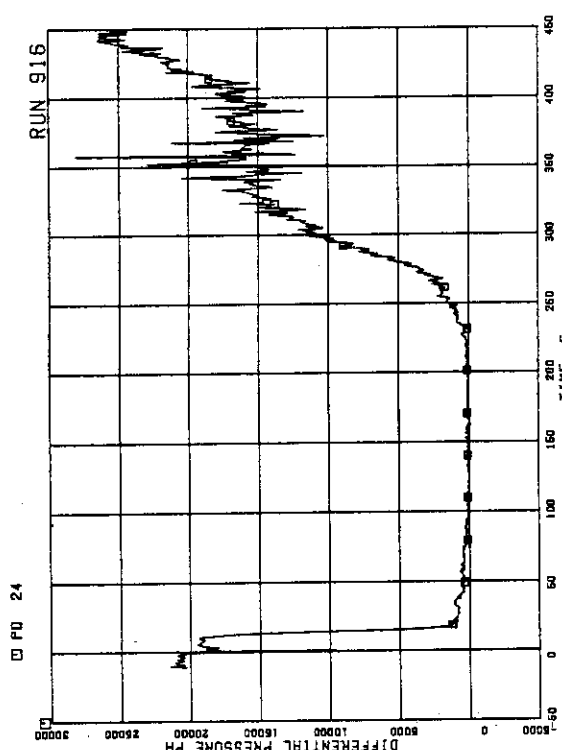


FIG. 5. 9 DC (DOWNCOMER) HEAD

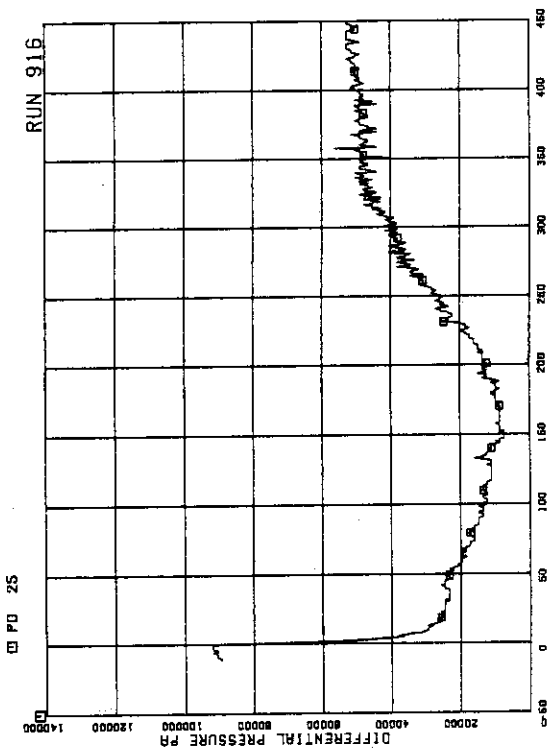


FIG. 5. 10 DIFFERENTIAL PRESSURE BETWEEN
PV BOTTOM AND TOP

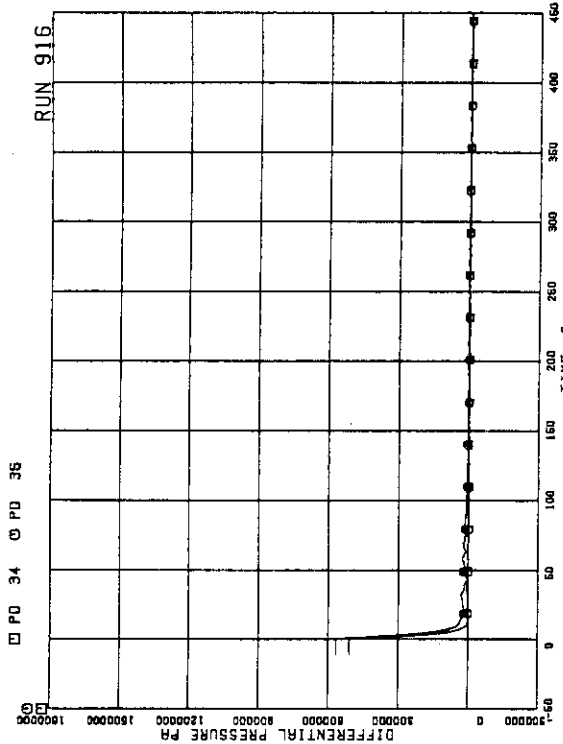


FIG. 5. 15 DIFFERENTIAL PRESSURE BETWEEN
MRP DELIVERY AND SUCTION

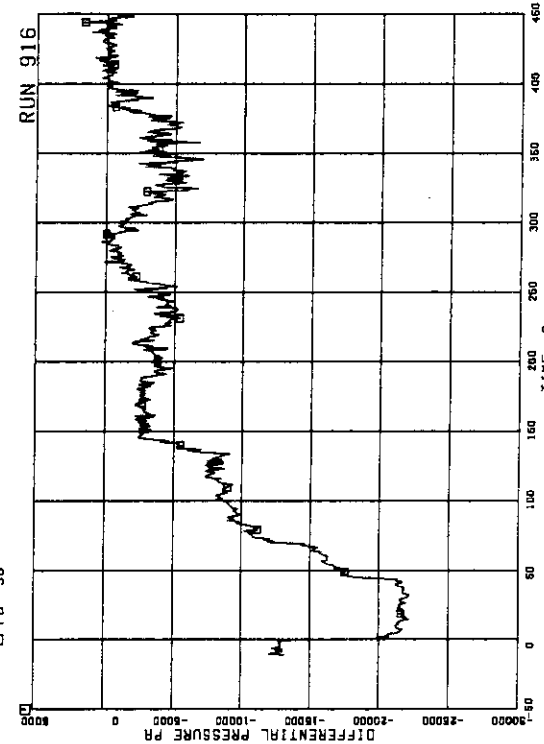


FIG. 5. 16 DIFFERENTIAL PRESSURE BETWEEN
DOWNCOMER BOTTOM AND MRP1 SUCTION

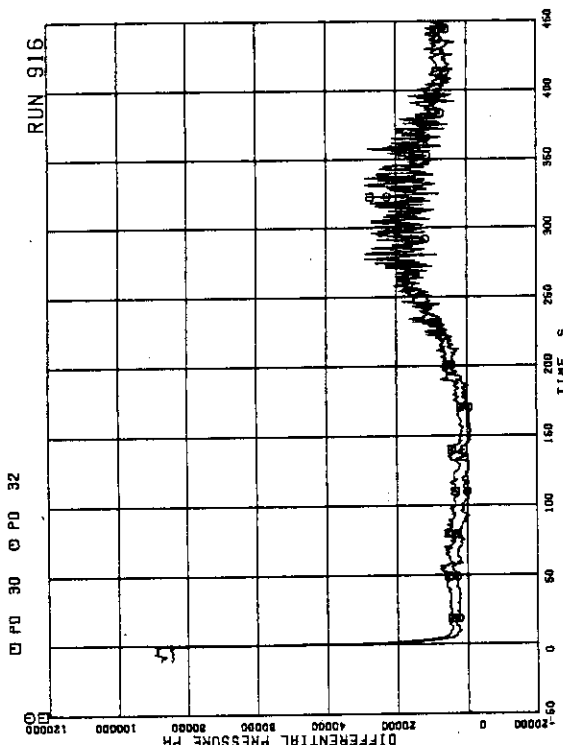


FIG. 5. 13 DIFFERENTIAL PRESSURE BETWEEN
JP-3,4 DISCHARGE AND SUCTION

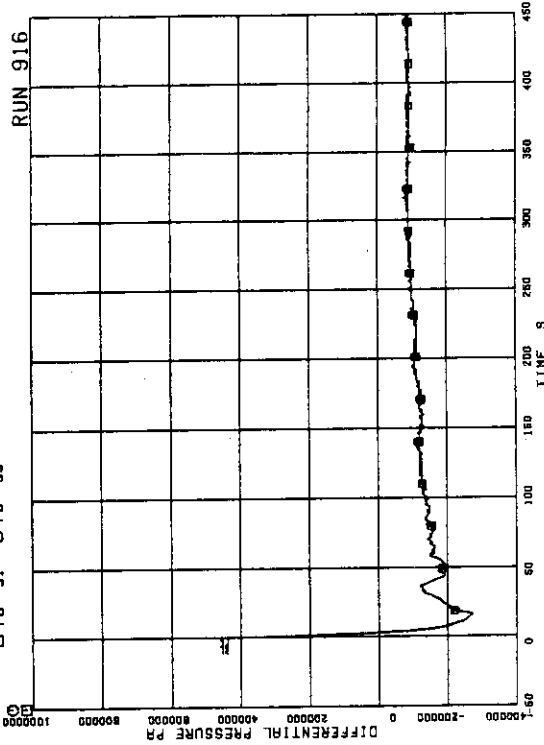


FIG. 5. 14 DIFFERENTIAL PRESSURE BETWEEN
JP-3,4 DRIVE AND SUCTION

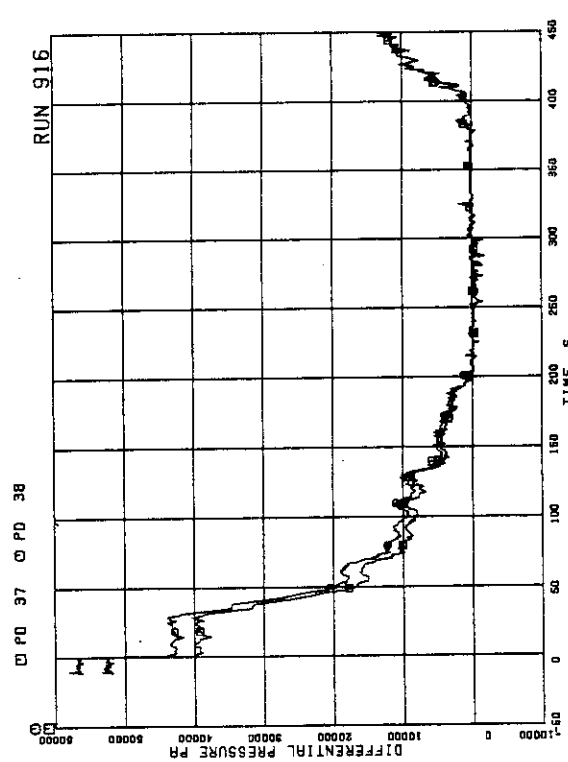


FIG. 5. 17 DIFFERENTIAL PRESSURE BETWEEN
MRP DELIVERY AND JP-1.2 DRIVE

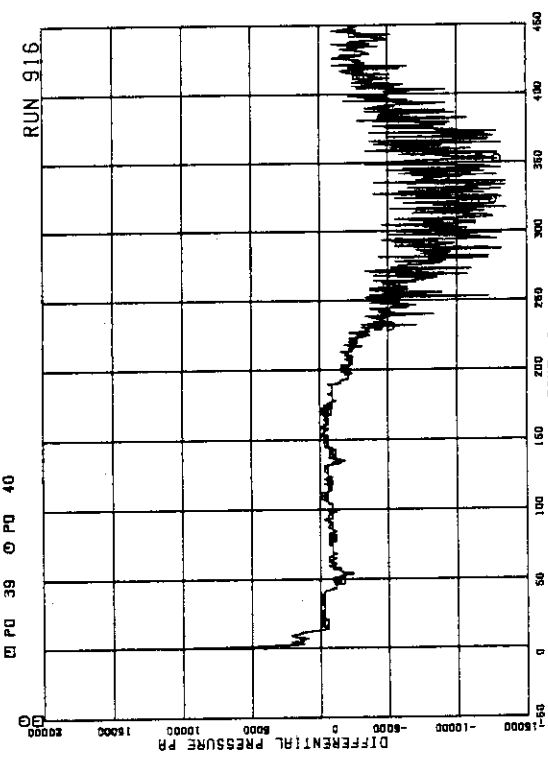


FIG. 5. 18 DIFFERENTIAL PRESSURE BETWEEN
DOWNCOMER MIDDLE AND JP-1.2 SUCTION

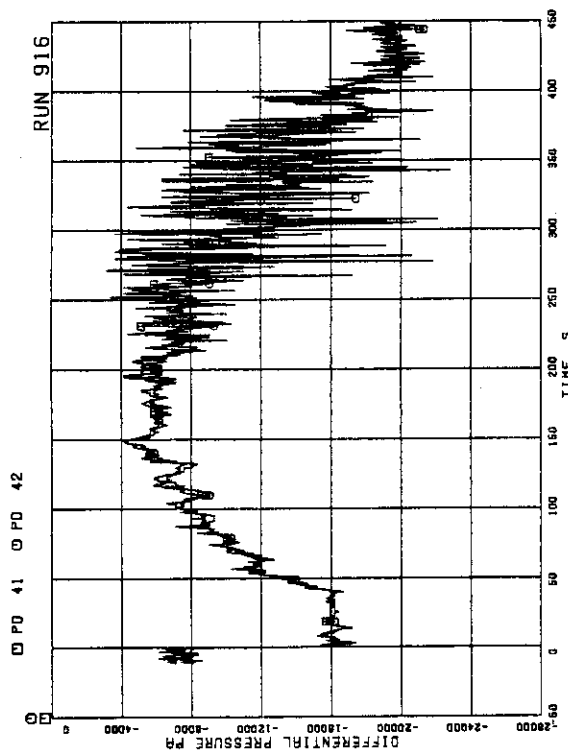


FIG. 5. 19 DIFFERENTIAL PRESSURE BETWEEN
JP-1.2 DISCHARGE AND LOWER PLENUM

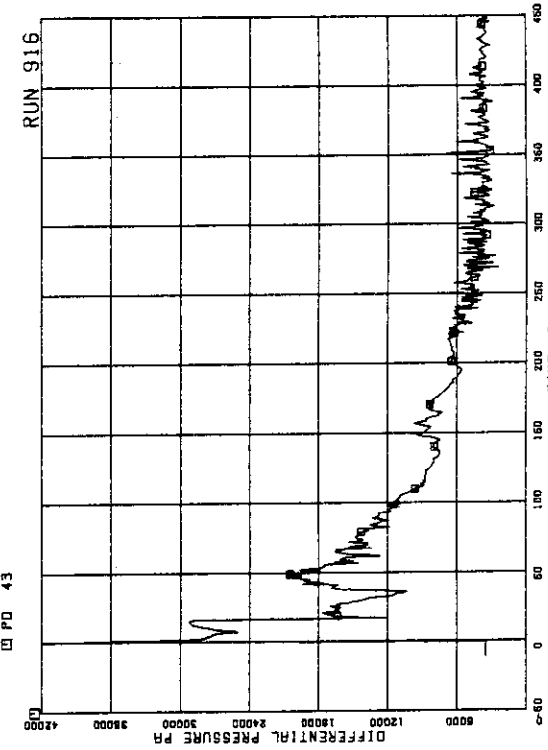


FIG. 5. 20 DIFFERENTIAL PRESSURE BETWEEN
DOWNCOMER BOTTOM AND BREAK B

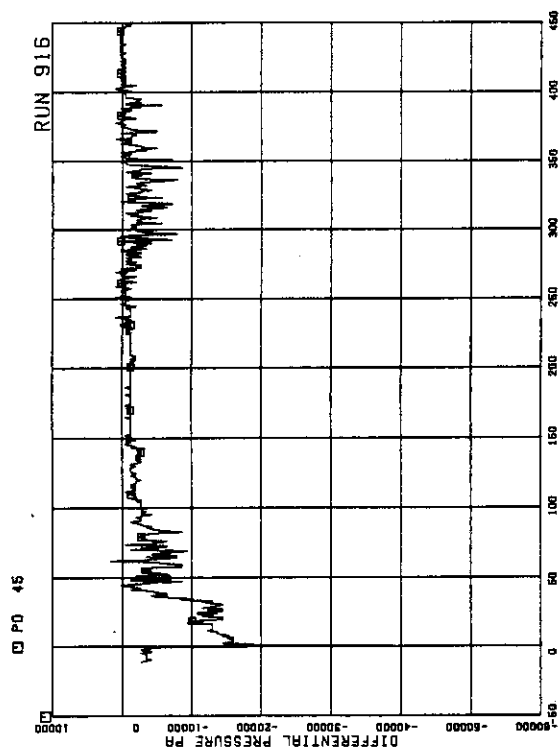


FIG.5. 21 DIFFERENTIAL PRESSURE BETWEEN
BREAK A AND MRP2 SUCTION

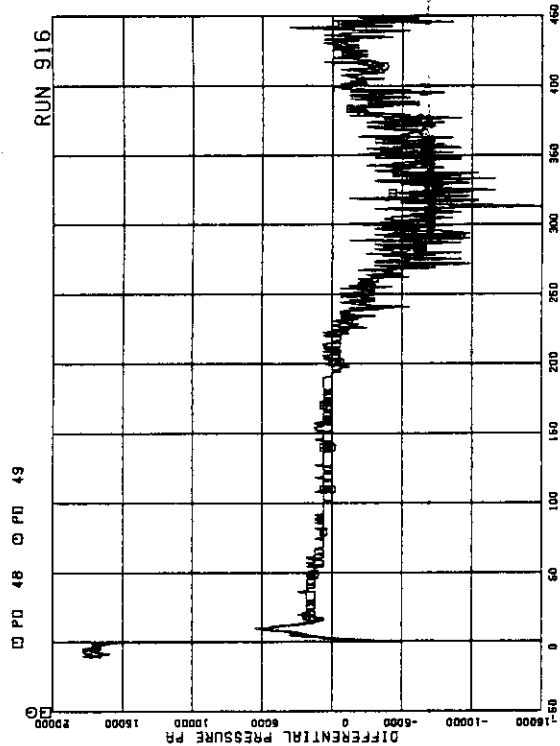


FIG.5. 23 DIFFERENTIAL PRESSURE BETWEEN
DOWNCOMER MIDDLE AND JP-3,4 SUCTION

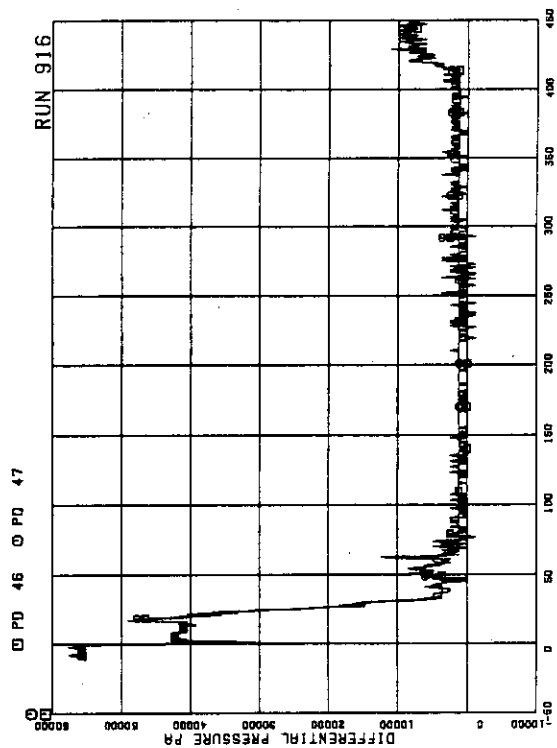


FIG.5. 22 DIFFERENTIAL PRESSURE BETWEEN
MRP DELIVERY AND JP-3,4 DRIVE

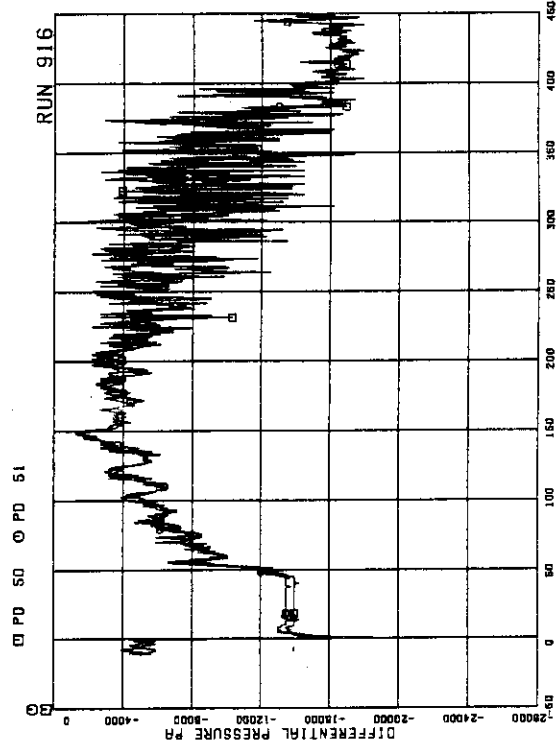


FIG.5. 24 DIFFERENTIAL PRESSURE BETWEEN
JP-3,4 DISCHARGE AND CONFLUENCE

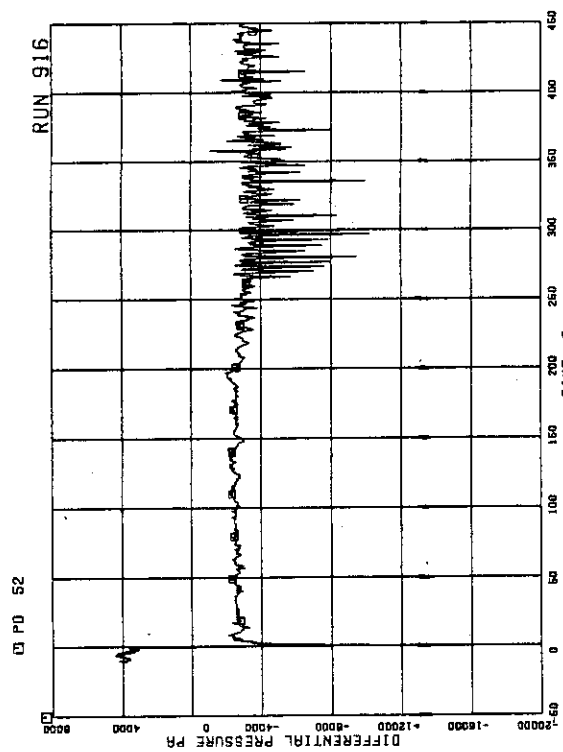


FIG. 5. 25 DIFFERENTIAL PRESSURE BETWEEN JP-3.4 CONFLUENCE IN BROKEN LOOP AND LP

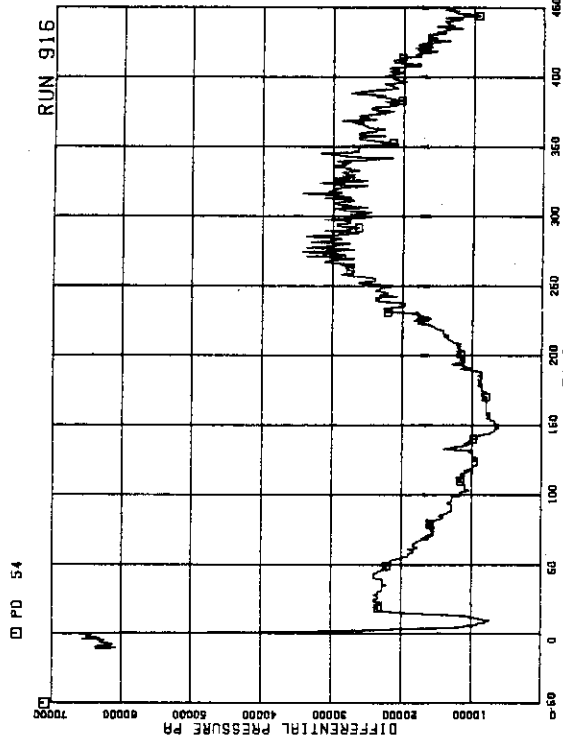


FIG. 5. 27 DIFFERENTIAL PRESSURE BETWEEN LOWER PLENUM AND DOWNCOMER BOTTOM

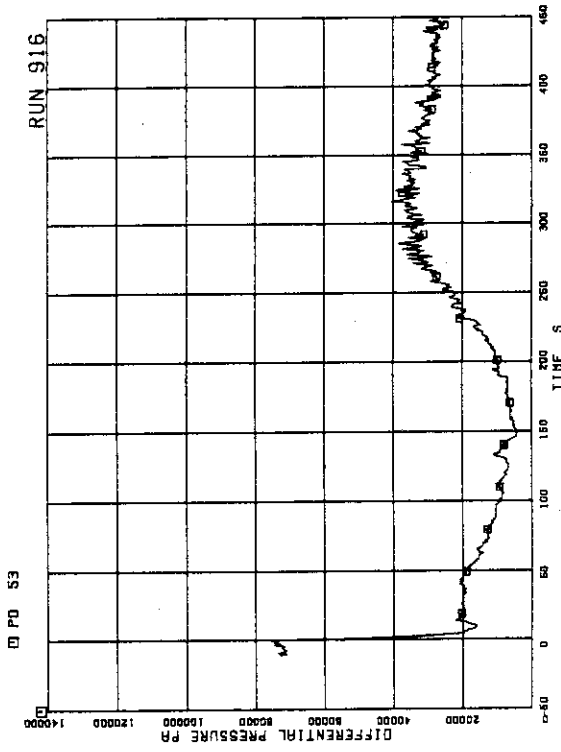


FIG. 5. 26 DIFFERENTIAL PRESSURE BETWEEN LOWER PLENUM AND DOWNCOMER MIDDLE

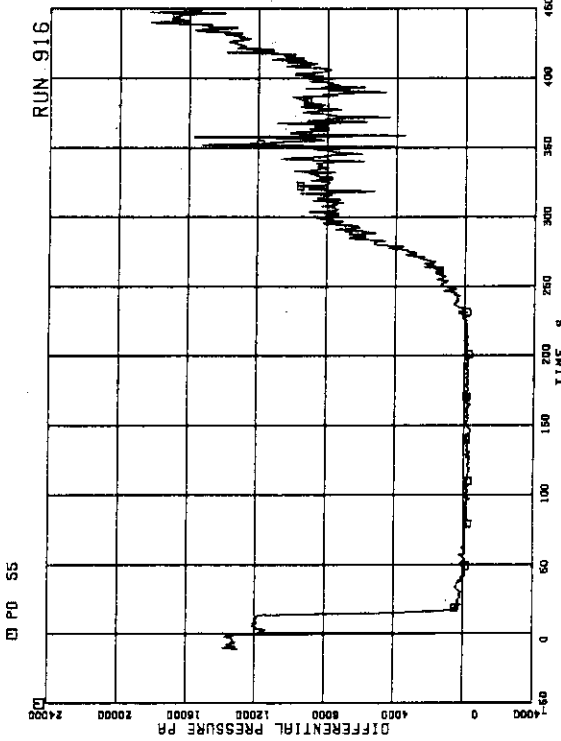
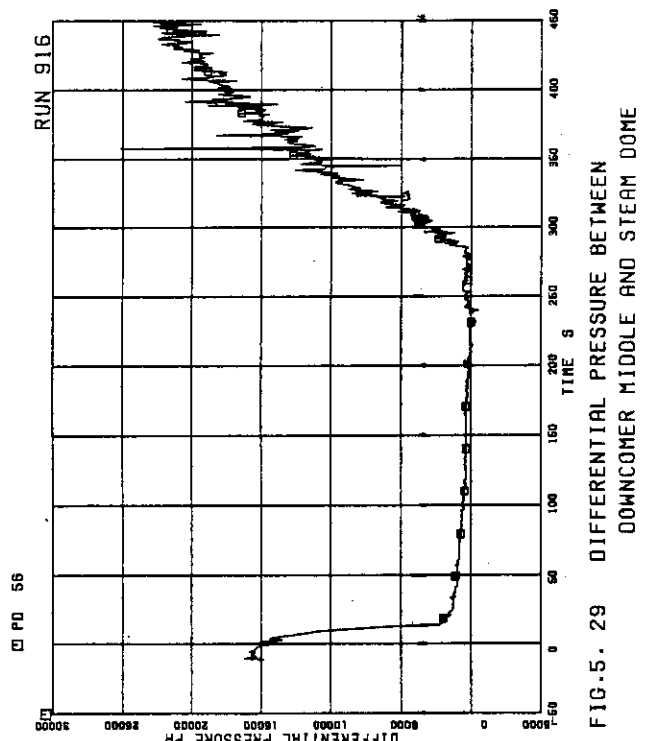
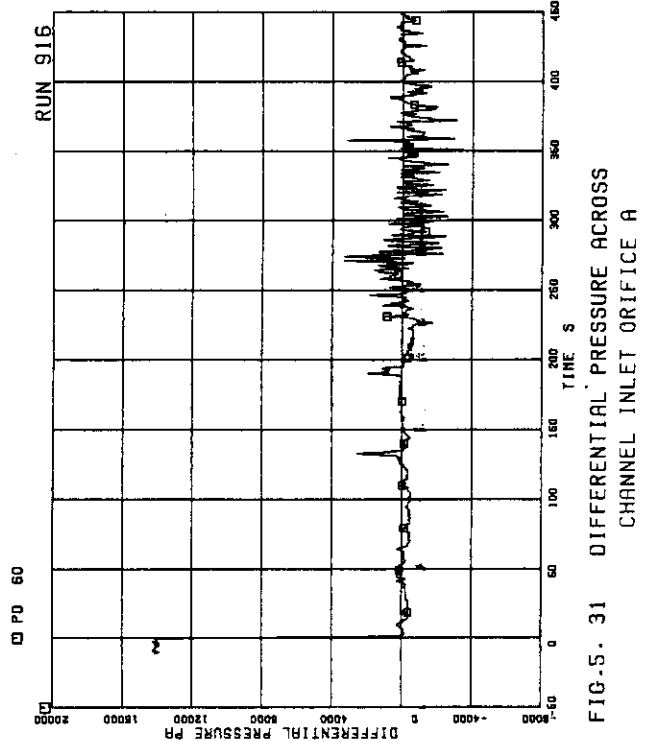
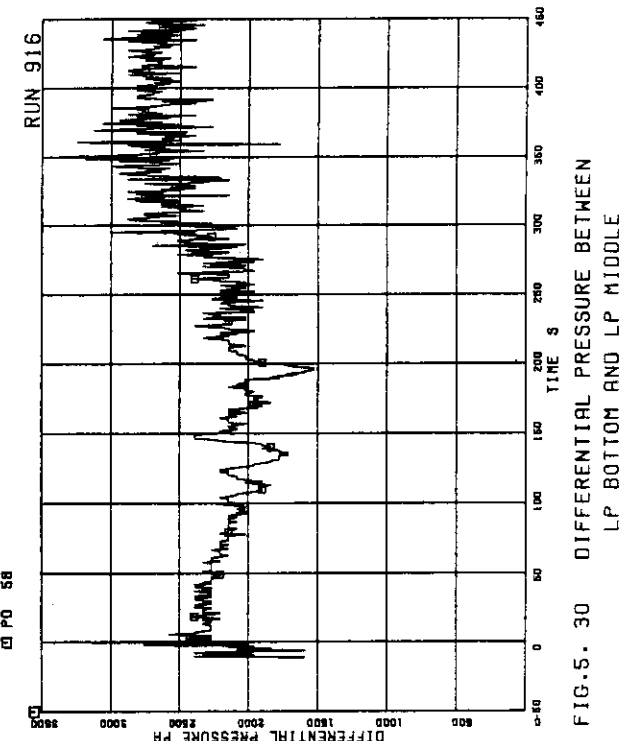
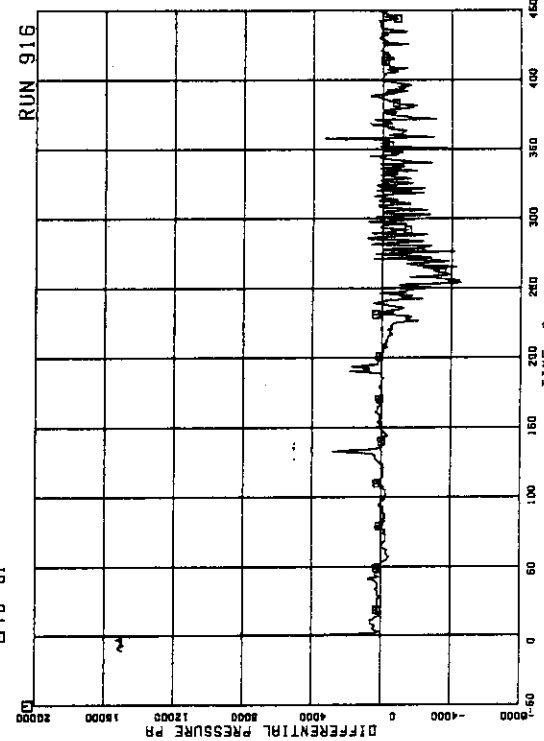


FIG. 5. 28 DIFFERENTIAL PRESSURE BETWEEN DOWNCOMER BOTTOM AND DOWNCOMER MIDDLE

FIG. 5. 29 DIFFERENTIAL PRESSURE BETWEEN
DOWNCOMER MIDDLE AND STEAM DOMEFIG. 5. 31 DIFFERENTIAL PRESSURE ACROSS
CHANNEL INLET ORIFICE AFIG. 5. 30 DIFFERENTIAL PRESSURE BETWEEN
LP BOTTOM AND LP MIDDLEFIG. 5. 32 DIFFERENTIAL PRESSURE ACROSS
CHANNEL INLET ORIFICE B

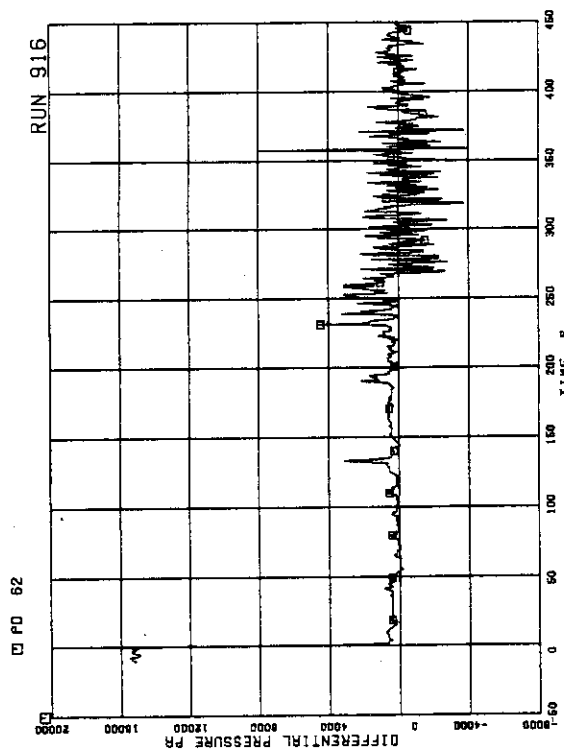


FIG. 5. 33 DIFFERENTIAL PRESSURE ACROSS CHANNEL INLET ORIFICE C

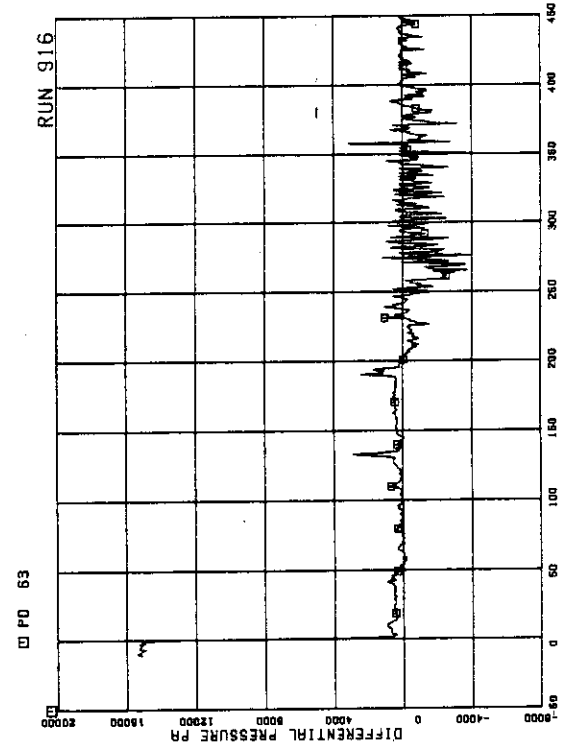


FIG. 5. 34 DIFFERENTIAL PRESSURE ACROSS CHANNEL INLET ORIFICE D

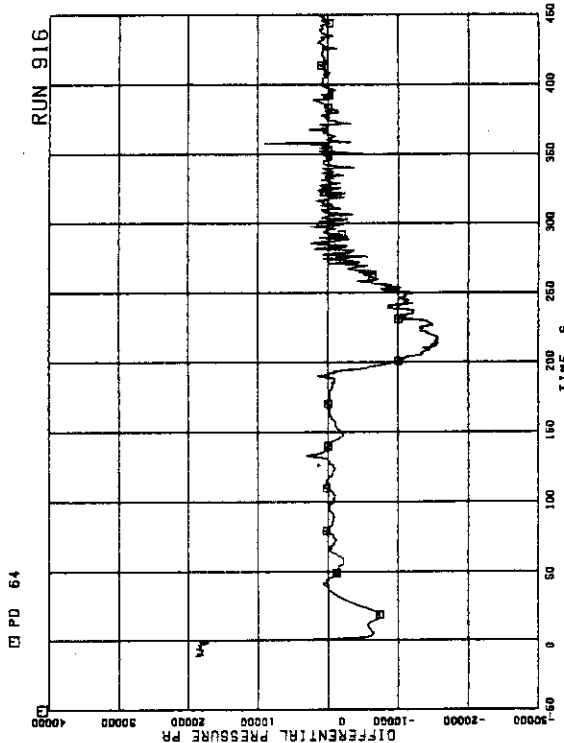


FIG. 5. 35 DIFFERENTIAL PRESSURE ACROSS BYPASS HOLE

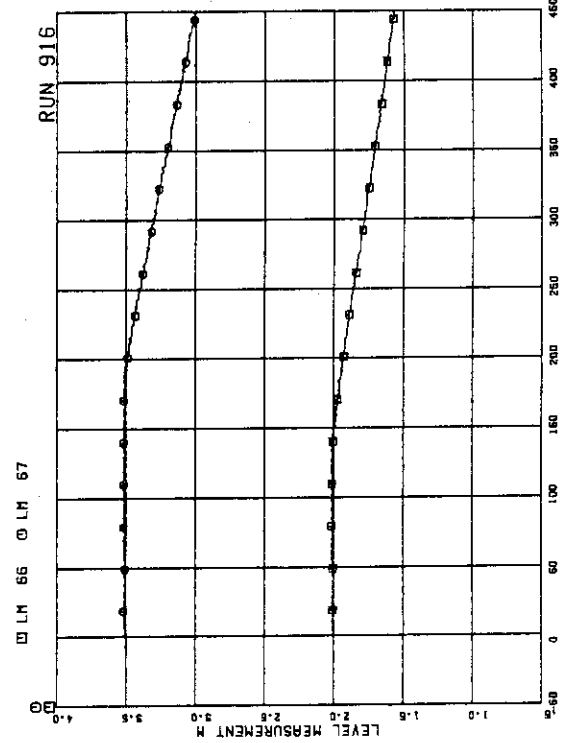


FIG. 5. 36 LIQUID LEVELS IN ECCS TANKS

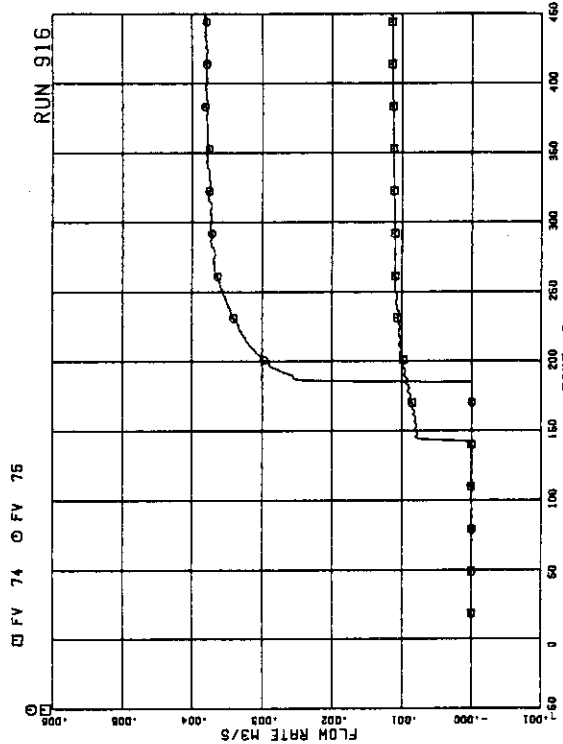


FIG. 5. 39 ECC INJECTION FLOW RATE

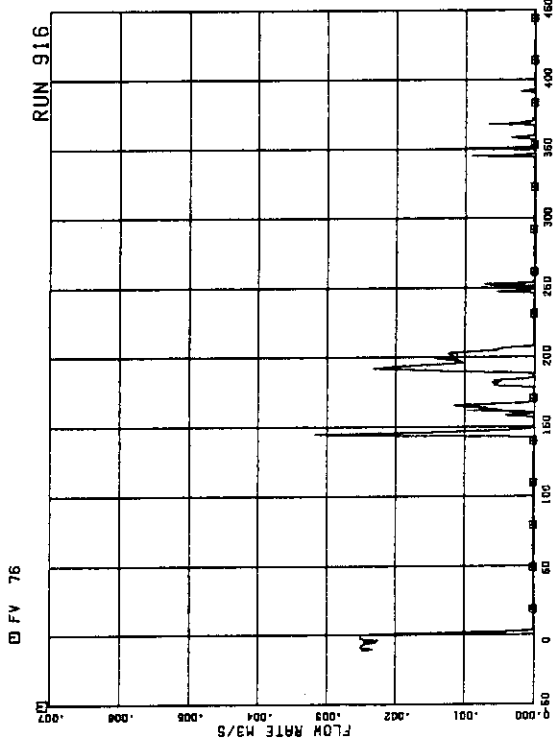


FIG. 5. 40 FEEDWATER FLOW RATE

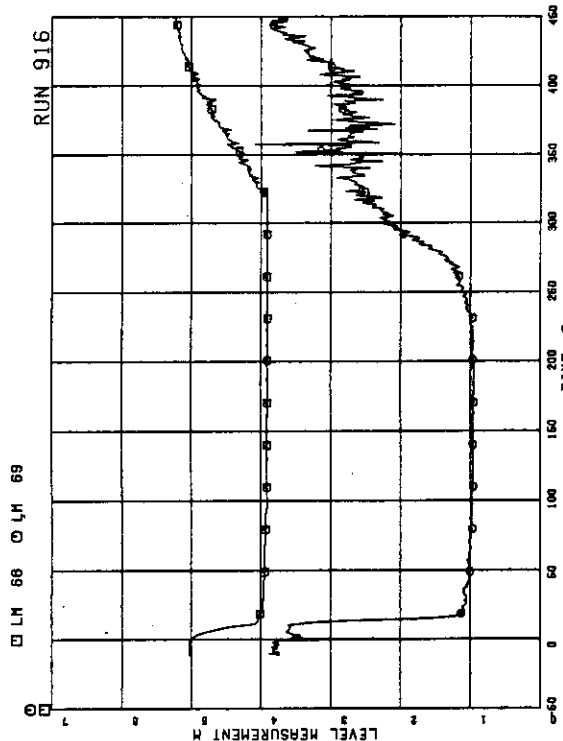


FIG. 5. 37 LIQUID LEVELS IN DOWNCOMER

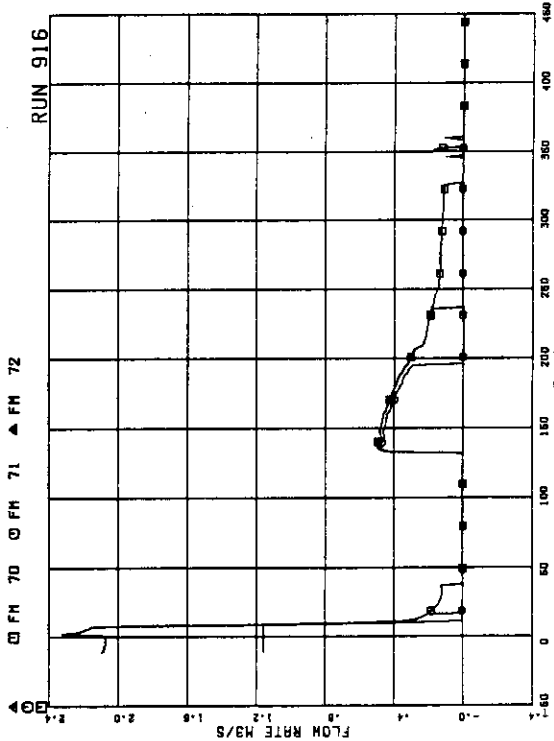
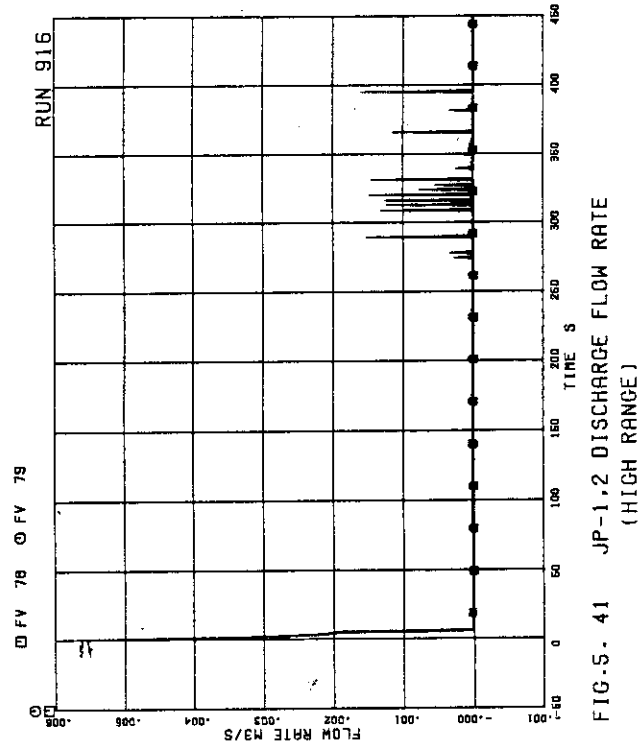
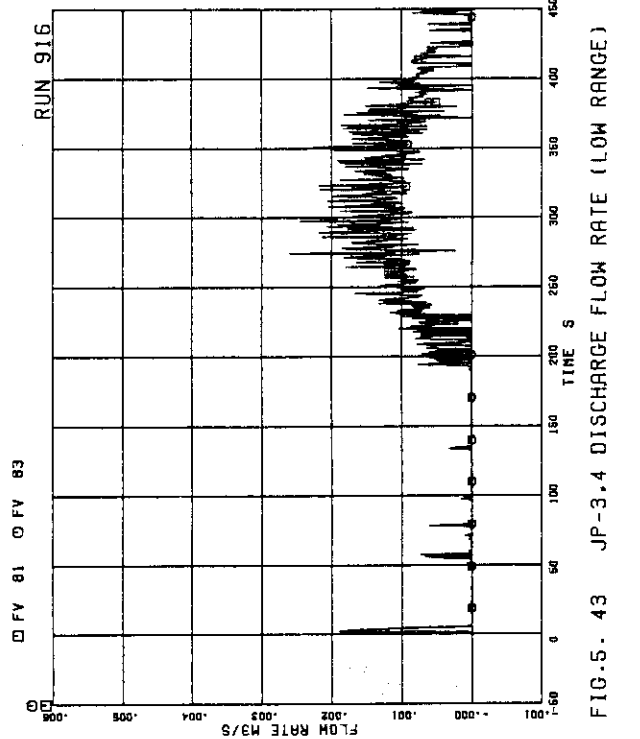
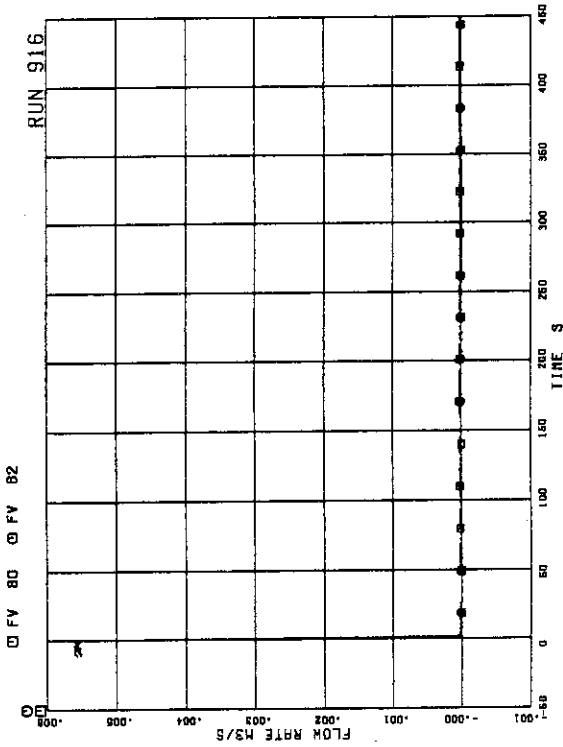


FIG. 5. 38 MASS FLOW RATE IN MSL

FIG. 5. 41 JP-1,2 DISCHARGE FLOW RATE
(HIGH RANGE)FIG. 5. 43 JP-3,4 DISCHARGE FLOW RATE
(LOW RANGE)FIG. 5. 44 MRP DISCHARGE FLOW RATE
(HIGH RANGE)

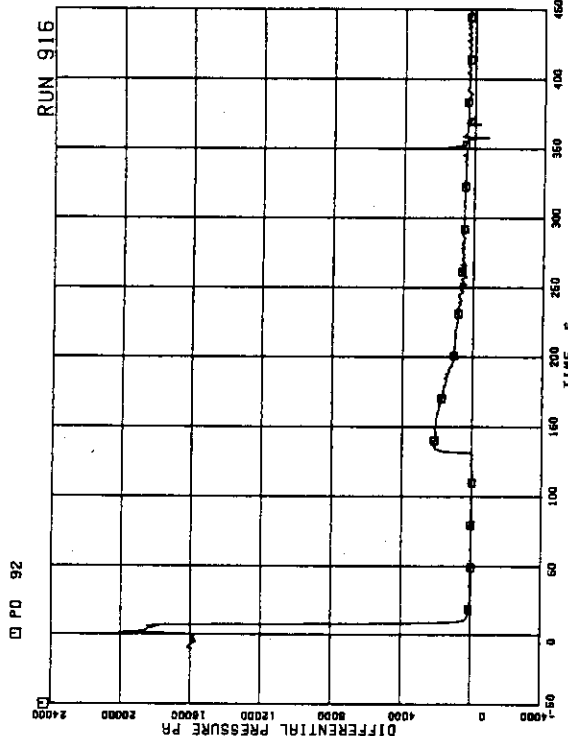


FIG. 5. 47 DIFFERENTIAL PRESSURE ACROSS
ORIFICE FLOWMETER F-3

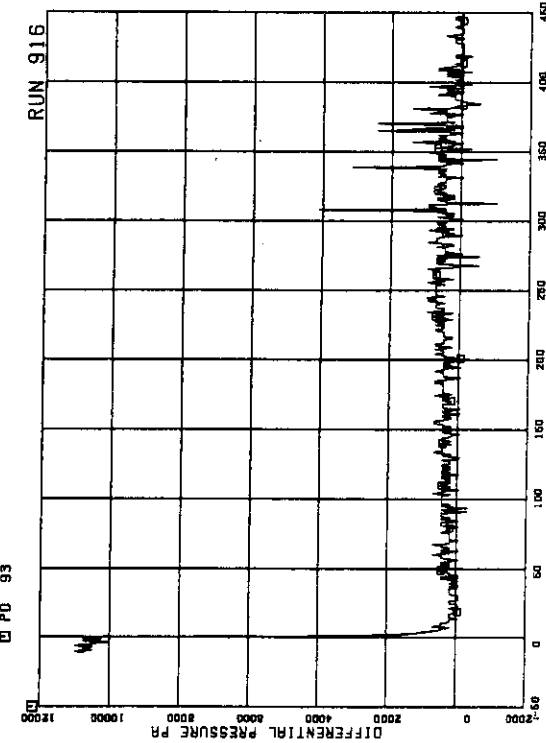


FIG. 5. 48 DIFFERENTIAL PRESSURE ACROSS
VENTURI FLOWMETER F-17

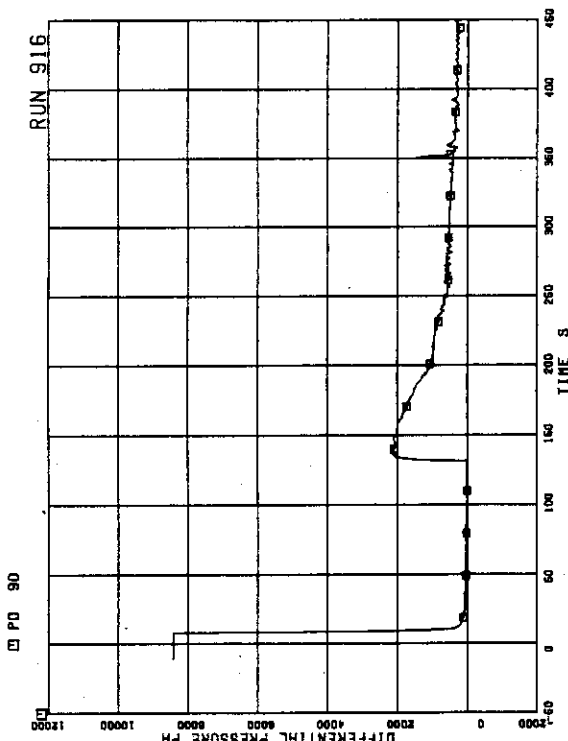


FIG. 5. 45 DIFFERENTIAL PRESSURE ACROSS
ORIFICE FLOWMETER F-1

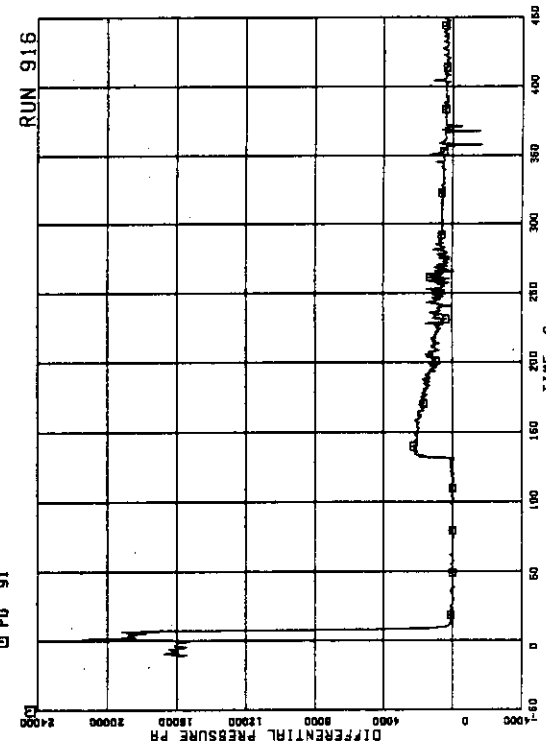


FIG. 5. 46 DIFFERENTIAL PRESSURE ACROSS
ORIFICE FLOWMETER F-2

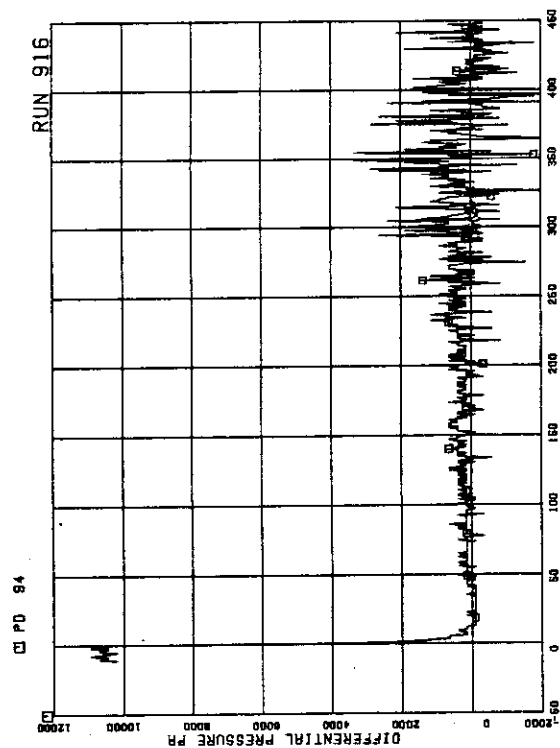


FIG. 5. 49 DIFFERENTIAL PRESSURE ACROSS VENTURI FLOWMETER F-18

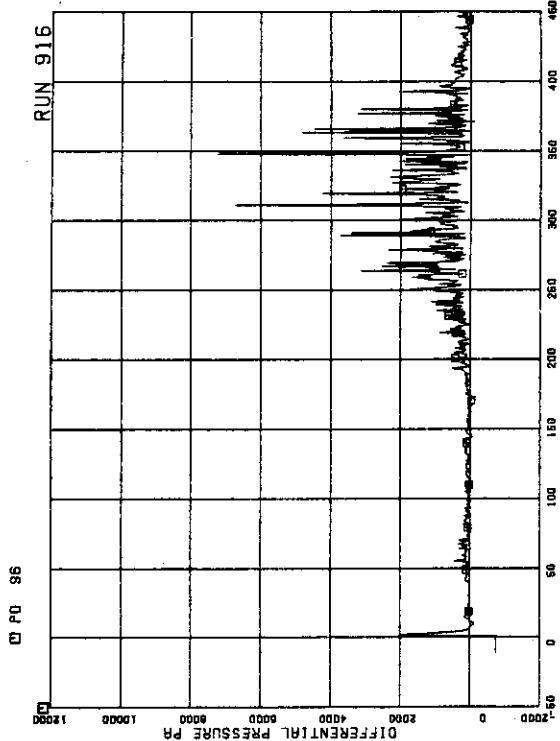


FIG. 5. 51 DIFFERENTIAL PRESSURE ACROSS ORIFICE FLOWMETER F-20

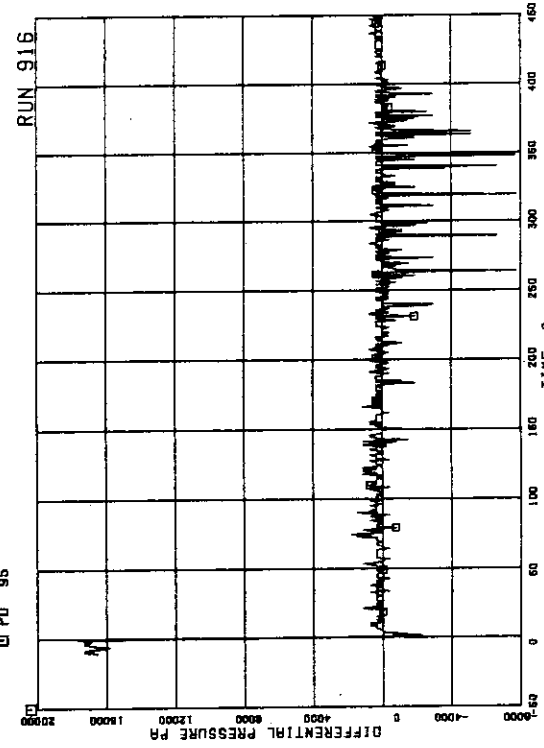


FIG. 5. 50 DIFFERENTIAL PRESSURE ACROSS ORIFICE FLOWMETER F-19

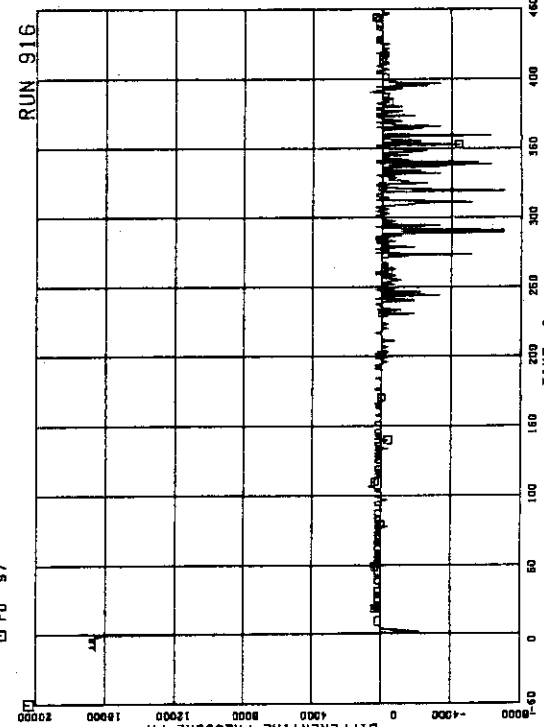


FIG. 5. 52 DIFFERENTIAL PRESSURE ACROSS ORIFICE FLOWMETER F-21

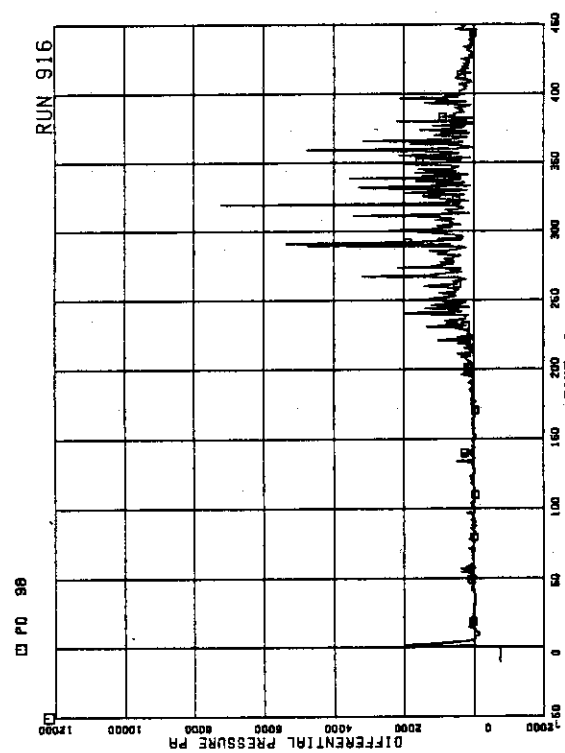


FIG. 5. 53 DIFFERENTIAL PRESSURE ACROSS
ORIFICE FLOWMETER F-22

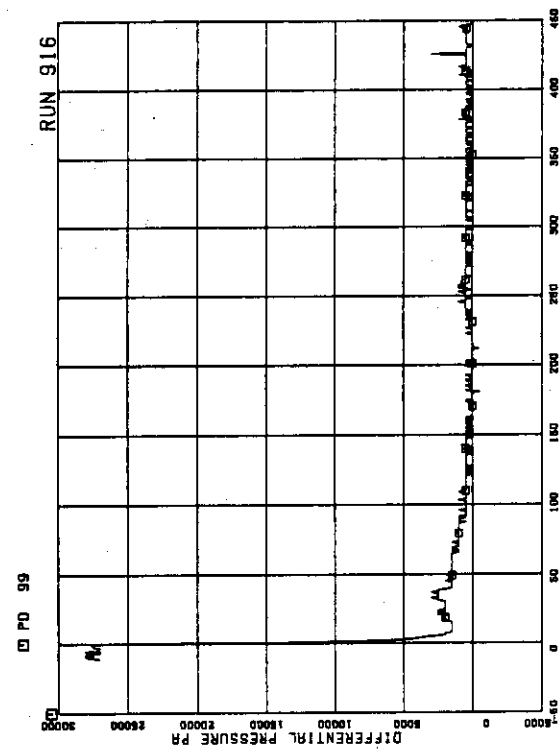


FIG. 5. 54 DIFFERENTIAL PRESSURE ACROSS
VENTURI FLOWMETER F-27

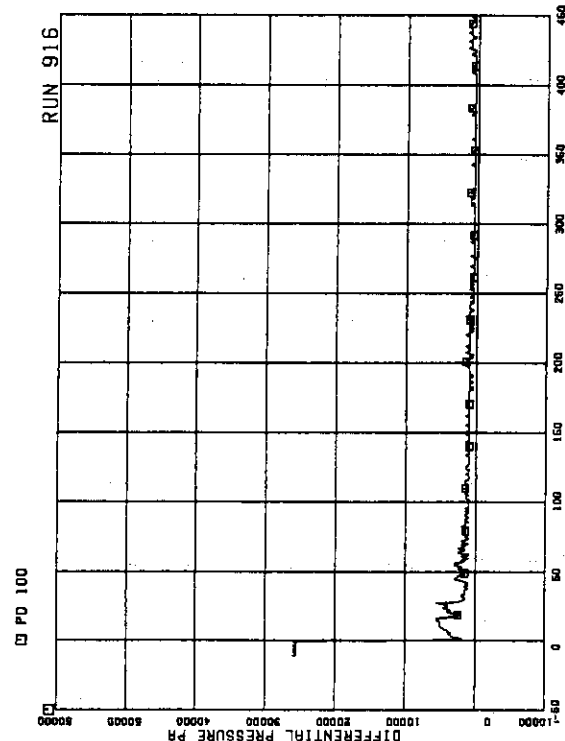


FIG. 5. 55 DIFFERENTIAL PRESSURE ACROSS
VENTURI FLOWMETER F-28

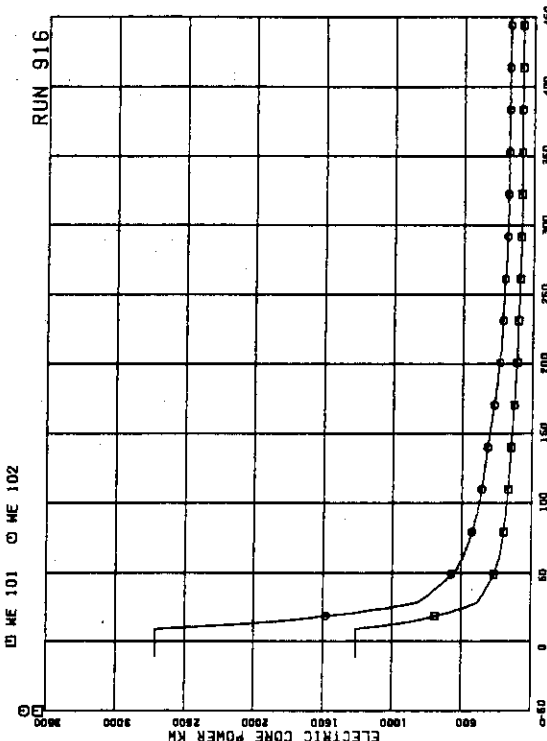


FIG. 5. 56 ELECTRIC CORE POWER

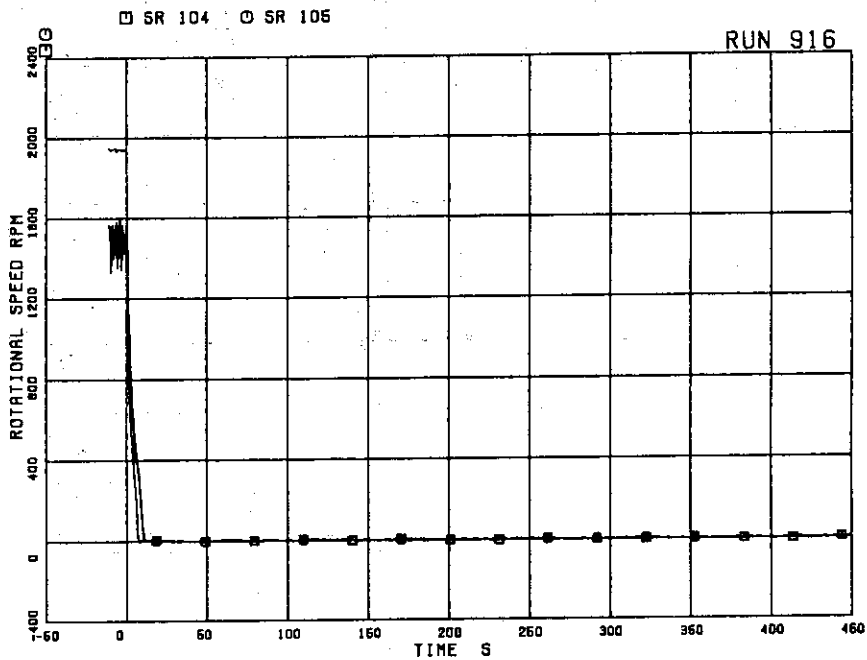


FIG.5. 57 MRP REVOLUTION

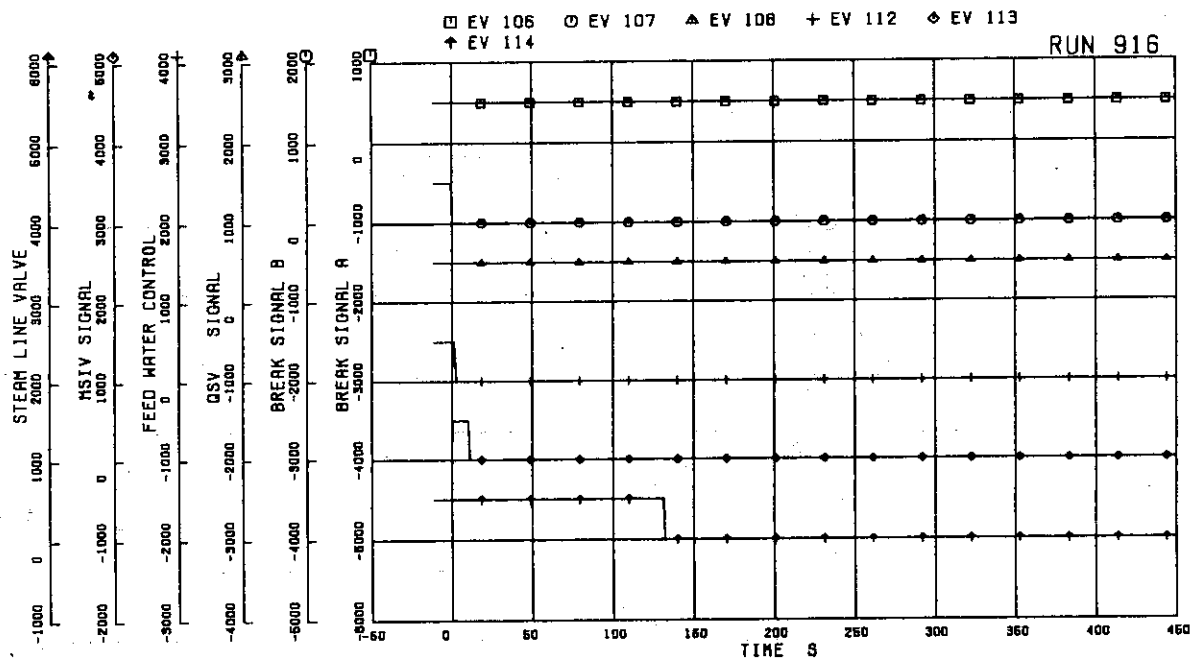


FIG.5. 58 VALVE OPERATION SIGNALS

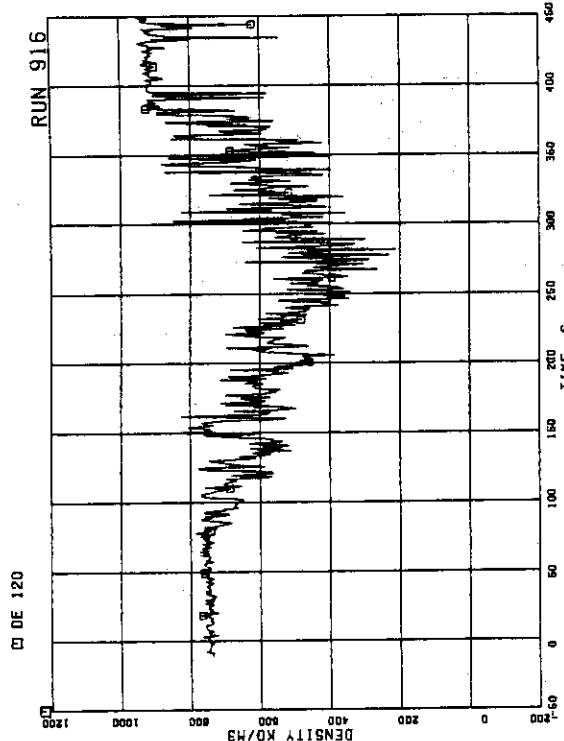


FIG.5. 61 FLUID DENSITY AT JP-1,2 OUTLET. BEAM A

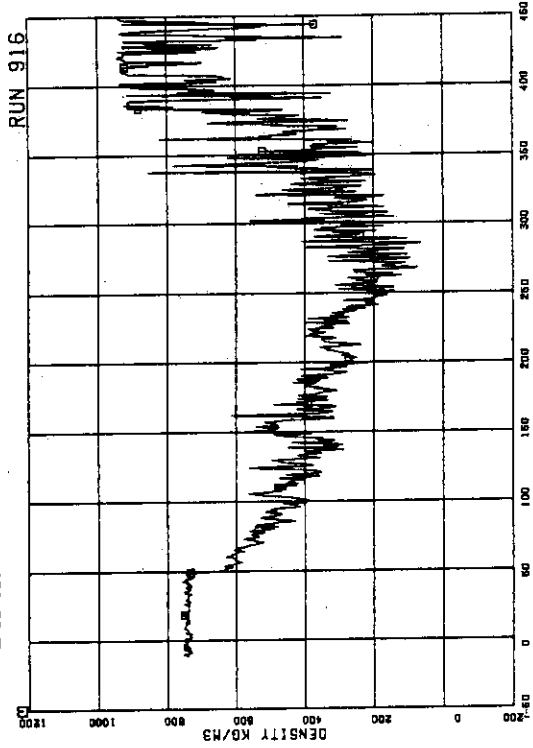


FIG.5. 62 FLUID DENSITY AT JP-1,2 OUTLET. BEAM B

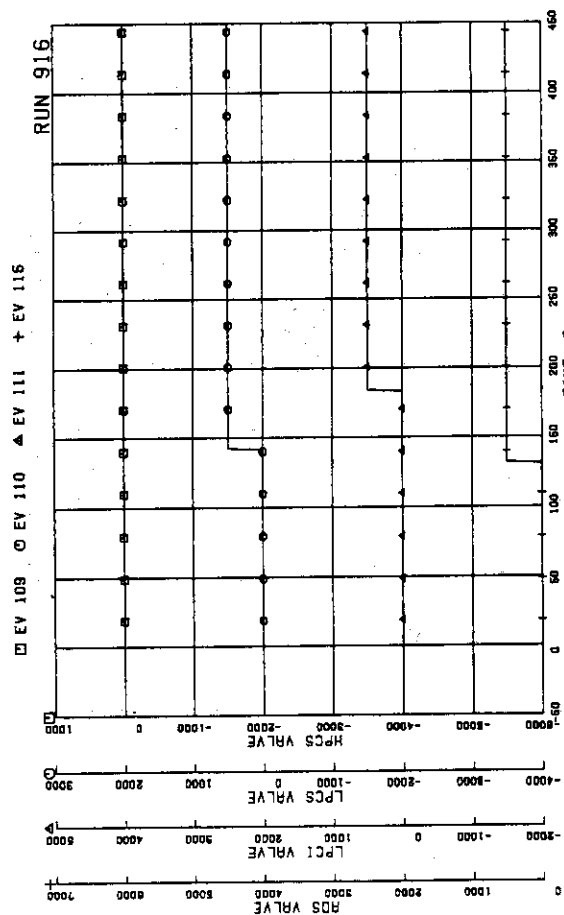


FIG.5. 59 ECCS OPERATION SIGNALS

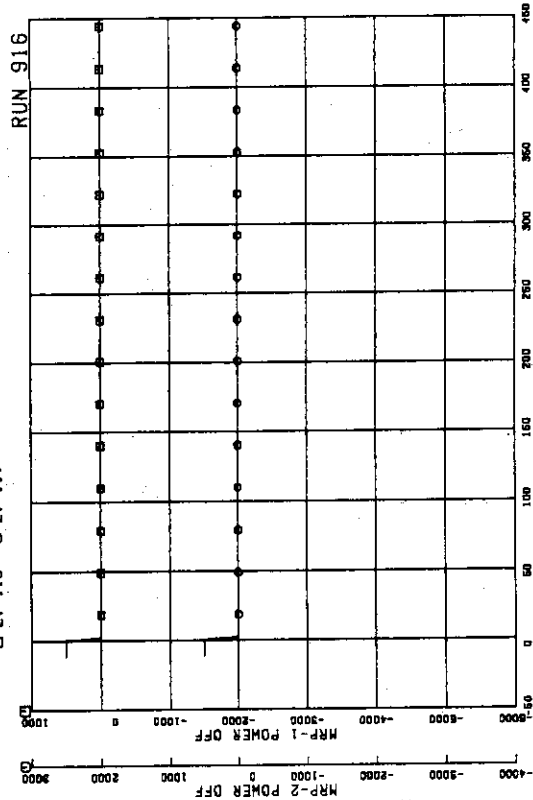


FIG.5. 60 MRP OPERATION SIGNALS

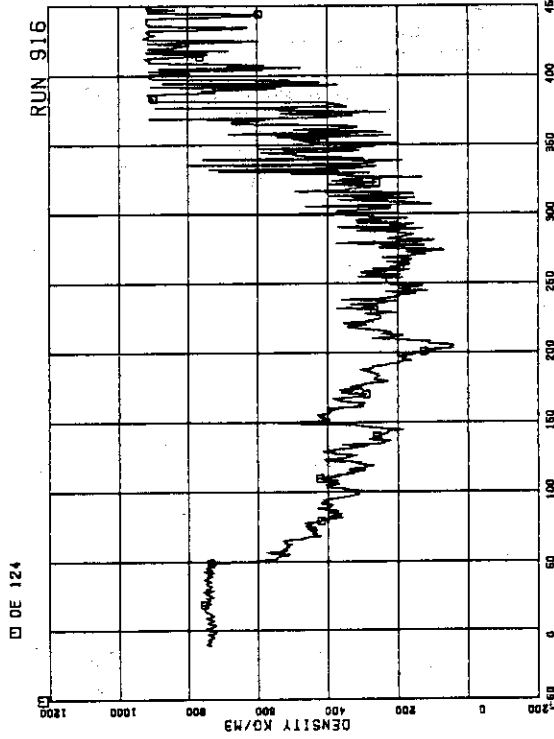


FIG. 5. 65 FLUID DENSITY AT JP-3.4 OUTLET, BEAM B

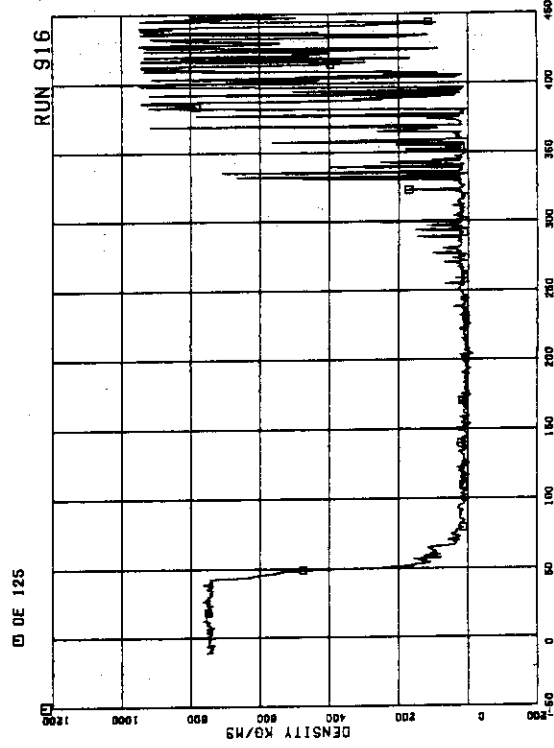


FIG. 5. 66 FLUID DENSITY AT JP-3.4 OUTLET, BEAM C.

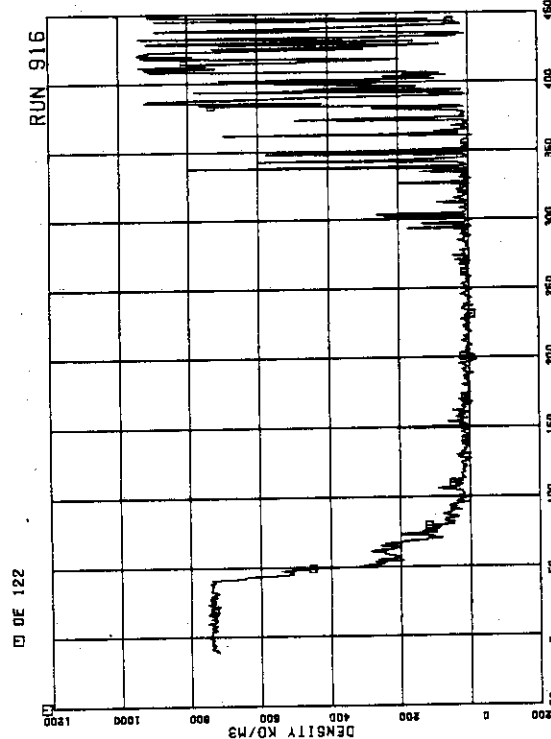


FIG. 5. 63 FLUID DENSITY AT JP-1.2 OUTLET, BEAM C

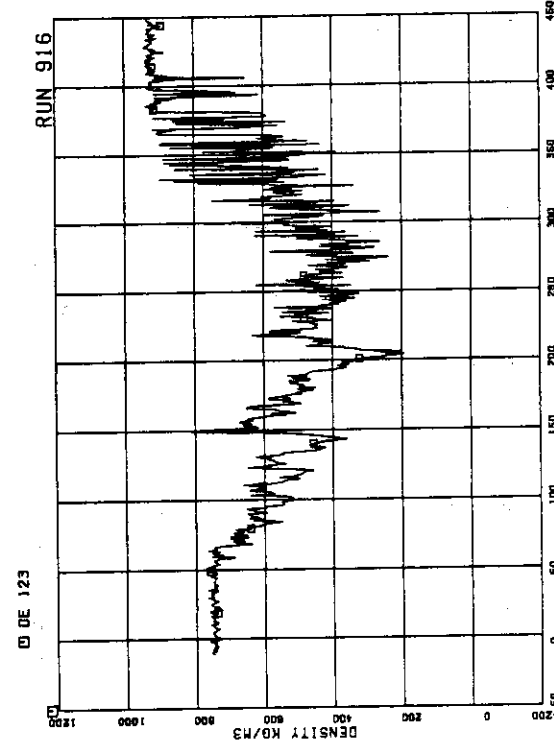


FIG. 5. 64 FLUID DENSITY AT JP-3.4 OUTLET, BEAM A

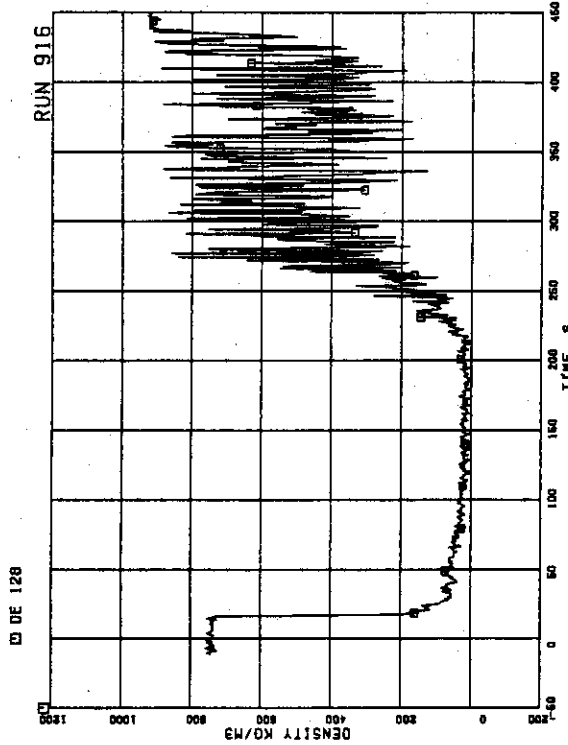


FIG.5. 69 FLUID DENSITY AT PV SIDE OF BREAK.
BEAM A

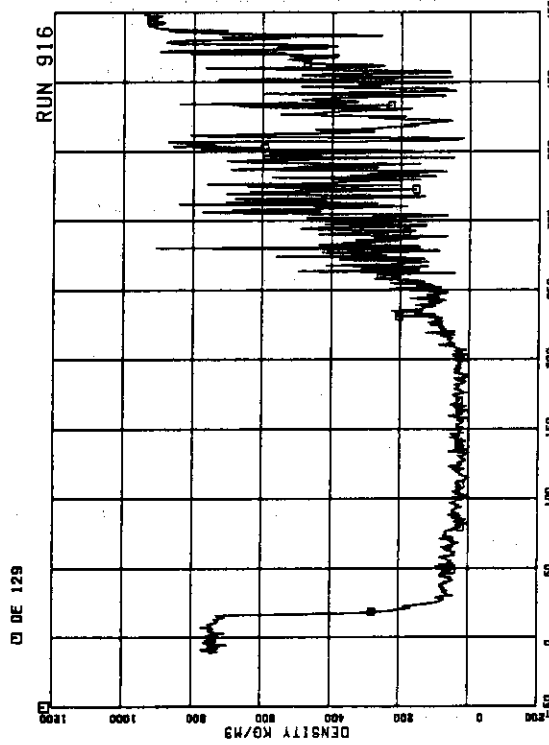


FIG.5. 70 FLUID DENSITY AT PV SIDE OF BREAK.
BEAM B

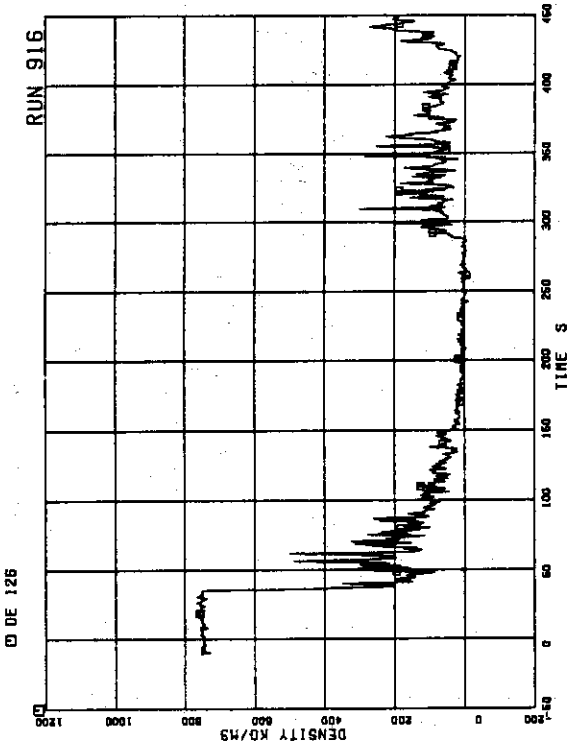


FIG.5. 67 FLUID DENSITY AT MRP SIDE OF BREAK.
BEAM A

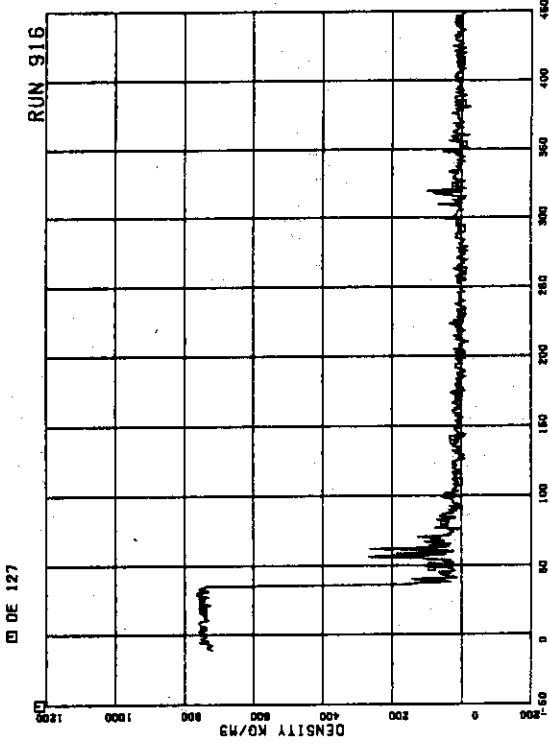
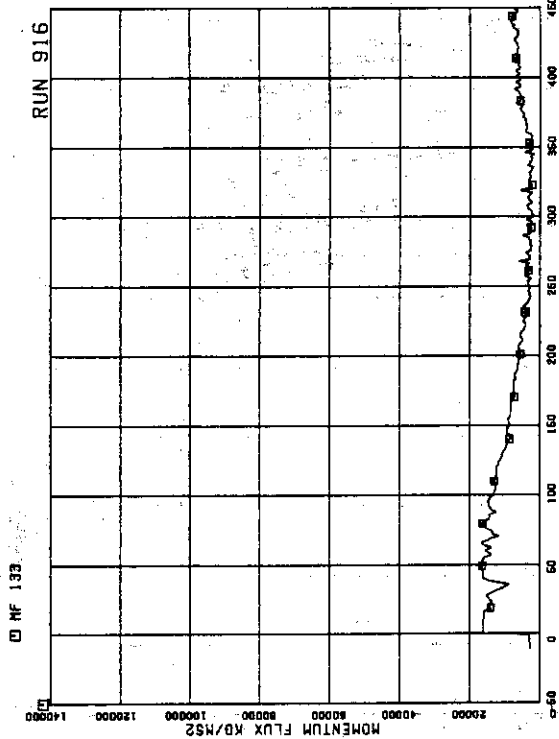
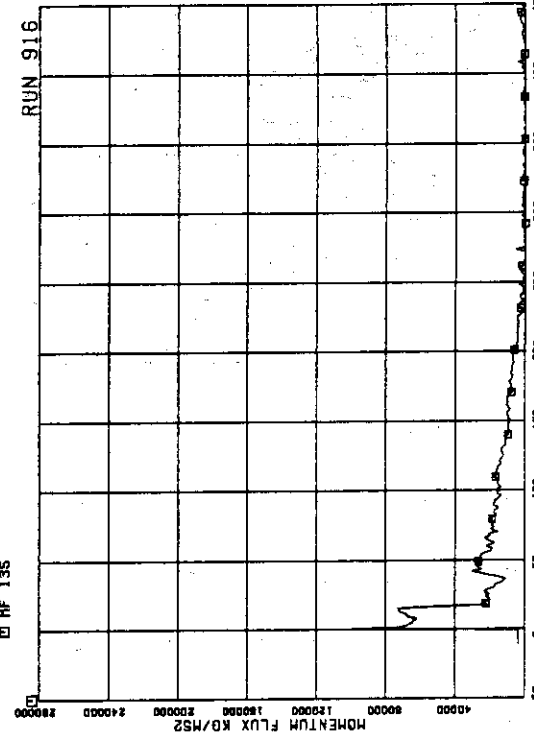
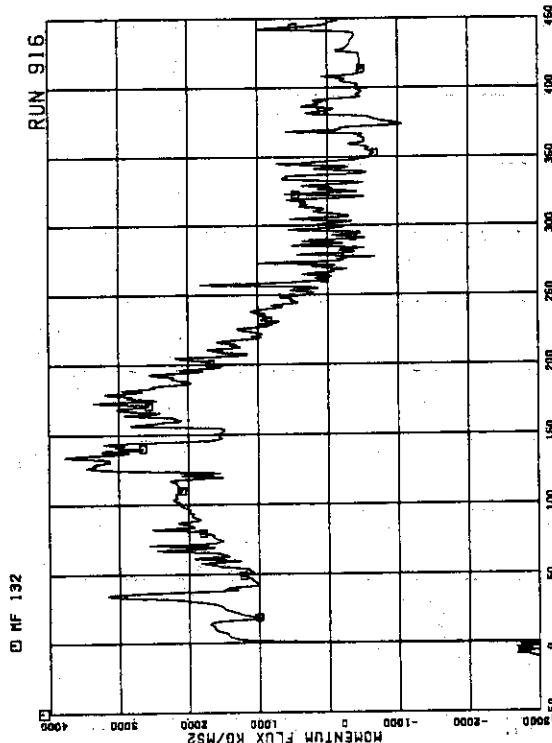
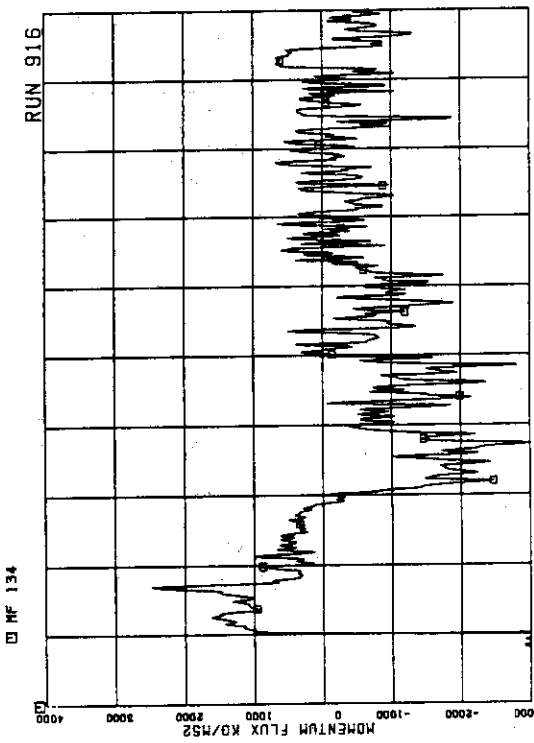


FIG.5. 68 FLUID DENSITY AT MRP SIDE OF BREAK.
BEAM B

FIG. 5. 71 MOMENTUM FLUX AT BREAK A SPOOL PIECE
(LOW RANGE)FIG. 5. 73 MOMENTUM FLUX AT BREAK B SPOOL PIECE
(LOW RANGE)FIG. 5. 71 MOMENTUM FLUX AT BREAK A SPOOL PIECE
(HIGH RANGE)FIG. 5. 72 MOMENTUM FLUX AT BREAK B SPOOL PIECE
(HIGH RANGE)

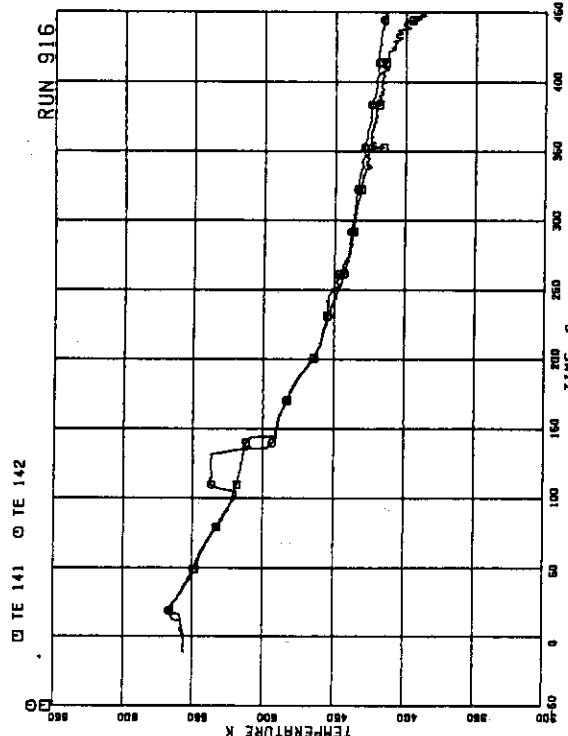


FIG. 5. 77 FLUID TEMPERATURES IN DOWNCOMER

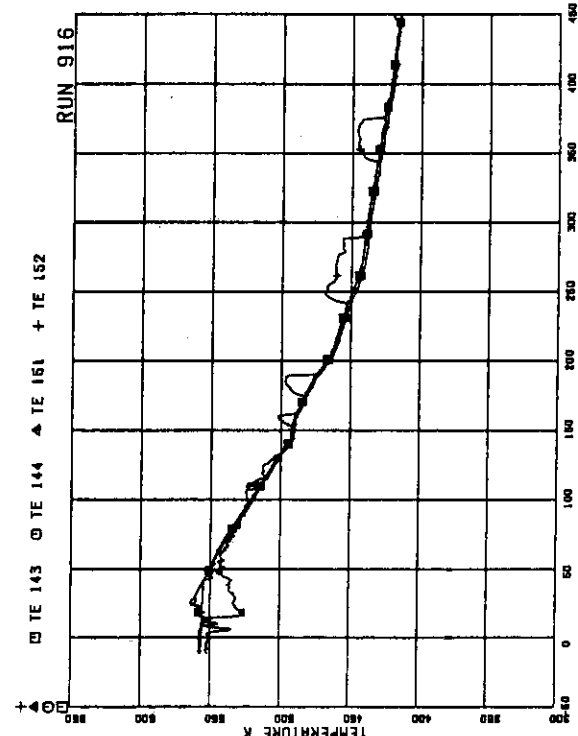


FIG. 5. 78 FLUID TEMPERATURES IN INTACT RECIRCULATION LOOP

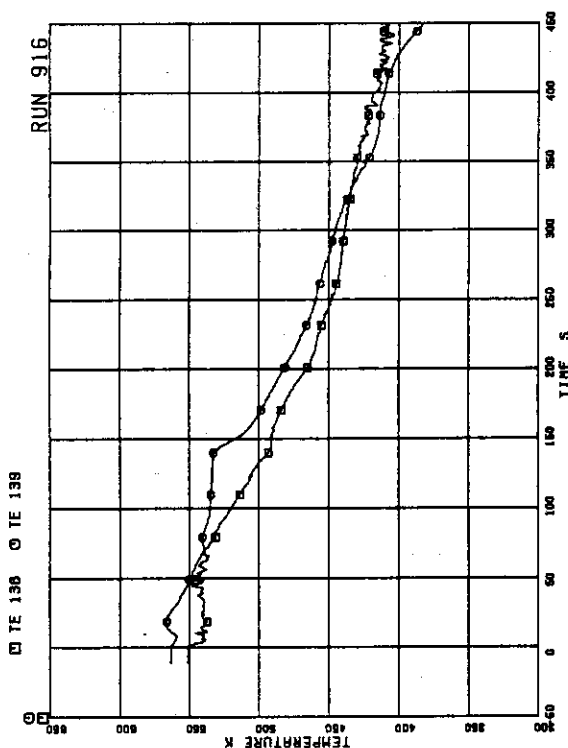


FIG. 5. 75 FLUID TEMPERATURES IN LOWER PLENUM AND UPPER PLENUM

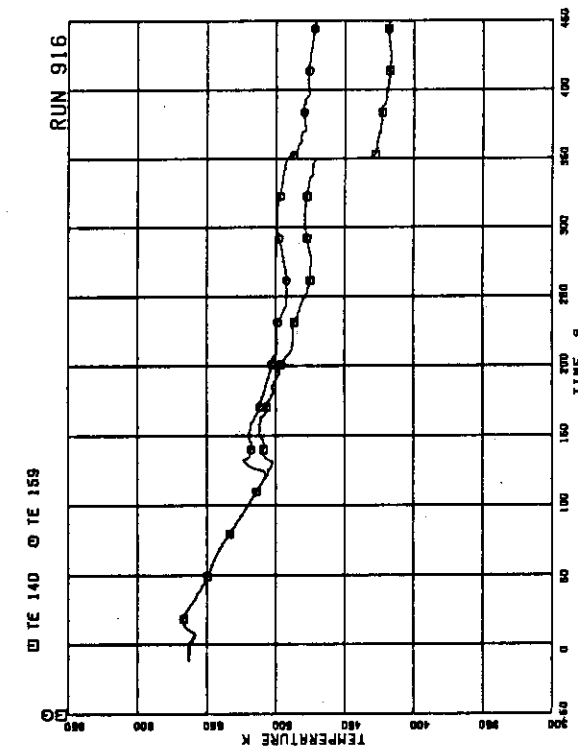


FIG. 5. 76 FLUID TEMPERATURES IN STEAM DOME AND MSL

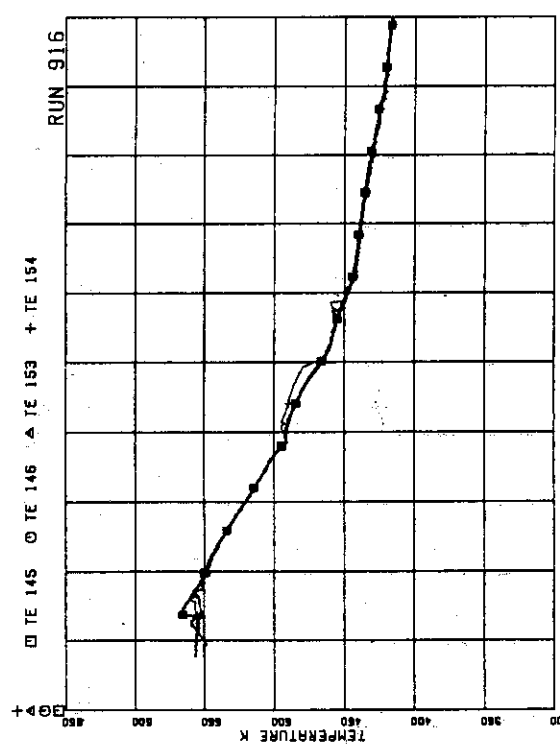


FIG. 5-79 FLUID TEMPERATURES IN BROKEN RECIRCULATION LOOP

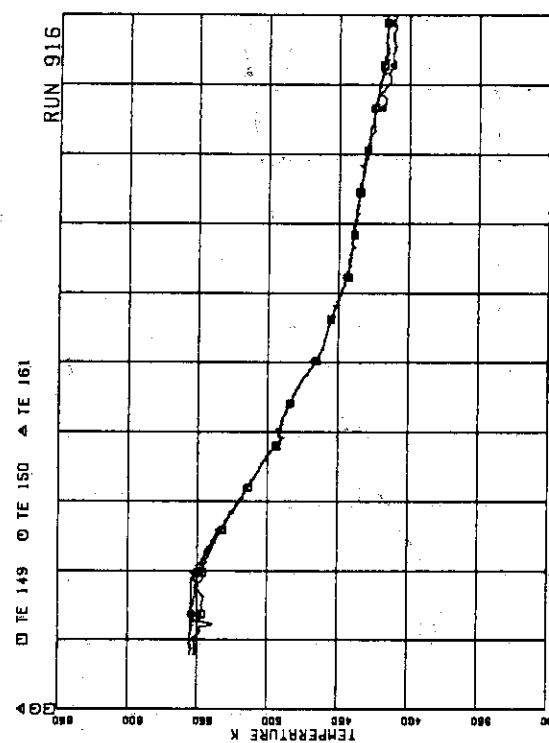


FIG. 5-81 FLUID TEMPERATURES AT JP-3,4 OUTLET

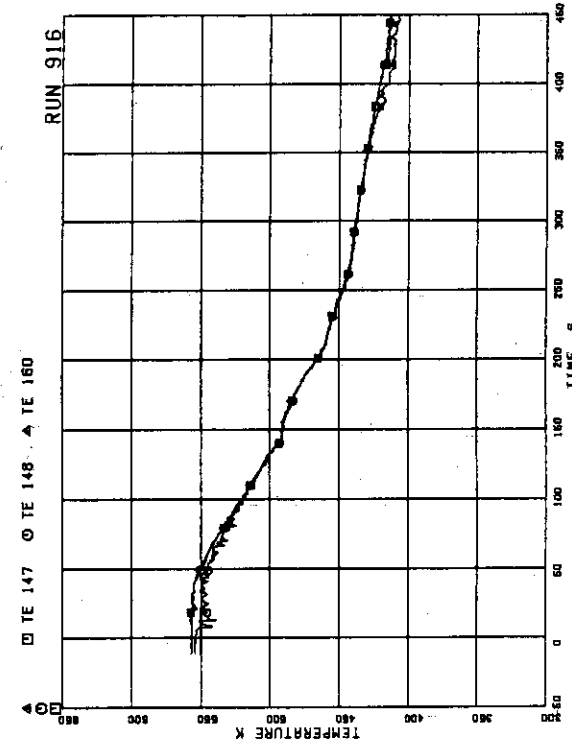


FIG. 5-80 FLUID TEMPERATURES AT JP-1,2 OUTLET

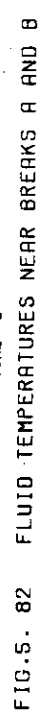


FIG. 5-82 FLUID TEMPERATURES NEAR BREAKS A AND B

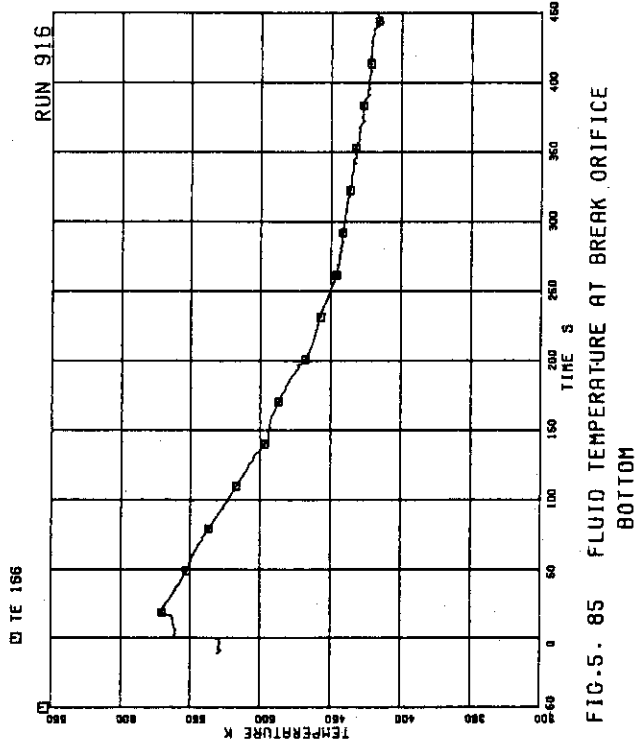


FIG. 5. 85 FLUID TEMPERATURE AT BREAK ORIFICE BOTTOM

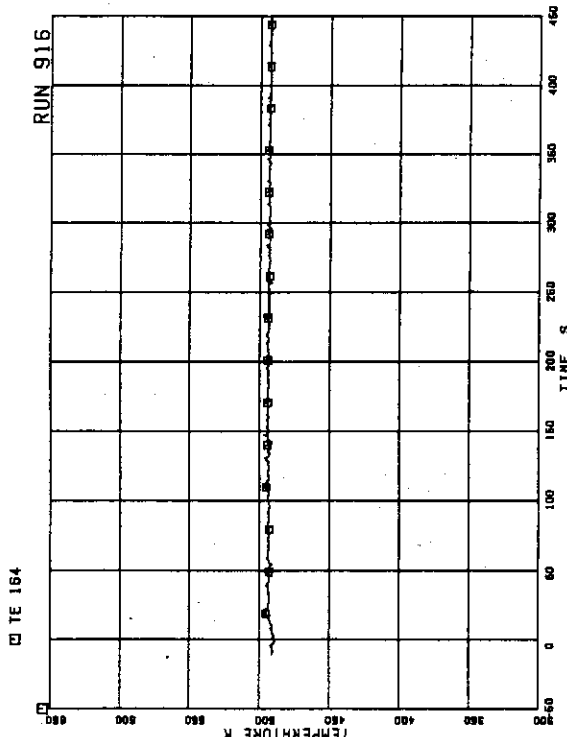


FIG. 5. 83 FEEDWATER TEMPERATURE

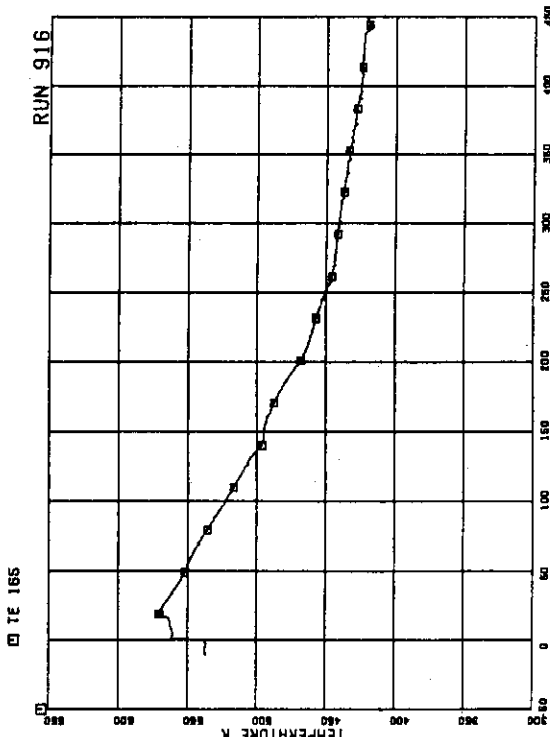


FIG. 5. 84 FLUID TEMPERATURE AT BREAK ORIFICE TOP

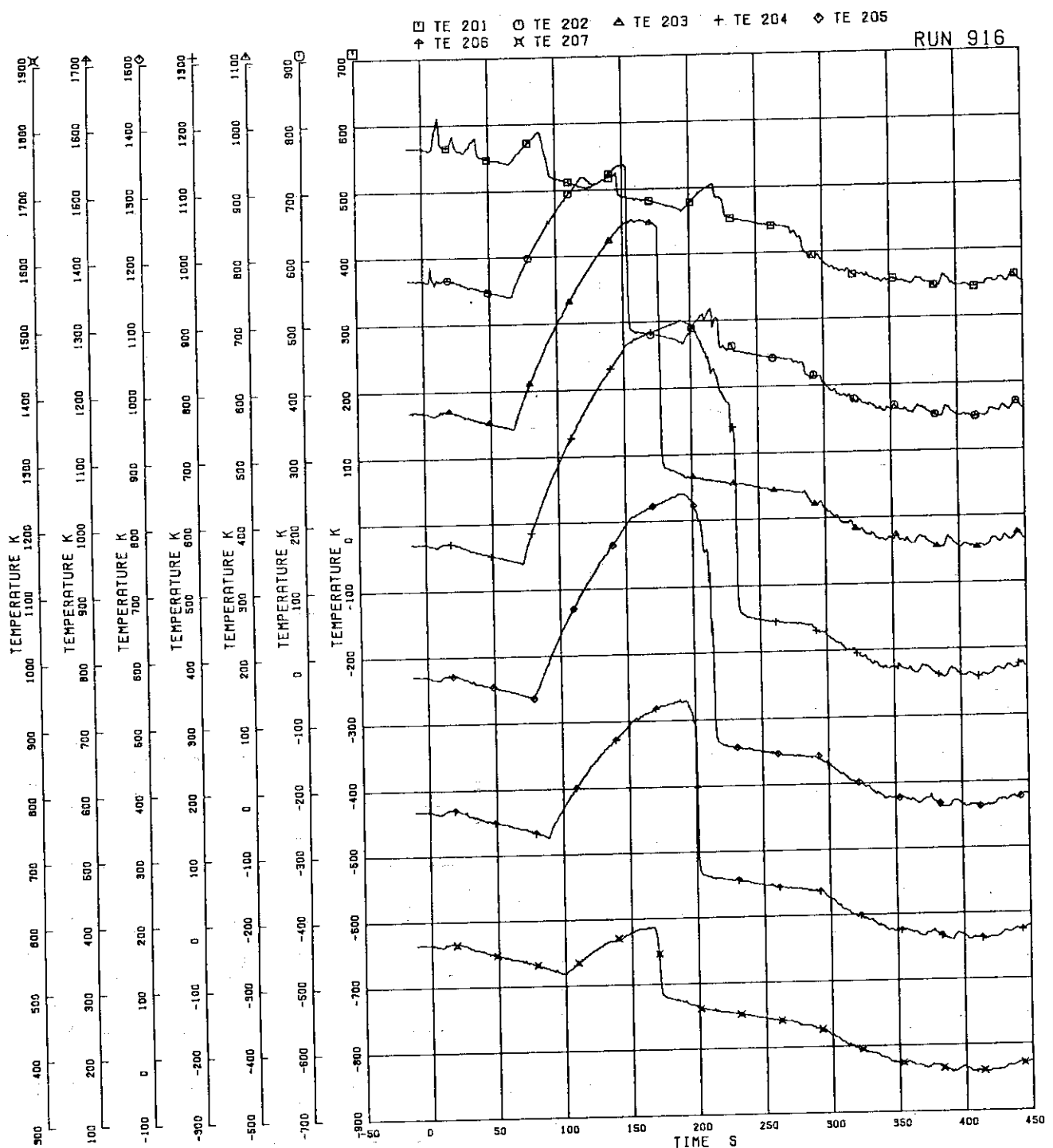


FIG. 5. 86 SURFACE TEMPERATURES OF FUEL ROD A11

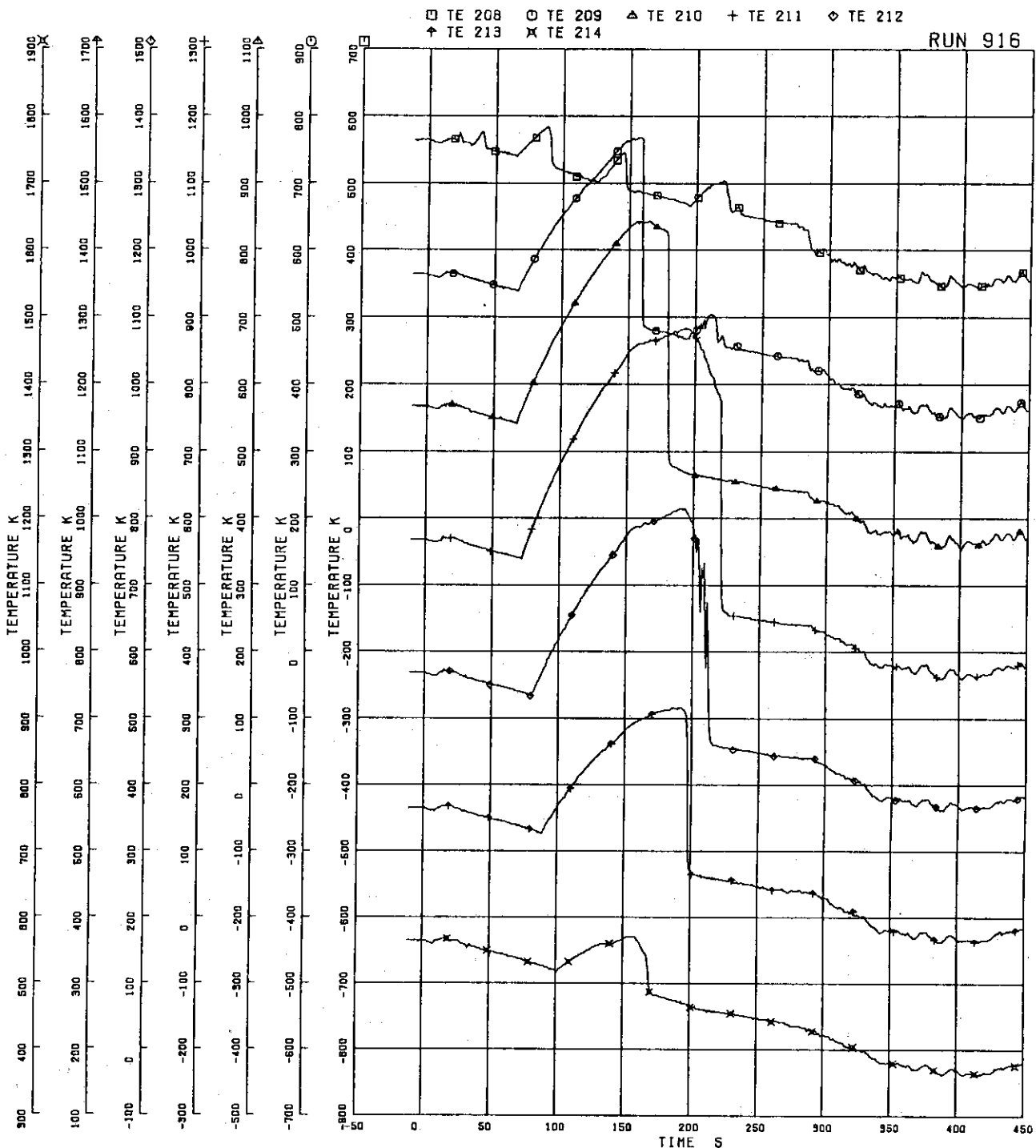


FIG. 5. 87 SURFACE TEMPERATURES OF FUEL ROD A12

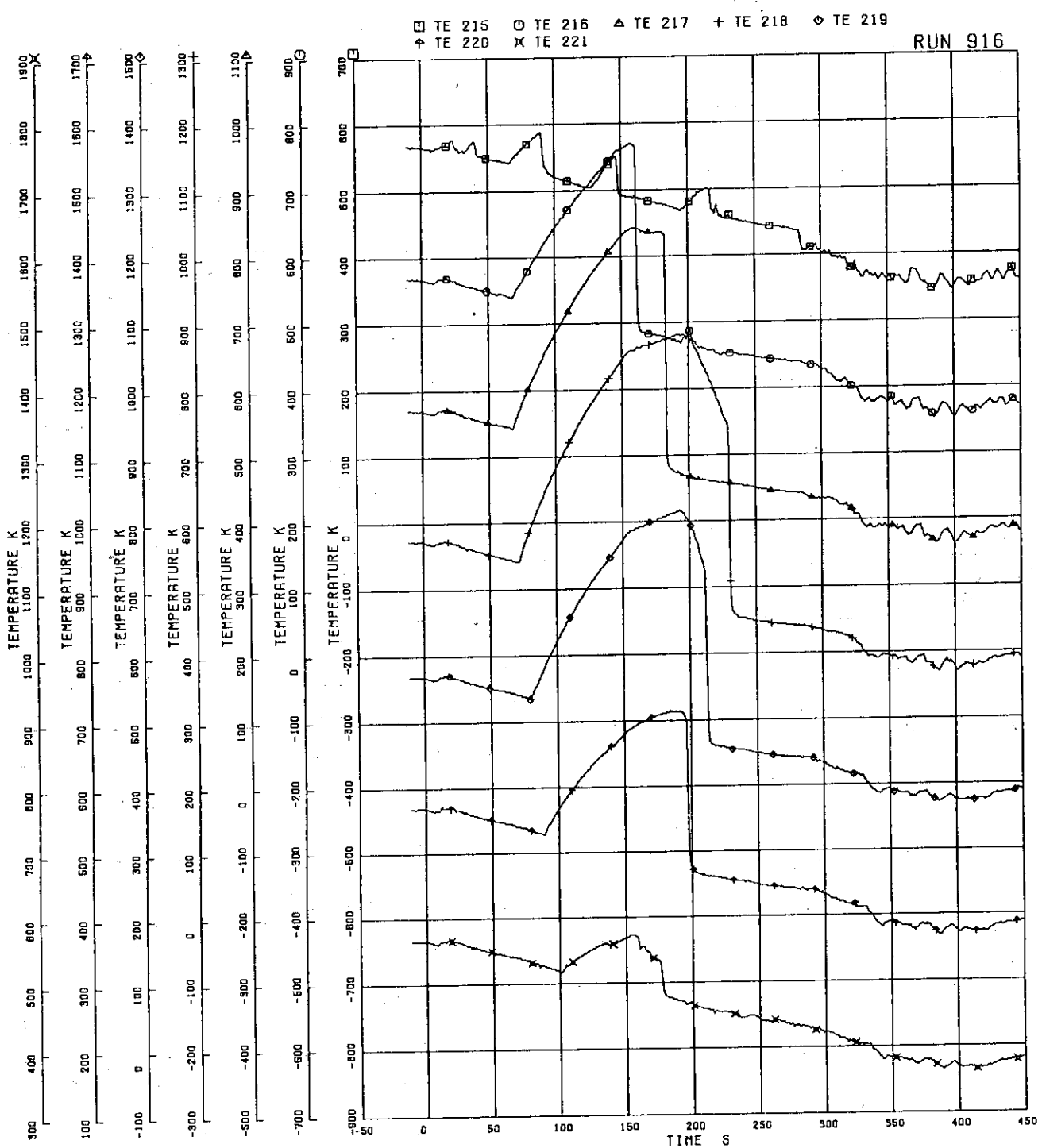


FIG. 5. 88 SURFACE TEMPERATURES OF FUEL ROD A13

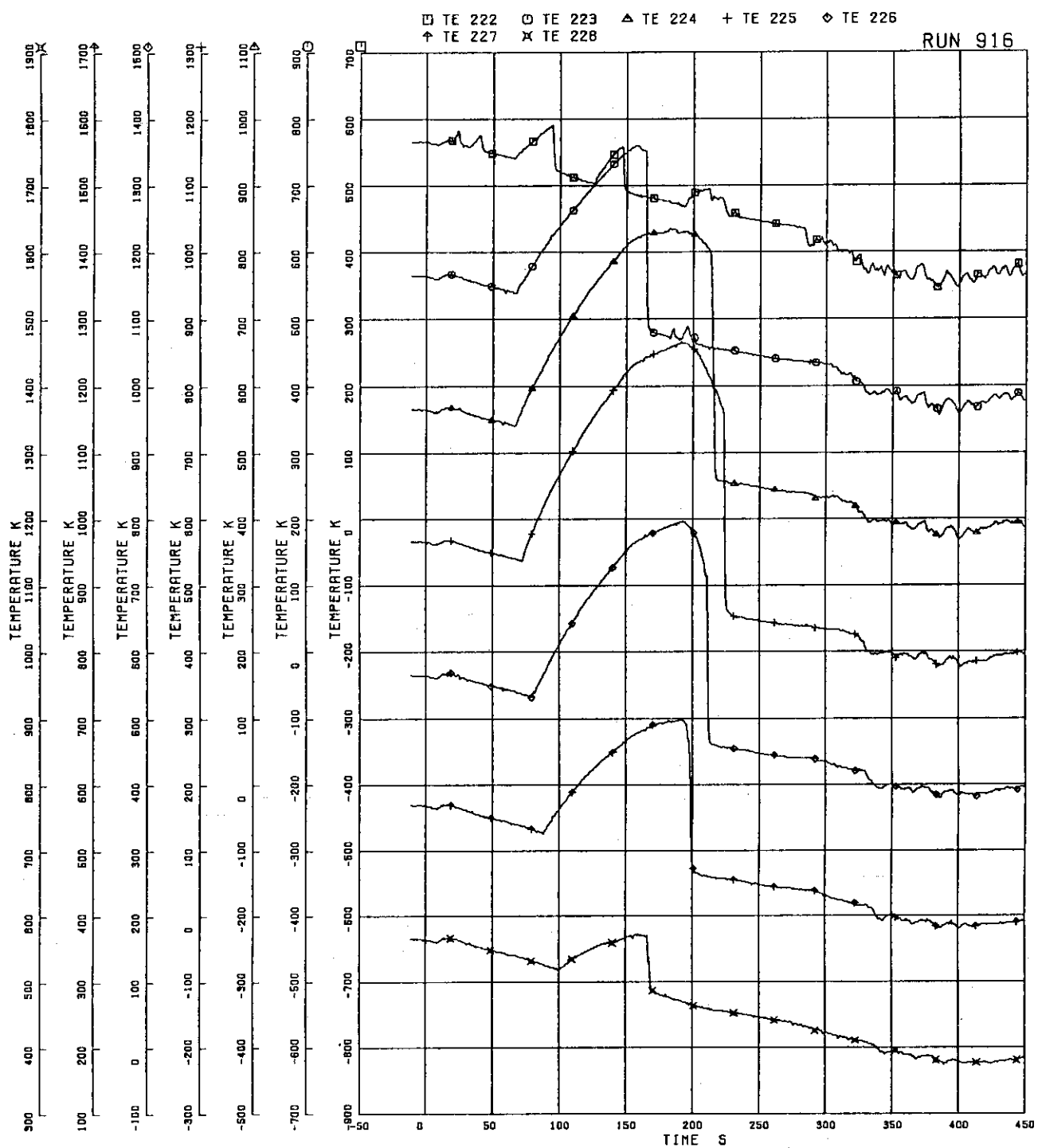


FIG. 5. 89 SURFACE TEMPERATURES OF FUEL ROD A14

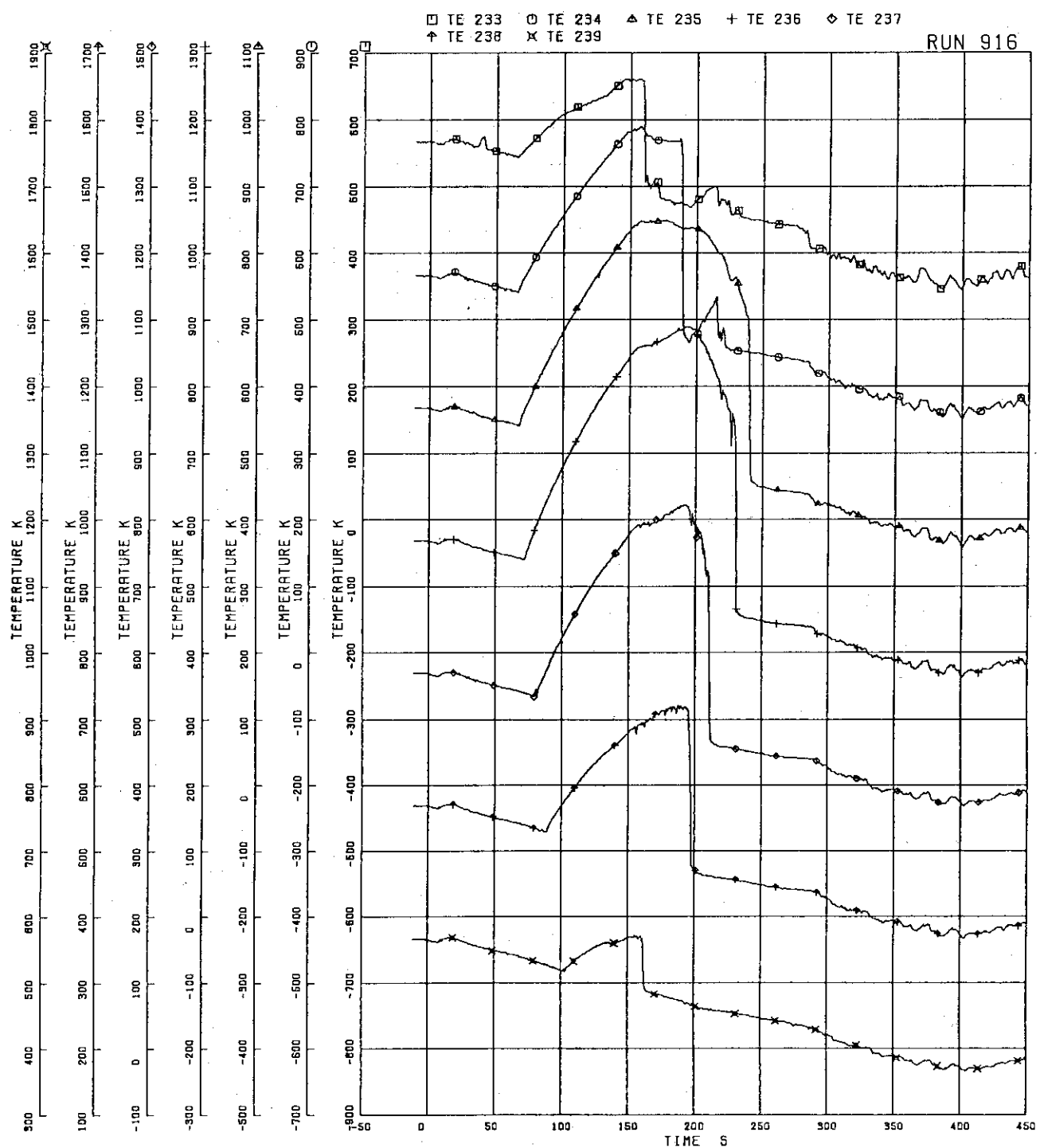


FIG. 5. 90 SURFACE TEMPERATURES OF FUEL ROD A22

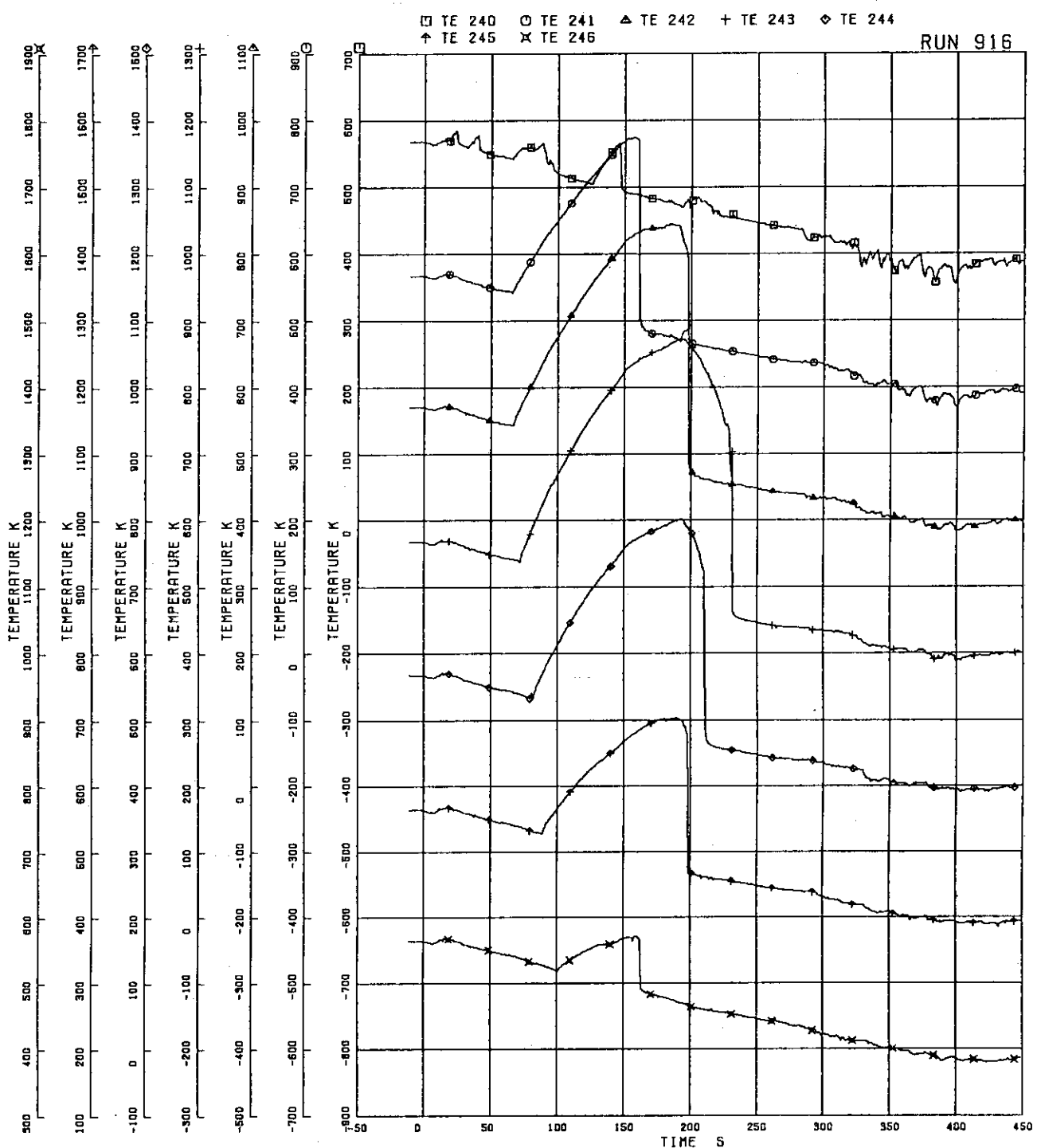


FIG. 5. 91 SURFACE TEMPERATURES OF FUEL ROD A24

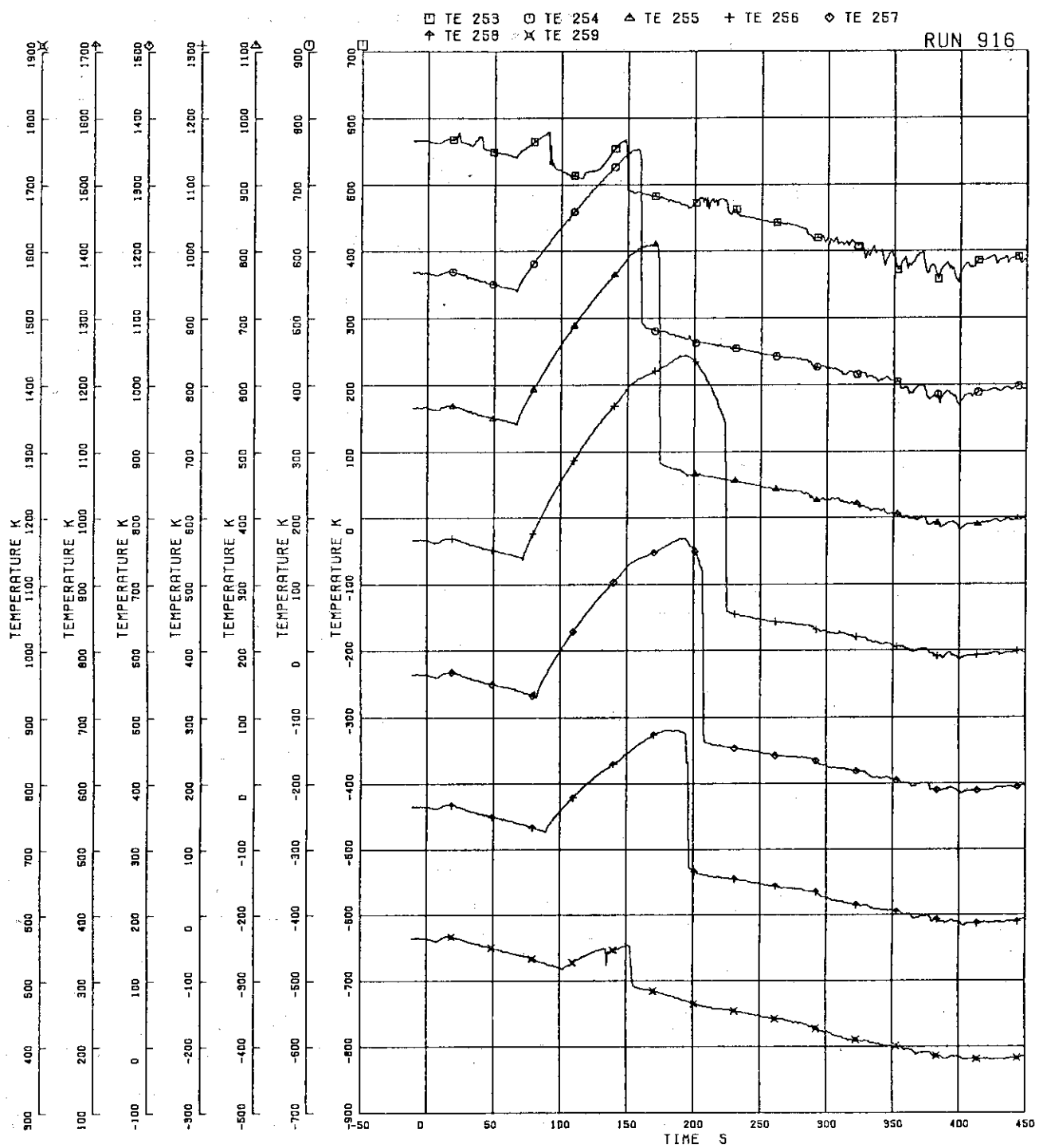


FIG. 5. 92 SURFACE TEMPERATURES OF FUEL ROD A33

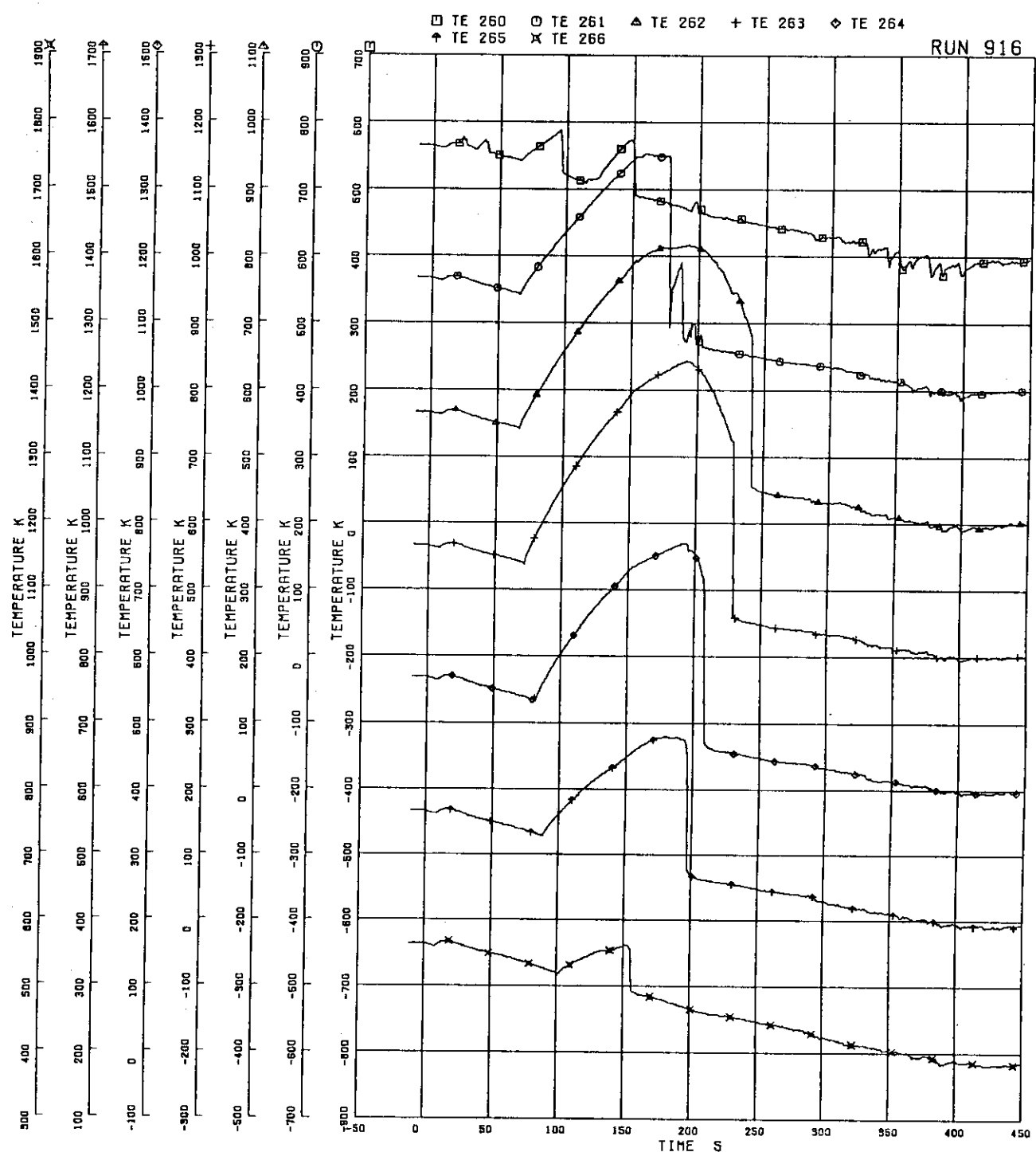


FIG. 5. 93 SURFACE TEMPERATURES OF FUEL ROD A34

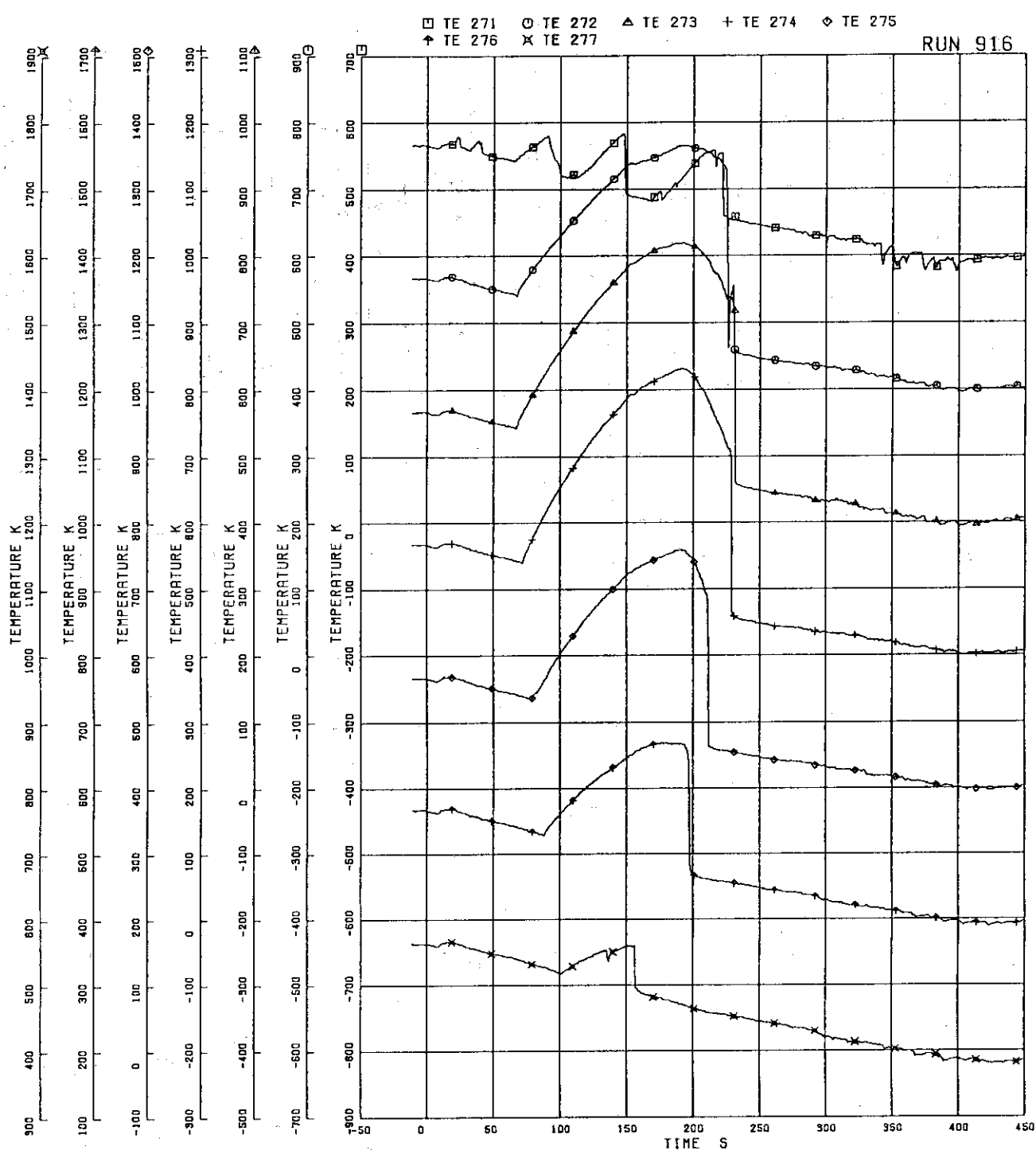


FIG. 5. 94 SURFACE TEMPERATURES OF FUEL ROD A44

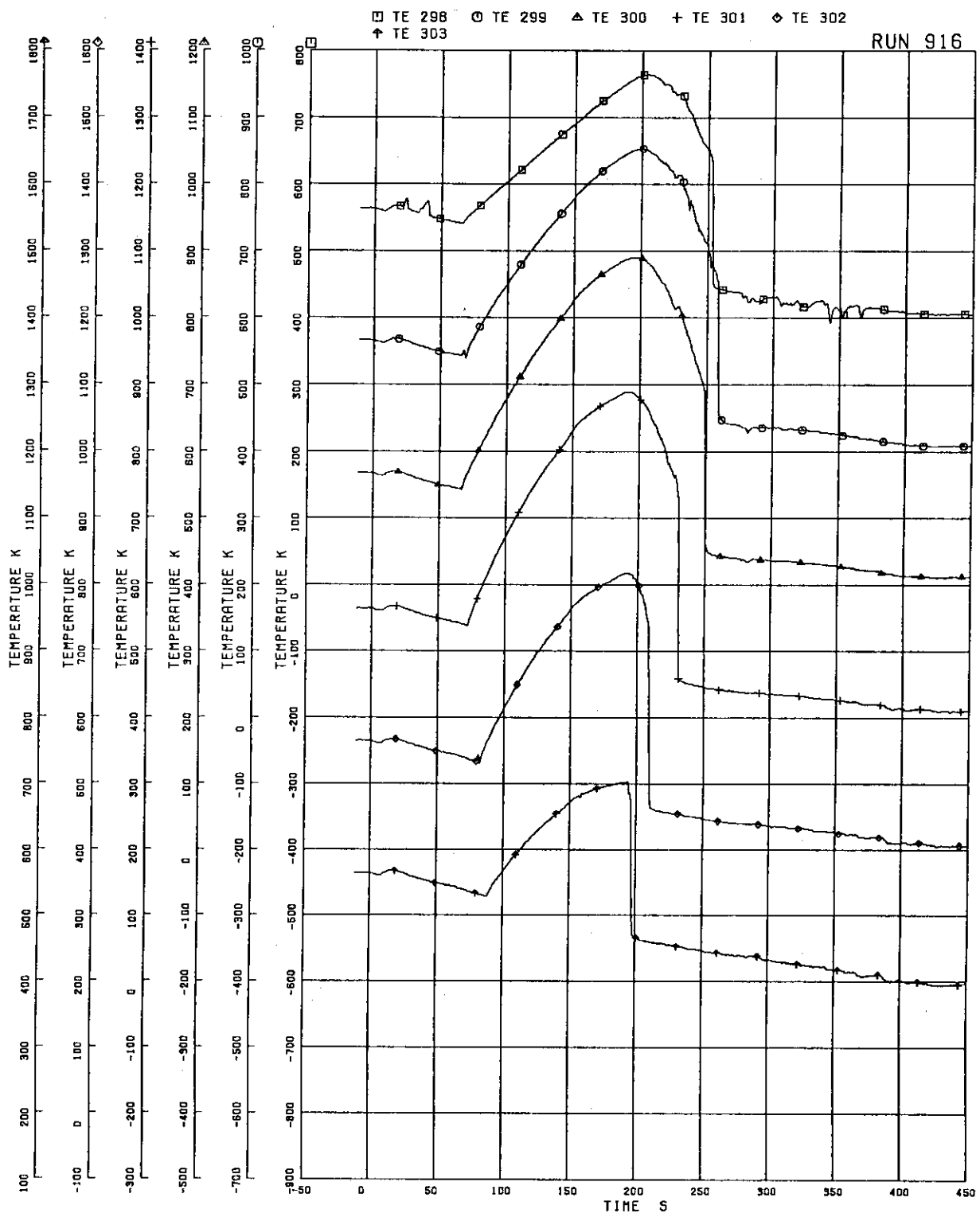


FIG. 5. 95 SURFACE TEMPERATURES OF FUEL ROD A77

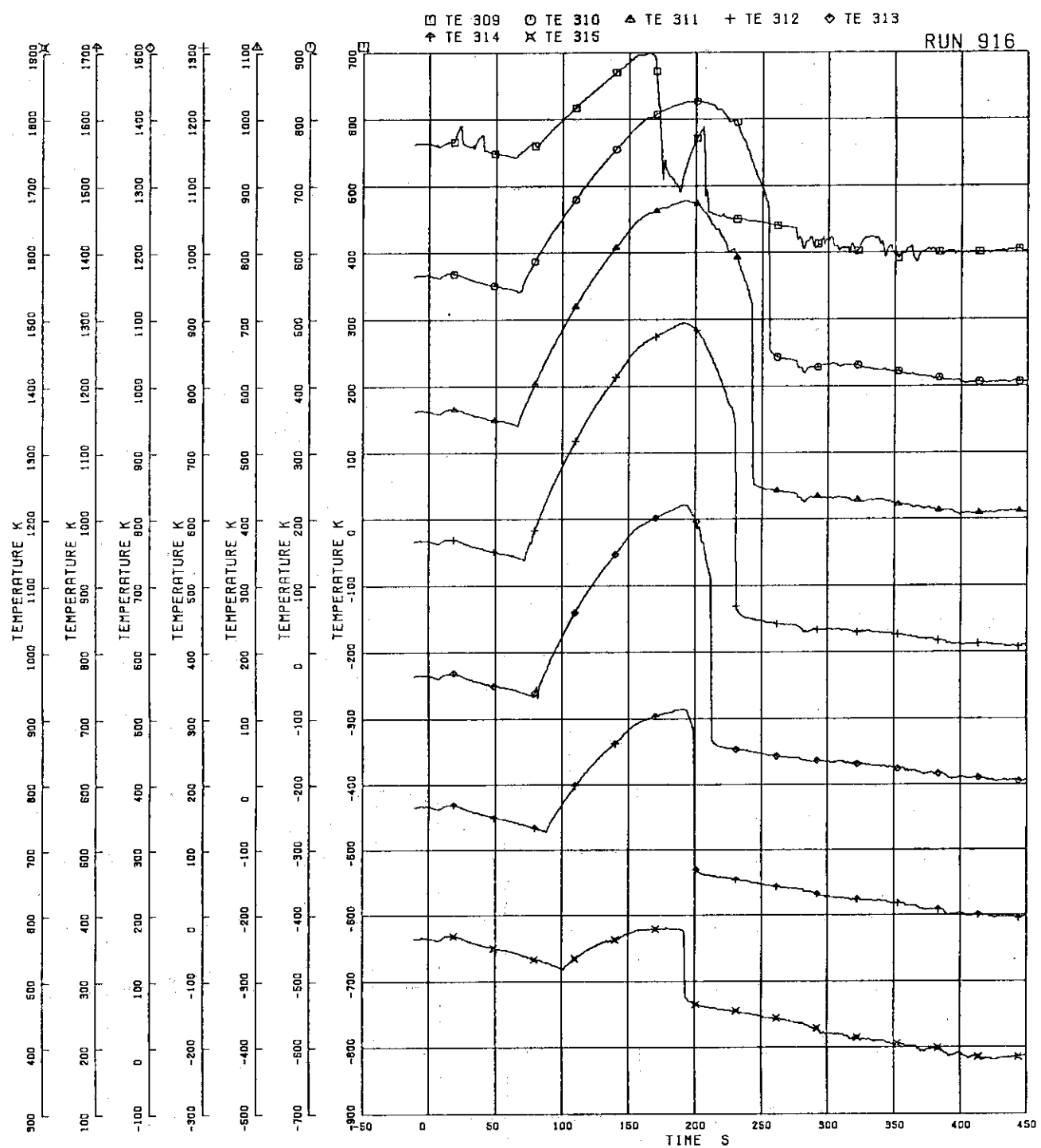


FIG. 5-96 SURFACE TEMPERATURES OF FUEL ROD A85

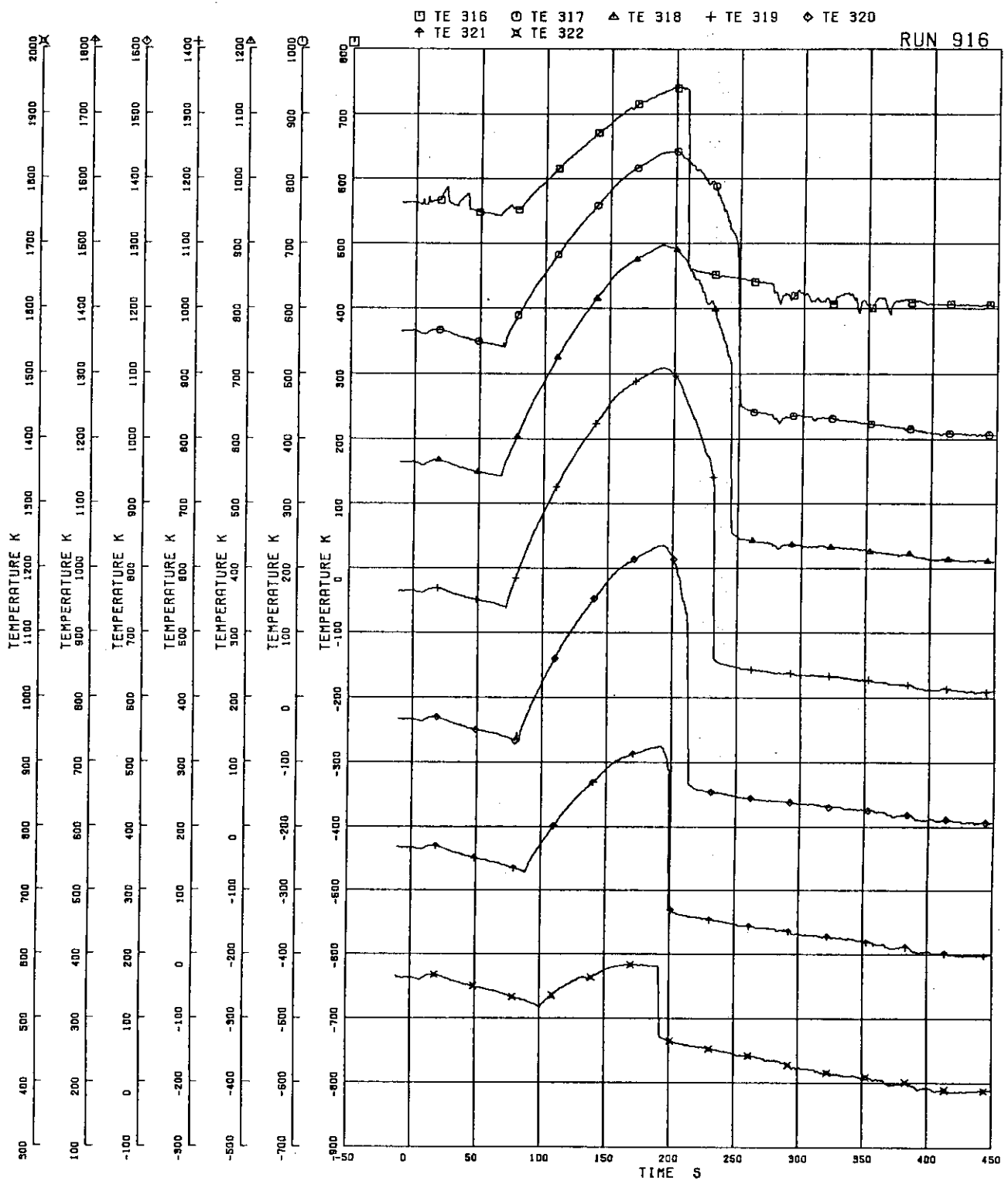


FIG. 5. 97 SURFACE TEMPERATURES OF FUEL ROD A87

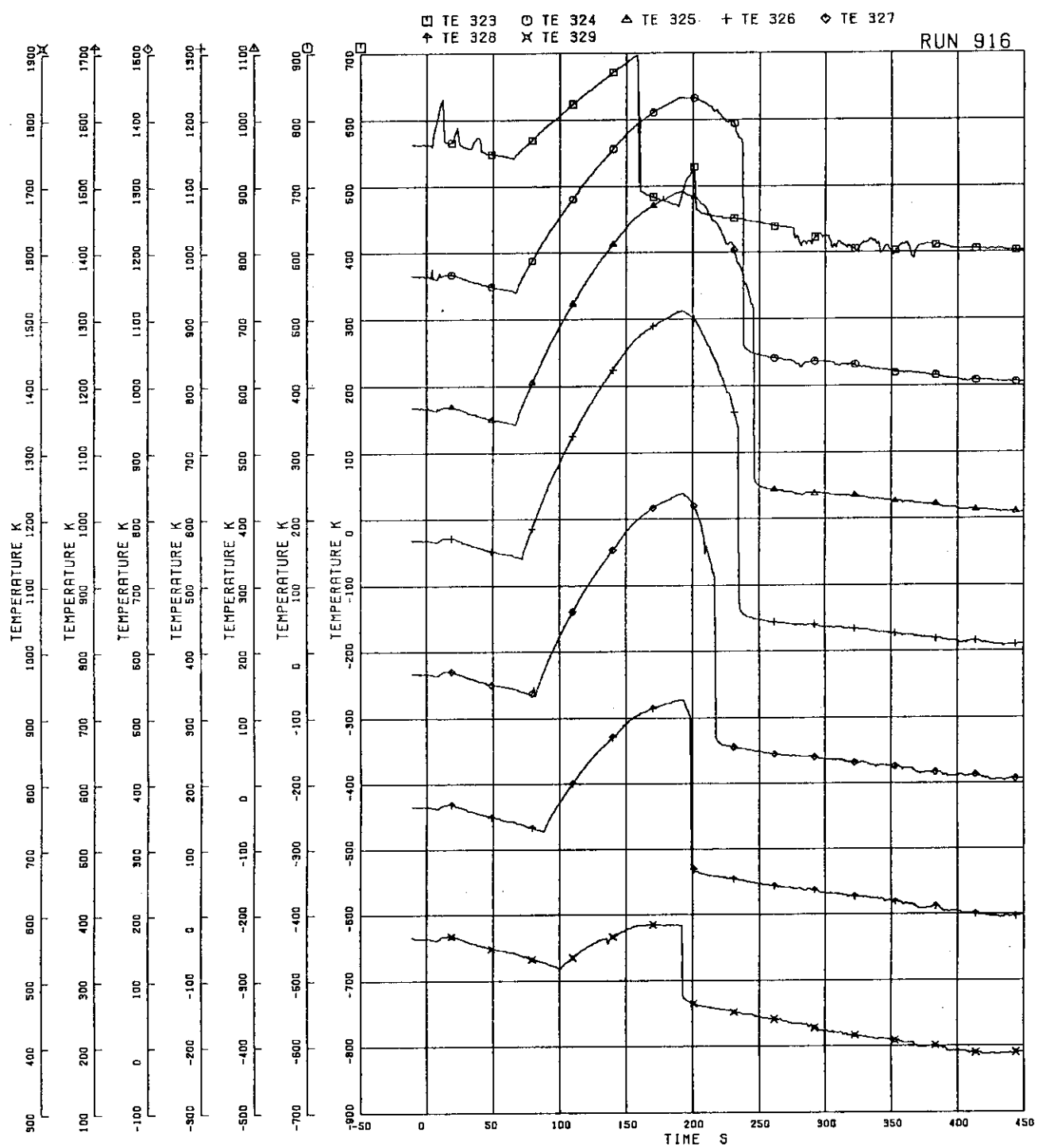


FIG. 5. 98 SURFACE TEMPERATURES OF FUEL ROD A88

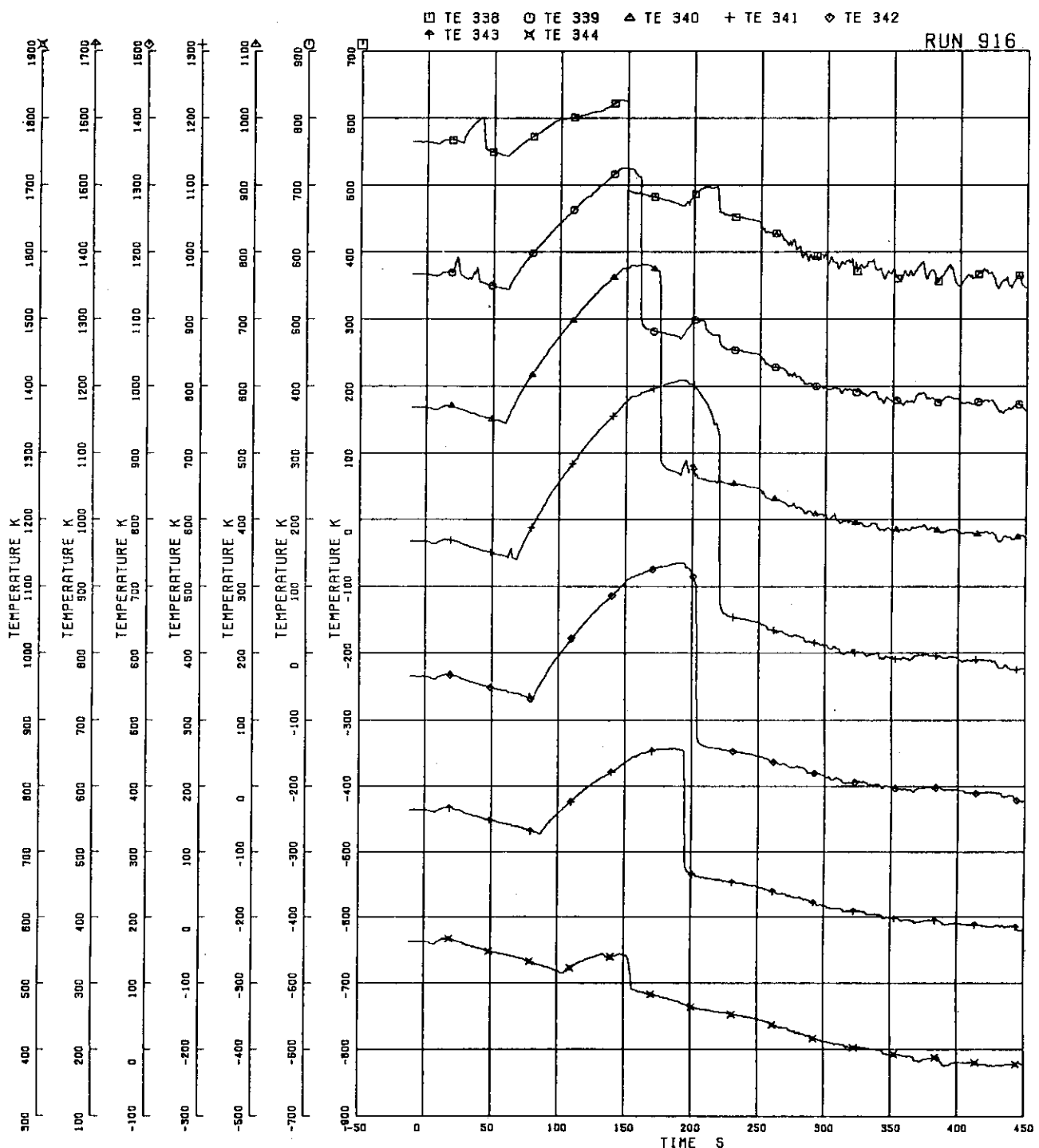


FIG. 5. 99 SURFACE TEMPERATURES OF FUEL ROD B22

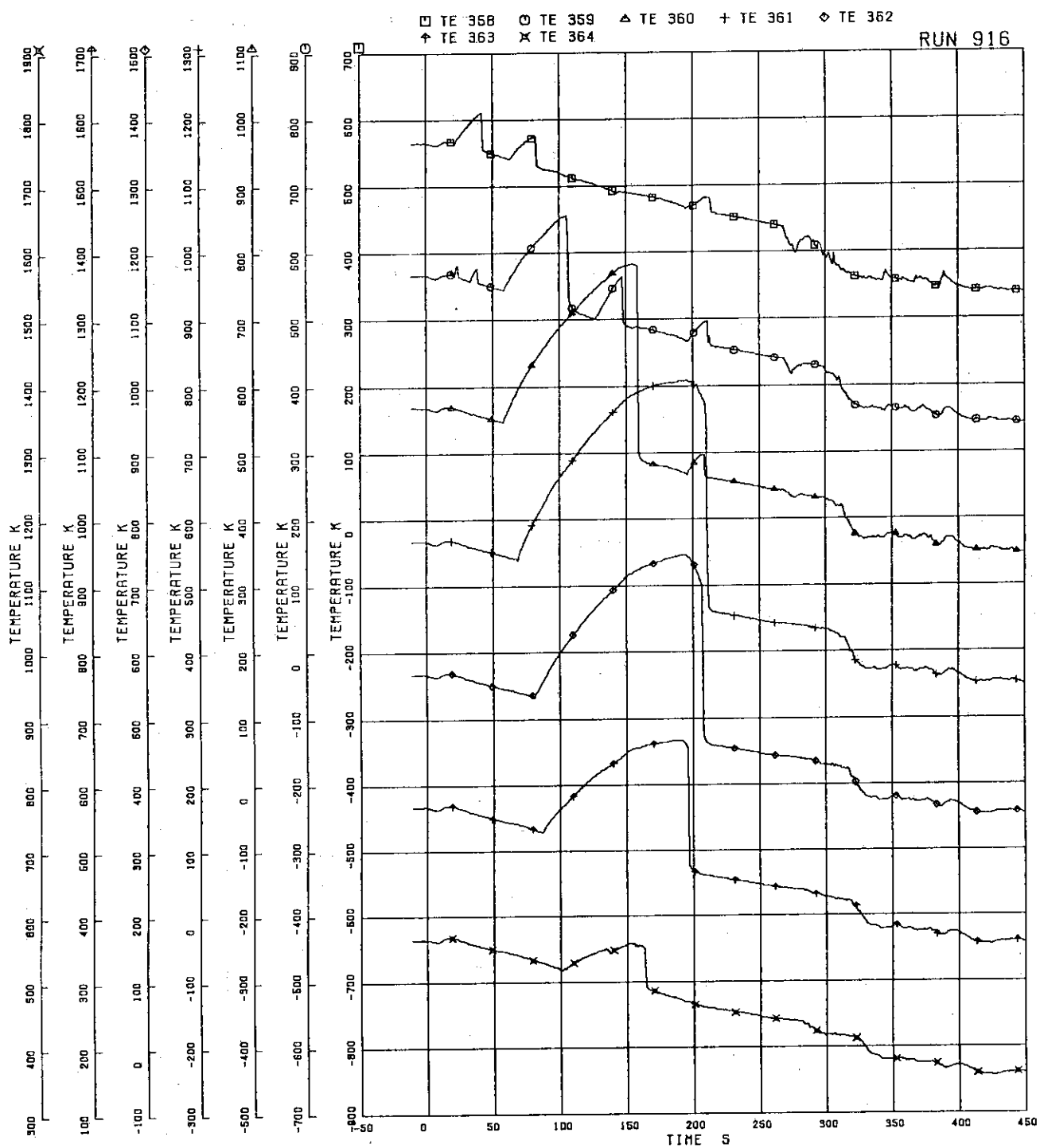


FIG.5.100. SURFACE TEMPERATURES OF FUEL ROD C11

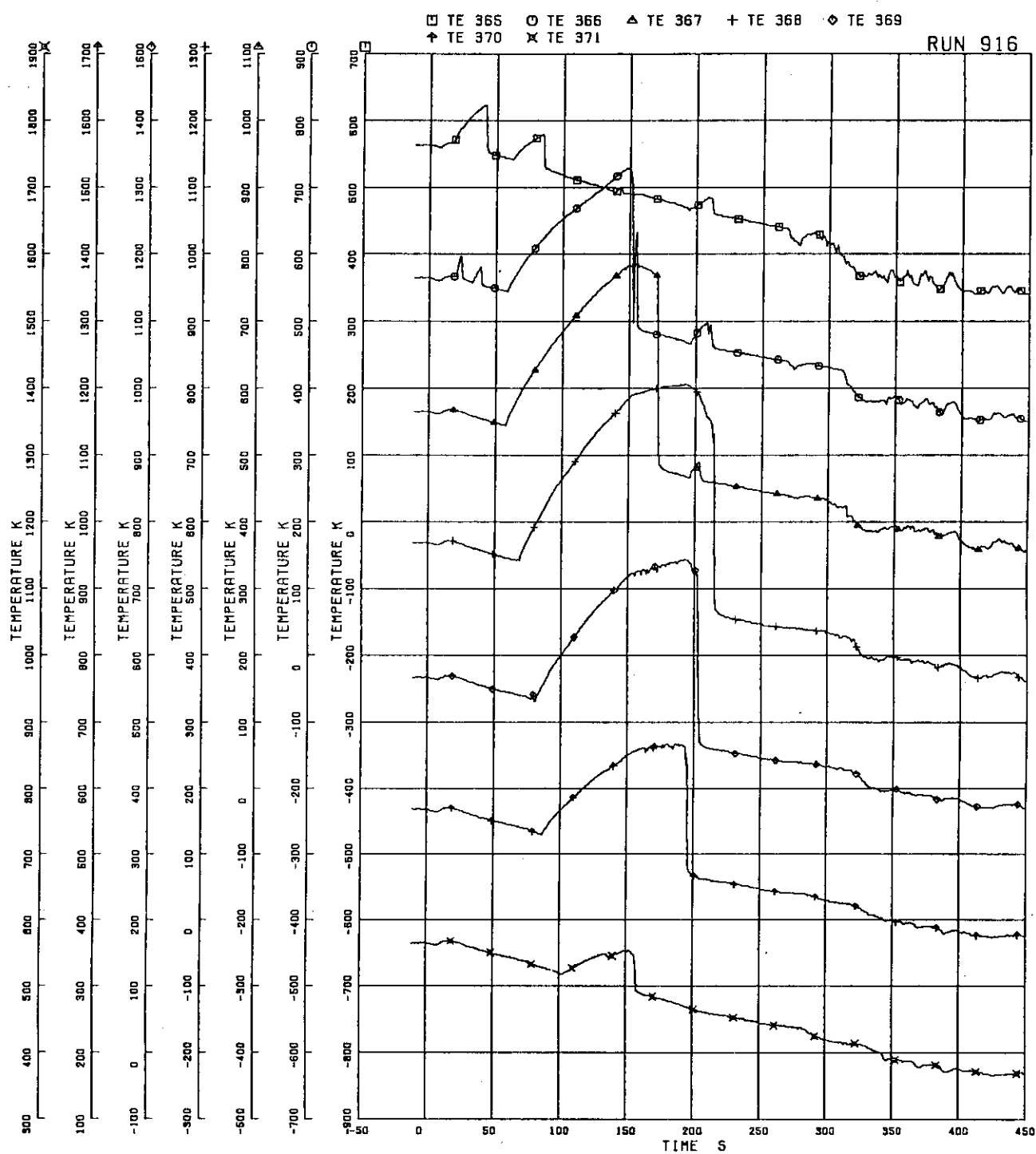


FIG. 5.101 SURFACE TEMPERATURES OF FUEL ROD C13

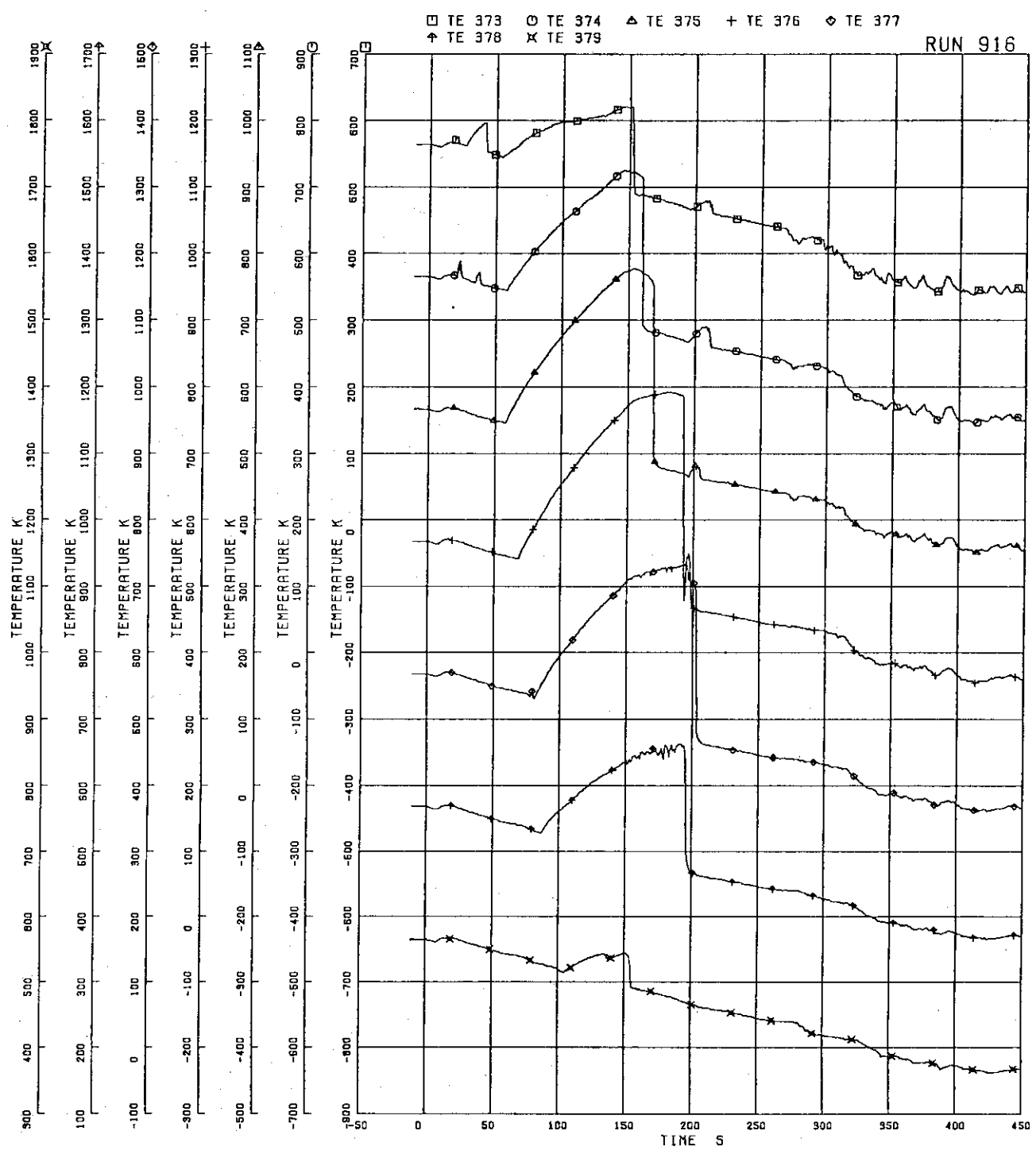


FIG.5.102 SURFACE TEMPERATURES OF FUEL ROD C22

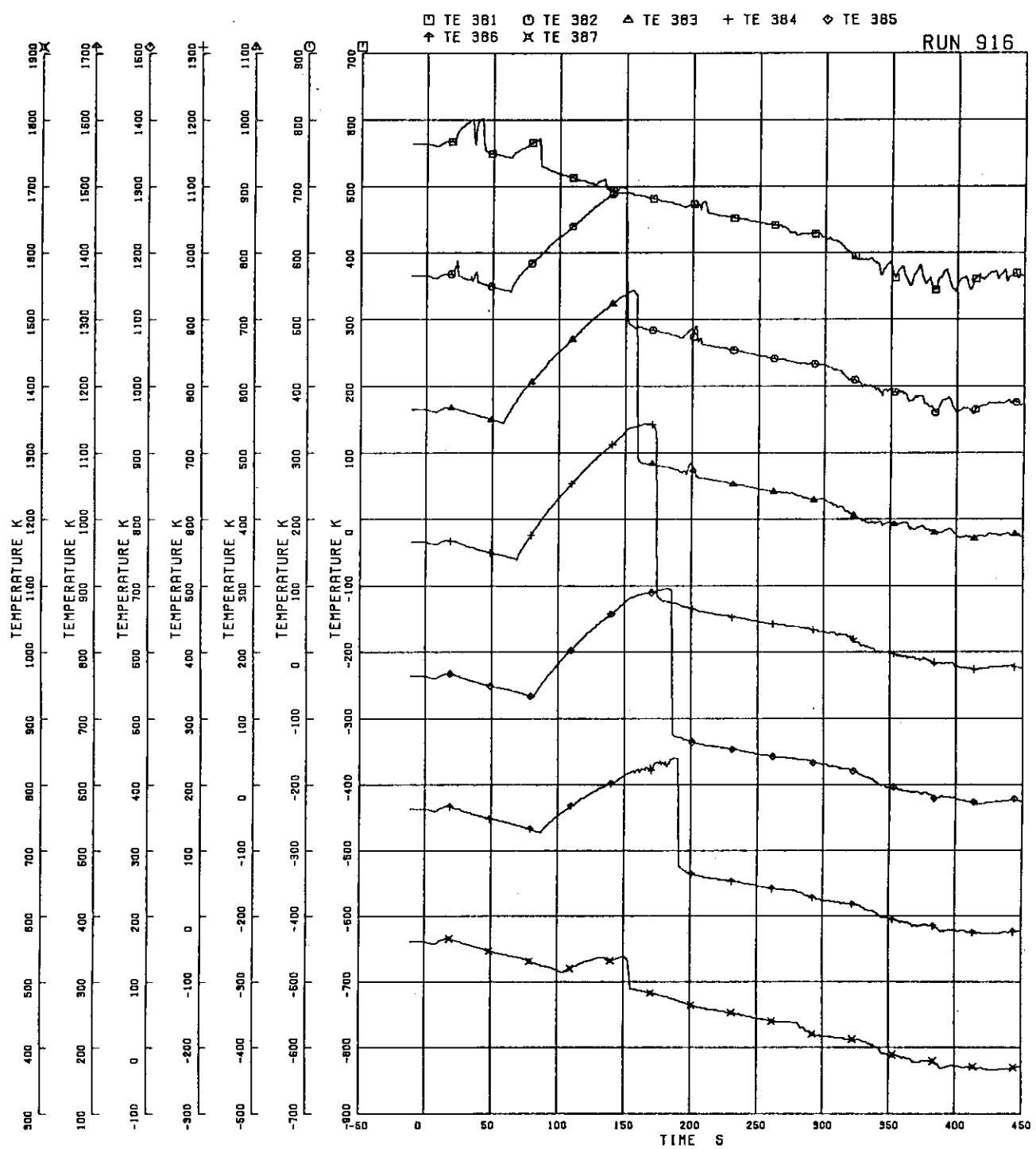


FIG.5.103 SURFACE TEMPERATURES OF FUEL ROD C33

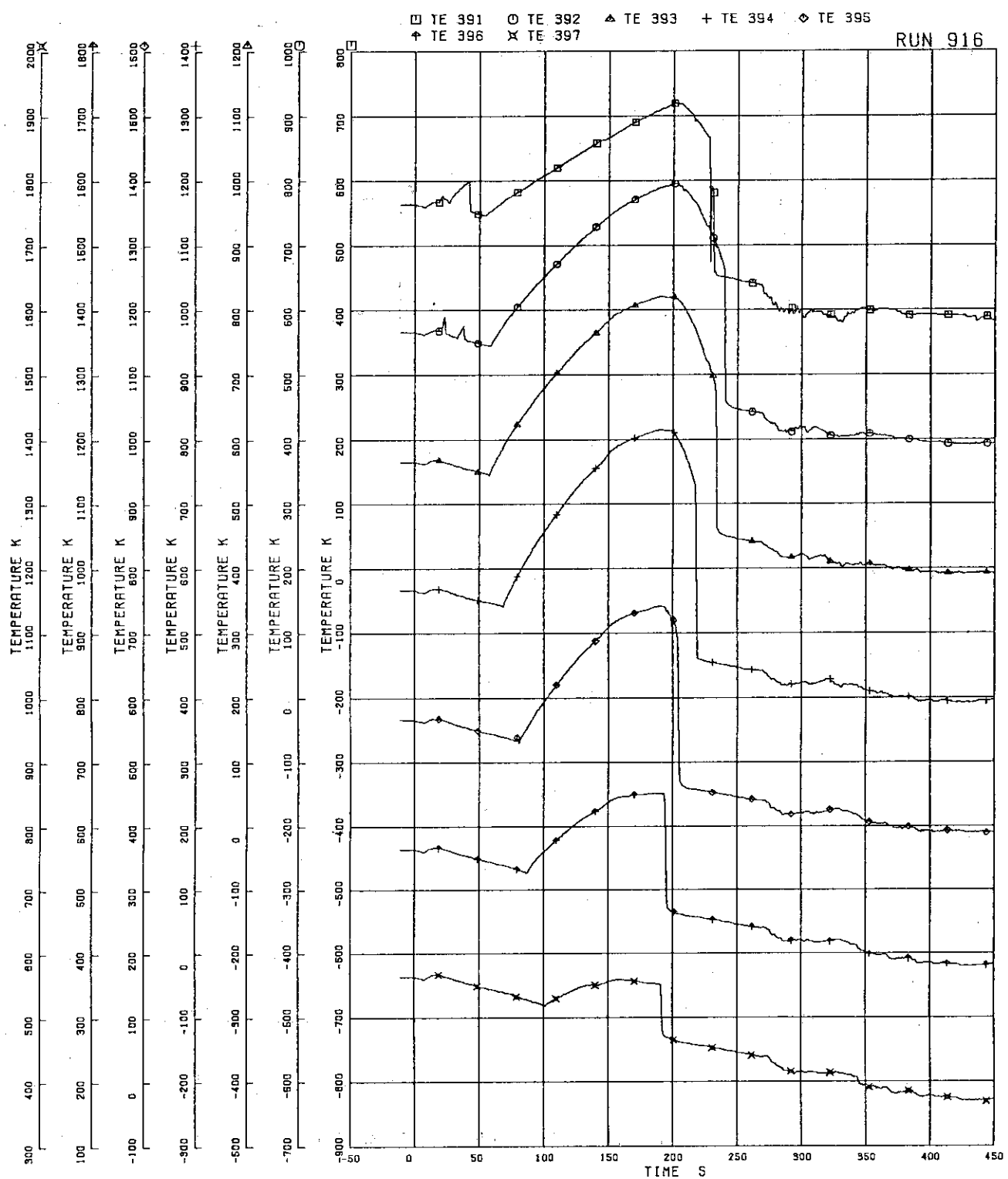


FIG.5.104 SURFACE TEMPERATURES OF FUEL ROD C77

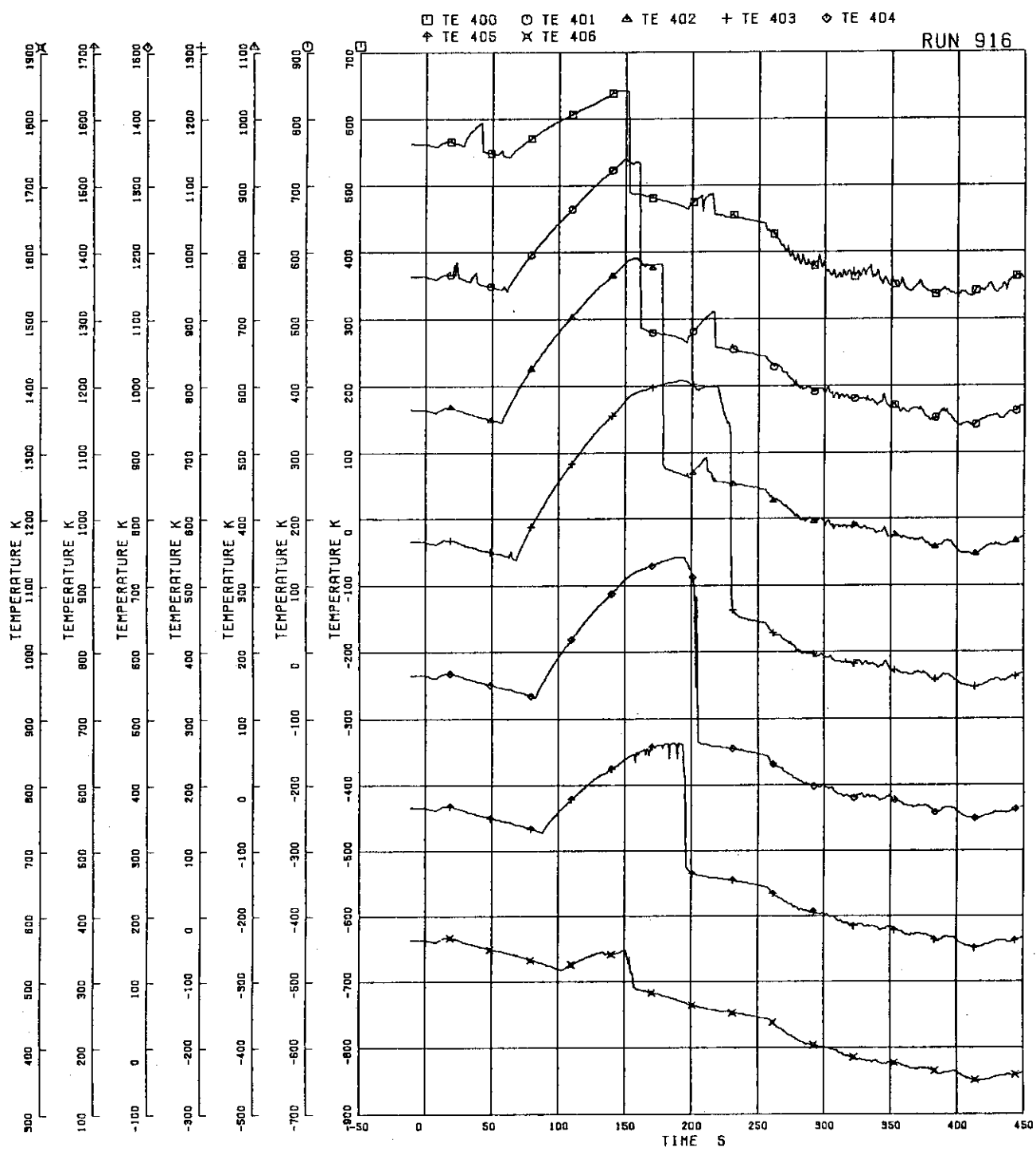


FIG.5.105 SURFACE TEMPERATURES OF FUEL ROD D22

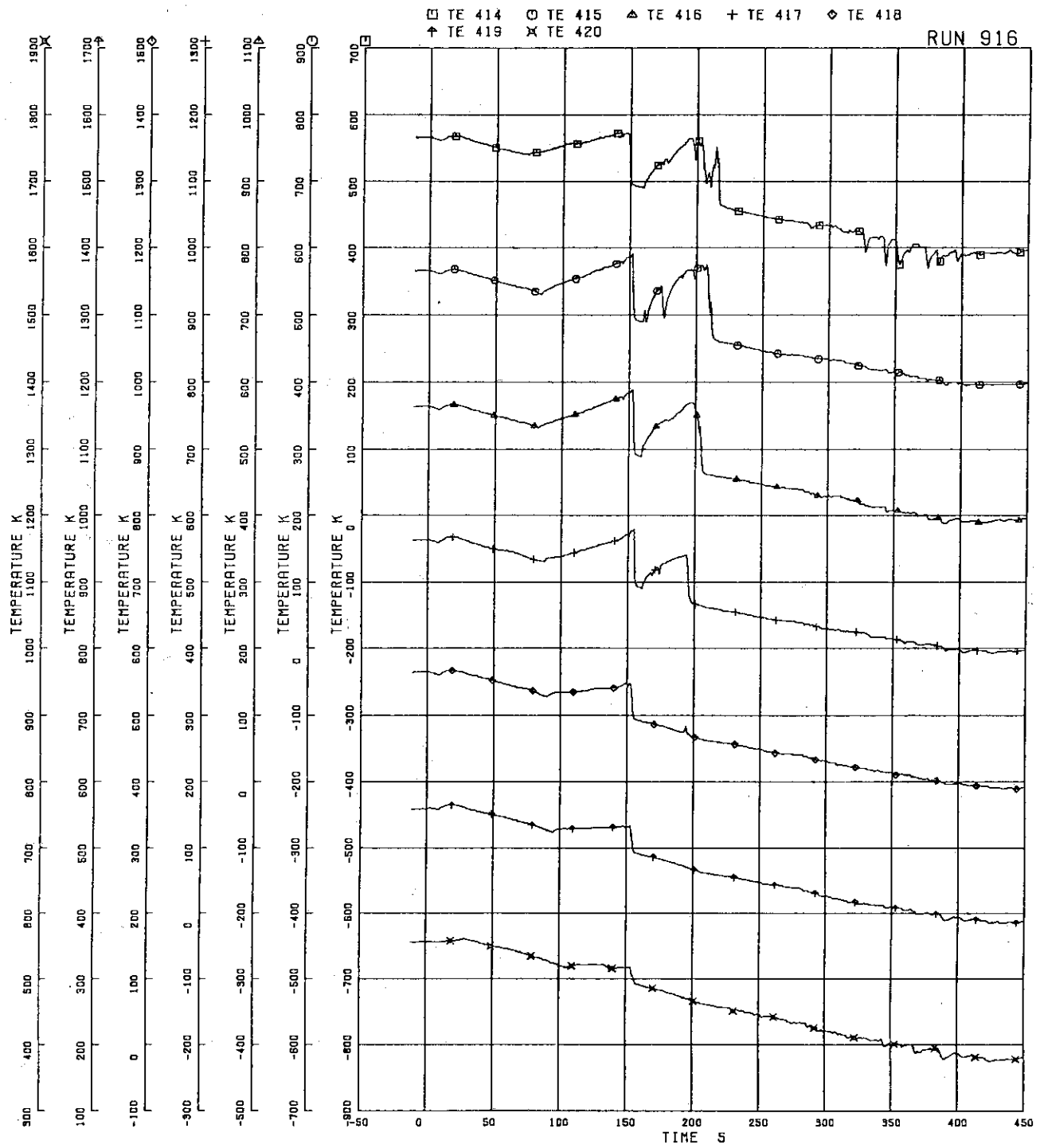


FIG.5.106 SURFACE TEMPERATURES OF
WATER ROD SIMULATOR A45

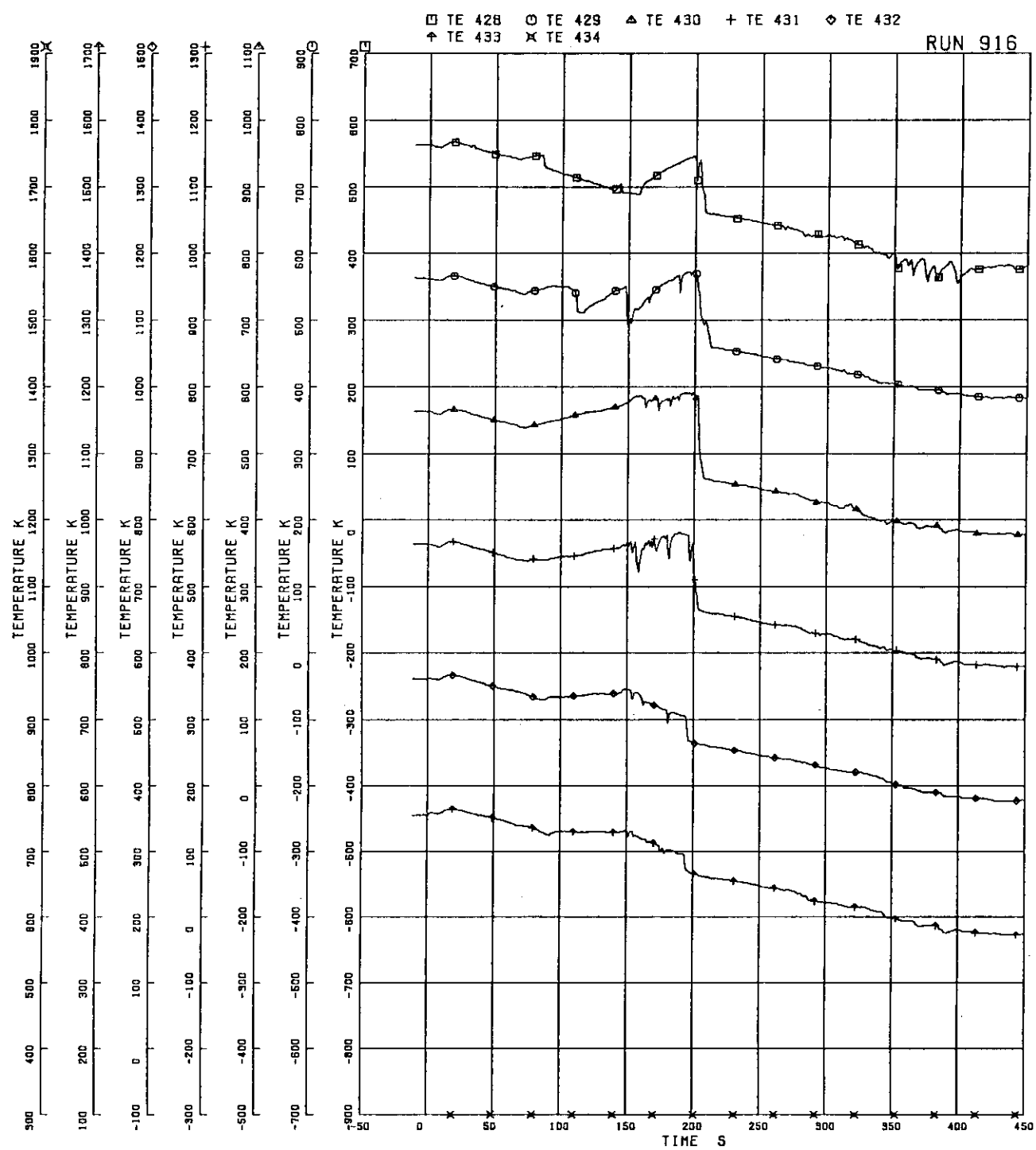


FIG.5.107 SURFACE TEMPERATURES OF
WATER ROD SIMULATOR C45

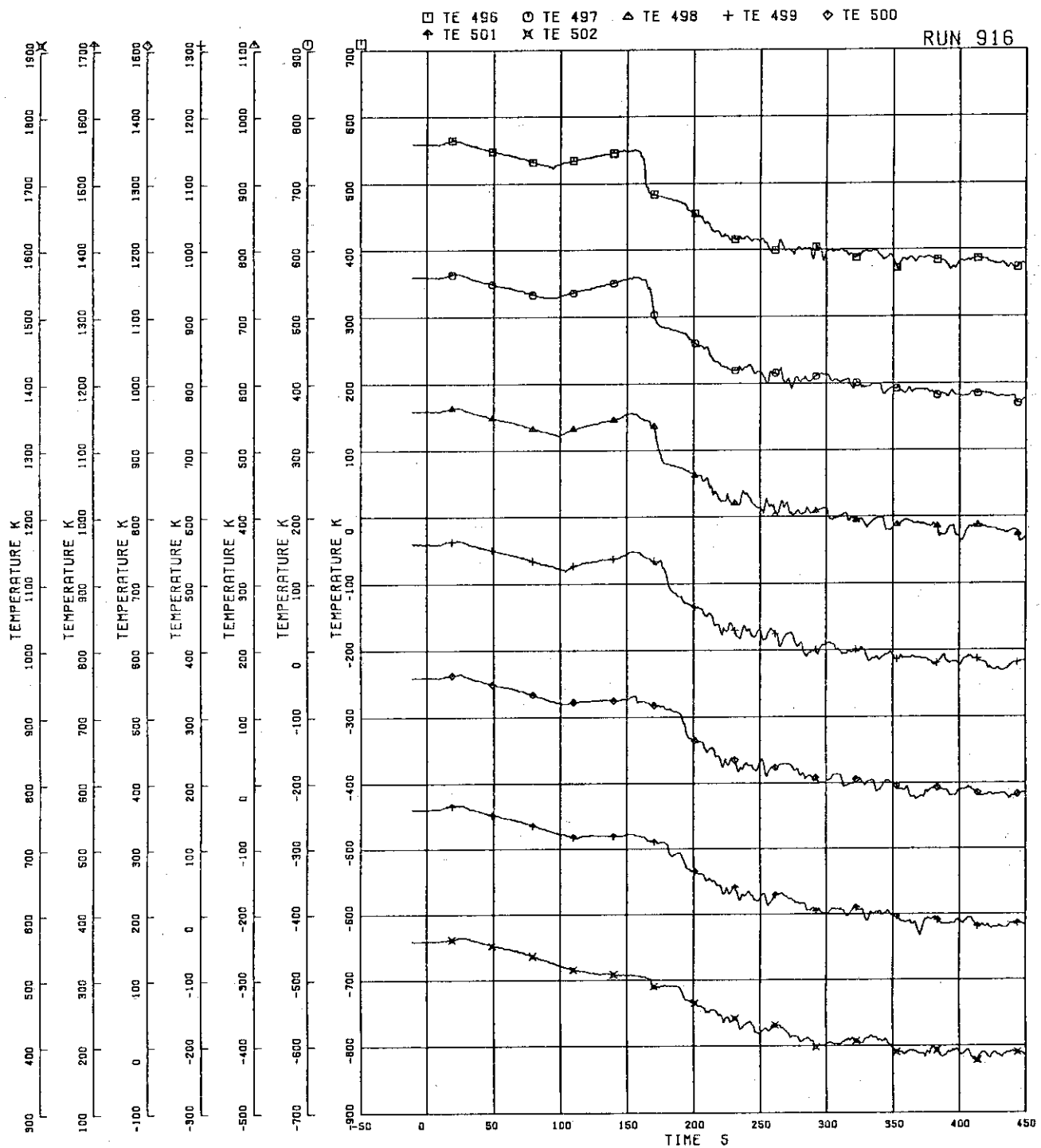


FIG.5.108 INNER SURFACE TEMPERATURES OF CHANNEL BOX A, LOCATION A1

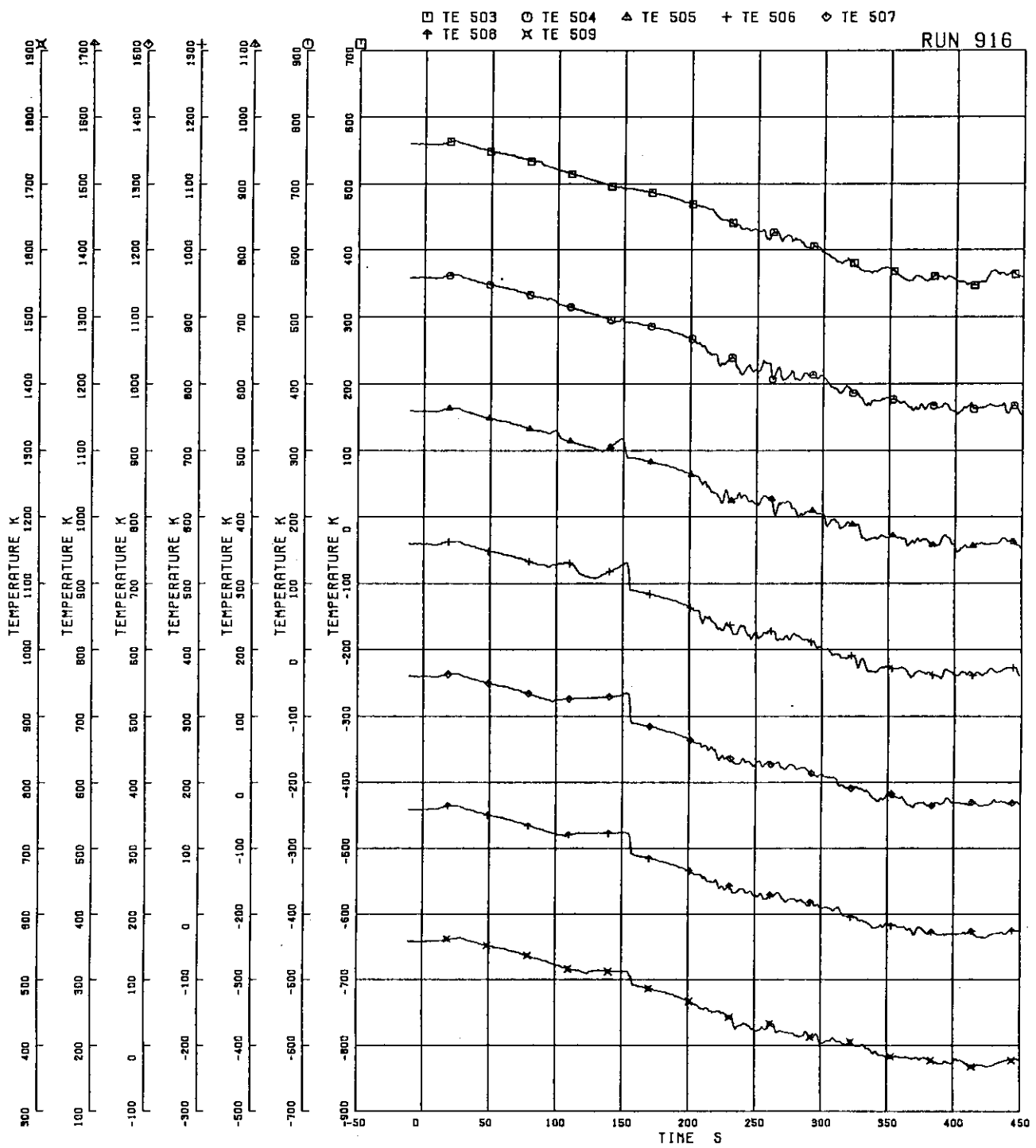


FIG.5.109 INNER SURFACE TEMPERATURES OF CHANNEL BOX A, LOCATION A2

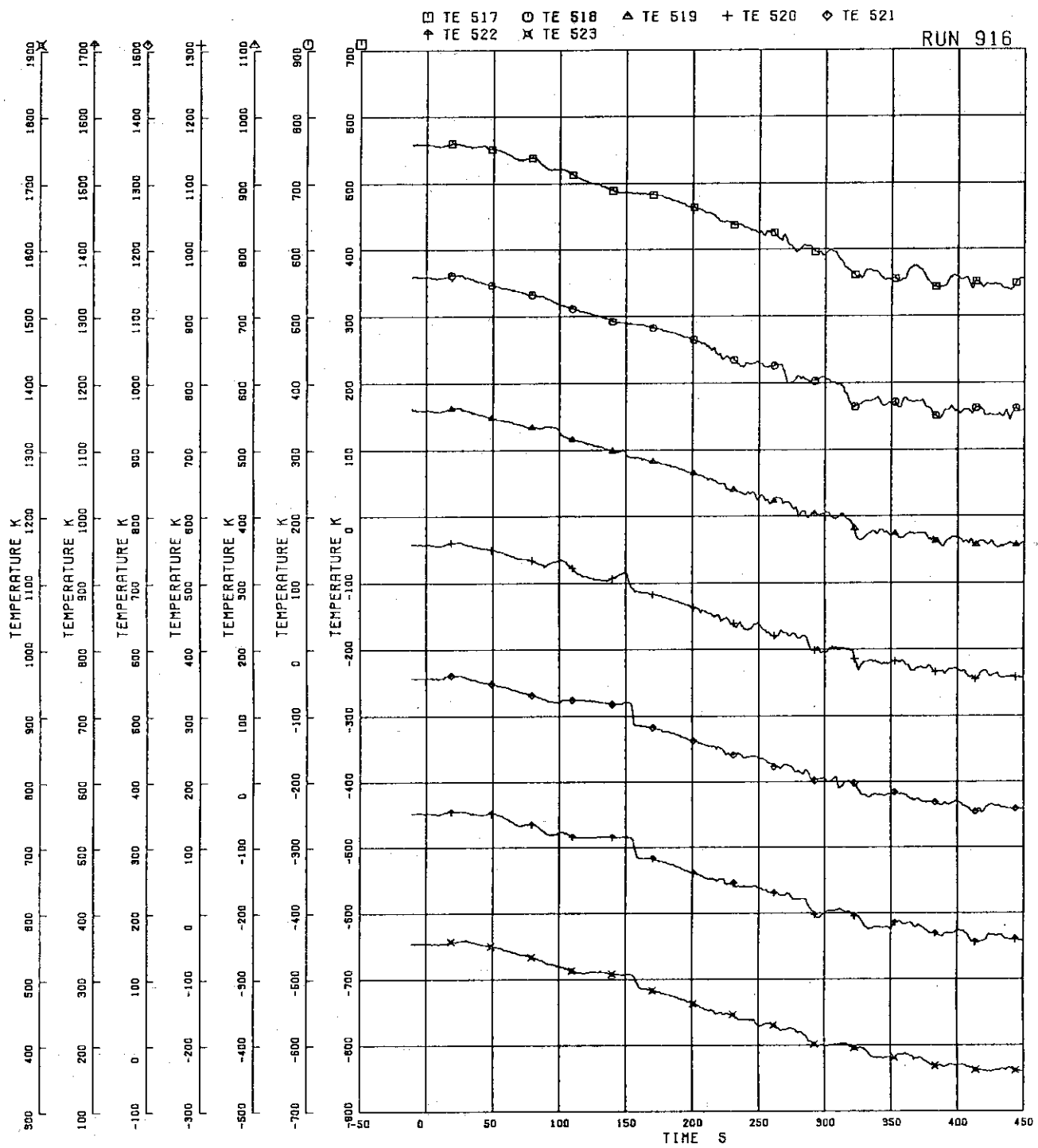


FIG.5.110 INNER SURFACE TEMPERATURES OF CHANNEL BOX C

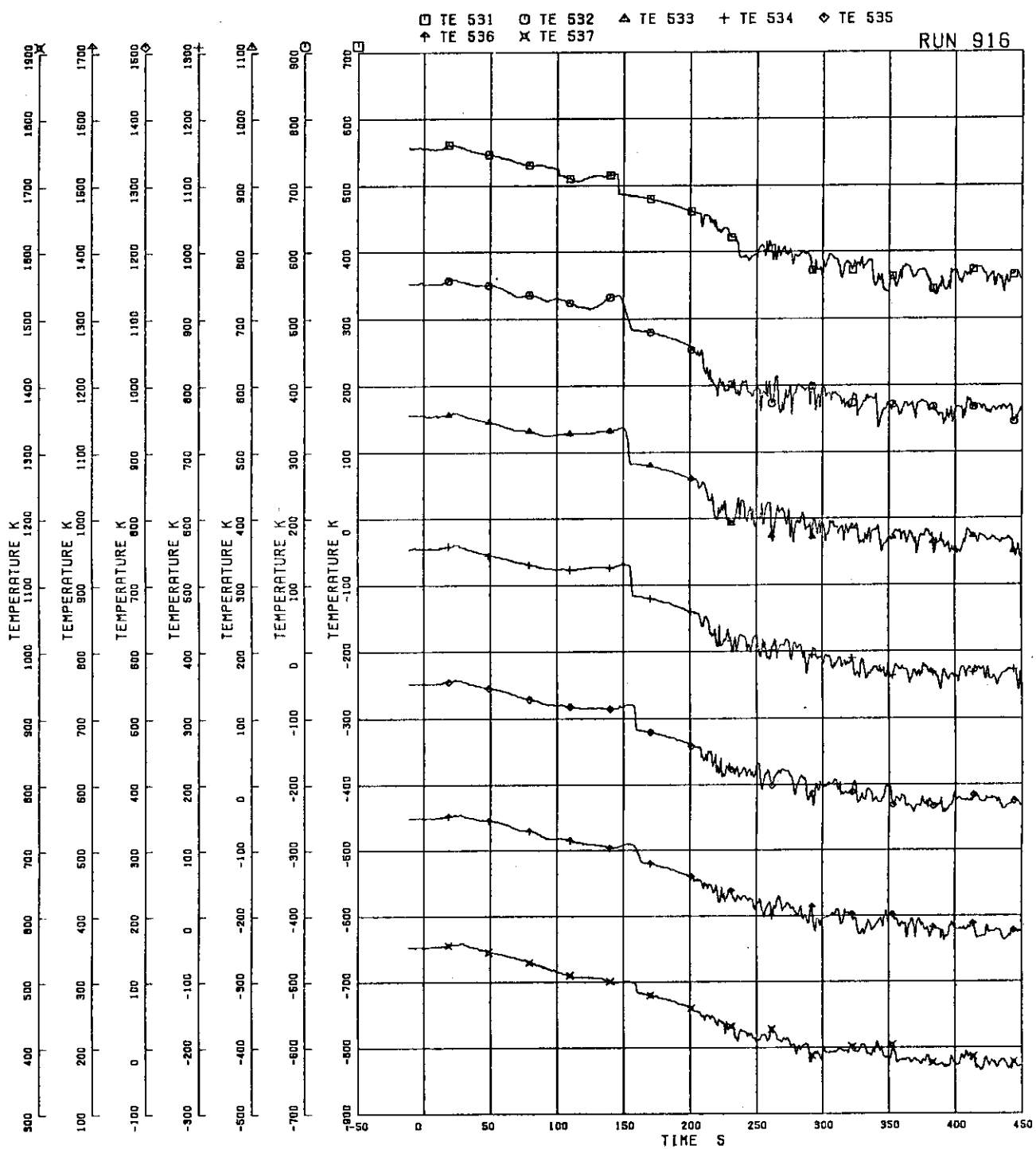


FIG.5.111 OUTER SURFACE TEMPERATURES OF CHANNEL BOX A

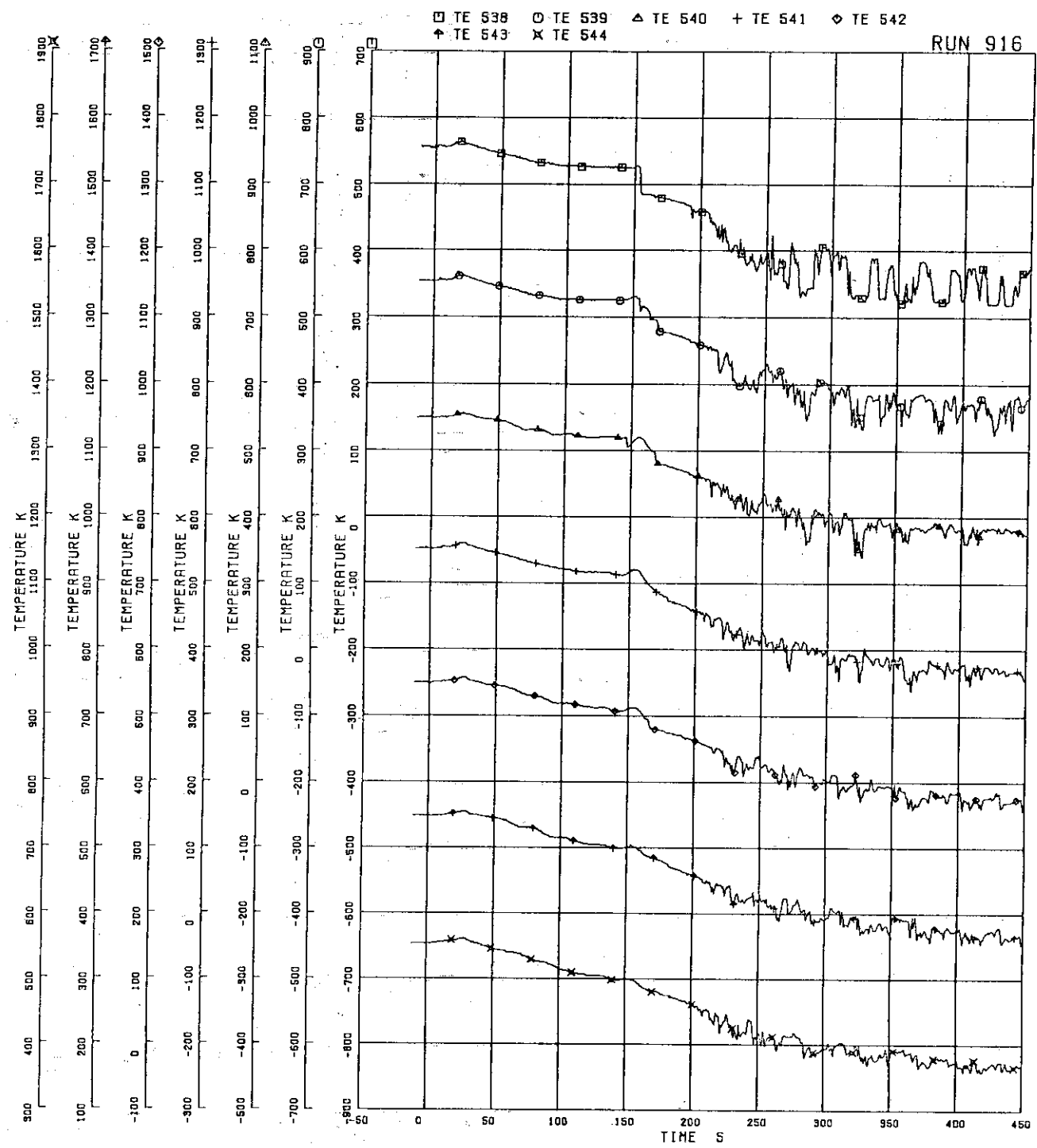


FIG.5.112 OUTER SURFACE TEMPERATURES OF CHANNEL BOX C

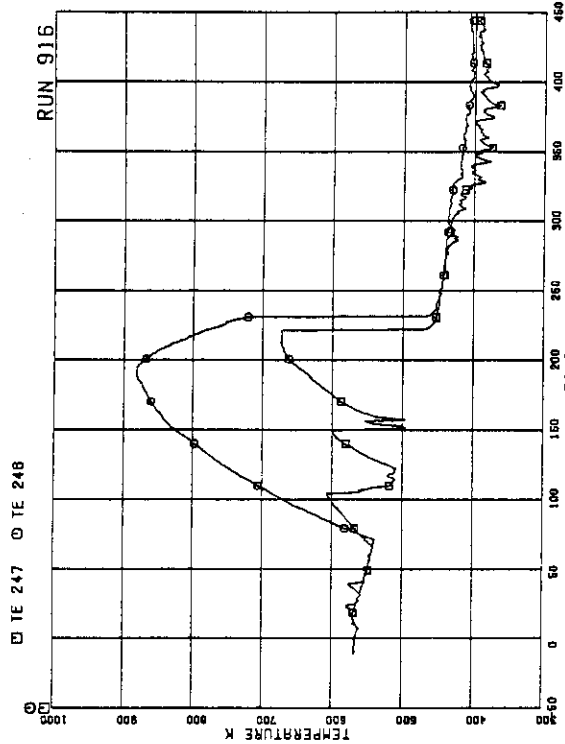


FIG. 5.115 SURFACE TEMPERATURES OF FUEL ROD A26
AT POSITIONS 1 AND 4

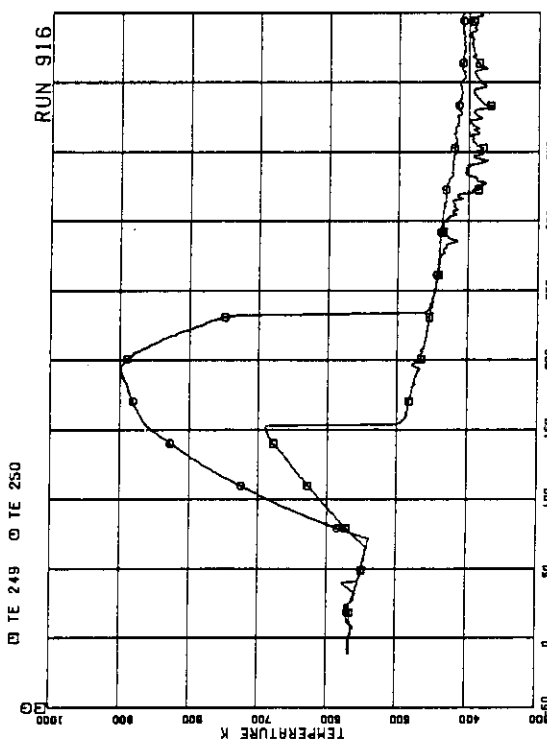


FIG. 5.116 SURFACE TEMPERATURES OF FUEL ROD A26
AT POSITIONS 1 AND 4

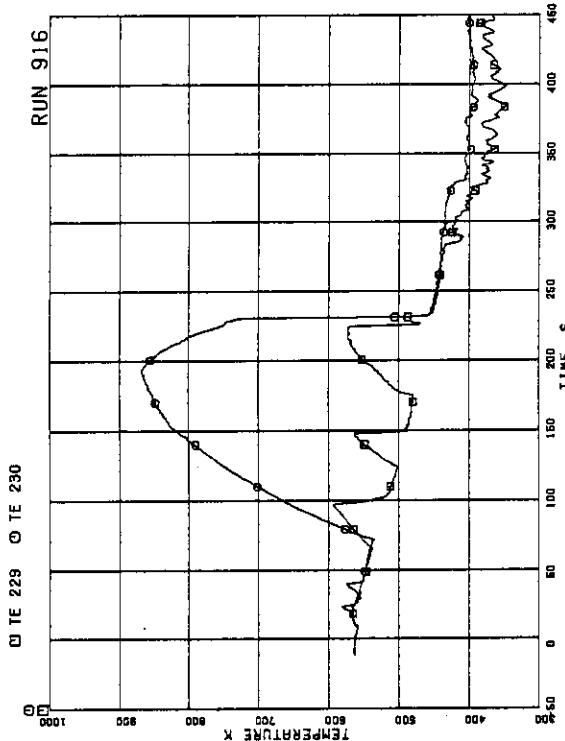


FIG. 5.113 SURFACE TEMPERATURES OF FUEL ROD A15
AT POSITIONS 1 AND 4

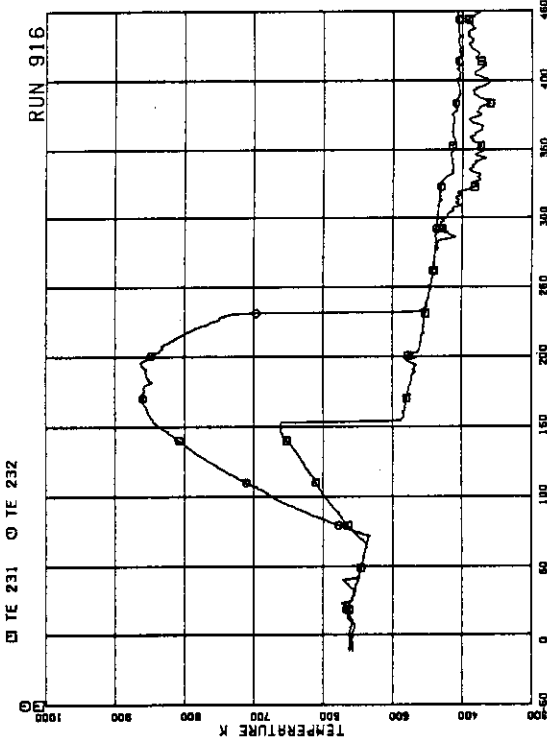


FIG. 5.114 SURFACE TEMPERATURES OF FUEL ROD A17
AT POSITIONS 1 AND 4

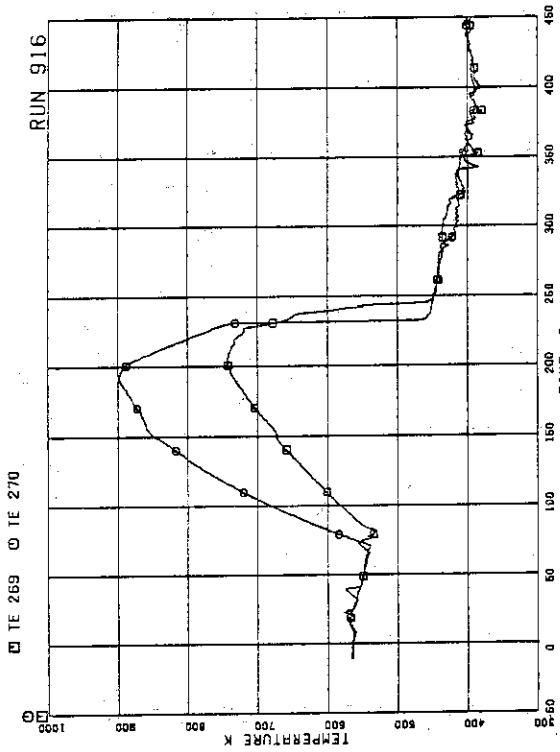


FIG. 5.119 SURFACE TEMPERATURE OF FUEL ROD R42
AT POSITION 1 AND 4

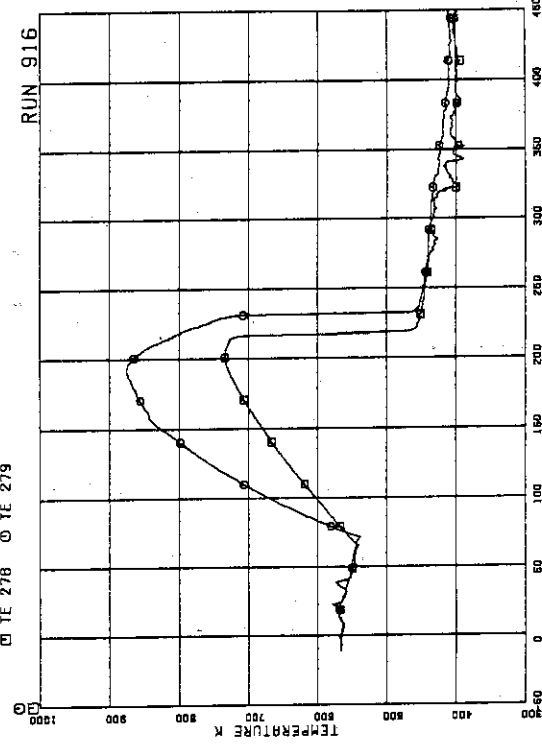


FIG. 5.120 SURFACE TEMPERATURES OF FUEL ROD R42
AT POSITIONS 1 AND 4

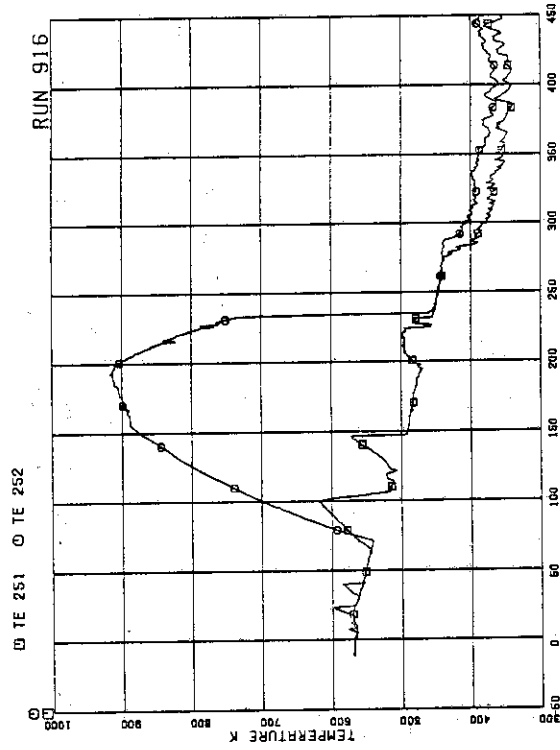


FIG. 5.117 SURFACE TEMPERATURES OF FUEL ROD R31
AT POSITIONS 1 AND 4

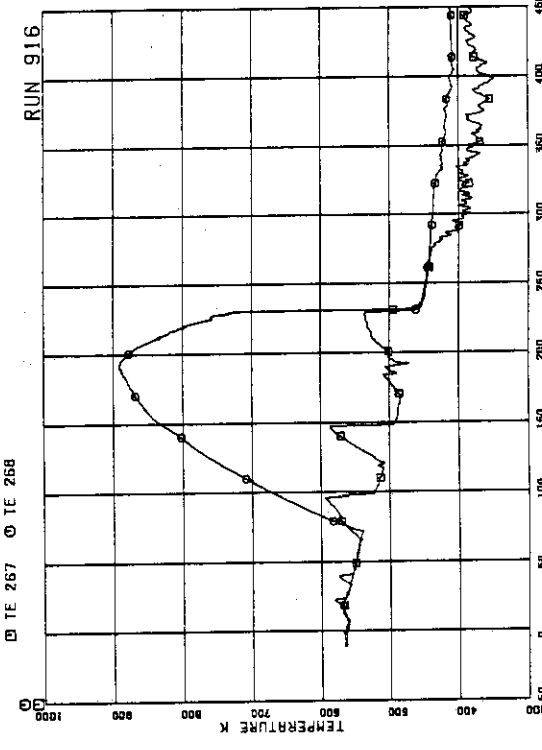


FIG. 5.118 SURFACE TEMPERATURES OF FUEL ROD R37
AT POSITIONS 1 AND 4

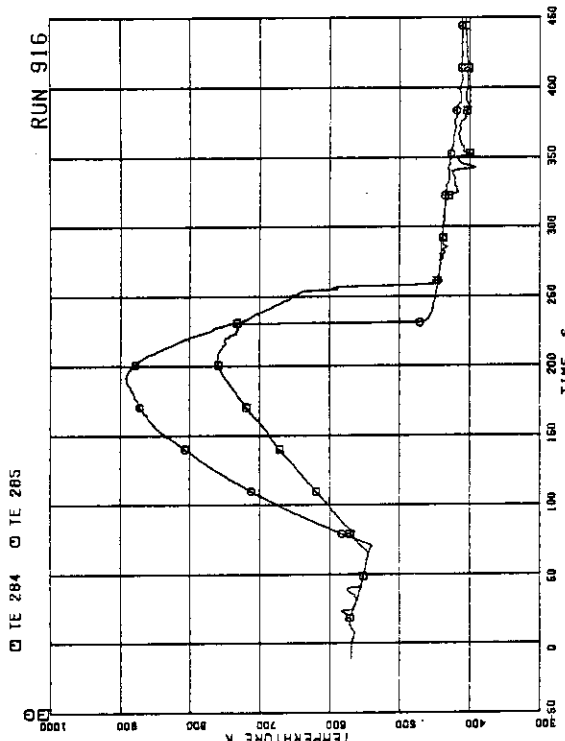


FIG.5.123 SURFACE TEMPERATURES OF FUEL ROD A57
AT POSITIONS 1 AND 4

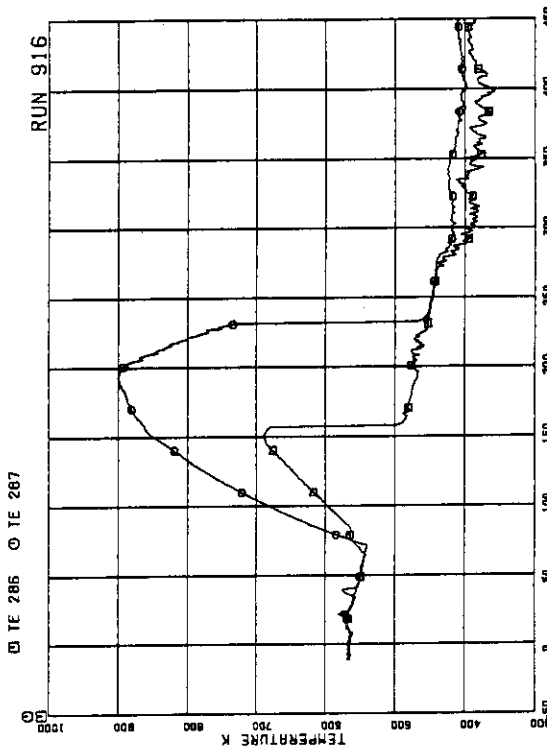


FIG.5.124 SURFACE TEMPERATURES OF FUEL ROD A57
AT POSITIONS 1 AND 4

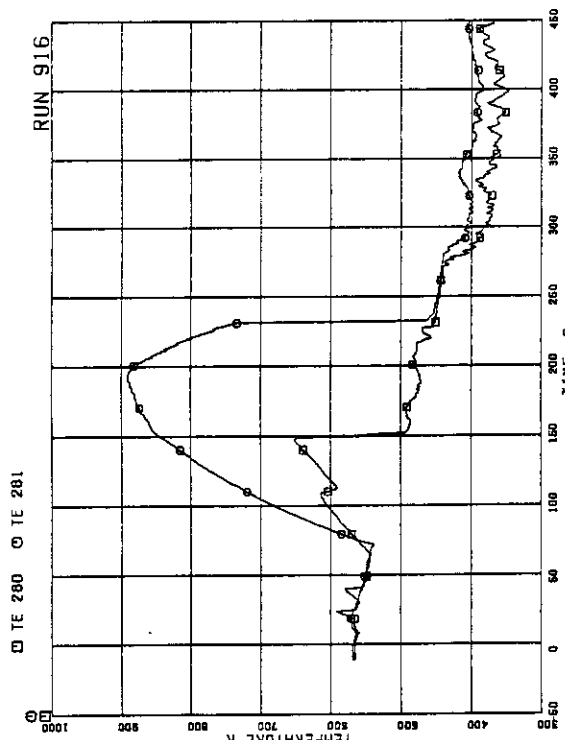


FIG.5.121 SURFACE TEMPERATURES OF FUEL ROD A51
AT POSITIONS 1 AND 4

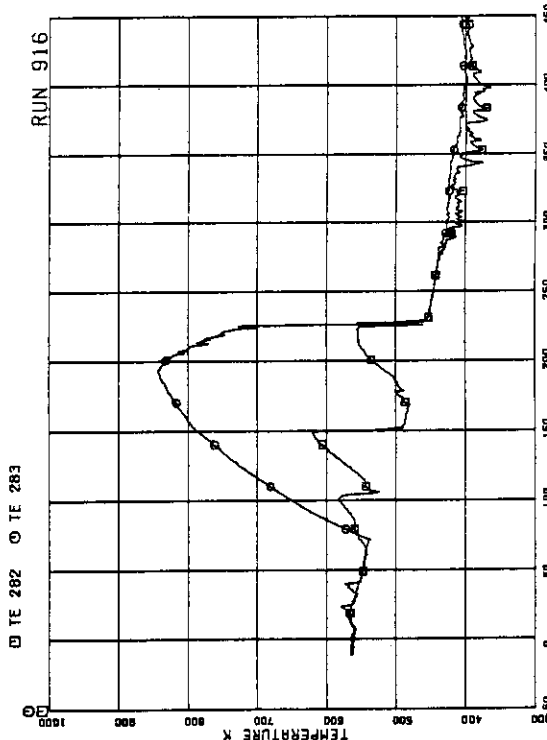


FIG.5.122 SURFACE TEMPERATURES OF FUEL ROD A53
AT POSITIONS 1 AND 4

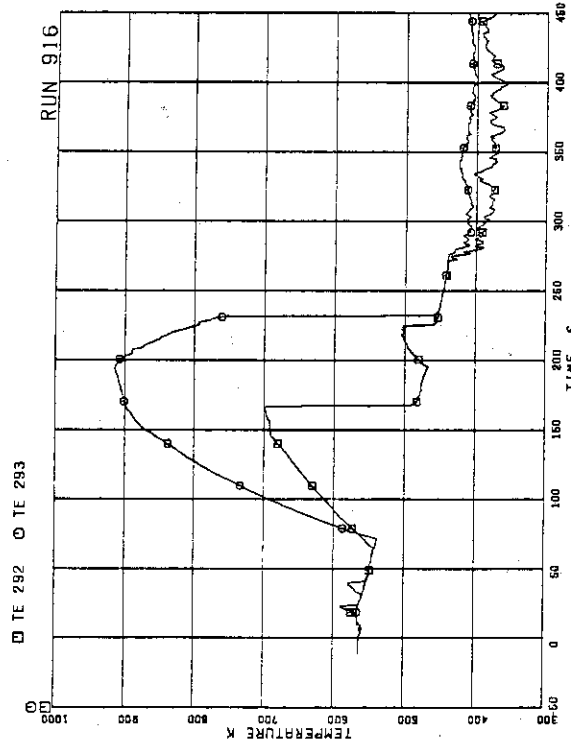


FIG.5.125 SURFACE TEMPERATURE OF FUEL ROD R66
AT POSITION 1 AND 4

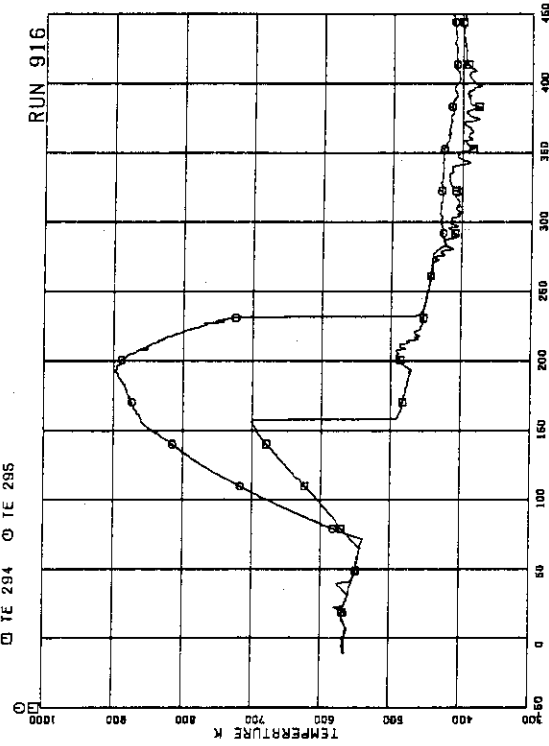


FIG.5.126 SURFACE TEMPERATURES OF FUEL ROD R68
AT POSITIONS 1 AND 4

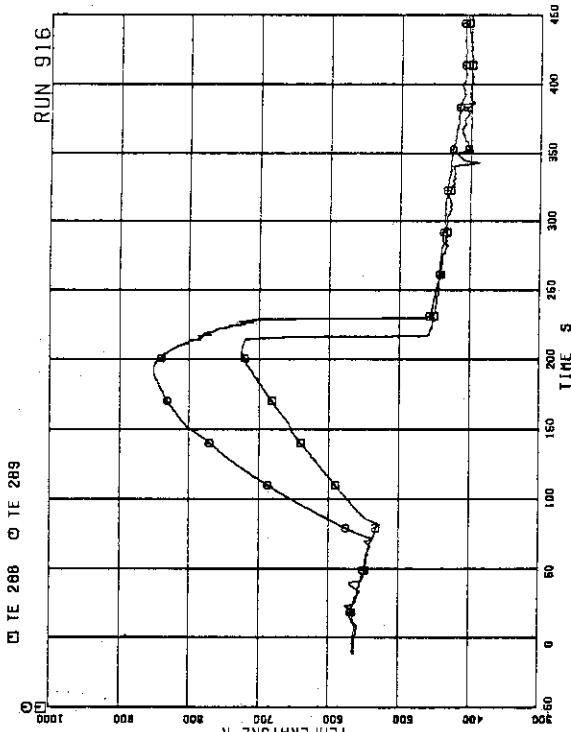


FIG.5.127 SURFACE TEMPERATURE OF FUEL ROD R71
AT POSITION 1 AND 4

FIG.5.128 SURFACE TEMPERATURES OF FUEL ROD R73
AT POSITIONS 1 AND 4

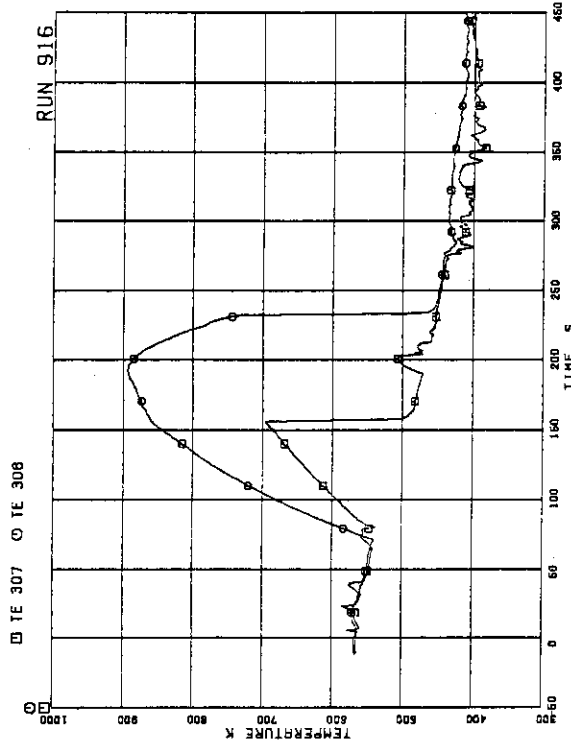


FIG.5.131 SURFACE TEMPERATURES OF FUEL ROD A84
AT POSITIONS 1 AND 4

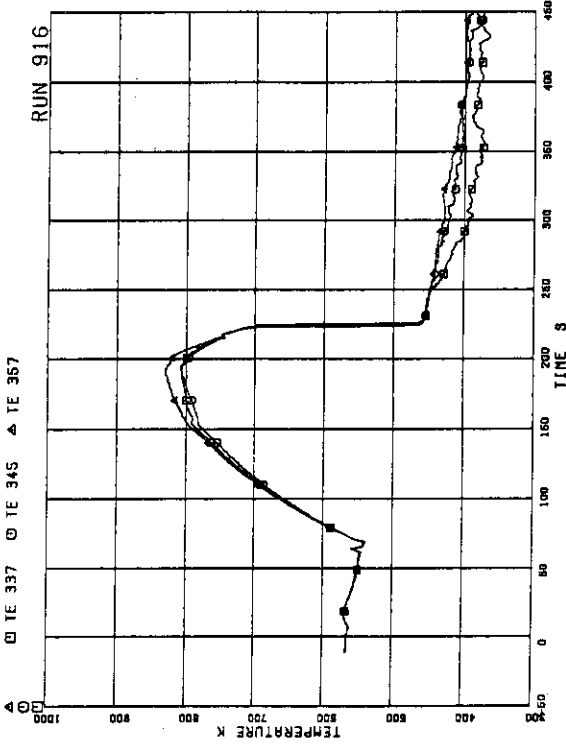


FIG.5.132 SURFACE TEMPERATURES OF FUEL RODS
A82, A84 AT POSITION 1 AND 4

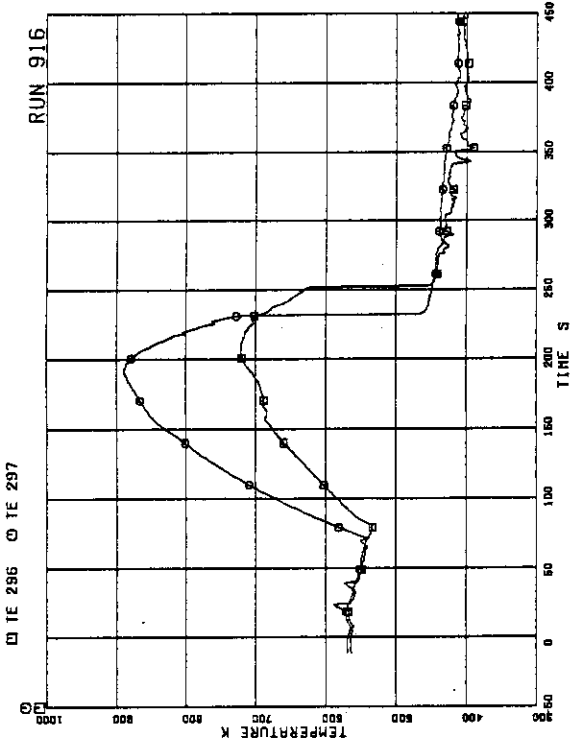


FIG.5.129 SURFACE TEMPERATURES OF FUEL ROD A75
AT POSITIONS 1 AND 4

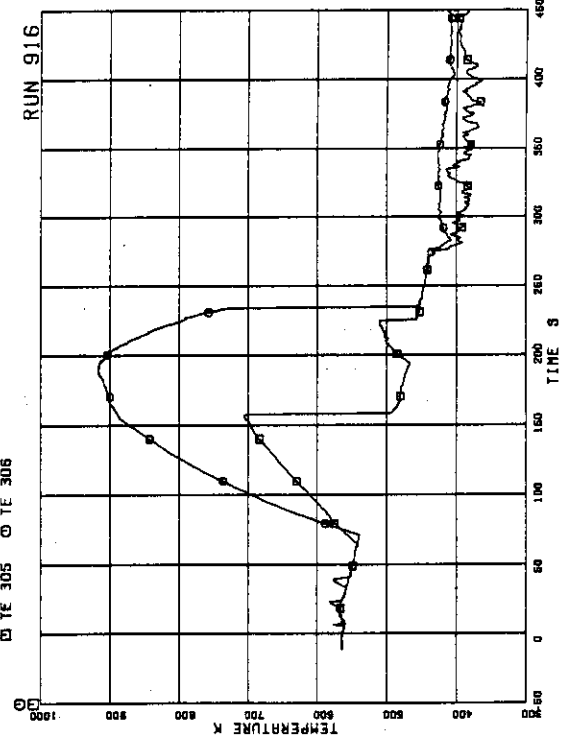


FIG.5.130 SURFACE TEMPERATURE OF FUEL ROD A82
AT POSITION 1 AND 4

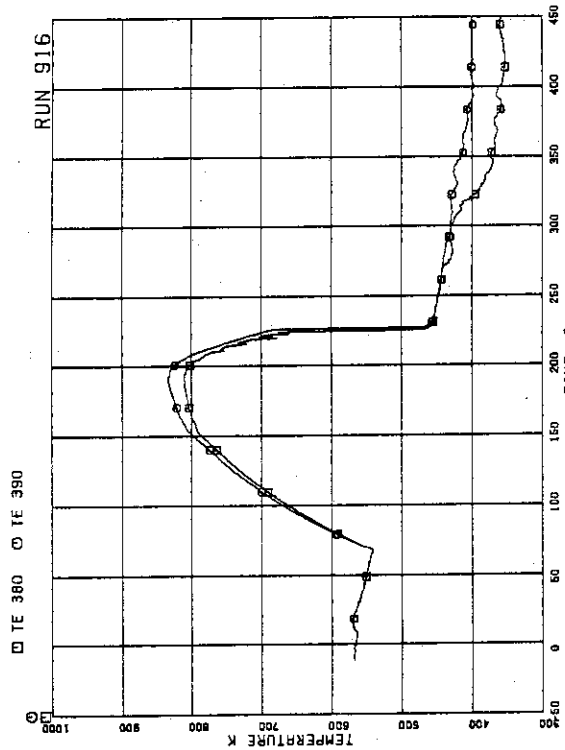


FIG.5.135 SURFACE TEMPERATURES OF FUEL RODS
C31,C68 AT POSITION 4

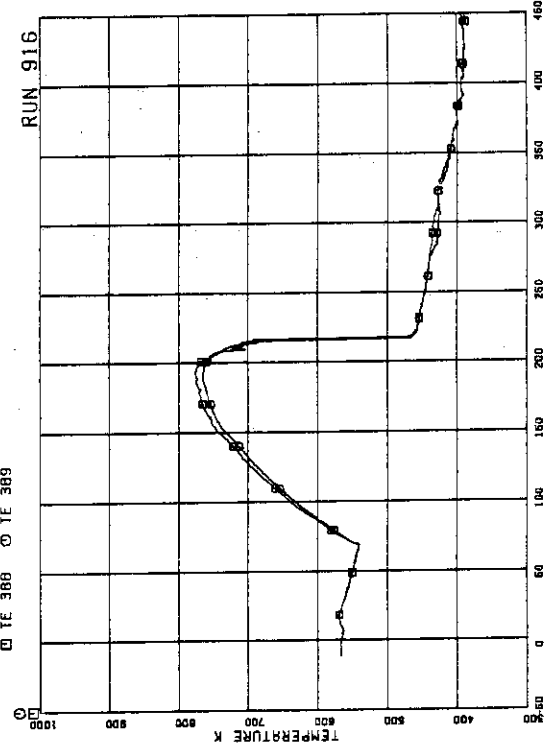


FIG.5.136 SURFACE TEMPERATURES OF FUEL RODS
C35,C66 AT POSITION 4

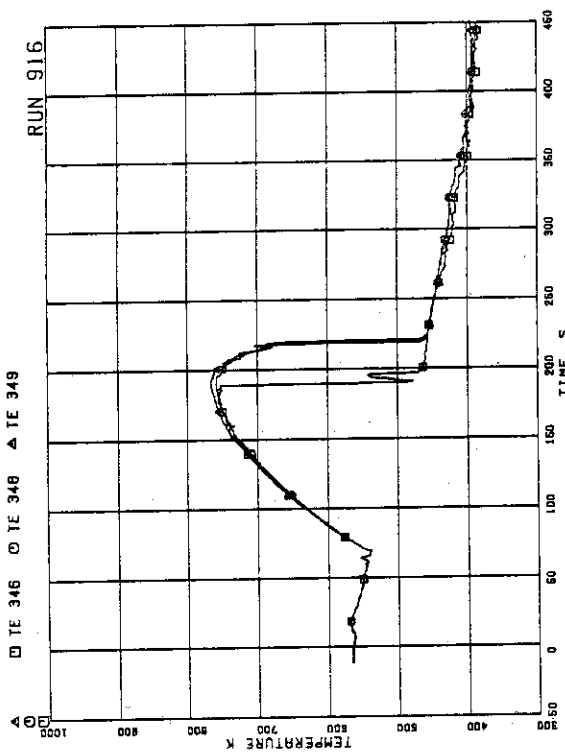


FIG.5.133 SURFACE TEMPERATURES OF FUEL RODS
B33,B53,B66 AT POSITION 4

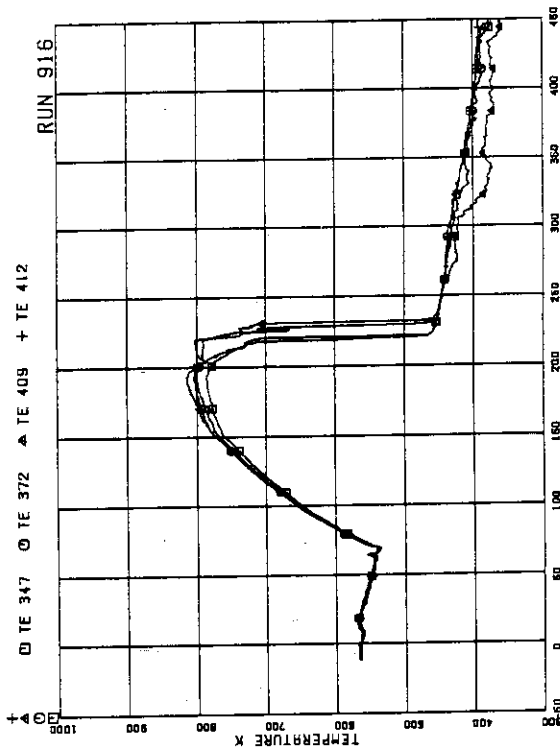


FIG.5.134 SURFACE TEMPERATURES OF FUEL RODS
B51,C15,D51,D77 AT POSITION 4

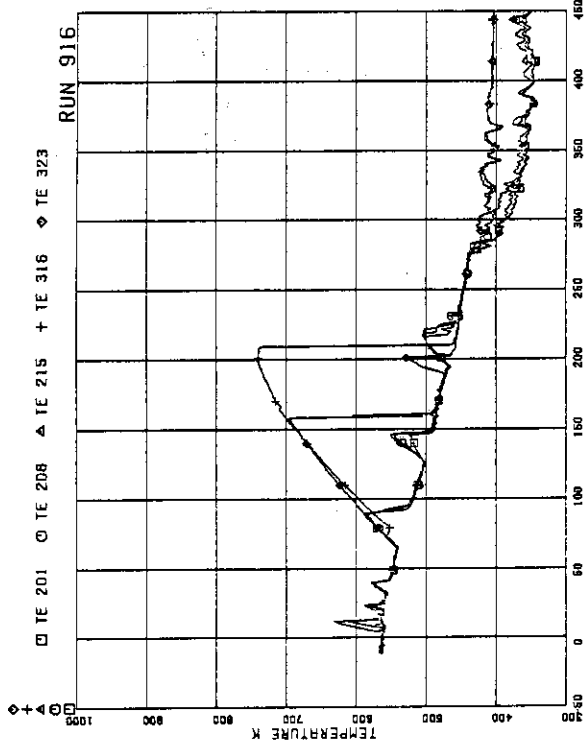


FIG. 5.139 SURFACE TEMPERATURES OF FUEL RODS
A11,A12,A13,A87,A88 AT POSITION 1

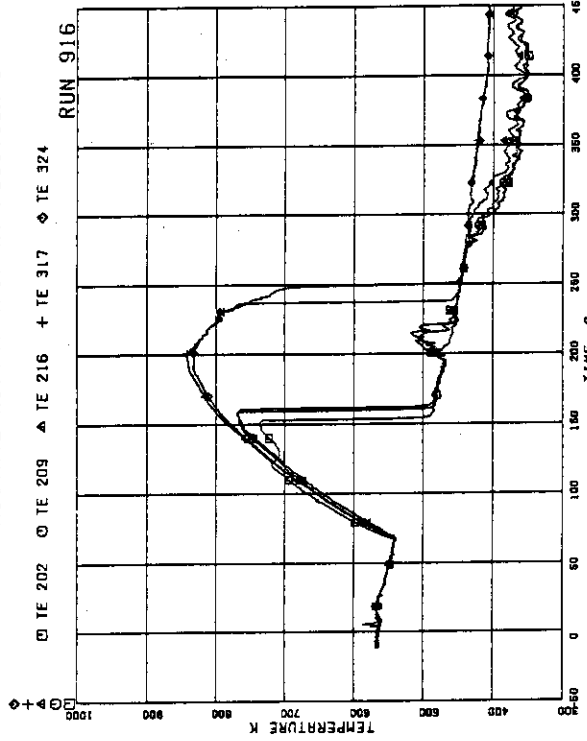


FIG. 5.140 SURFACE TEMPERATURES OF FUEL RODS
A11,A12,A13,A87,A88 AT POSITION 2

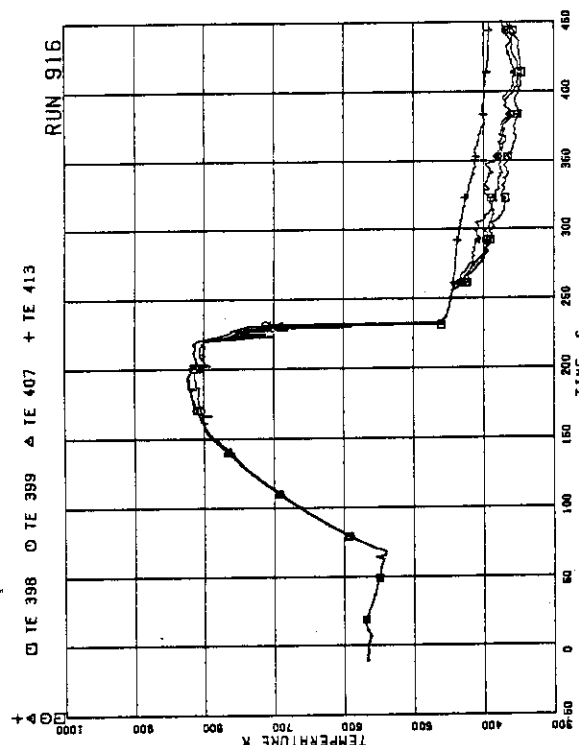


FIG. 5.137 SURFACE TEMPERATURES OF FUEL RODS
D11,D13,D31,D86 AT POSITION 4

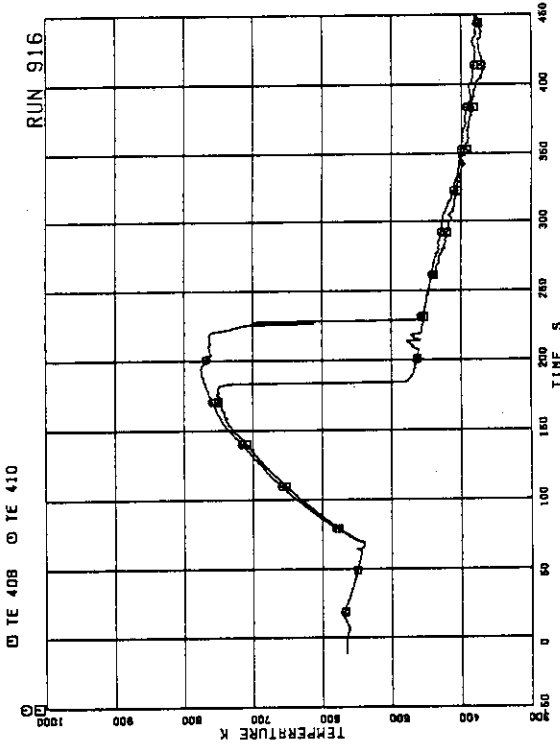


FIG. 5.138 SURFACE TEMPERATURES OF FUEL RODS
D33,D53 AT POSITION 4

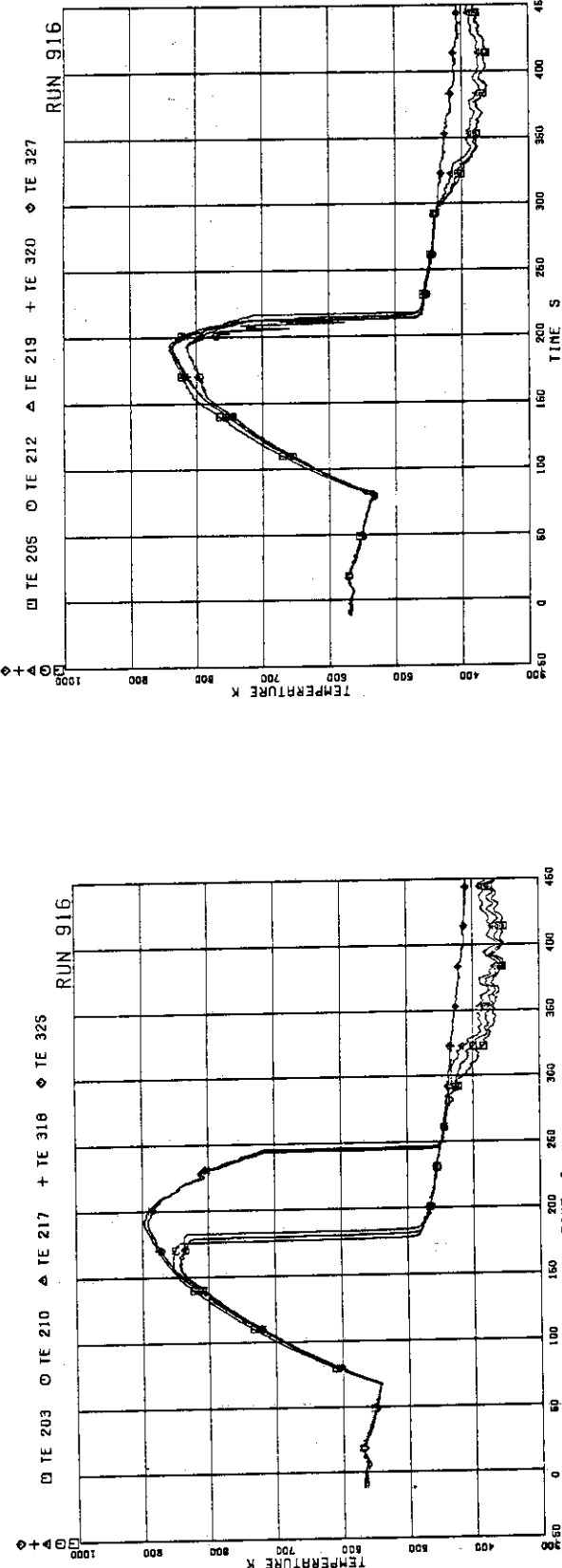


FIG. 5.141 SURFACE TEMPERATURES OF FUEL RODS
A11,A12,A13,A87,A88 AT POSITION 3

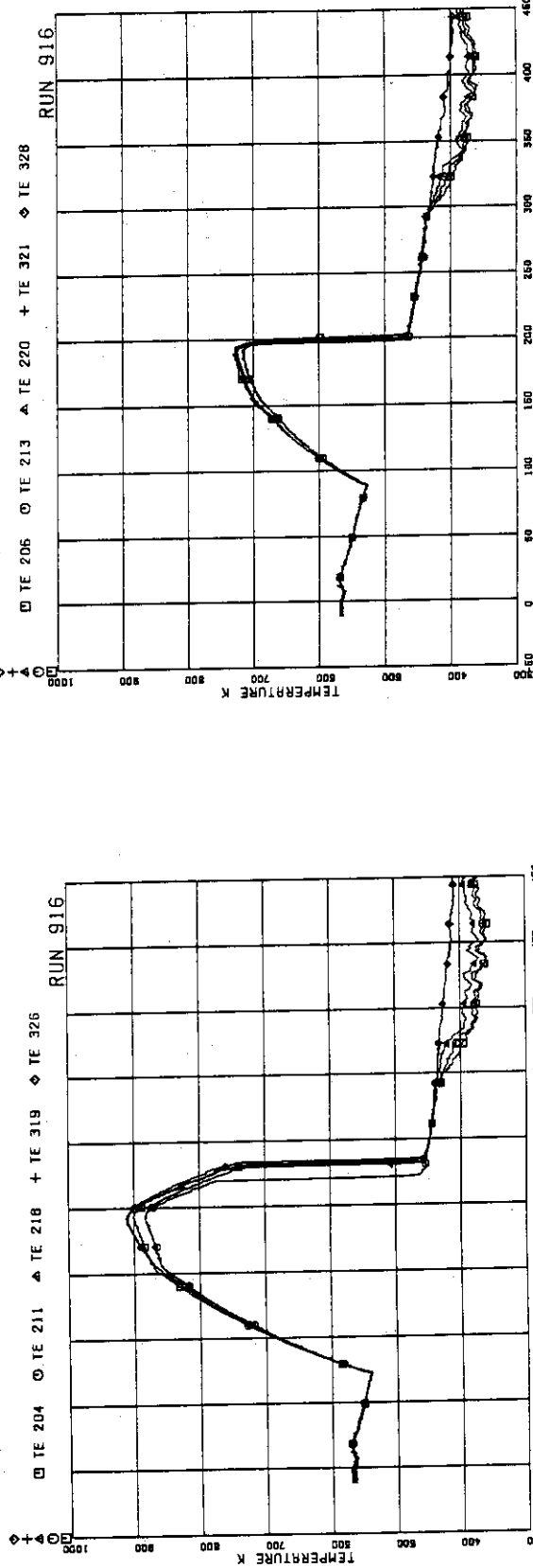


FIG. 5.142 SURFACE TEMPERATURES OF FUEL RODS
A11,A12,A13,A87,A88 AT POSITION 4

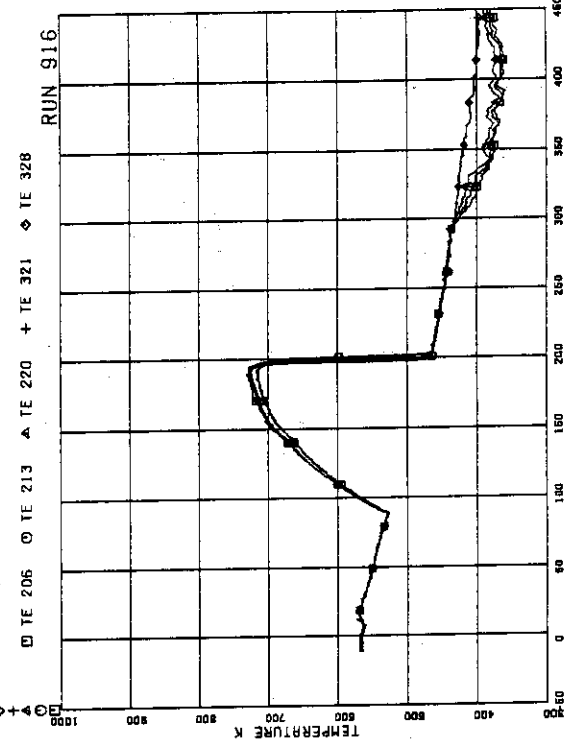


FIG. 5.143 SURFACE TEMPERATURES OF FUEL RODS
A11,A12,A13,A87,A88 AT POSITION 5

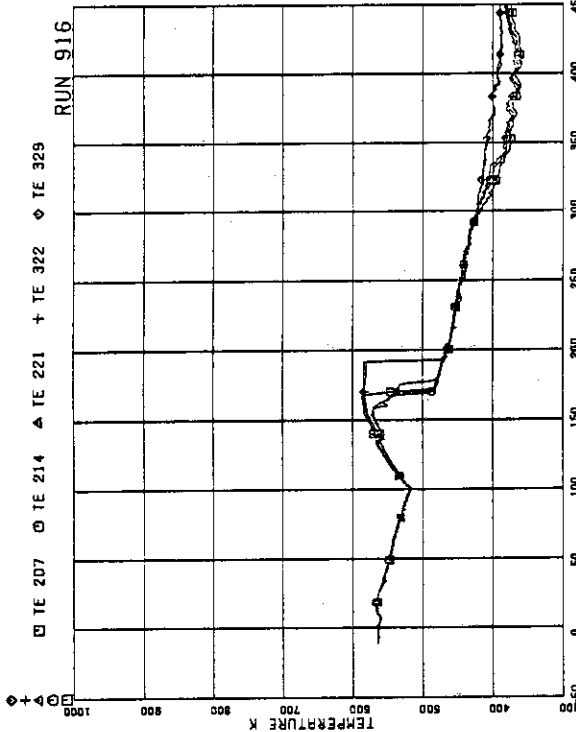


FIG. 5.145 SURFACE TEMPERATURES OF FUEL RODS
R11, R12, R13, R87, R88 AT POSITION 7
RUN 916

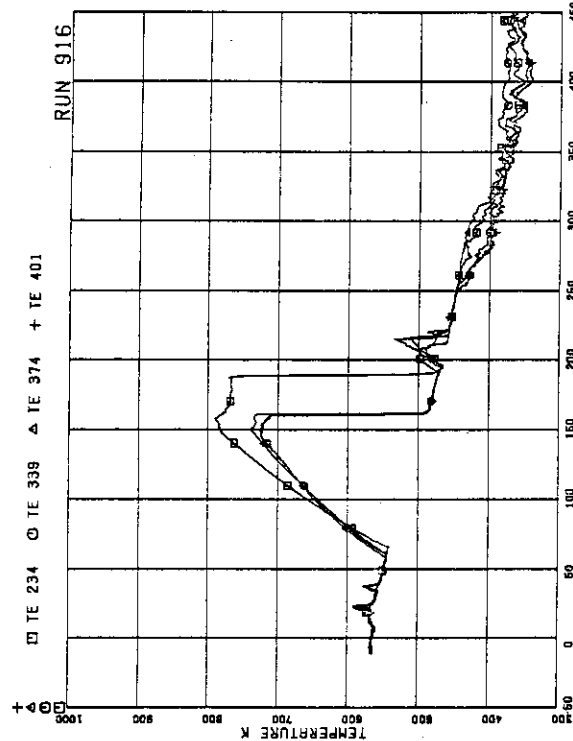


FIG. 5.147 SURFACE TEMPERATURES OF FUEL RODS
A22, B22, C22, D22 AT POSITION 2
RUN 916

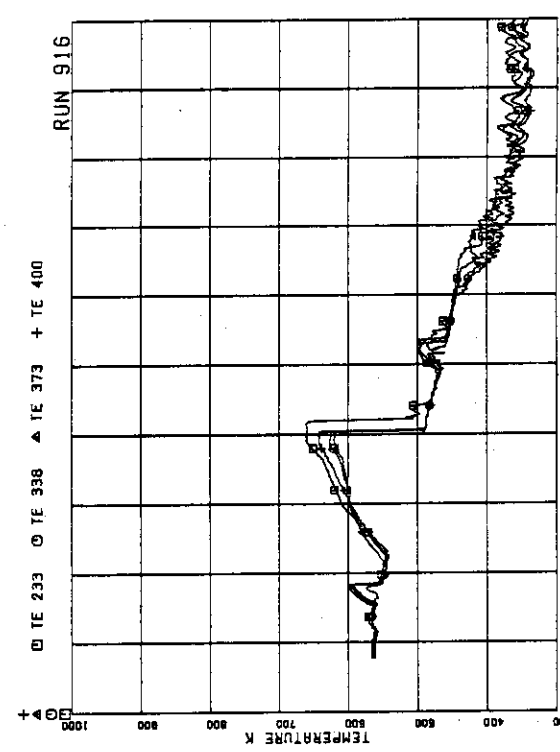


FIG. 5.148 SURFACE TEMPERATURES OF FUEL RODS
A22, B22, C22, D22 AT POSITION 3
RUN 916

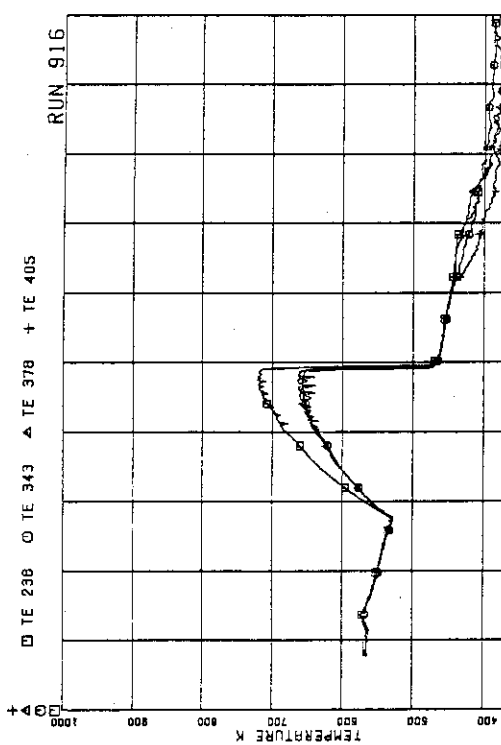


FIG.5.151 SURFACE TEMPERATURES OF FUEL RODS
A22,B22,C22,D22 AT POSITION 6

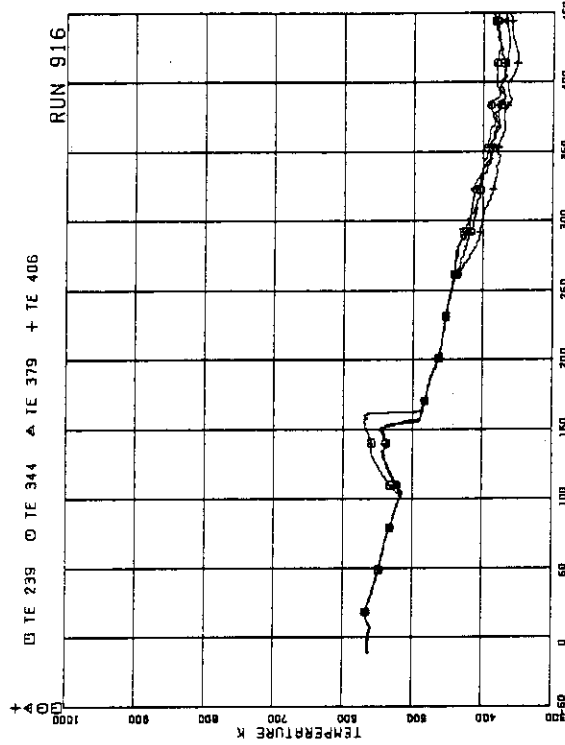


FIG.5.152 SURFACE TEMPERATURES OF FUEL RODS
A22,B22,C22,D22 AT POSITION 7

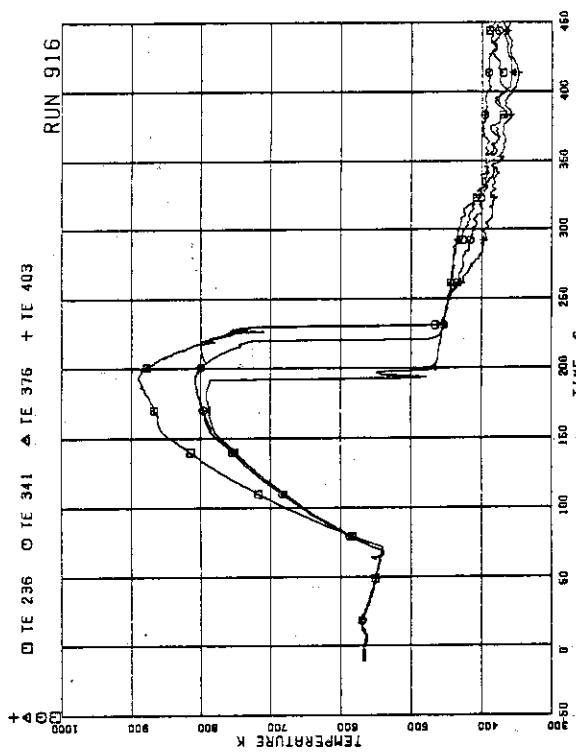


FIG.5.149 SURFACE TEMPERATURES OF FUEL RODS
A22,B22,C22,D22 AT POSITION 4

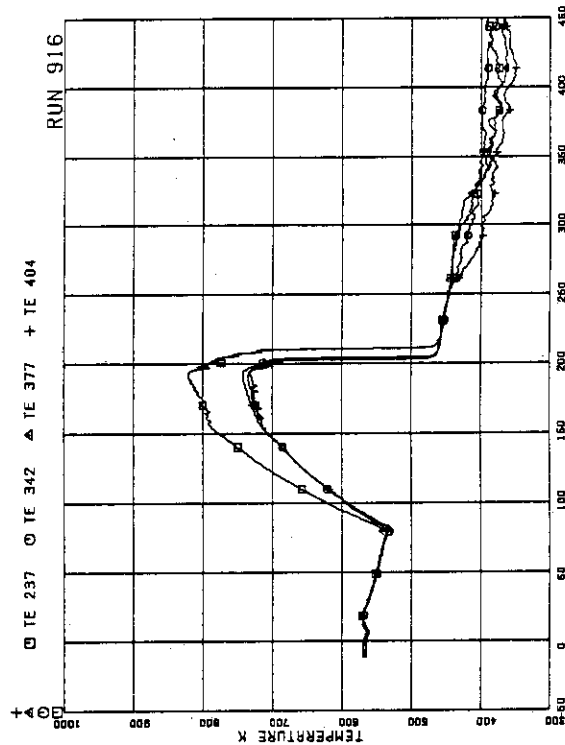
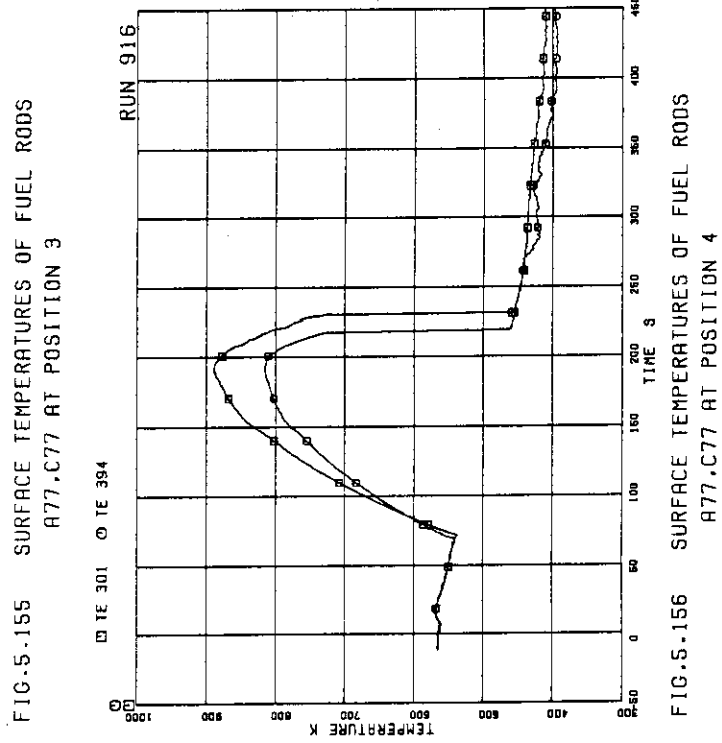
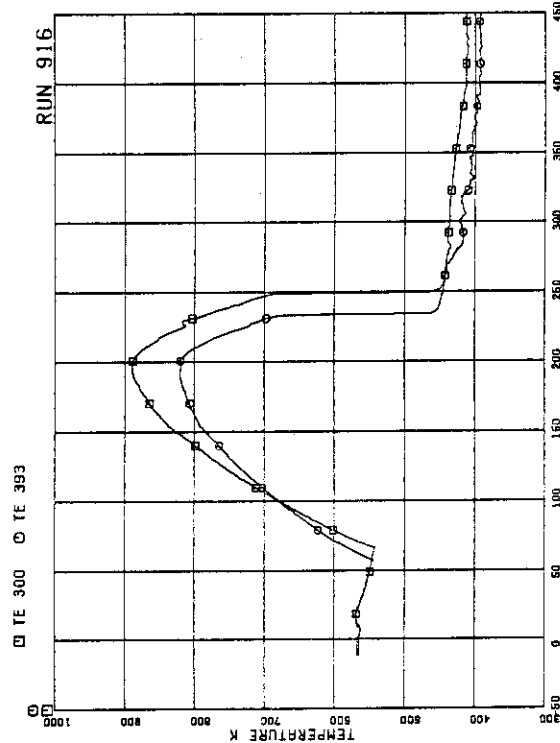
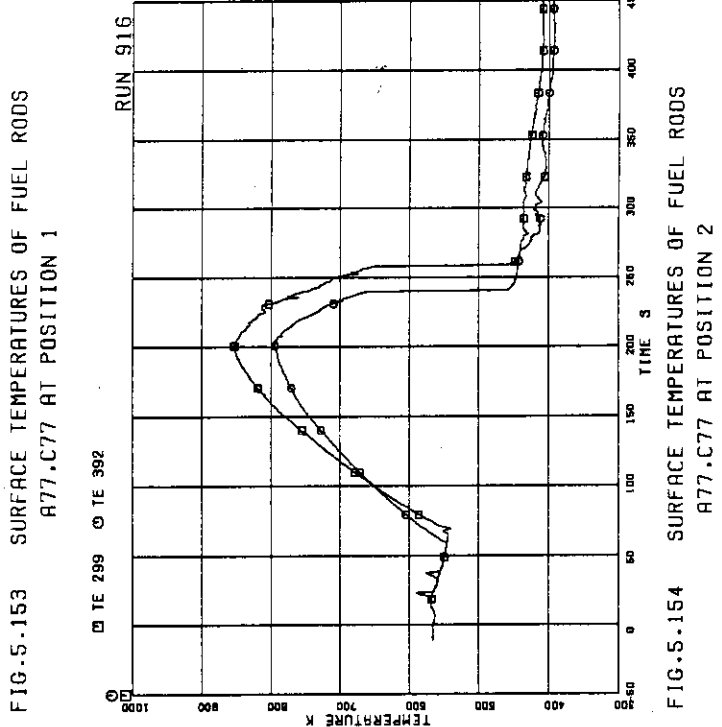
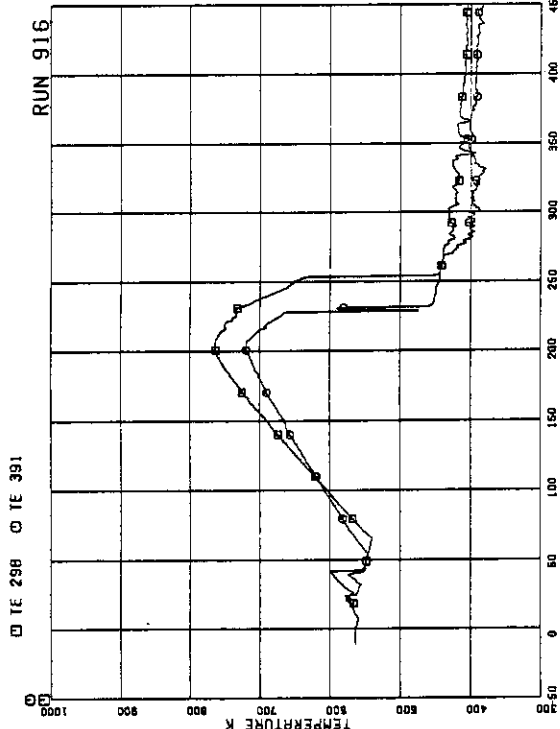


FIG.5.150 SURFACE TEMPERATURES OF FUEL RODS
A22,B22,C22,D22 AT POSITION 5



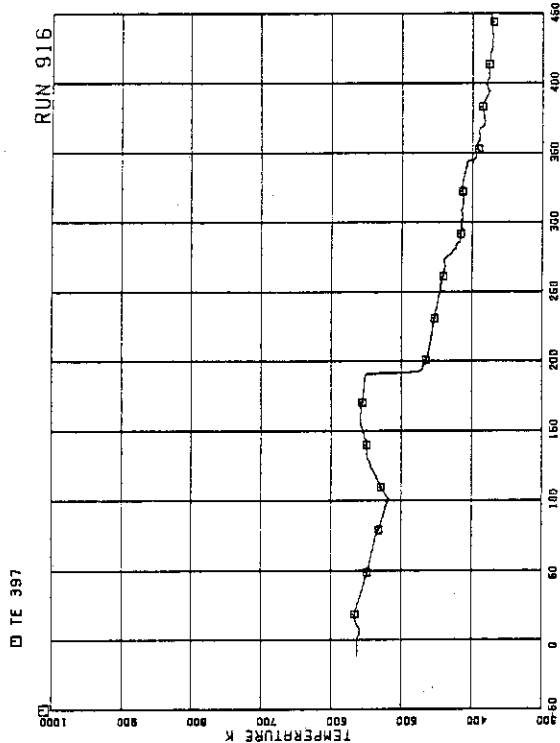


FIG.5.159 SURFACE TEMPERATURES OF FUEL RODS
C77 RODS AT POSITION 7

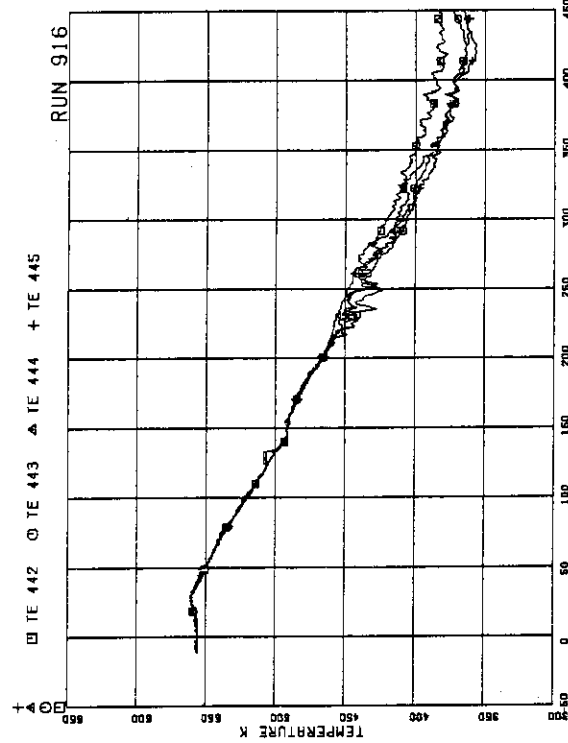


FIG.5.160 FLUID TEMPERATURES AT CHANNEL INLET

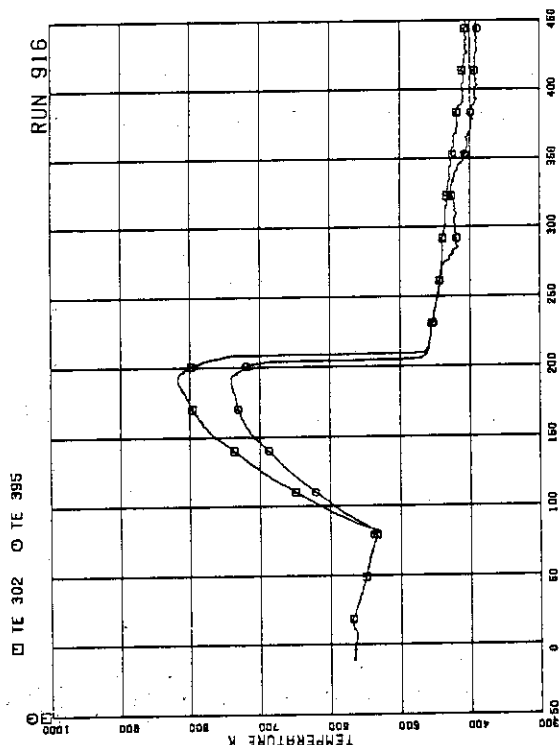


FIG.5.157 SURFACE TEMPERATURES OF FUEL RODS
A77,C77 AT POSITION 5

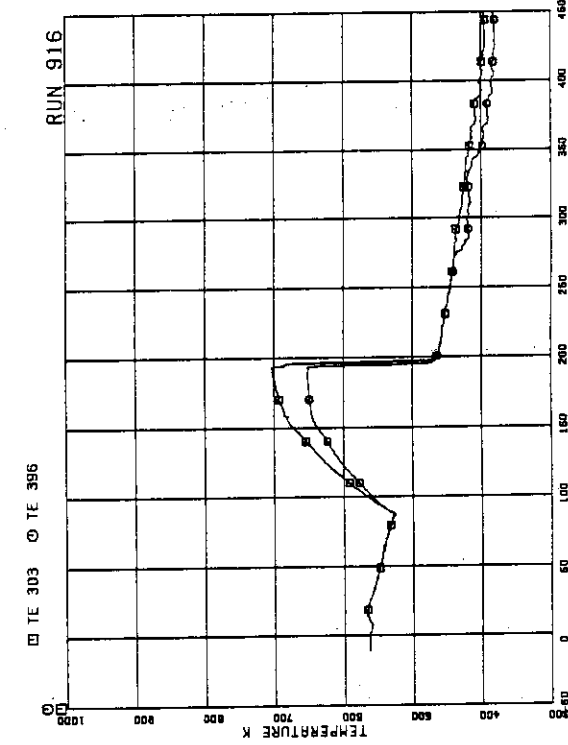


FIG.5.158 SURFACE TEMPERATURES OF FUEL RODS
A77,C77 AT POSITION 6

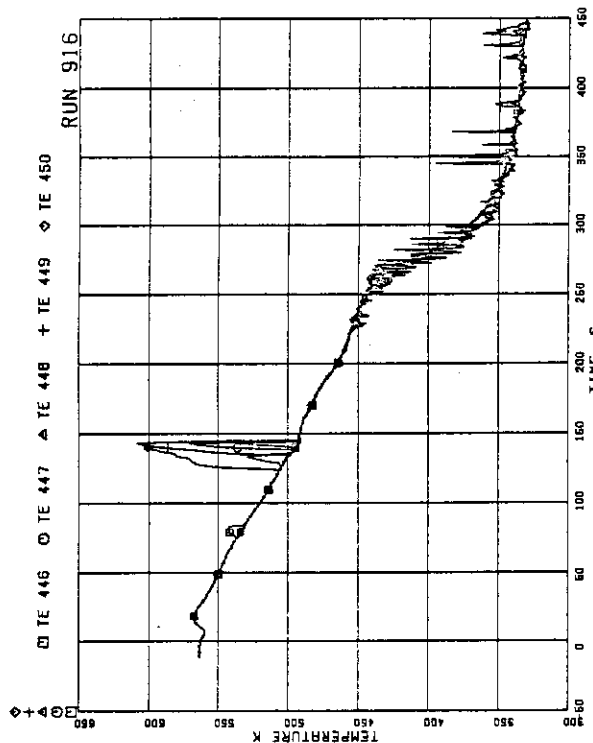


FIG.5.161 FLUID TEMPERATURES AT CHANNEL A OUTLET

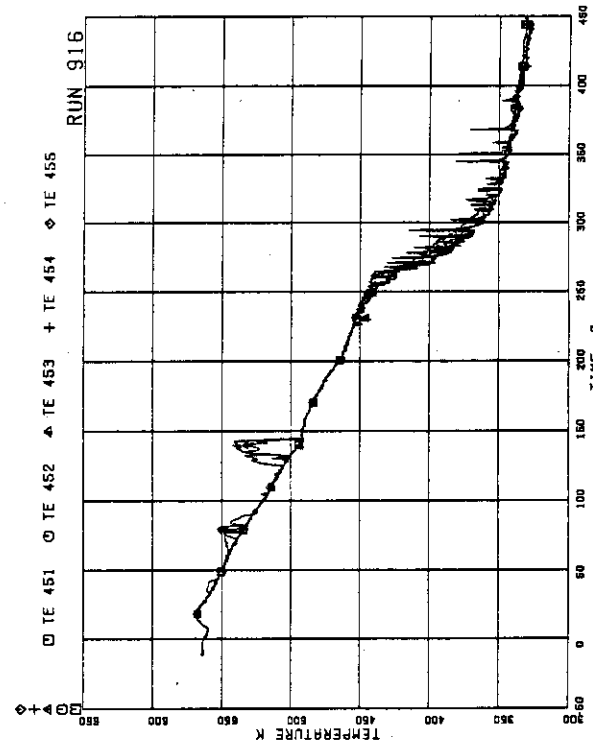


FIG.5.162 FLUID TEMPERATURES AT CHANNEL C OUTLET

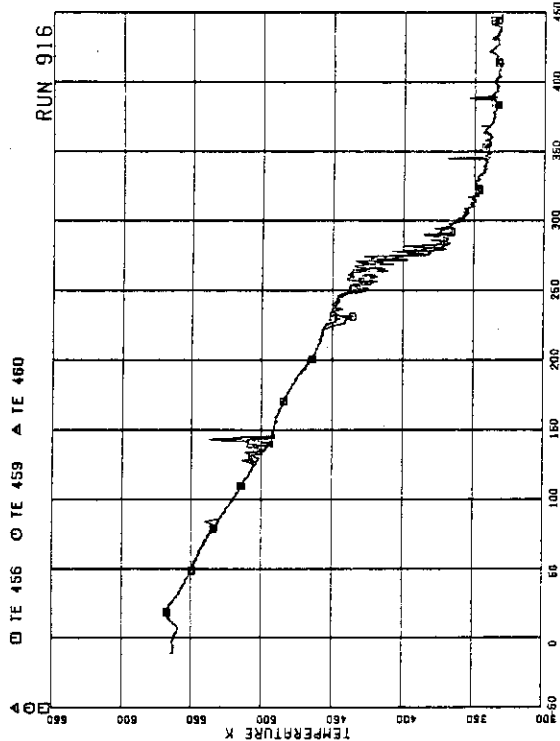


FIG.5.163 FLUID TEMPERATURES ABOVE UTP OF CHANNEL A, OPENINGS 1, 4, 5

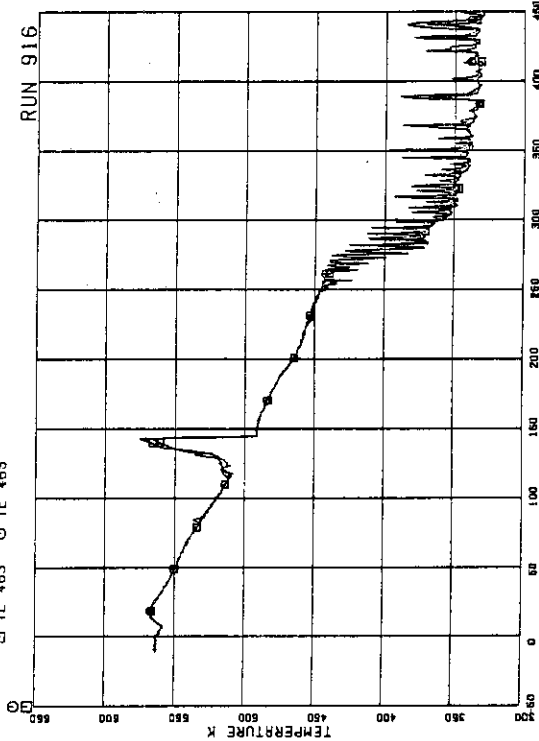


FIG.5.164 FLUID TEMPERATURES ABOVE UTP OF CHANNEL A, OPENINGS 8, 10

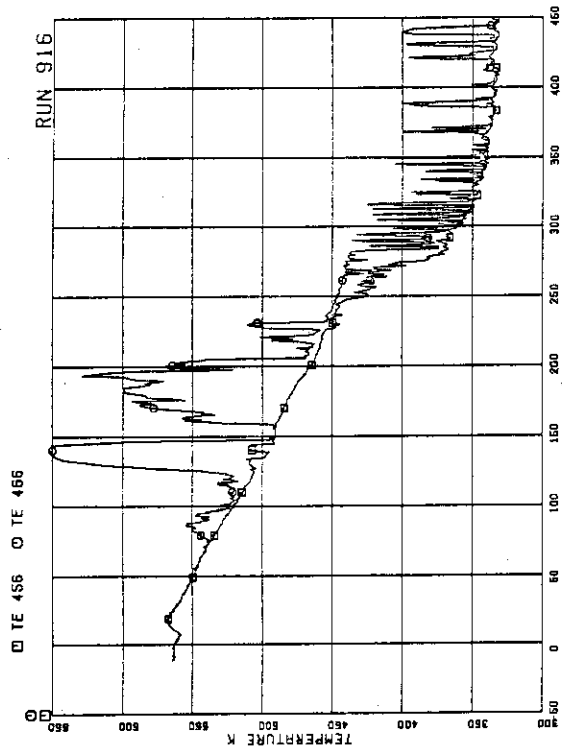


FIG.5.167 FLUID TEMPERATURES AT UTP IN
CHANNEL A, OPENING 1

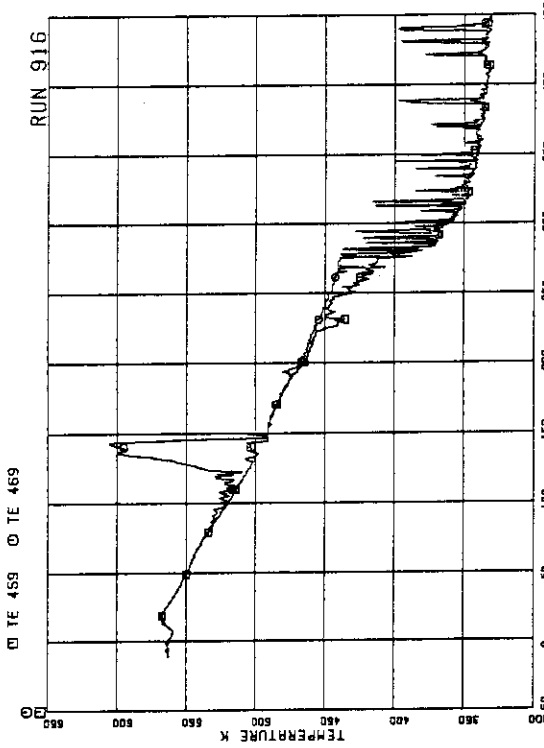


FIG.5.168 FLUID TEMPERATURES AT UTP IN
CHANNEL A, OPENING 4

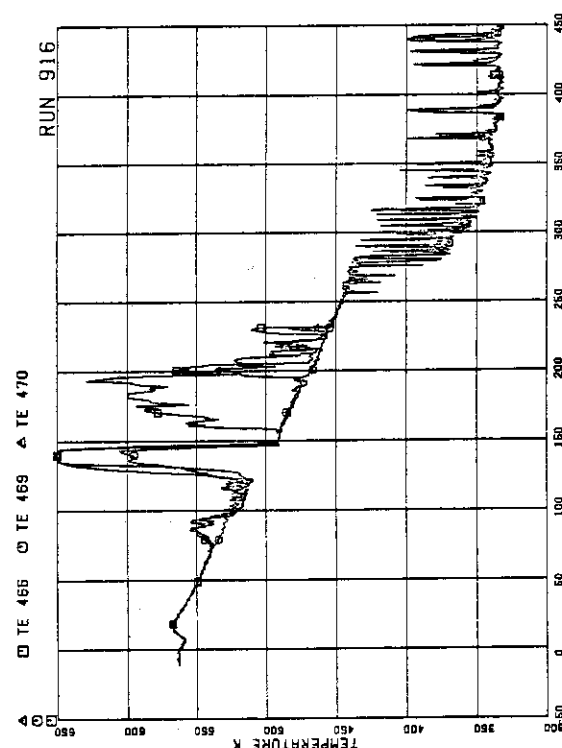


FIG.5.165 FLUID TEMPERATURES BELOW UTP OF
CHANNEL A, OPENINGS 1,4,5

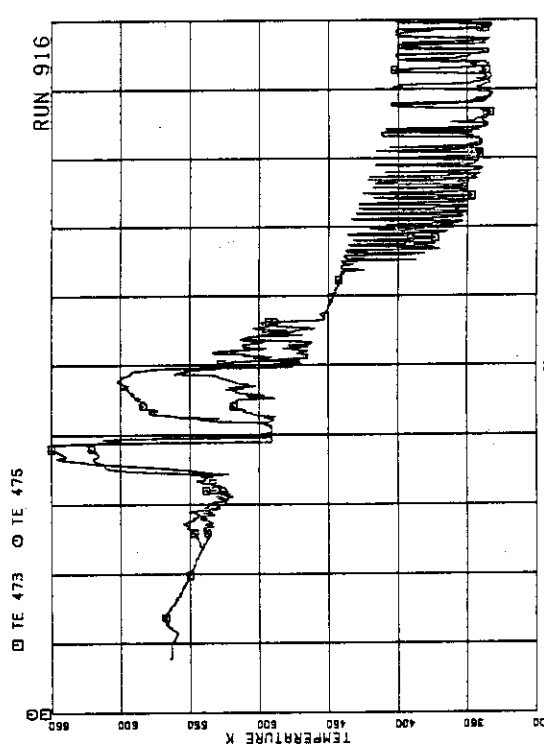


FIG.5.166 FLUID TEMPERATURES BELOW UTP OF
CHANNEL A, OPENINGS 8,10

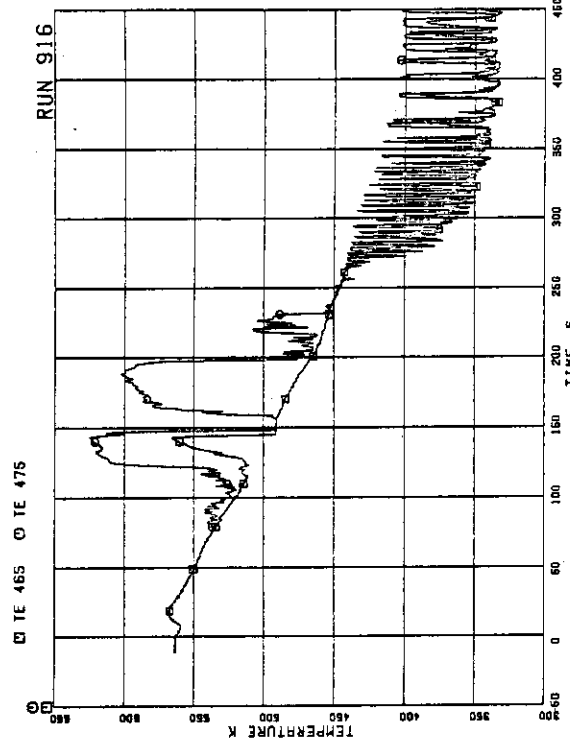


FIG.5.169 FLUID TEMPERATURES AT UTP IN CHANNEL A, OPENING 5

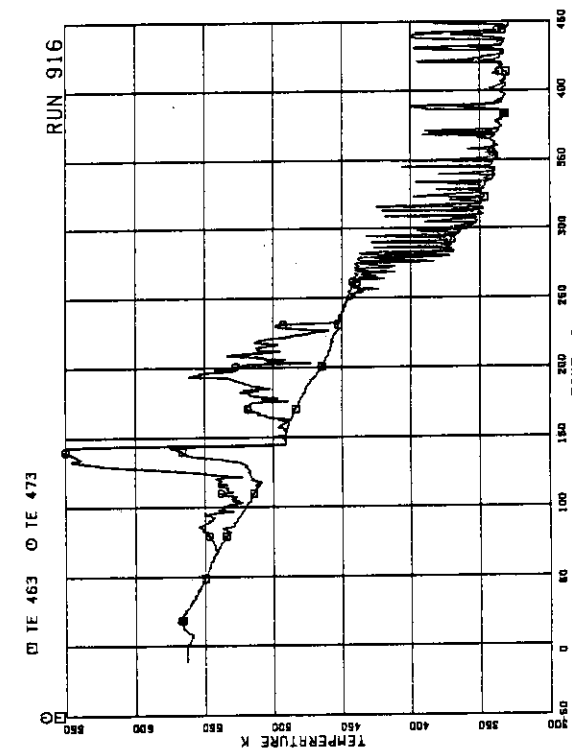


FIG.5.170 FLUID TEMPERATURES AT UTP IN CHANNEL A, OPENING 8

FIG.5.171 FLUID TEMPERATURES AT UTP IN CHANNEL A, OPENING 10

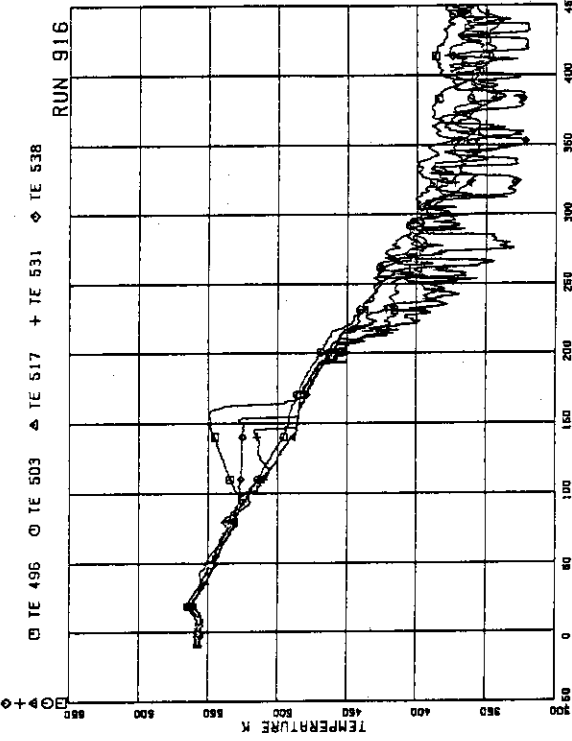


FIG.5.172 INNER AND OUTER SURFACE TEMPERATURES OF CHANNEL BOX AT POS.1

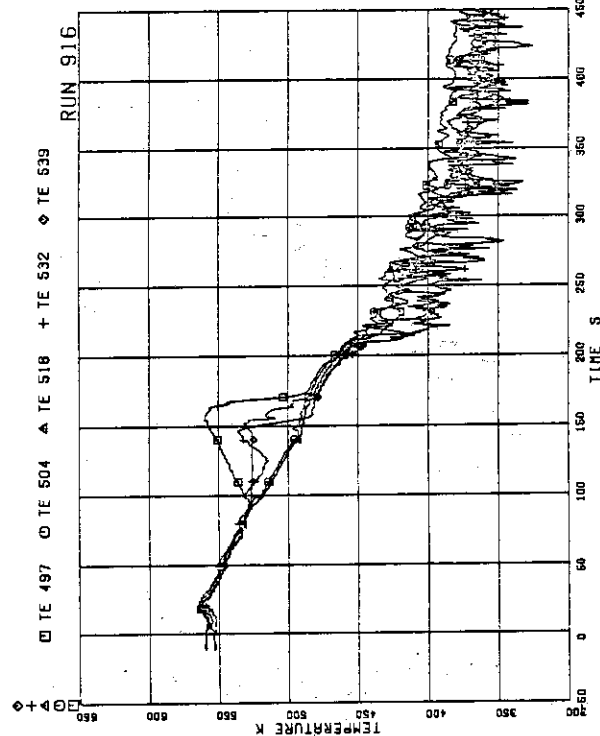


FIG.5.173 INNER AND OUTER SURFACE TEMPERATURES OF CHANNEL BOX AT POS.2

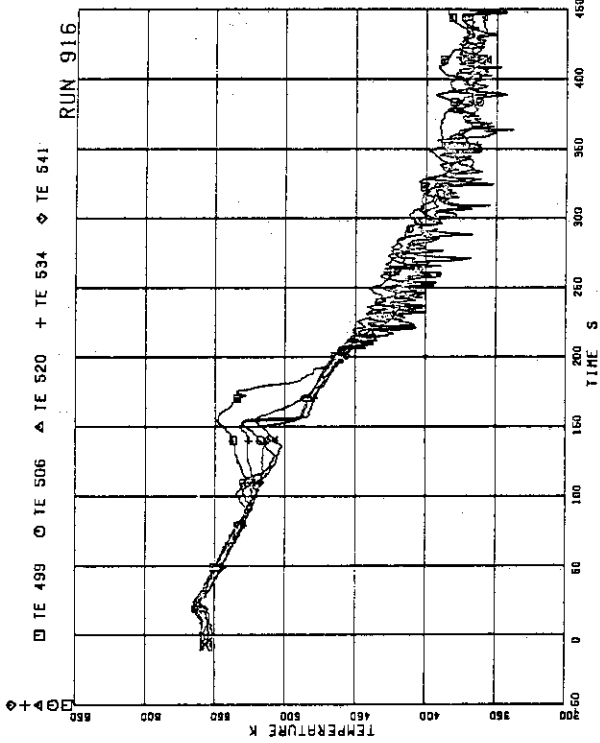


FIG.5.175 INNER AND OUTER SURFACE TEMPERATURES OF CHANNEL BOX AT POS.4

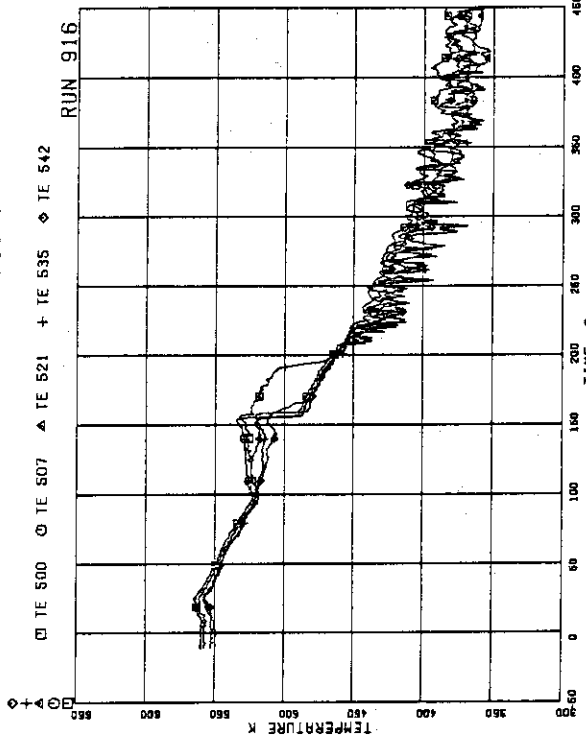


FIG.5.176 INNER AND OUTER SURFACE TEMPERATURES OF CHANNEL BOX AT POS.5

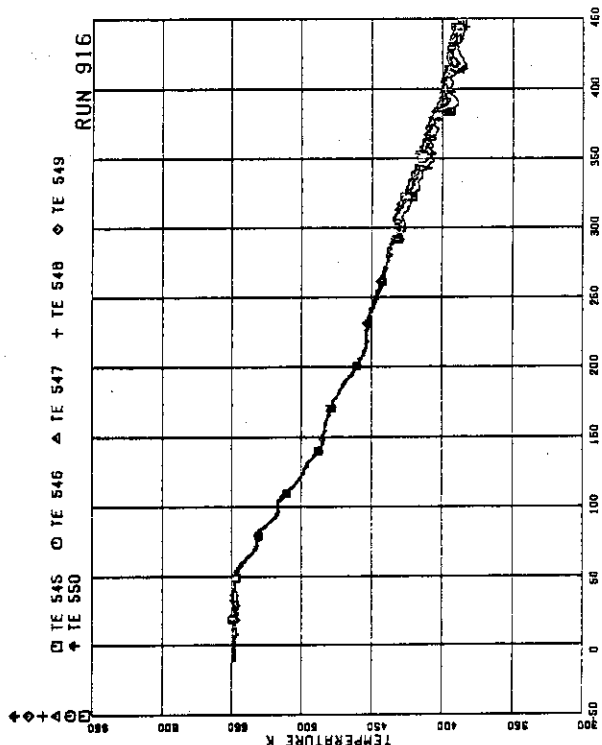


FIG. 5.179 FLUID TEMPERATURES IN LOWER PLENUM.
CENTER

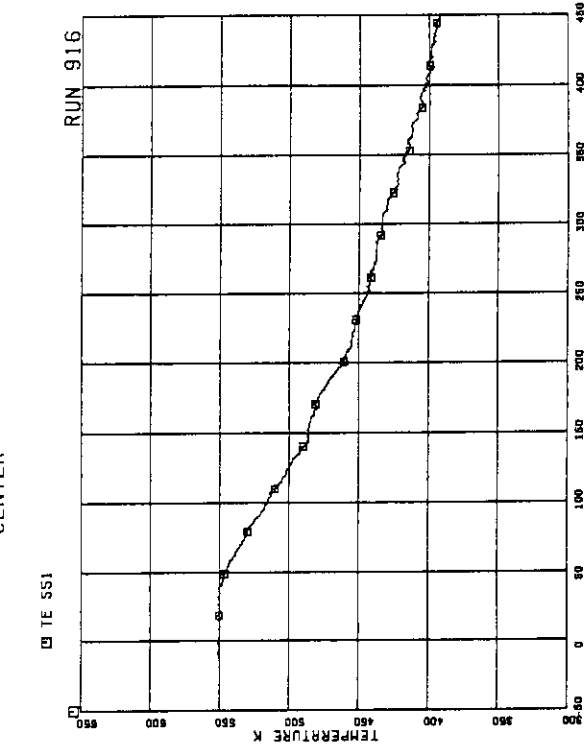


FIG. 5.180 FLUID TEMPERATURES IN LOWER PLENUM.
NORTH

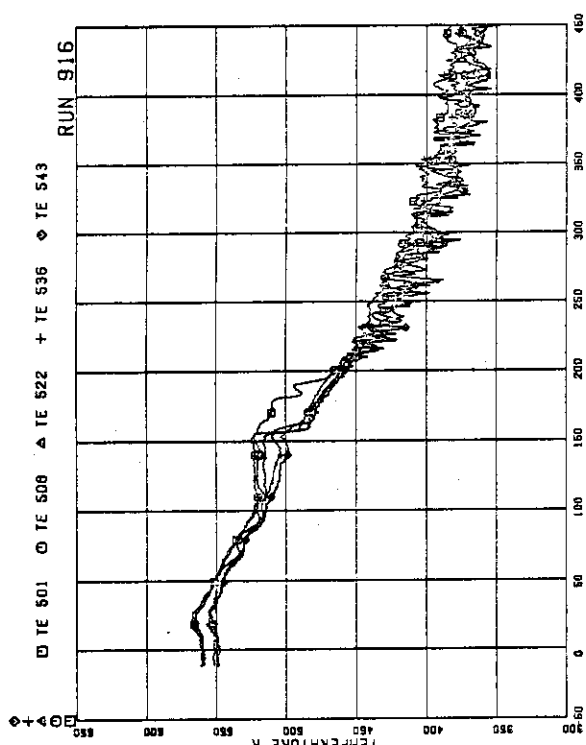


FIG. 5.177 INNER AND OUTER SURFACE TEMPERATURES
OF CHANNEL BOX AT POS. 6

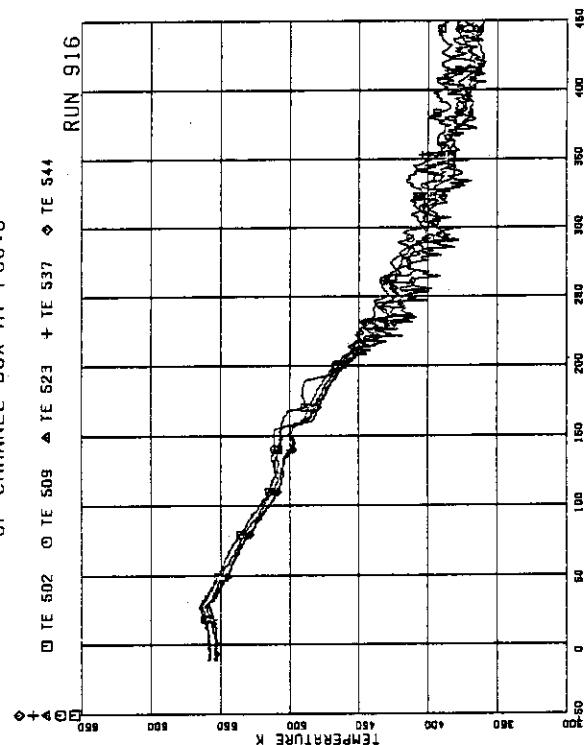


FIG. 5.178 INNER AND OUTER SURFACE TEMPERATURES
OF CHANNEL BOX AT POS. 7

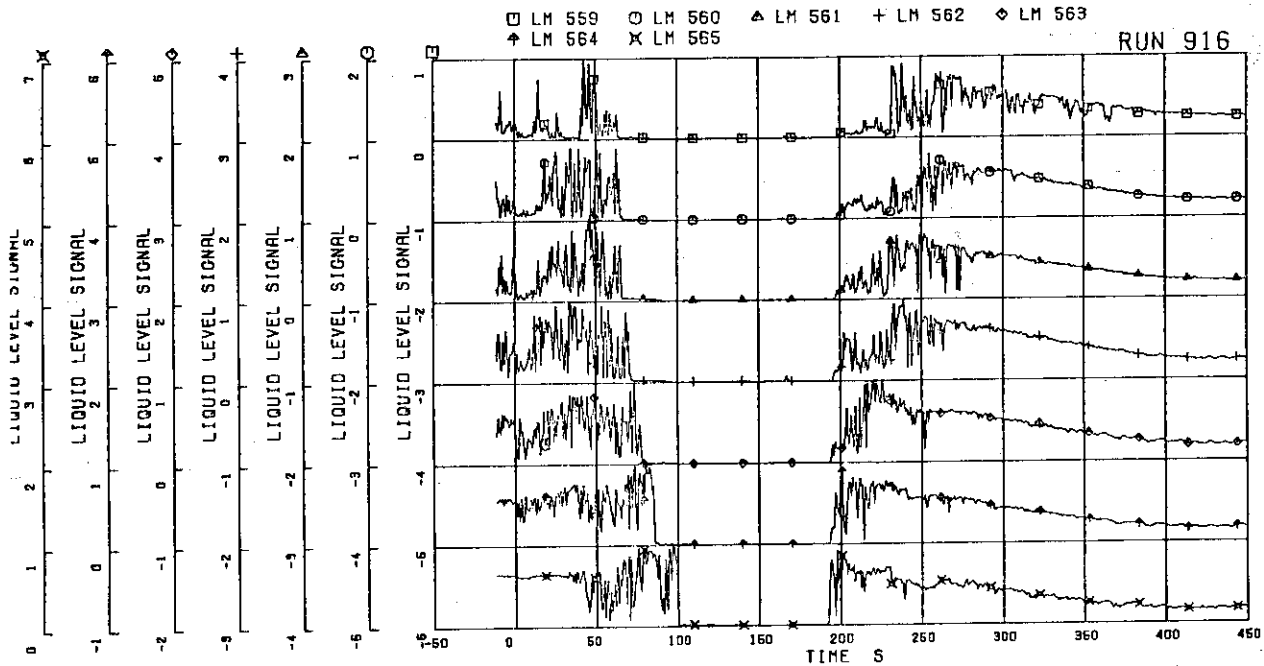


FIG.5.181 LIQUID LEVEL SIGNALS IN CHANNEL BOX A,
LOCATION A1

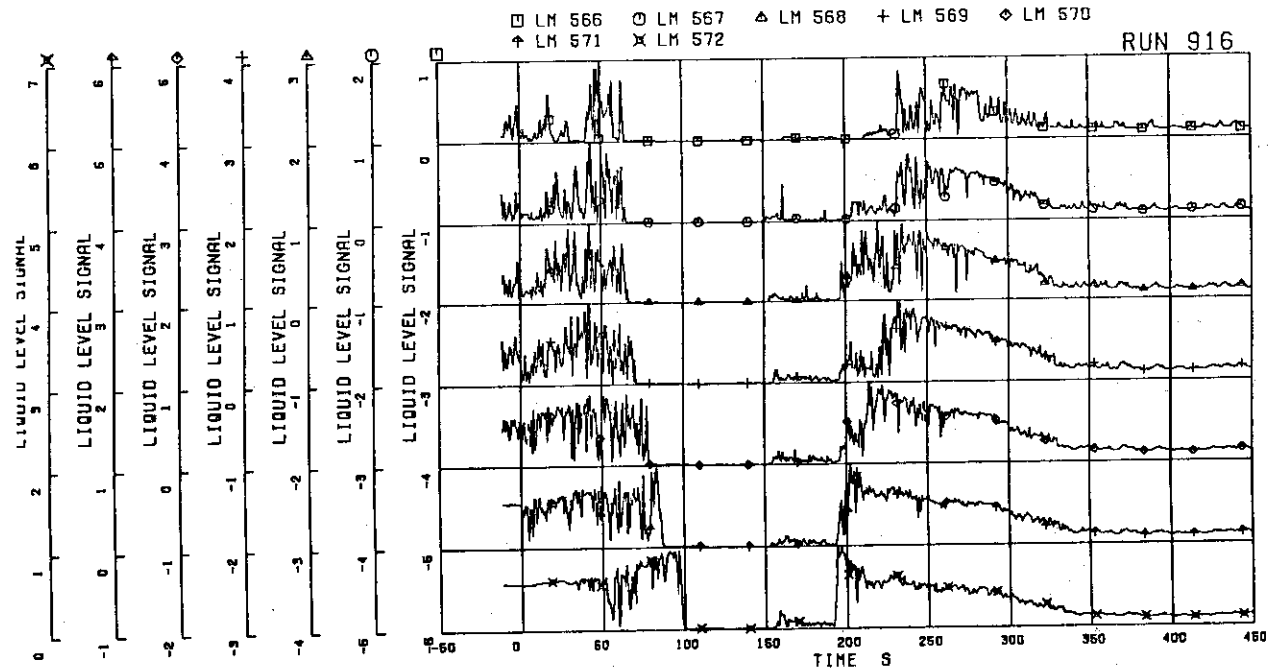


FIG.5.182 LIQUID LEVEL SIGNALS IN CHANNEL BOX A,
LOCATION A2

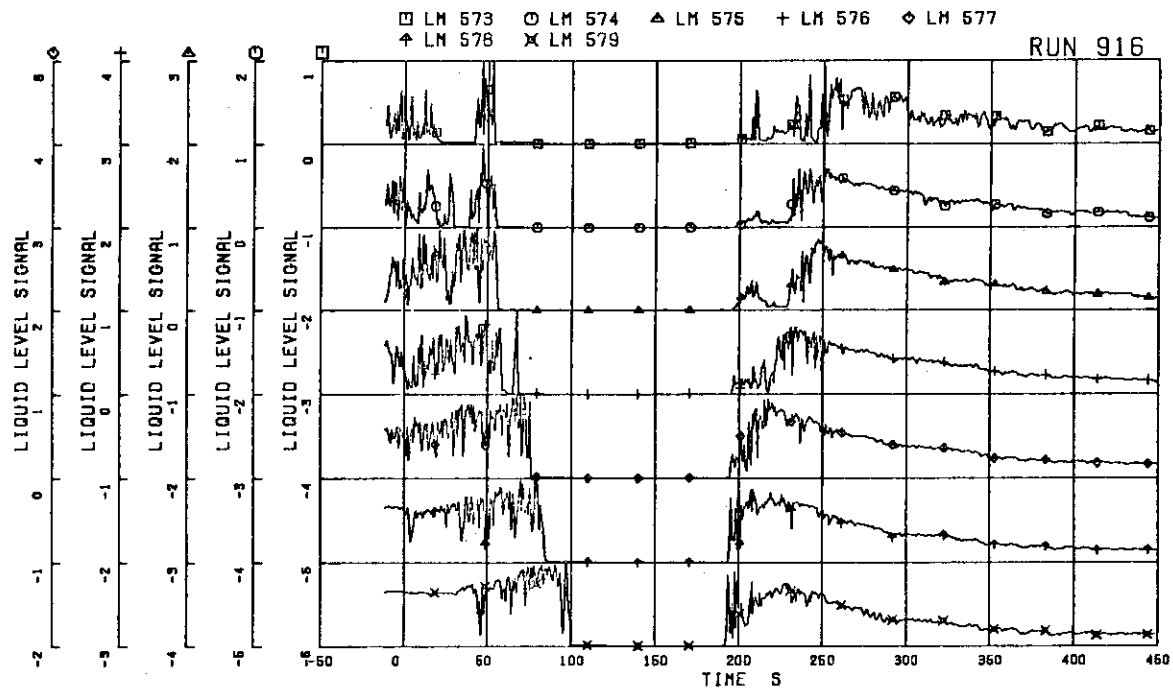


FIG.5.183 LIQUID LEVEL SIGNALS IN CHANNEL BOX B

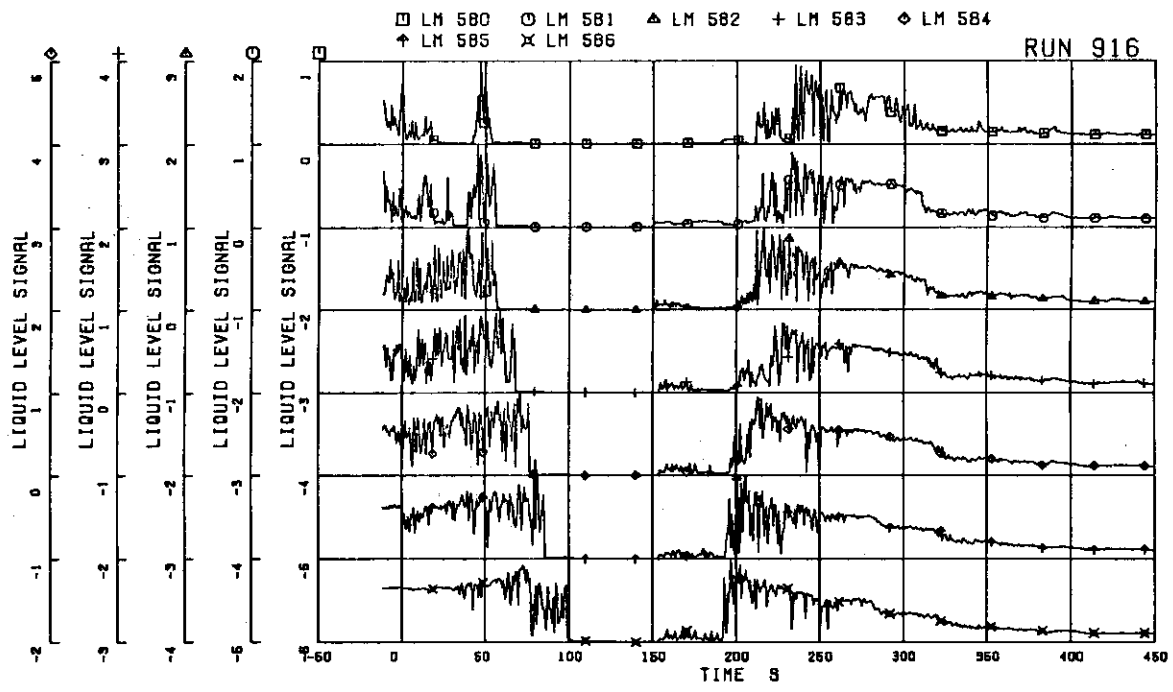


FIG.5.184 LIQUID LEVEL SIGNALS IN CHANNEL BOX C

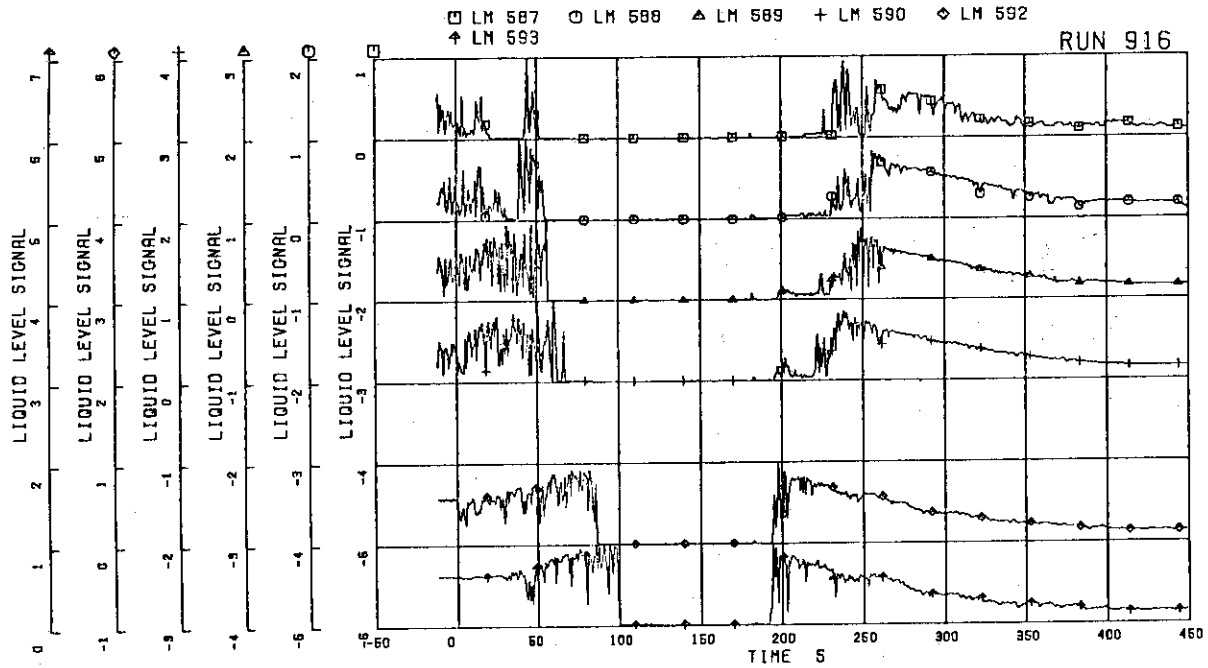
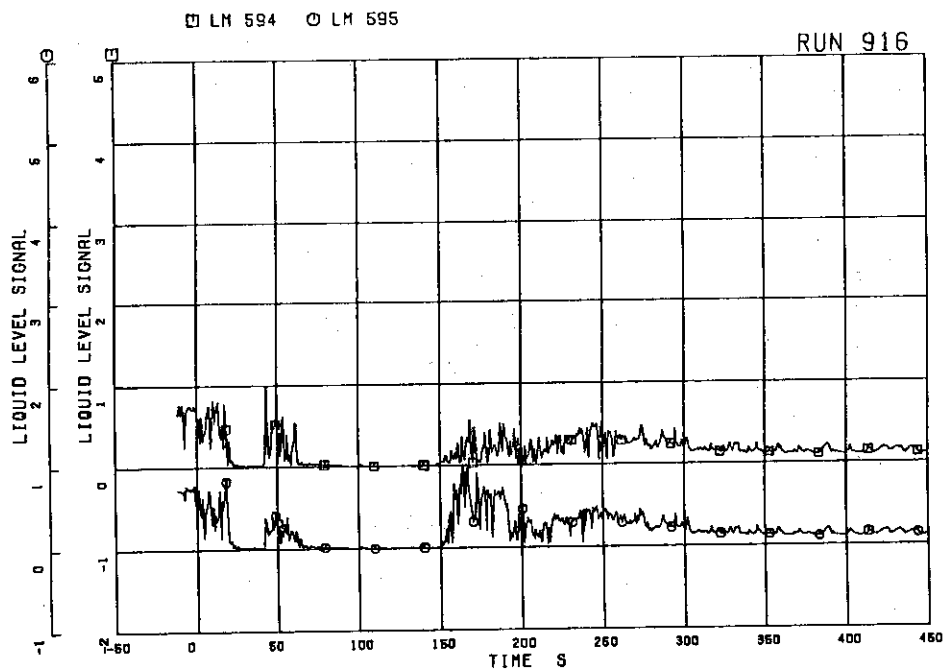


FIG.5.185 LIQUID LEVEL SIGNALS IN CHANNEL BOX D

FIG.5.186 LIQUID LEVEL SIGNAL IN CHANNEL A
OUTLET, LOCATION A1

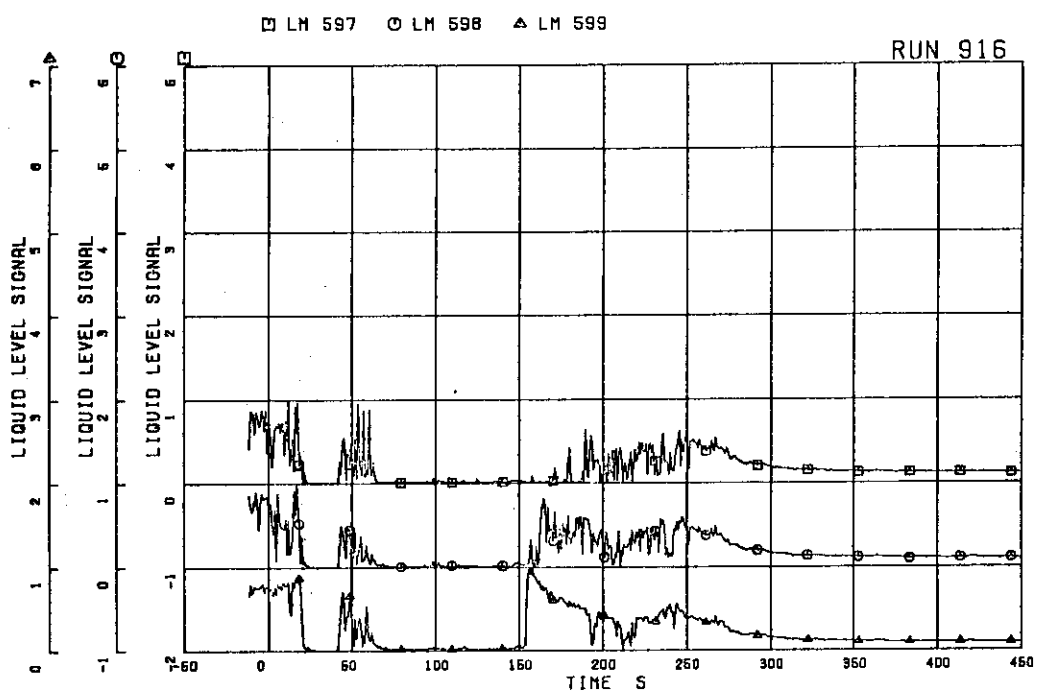


FIG.5.187 LIQUID LEVEL SIGNALS IN CHANNEL A
OUTLET, LOCATION A2

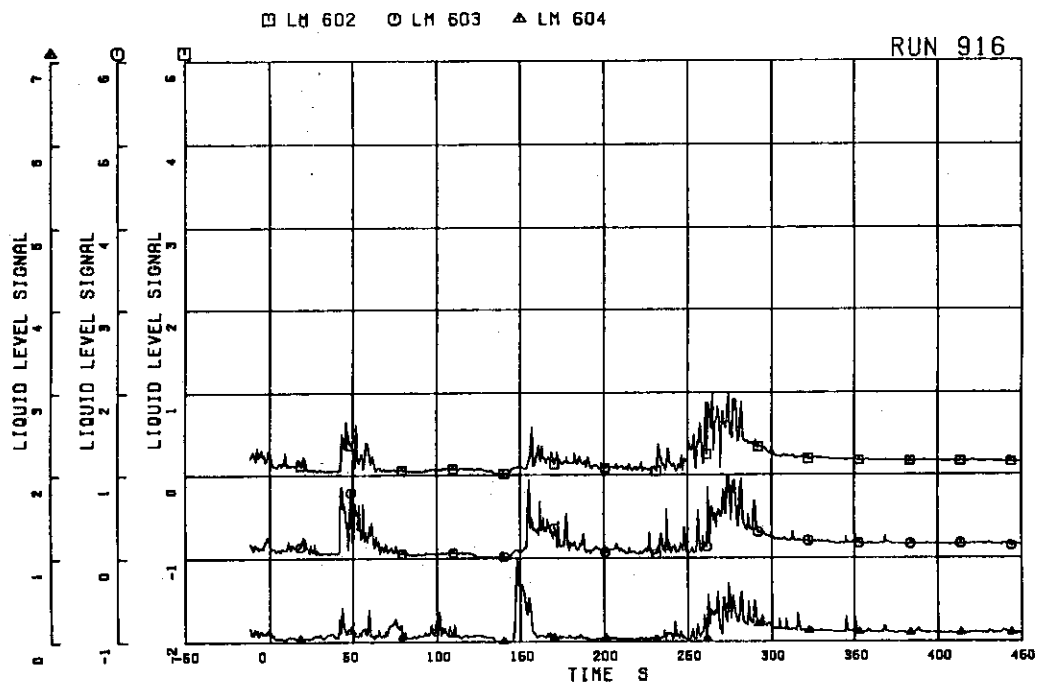


FIG.5.188 LIQUID LEVEL SIGNALS IN CHANNEL A
OUTLET CENTER

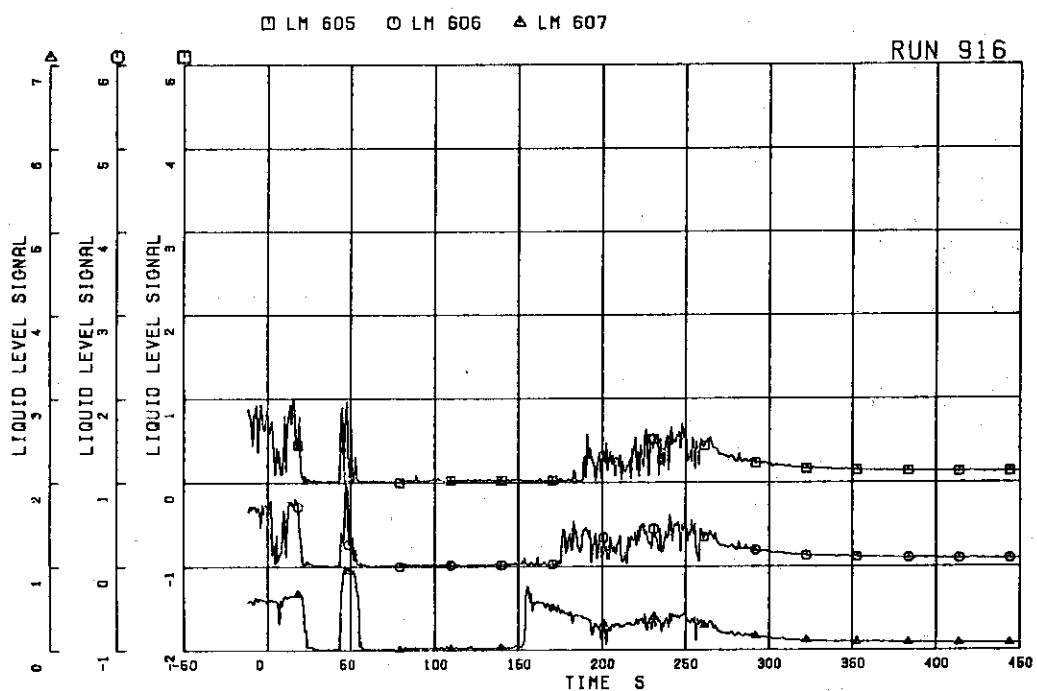


FIG.5.189 LIQUID LEVEL SIGNALS IN CHANNEL C
OUTLET LOCATION C1

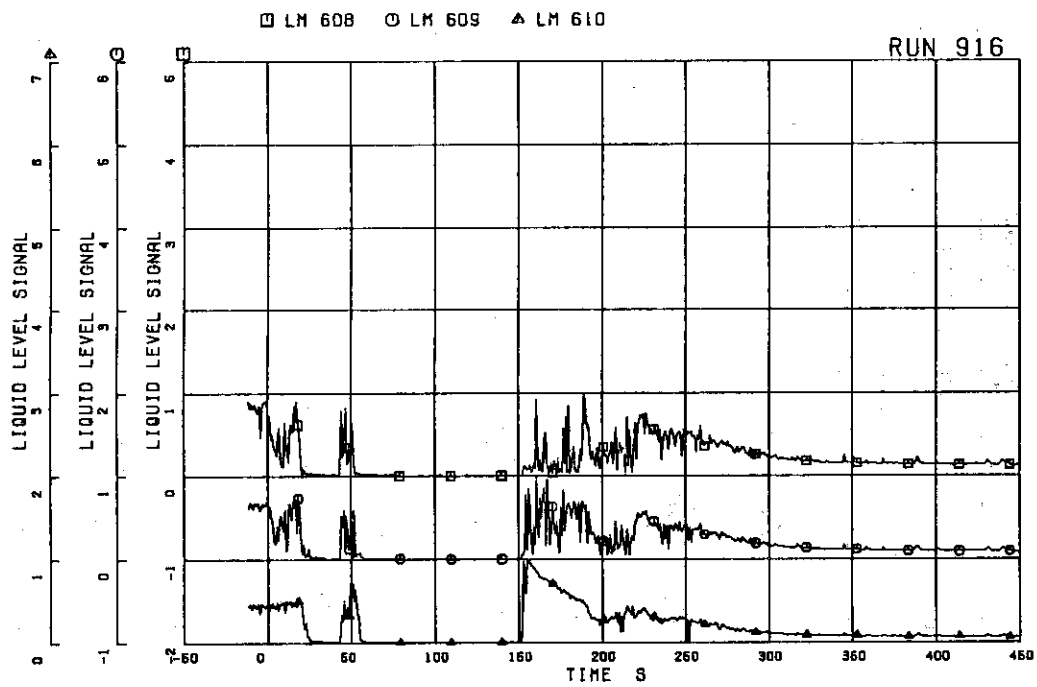


FIG.5.190 LIQUID LEVEL SIGNALS IN CHANNEL C
OUTLET LOCATION C2

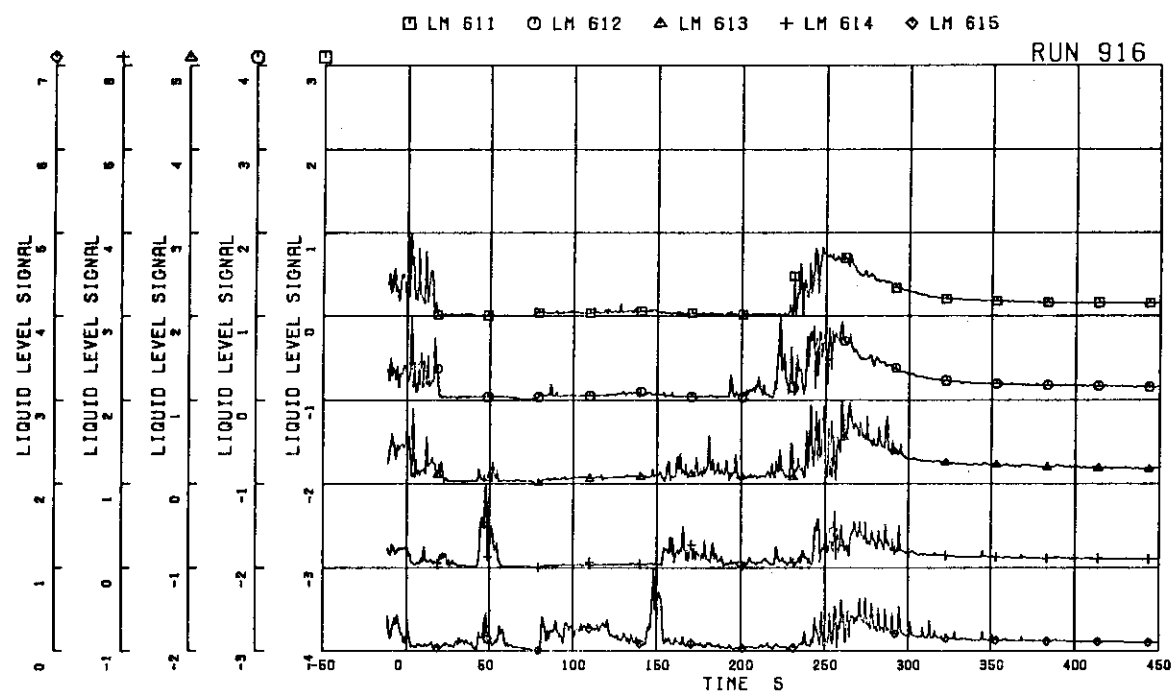


FIG.5.191 LIQUID LEVEL SIGNALS IN CHANNEL C
OUTLET CENTER

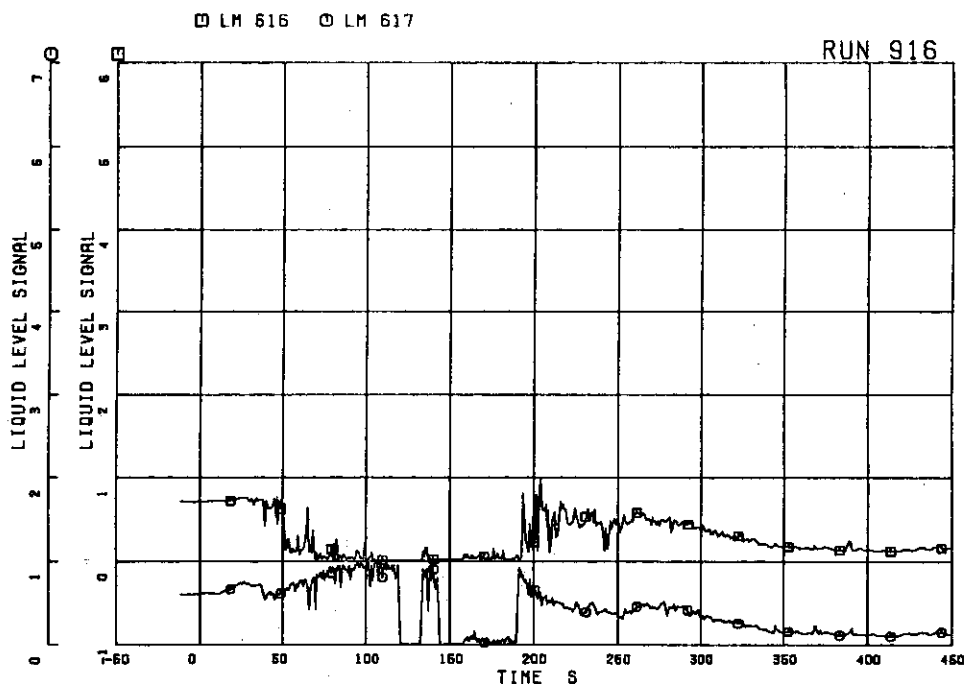
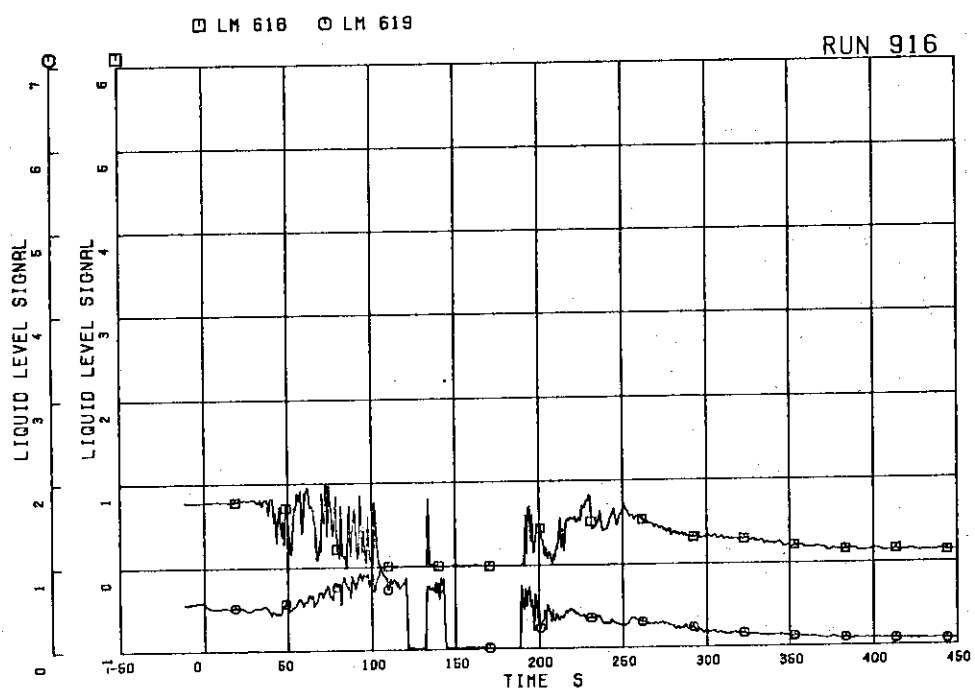
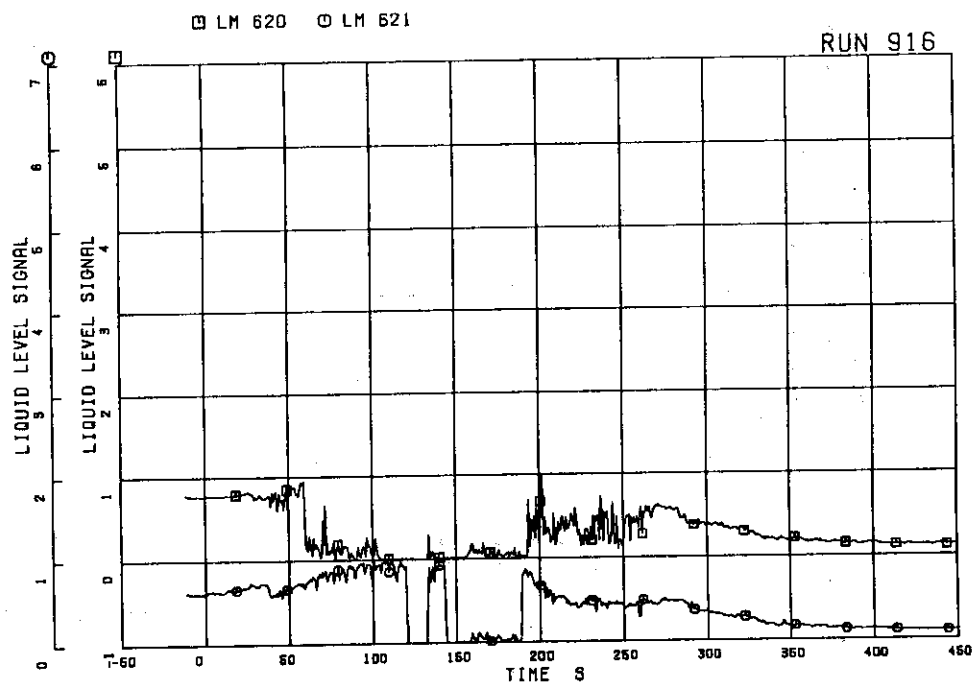
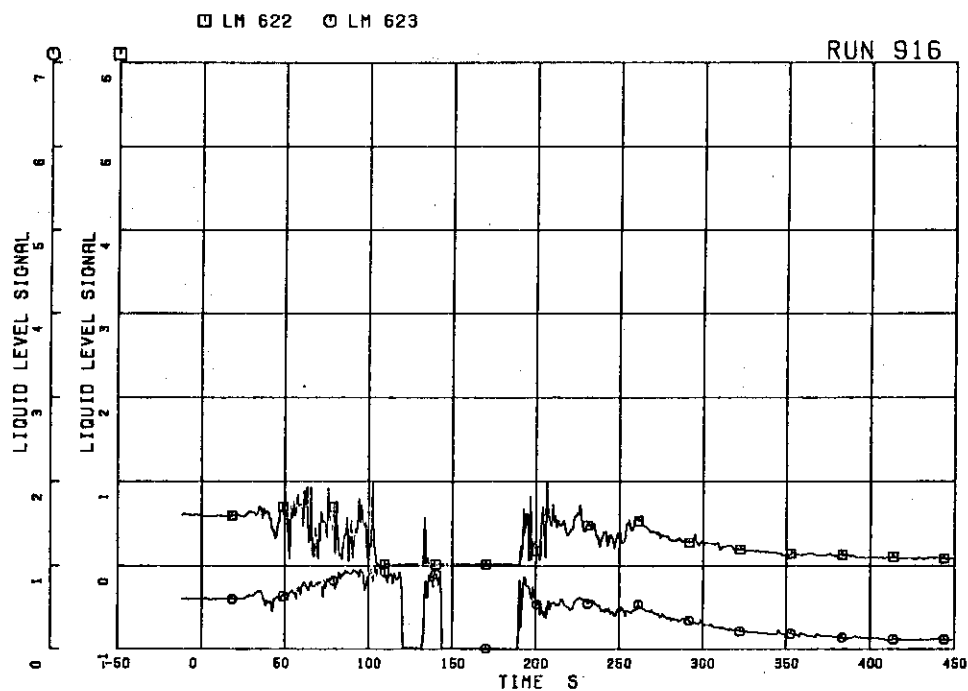
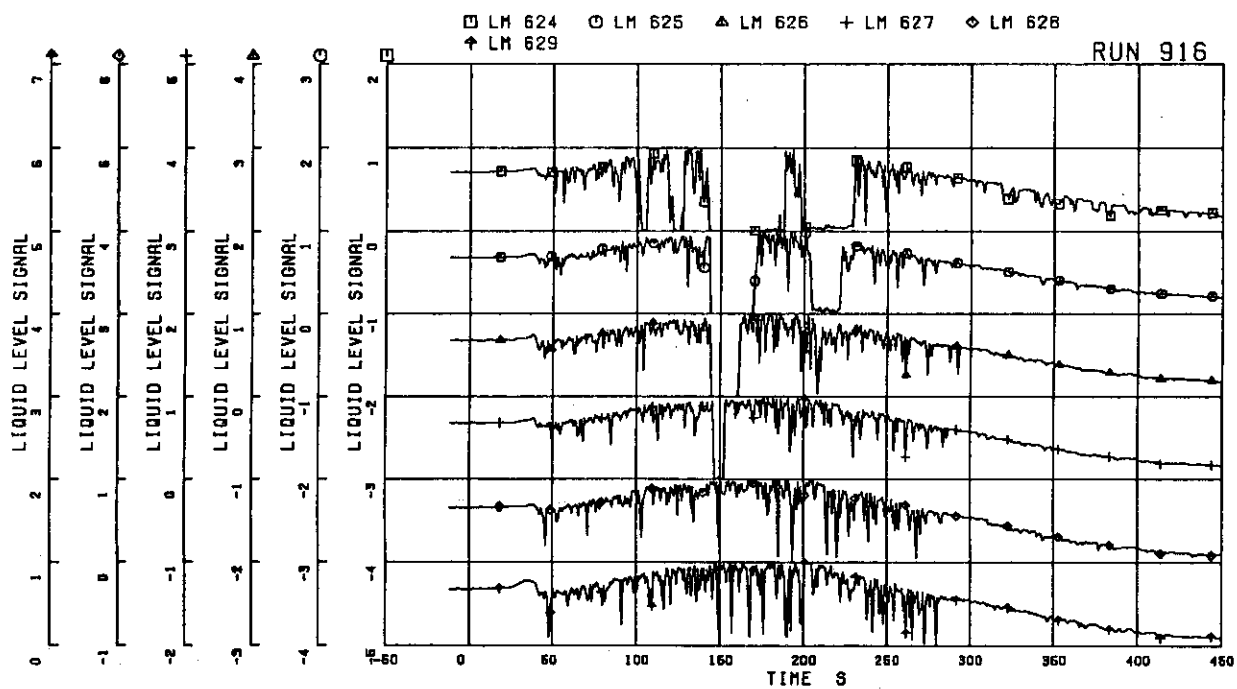
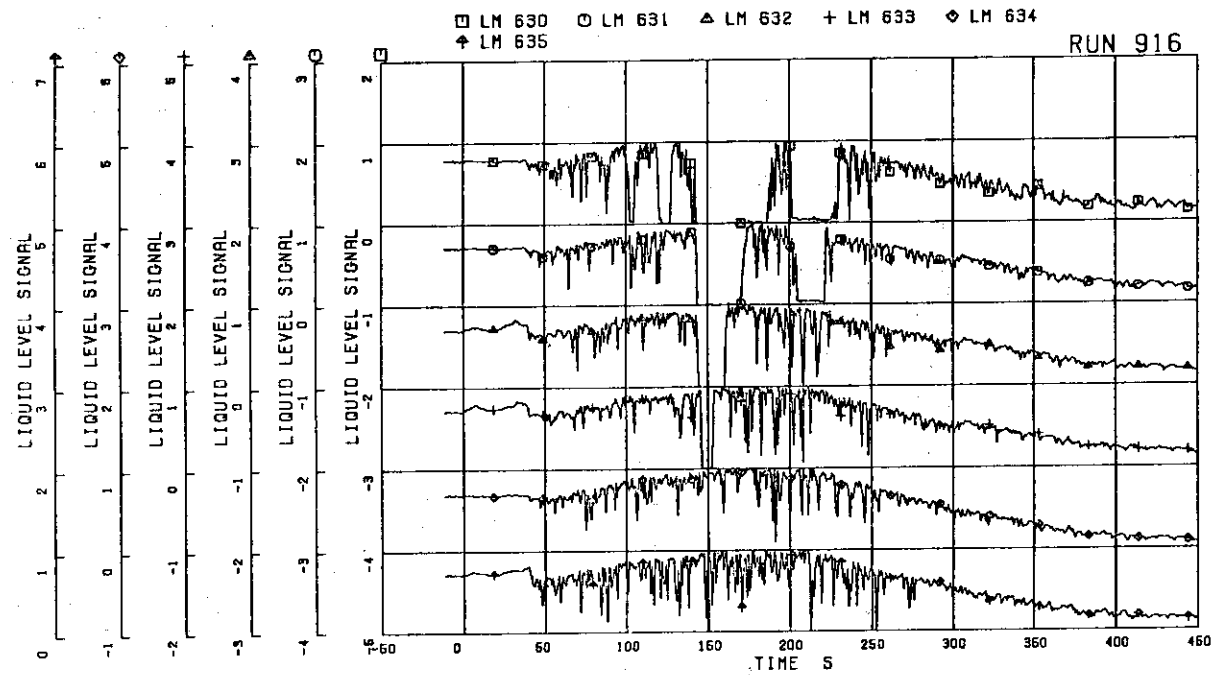
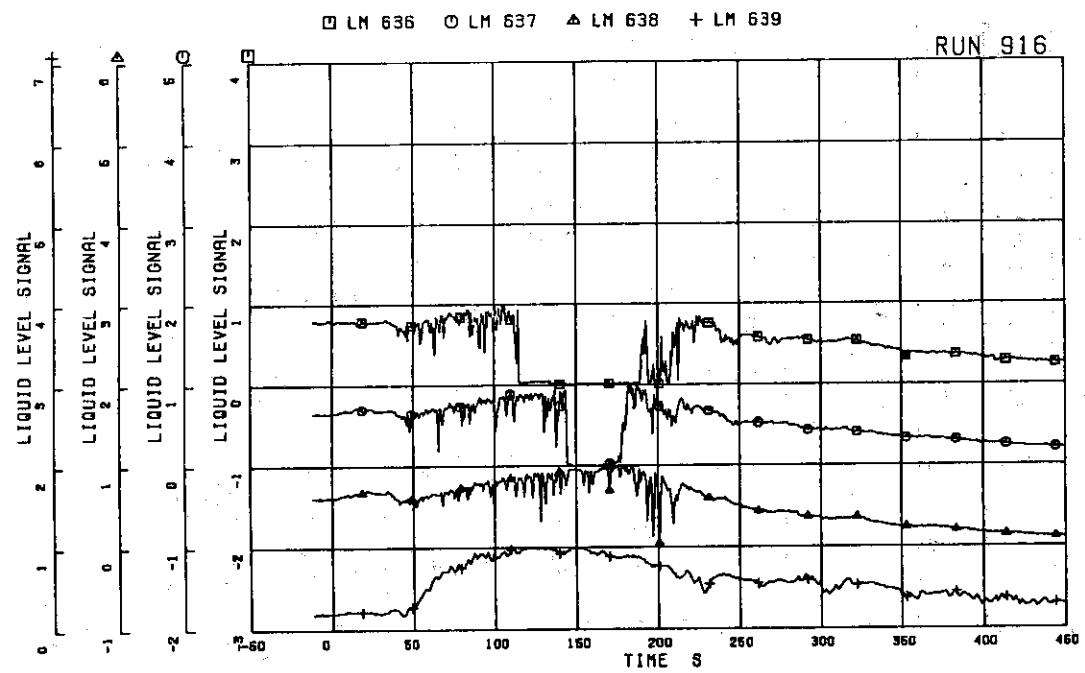


FIG.5.192 LIQUID LEVEL SIGNALS IN CHANNEL A
INLET

FIG.5.193 LIQUID LEVEL SIGNALS IN CHANNEL B
INLETFIG.5.194 LIQUID LEVEL SIGNALS IN CHANNEL C
INLET

FIG.5.195 LIQUID LEVEL SIGNALS IN CHANNEL D
INLETFIG.5.196 LIQUID LEVEL SIGNALS IN LOWER PLENUM,
NORTH

FIG.5.197 LIQUID LEVEL SIGNALS IN LOWER PLENUM,
SOUTHFIG.5.198 LIQUID LEVEL SIGNALS IN GUIDE TUBE,
NORTH

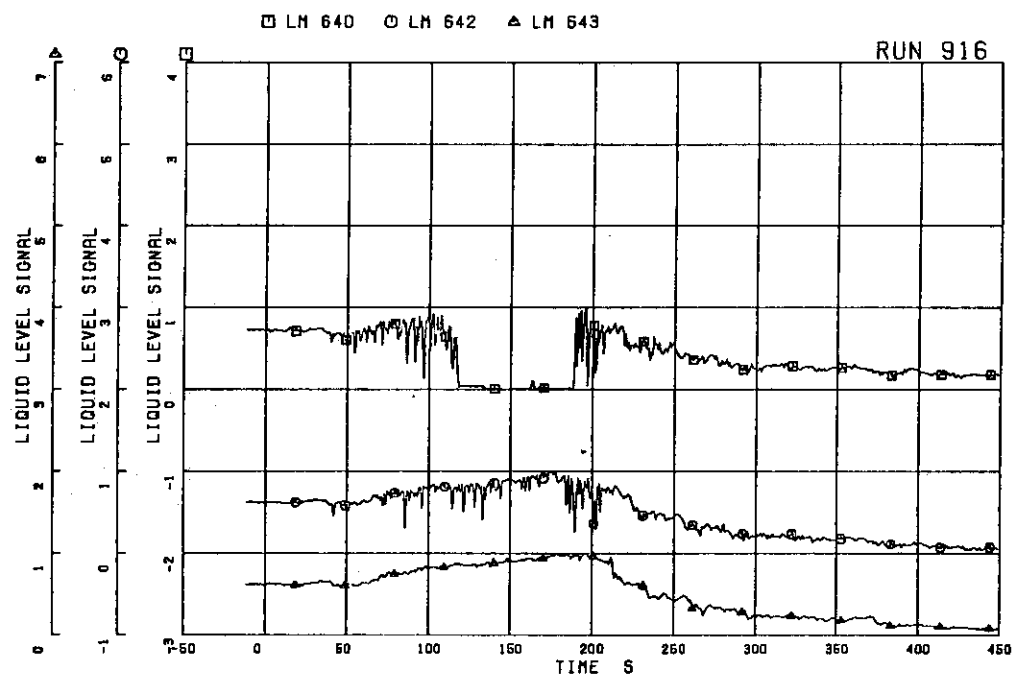


FIG.5.199 LIQUID LEVEL SIGNALS IN GUIDE TUBE,
SOUTH

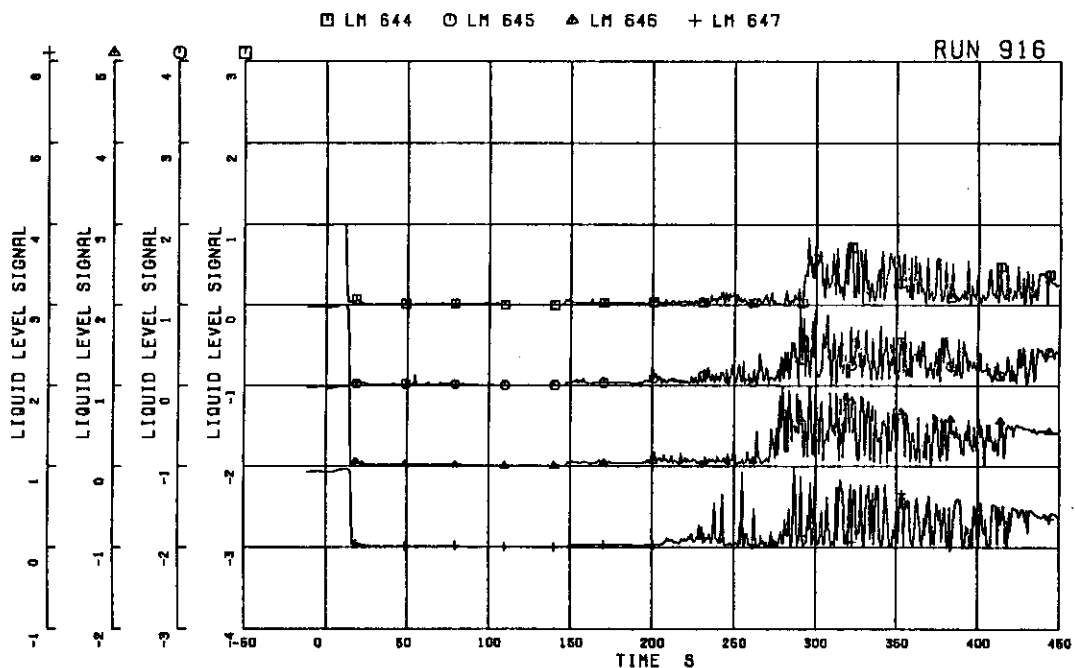


FIG.5.200 LIQUID LEVEL SIGNALS IN DOWNCOMER,
O SIDE

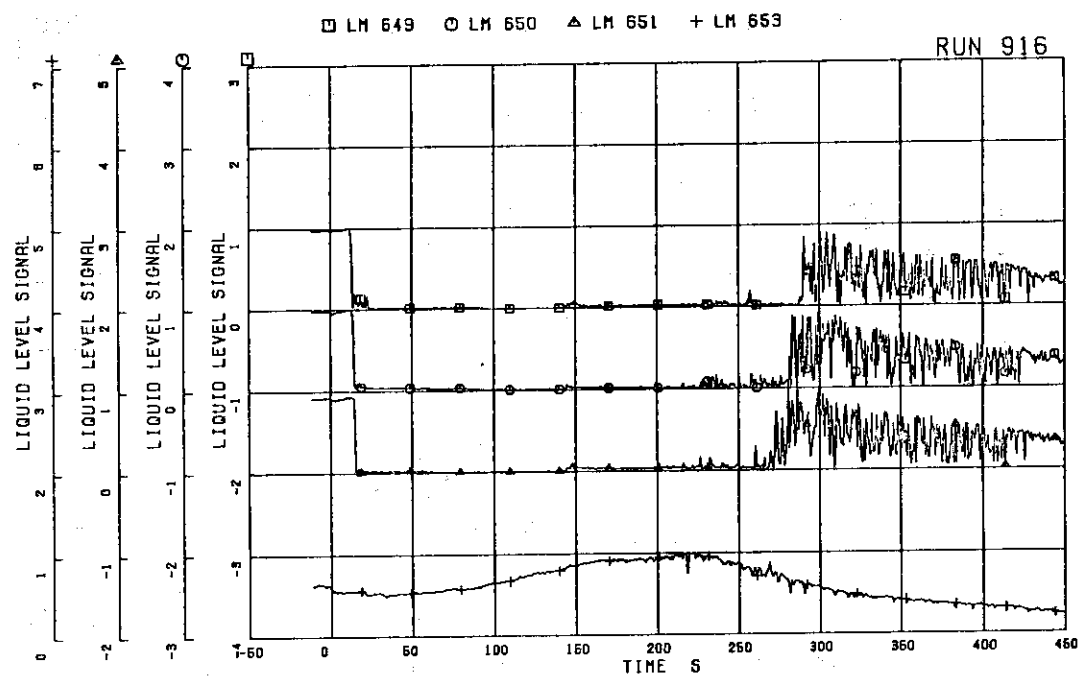


FIG.5.201 LIQUID LEVEL SIGNALS IN DOWNCOMER,
B SIDE

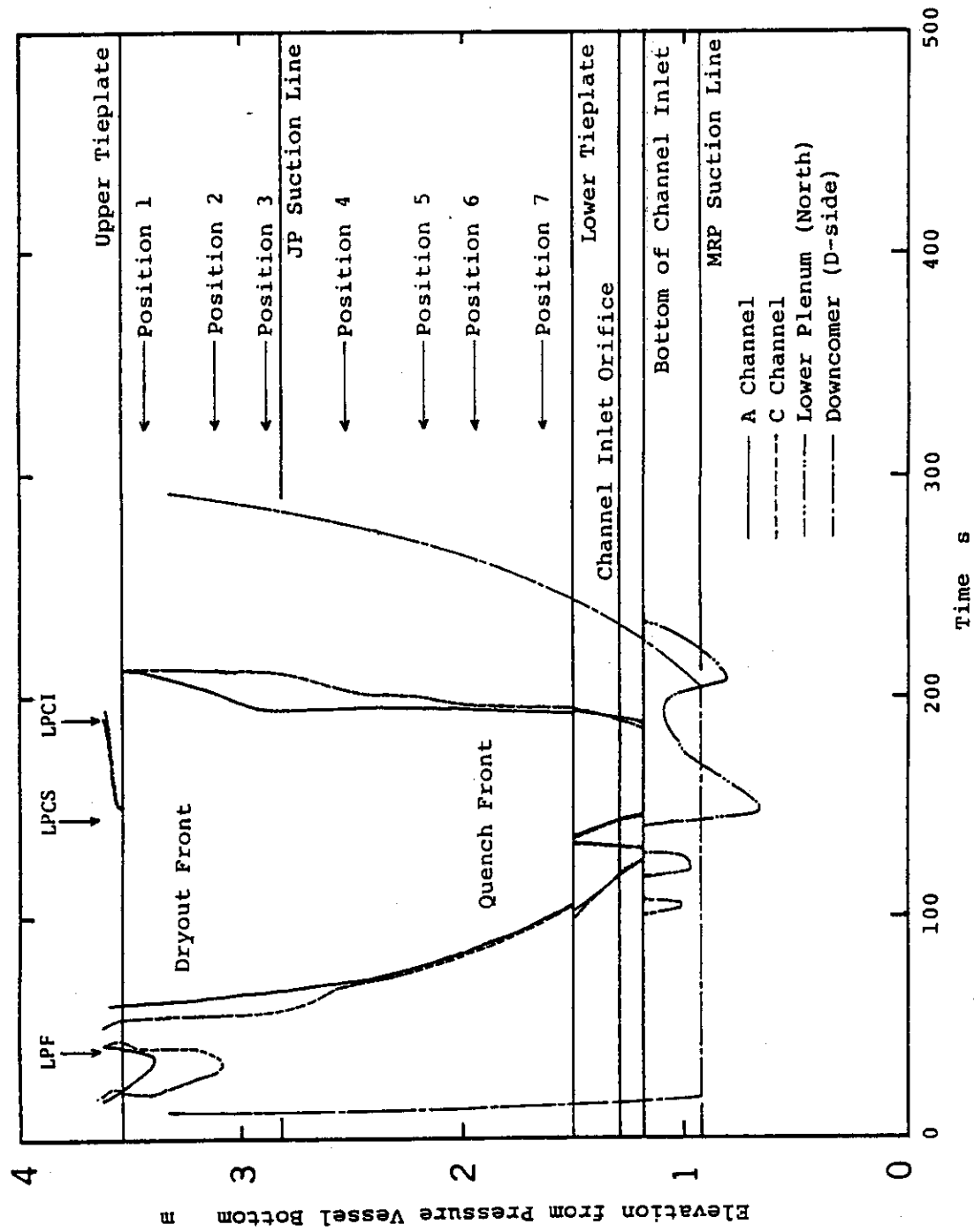


Fig. 5.202 Estimated liquid level in pressure vessel

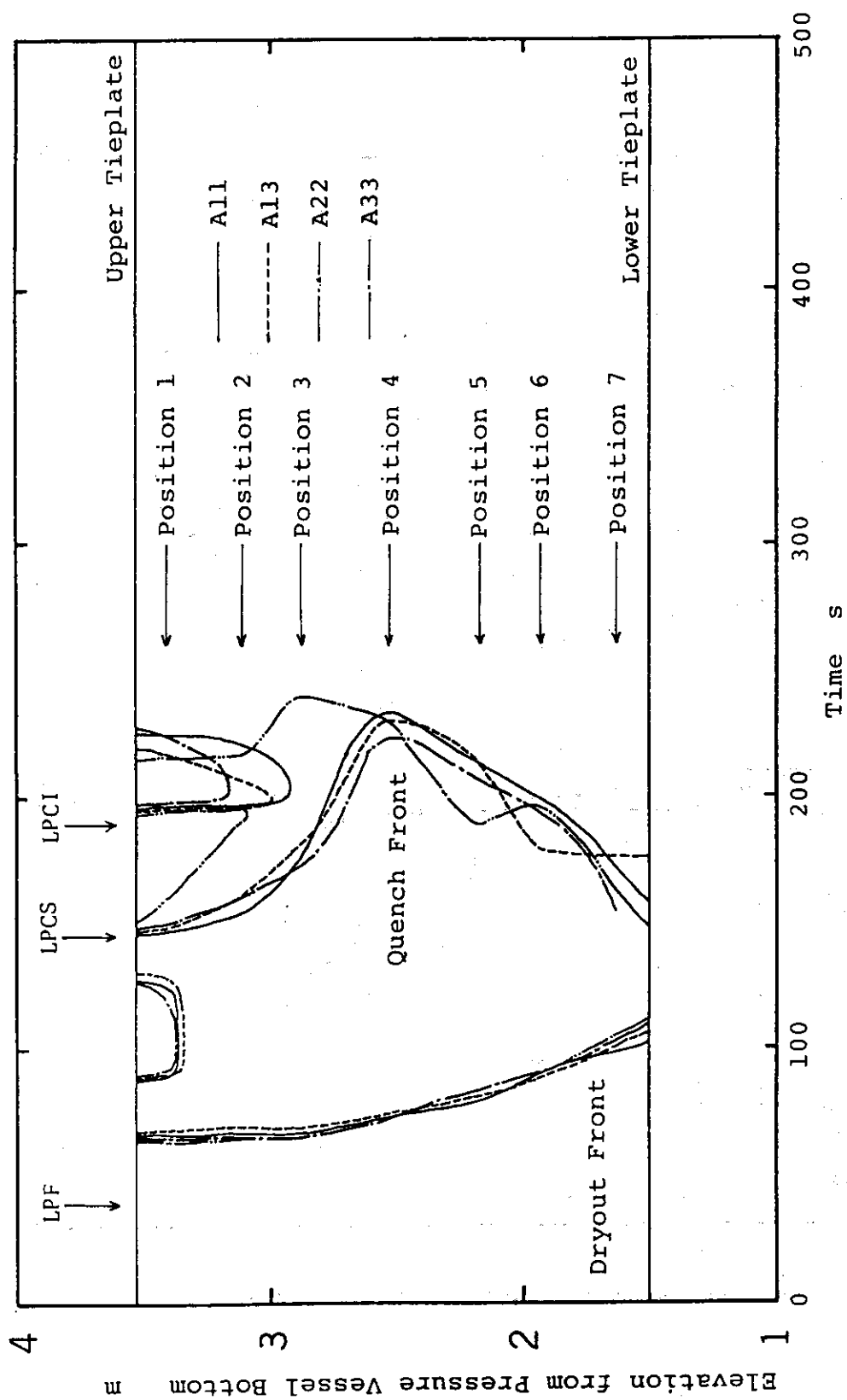


Fig. 5.203 Dryout and quench transients in channel A

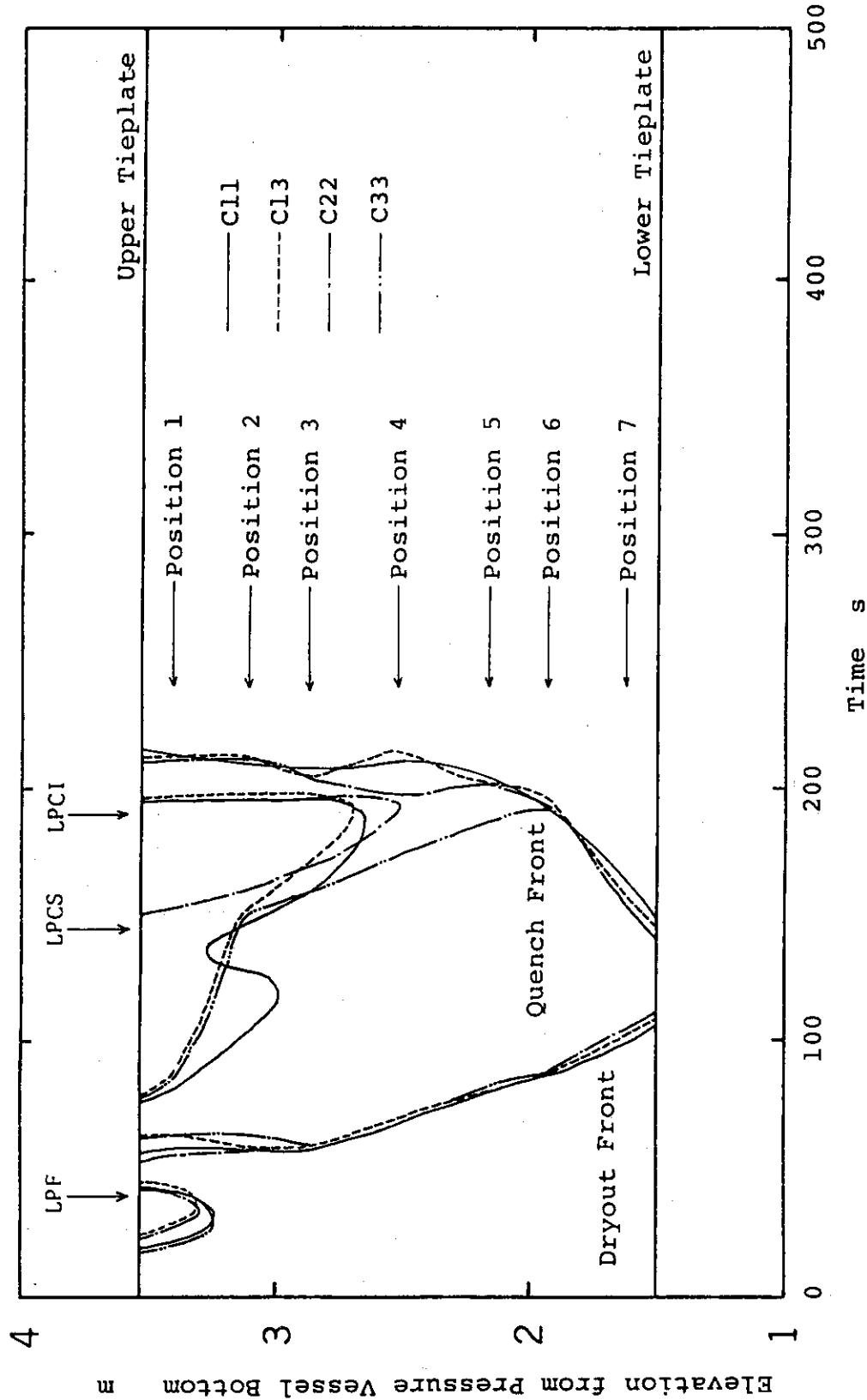


Fig. 5.204 Dryout and quench transients in channel C

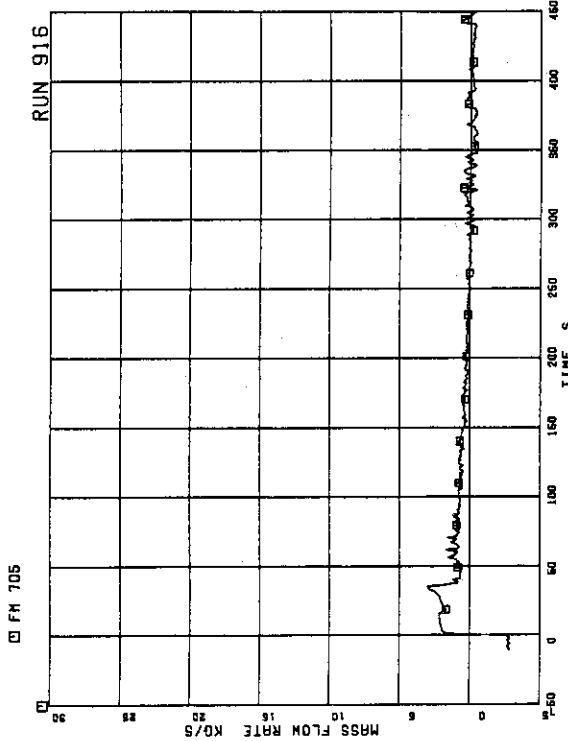


FIG.5.207 FLOW RATE AT MRP SIDE OF BREAK
(BASED ON LOW RANGE DRAG DISK DATA)

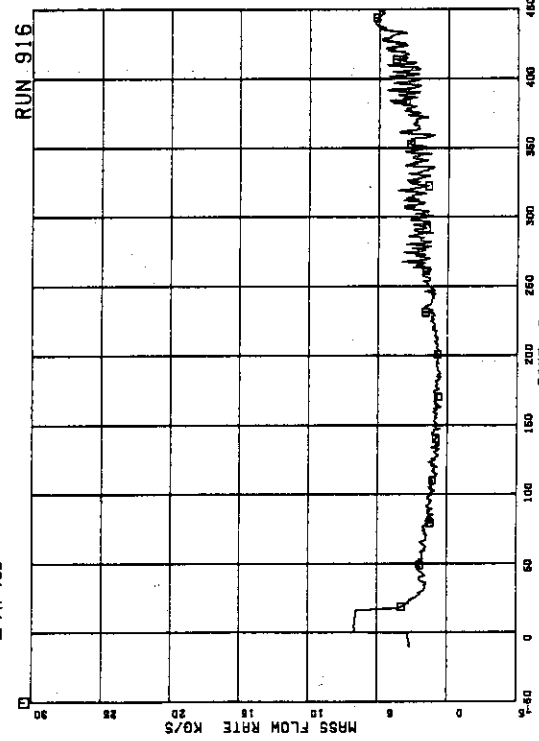


FIG.5.208 FLOW RATE AT PV SIDE OF BREAK
(BASED ON LOW RANGE DRAG DISK DATA)

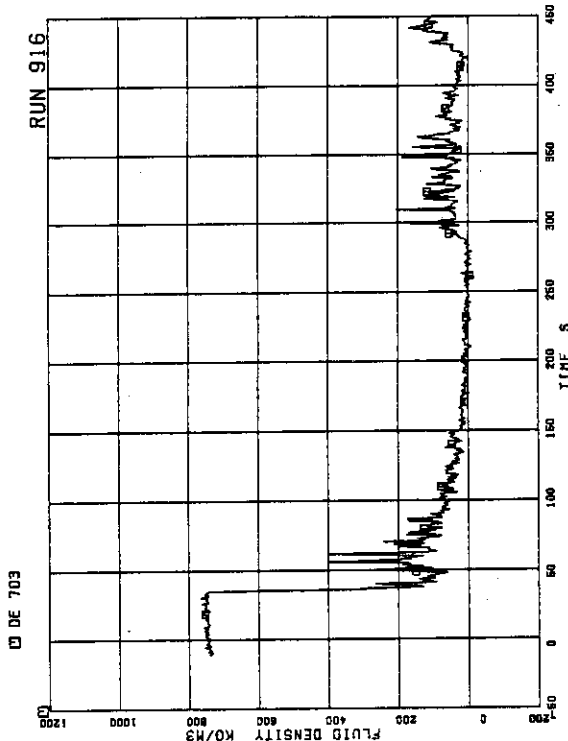


FIG.5.205 AVERAGE DENSITY AT MRP SIDE OF BREAK

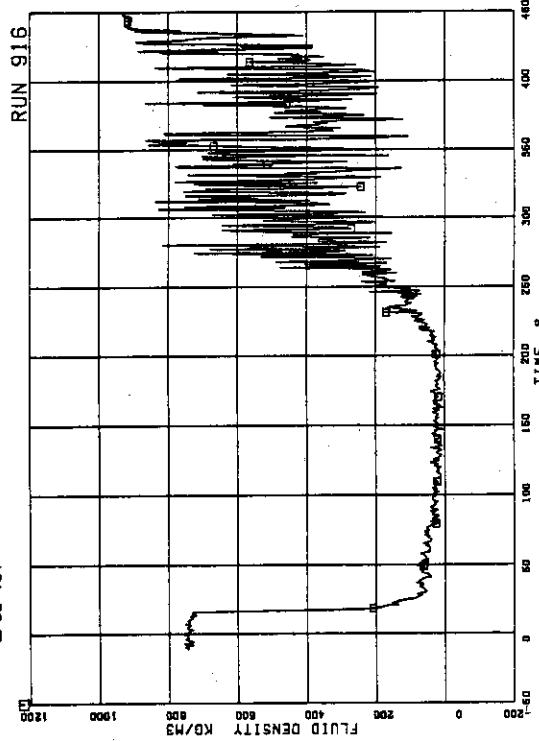


FIG.5.206 AVERAGE DENSITY AT PV SIDE OF BREAK

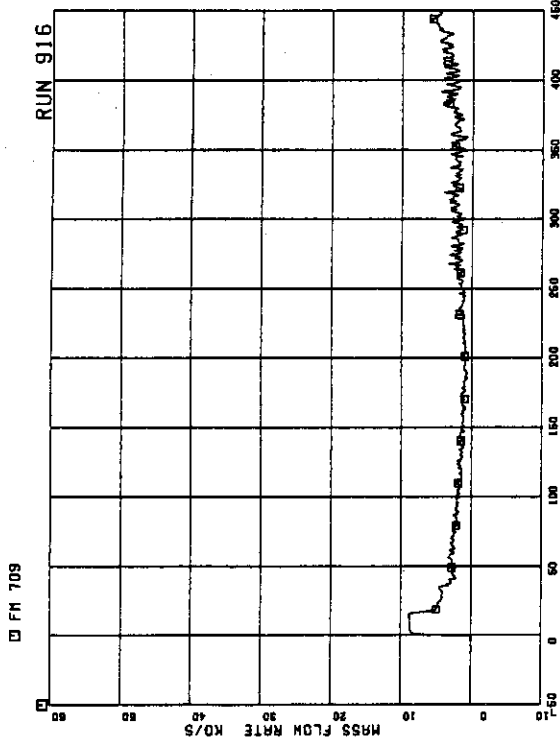


FIG.5.211 TOTAL DISCHARGE FLOW RATE FROM BREAK
(BASED ON LOW RANGE DRAG DISK DATA)

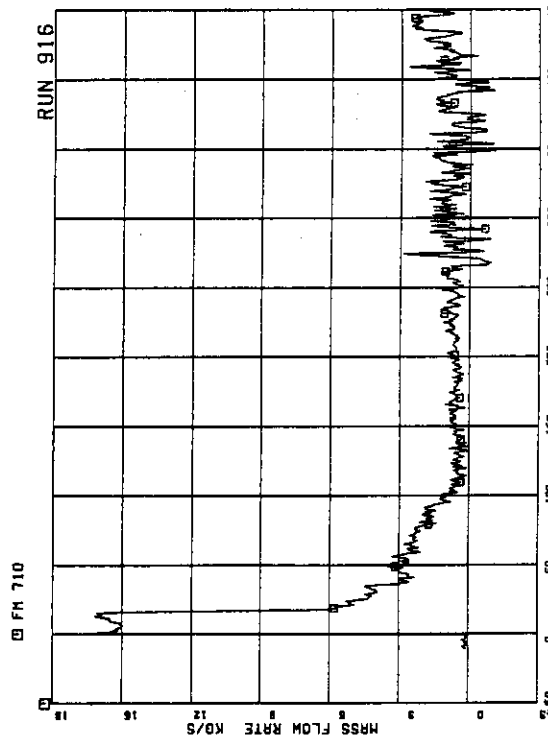


FIG.5.212 TOTAL DISCHARGE FLOW RATE FROM BREAK
(BASED ON HIGH RANGE DRAG DISK DATA)

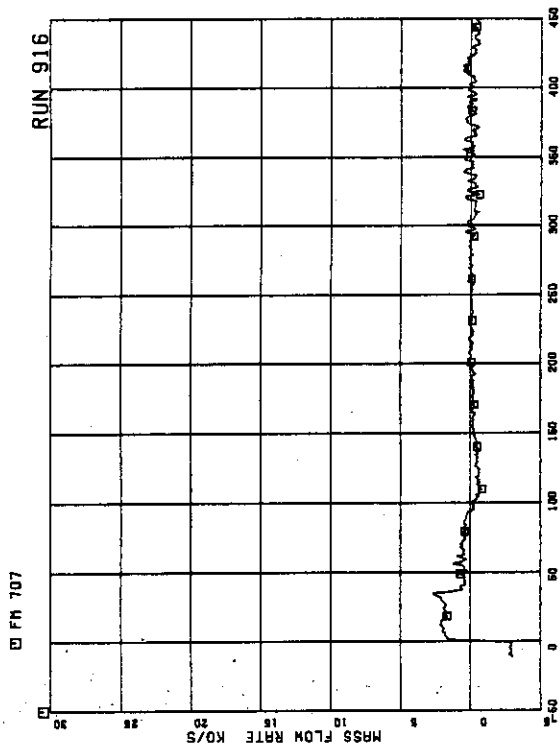


FIG.5.209 FLOW RATE AT MRP SIDE OF BREAK
(BASED ON HIGH RANGE DRAG DISK DATA)

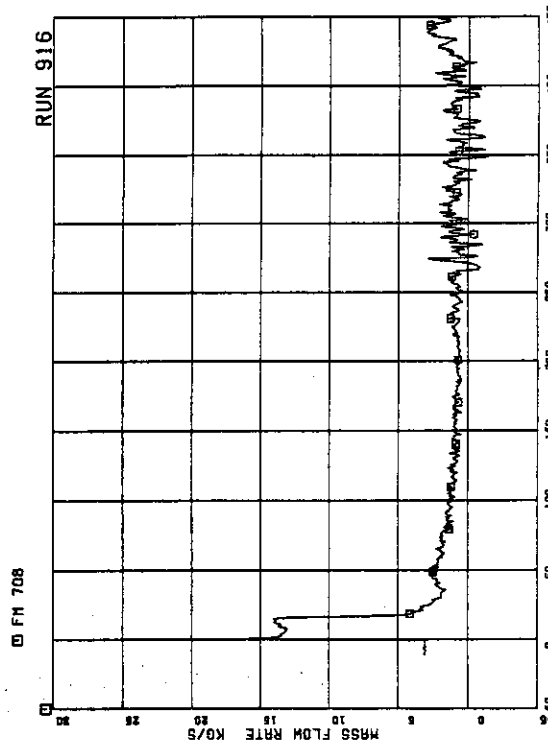


FIG.5.210 FLOW RATE AT PV SIDE OF BREAK
(BASED ON HIGH RANGE DRAG DISK DATA)

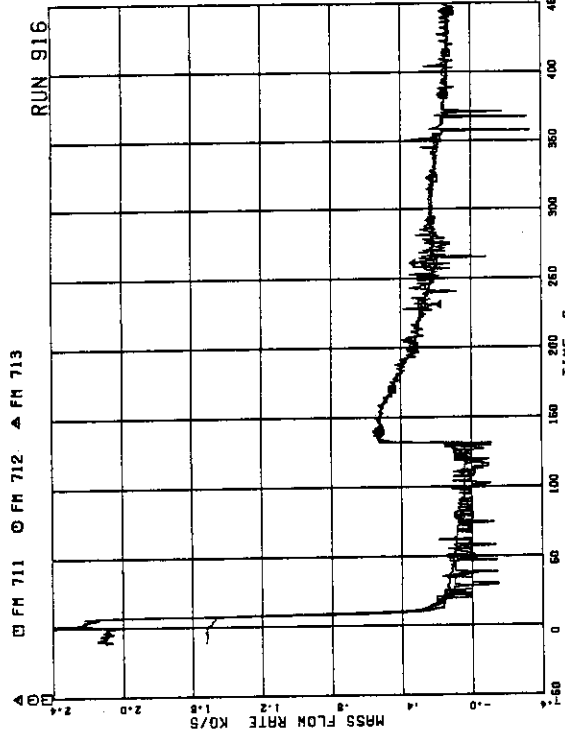


FIG.5.213 STEAM DISCHARGE FLOW RATE THROUGH MSL

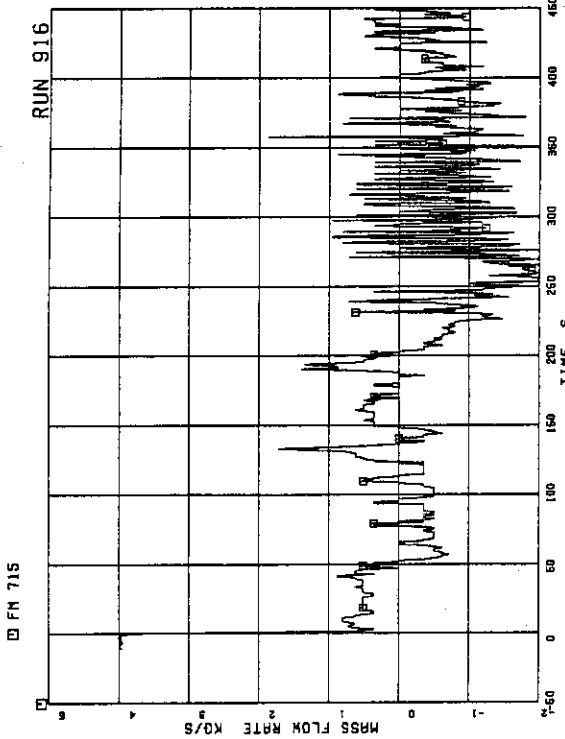


FIG.5.215 FLOW RATE AT CHANNEL B INLET

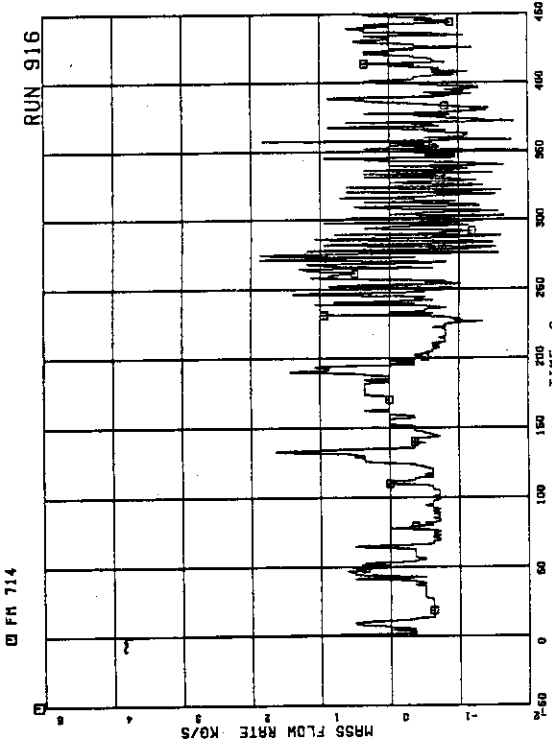


FIG.5.214 FLOW RATE AT CHANNEL A INLET

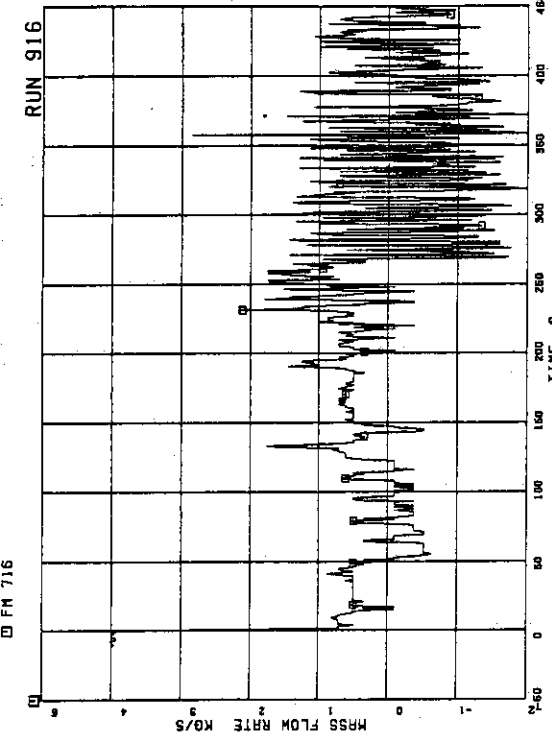


FIG.5.216 FLOW RATE AT CHANNEL C INLET

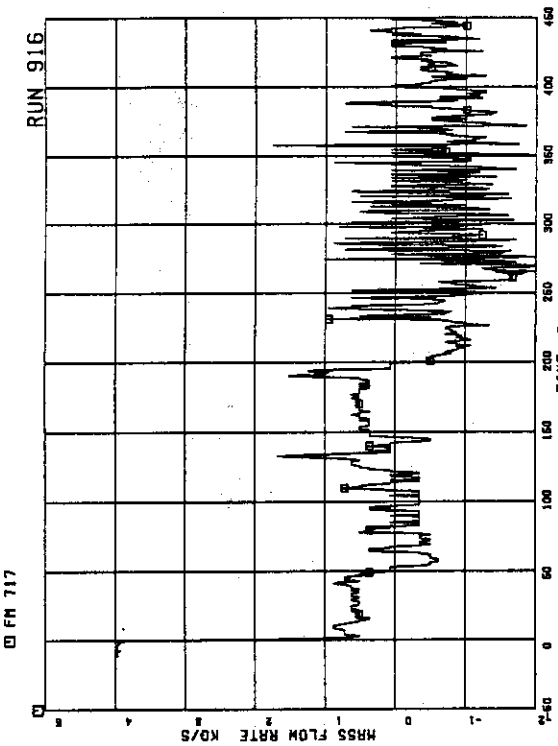


FIG.5.217 FLOW RATE AT CHANNEL D INLET

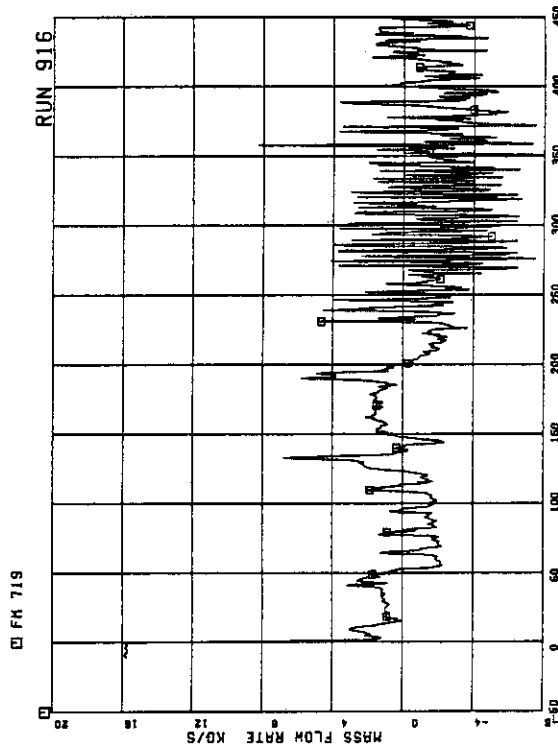


FIG.5.219 TOTAL CHANNEL INLET FLOW RATE

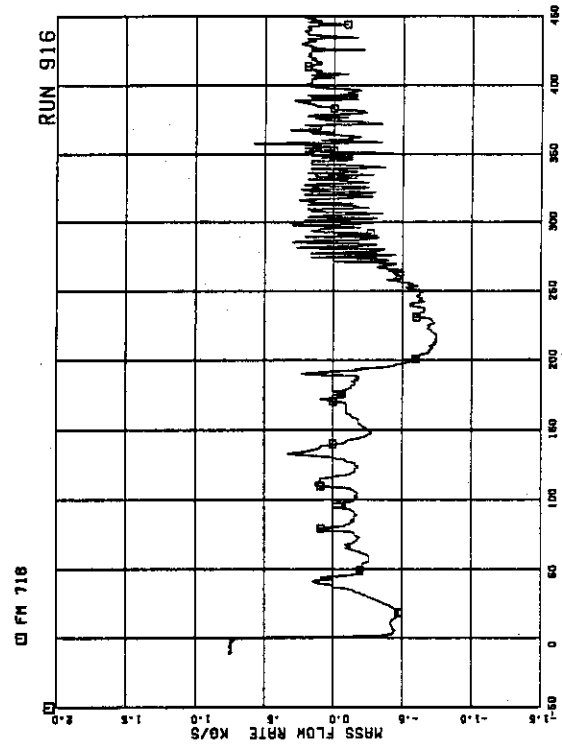


FIG.5.220 FLOW RATE AT JP-1,2 OUTLET
(HIGH RANGE)

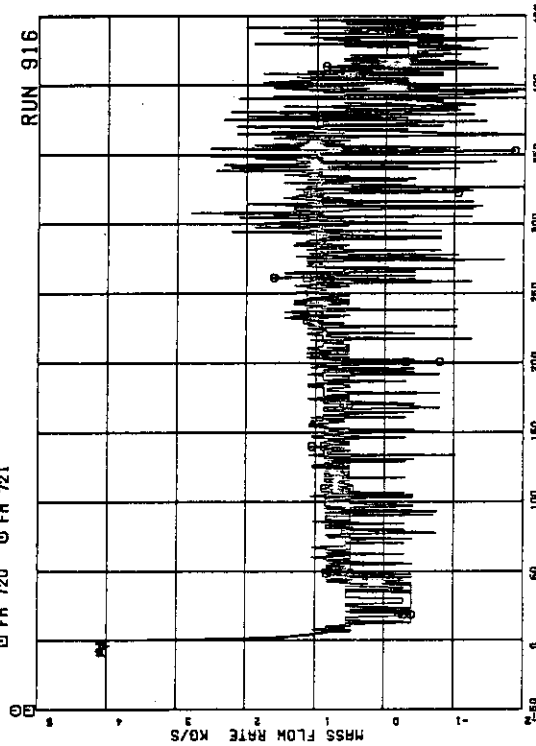


FIG.5.218 FLOW RATE AT BYPASS HOLE

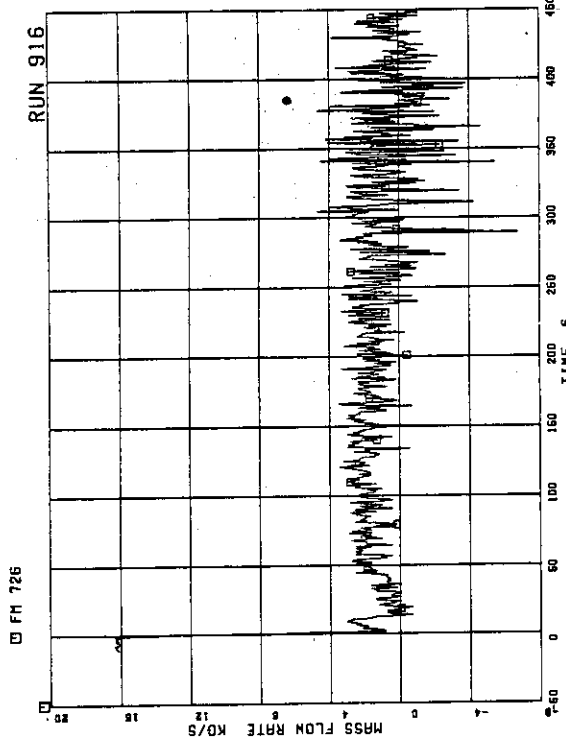
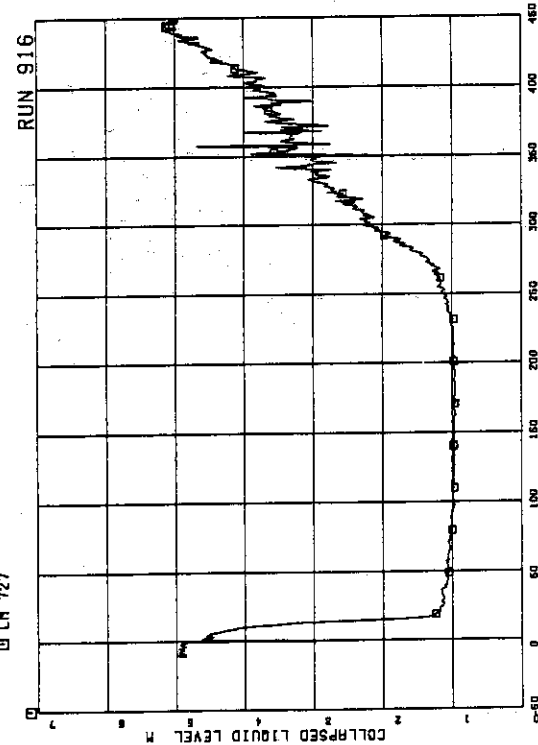
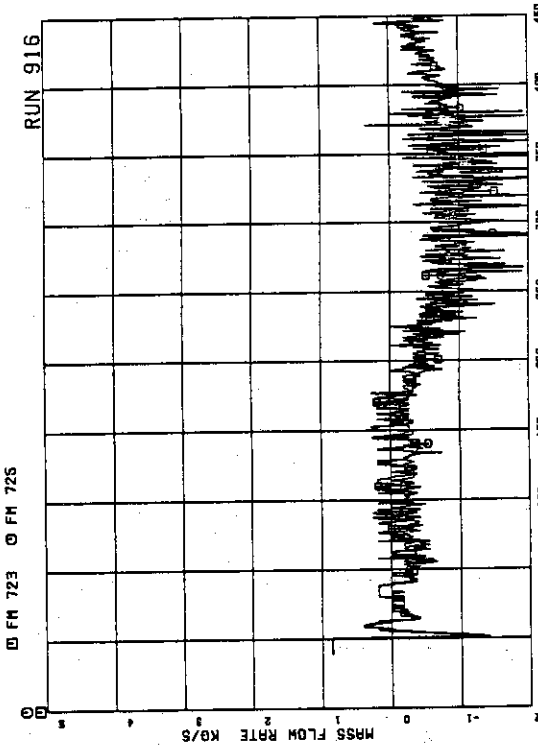
FIG.5.221 FLOW RATE AT JP-3,4 OUTLET
(HIGH RANGE)FIG.5.221 FLOW RATE AT JP-3,4 OUTLET
(HIGH RANGE)FIG.5.223 TOTAL JP OUTLET FLOW RATE
(HIGH RANGE)

FIG.5.224 COLLAPSED LIQUID LEVEL IN DOWNCOMER

FIG.5.222 FLOW RATE AT JP-3,4 OUTLET
(LOW RANGE)

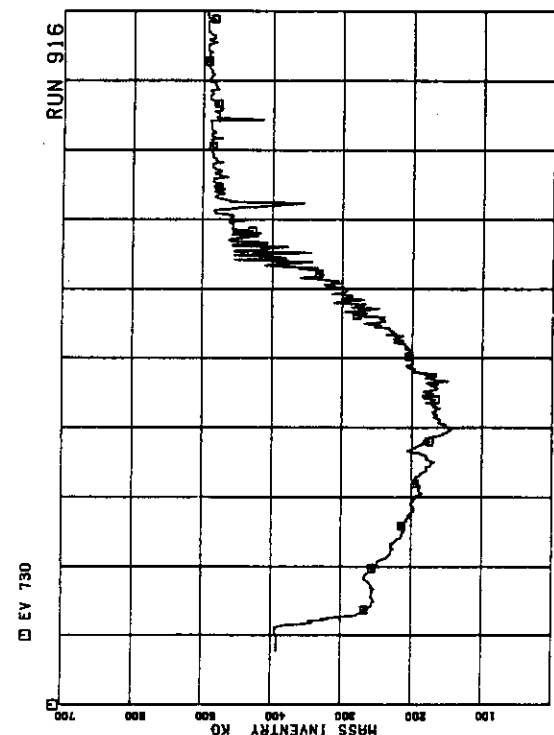


FIG.5.227 FLUID INVENTORY INSIDE CORE SHROUD

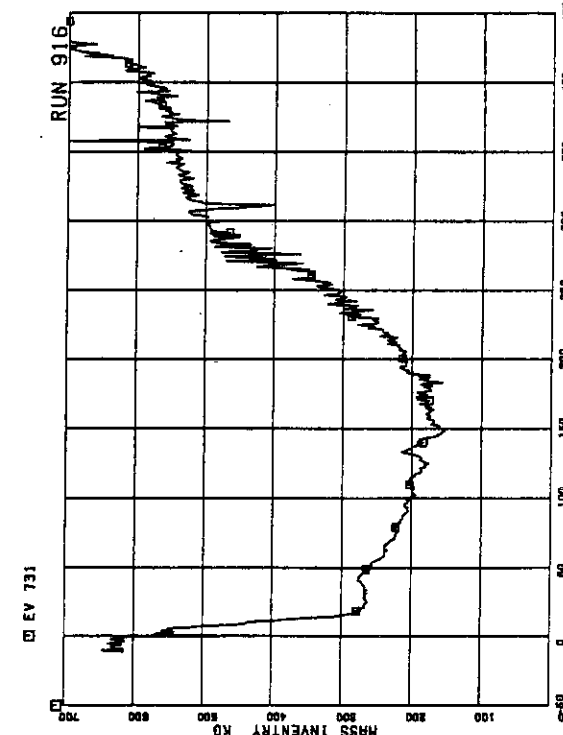


FIG.5.228 TOTAL FLUID INVENTORY IN PRESSURE VESSEL

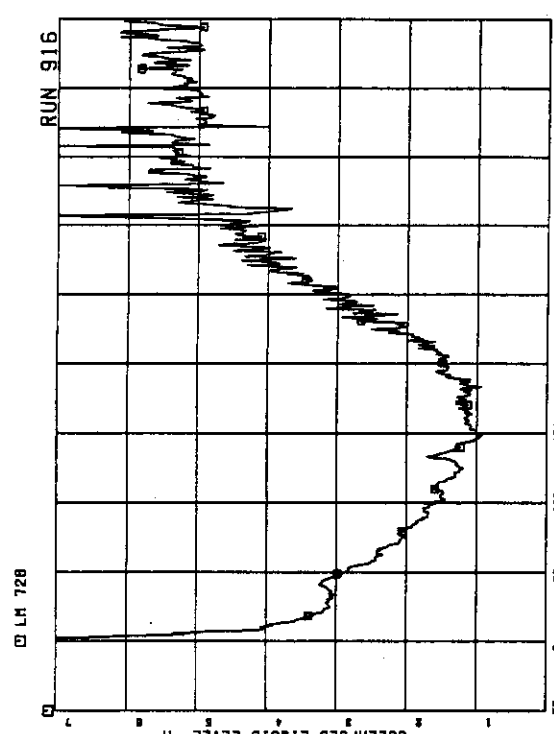


FIG.5.225 COLLAPSED LIQUID LEVEL INSIDE CORE SHROUD

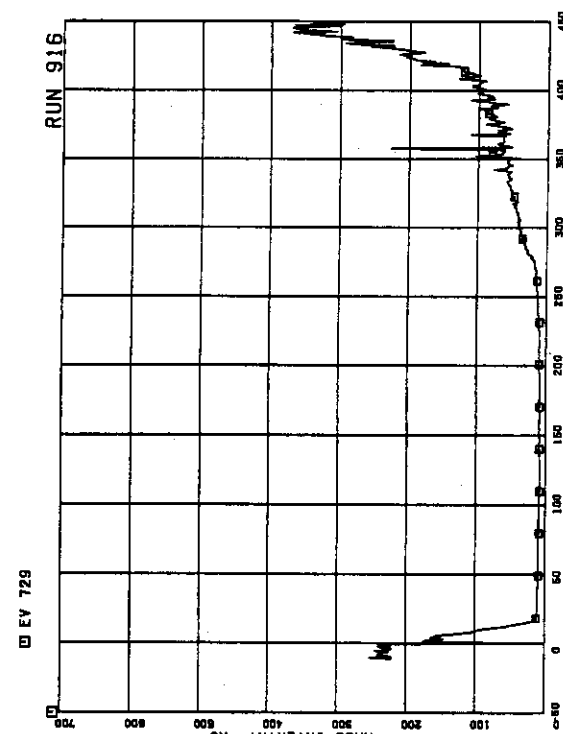


FIG.5.226 FLUID INVENTORY IN DOWNCOMER

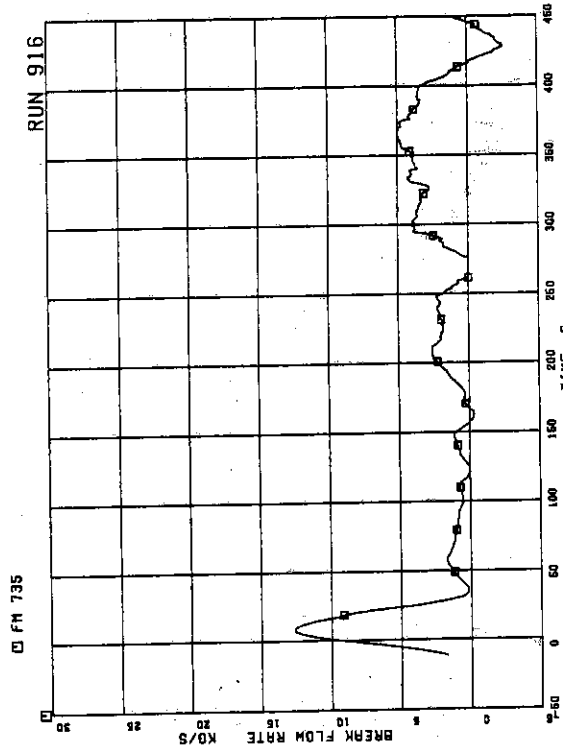


FIG.5.231 DISCHARGED FLOW RATE FROM BREAK

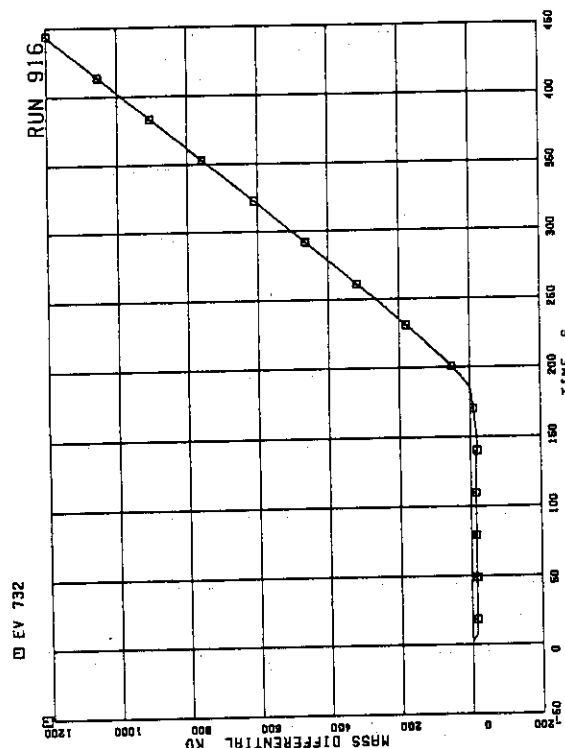


FIG.5.229 FLUID MASS INCREASE BY ECCS AND FW AND
DECREASE BY STEAM DISCHARGE FLOW

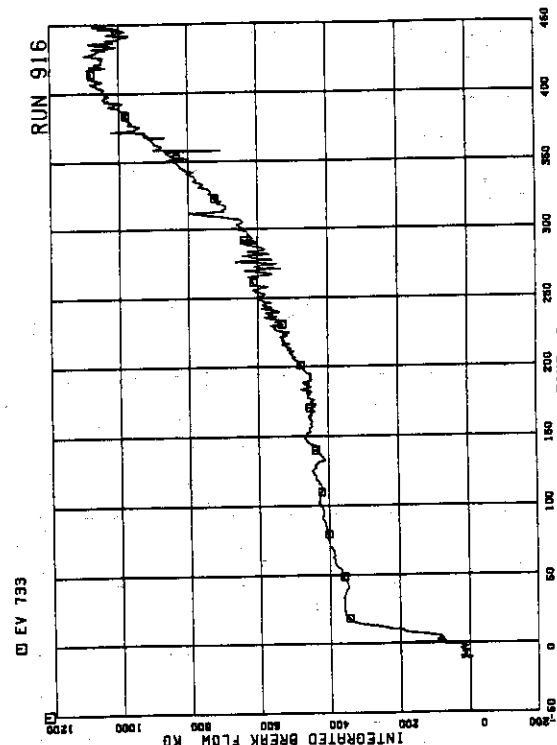


FIG.5.230 DISCHARGED FLUID MASS FROM BREAK

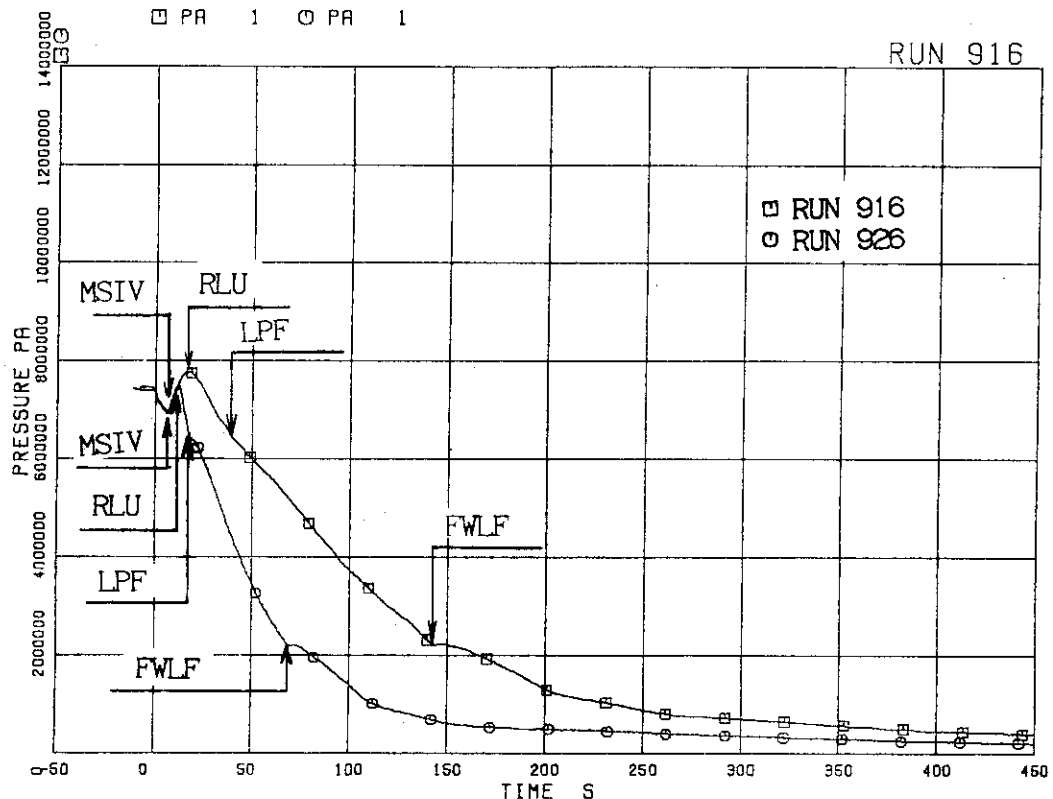


FIG. 6. 1 LOWER PLENUM PRESSURES

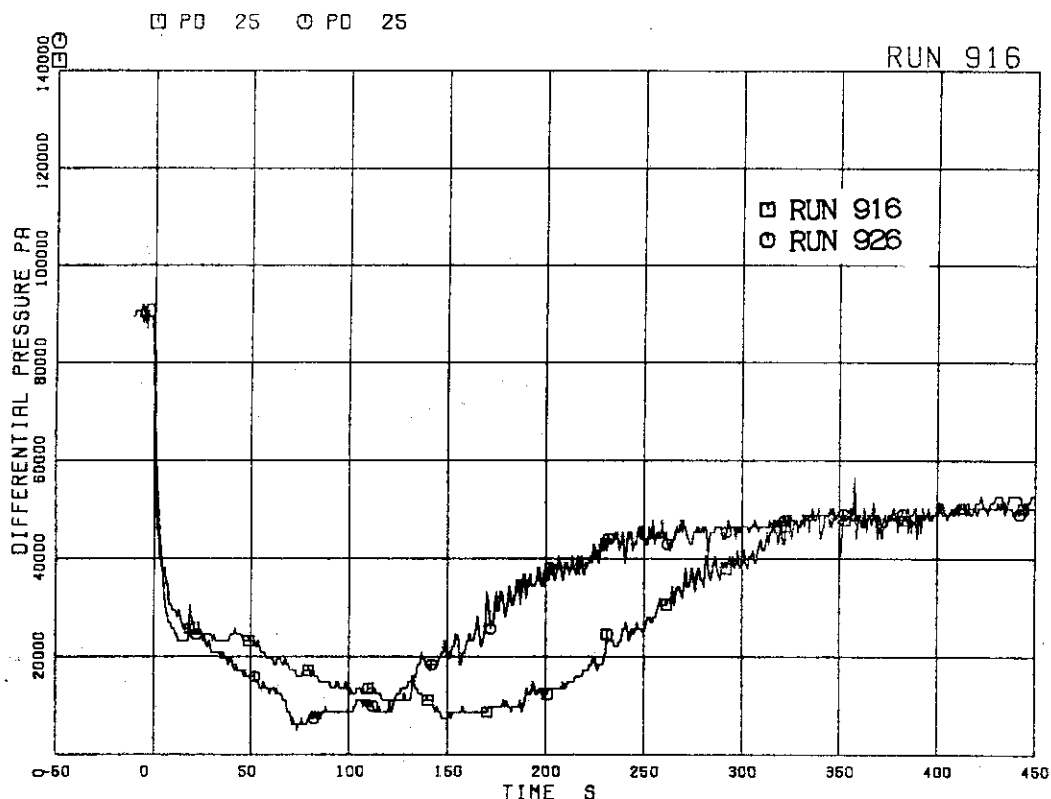


FIG. 6. 2 DIFFERENTIAL PRESSURES BETWEEN TOP AND BOTTOM OF PRESSURE VESSEL

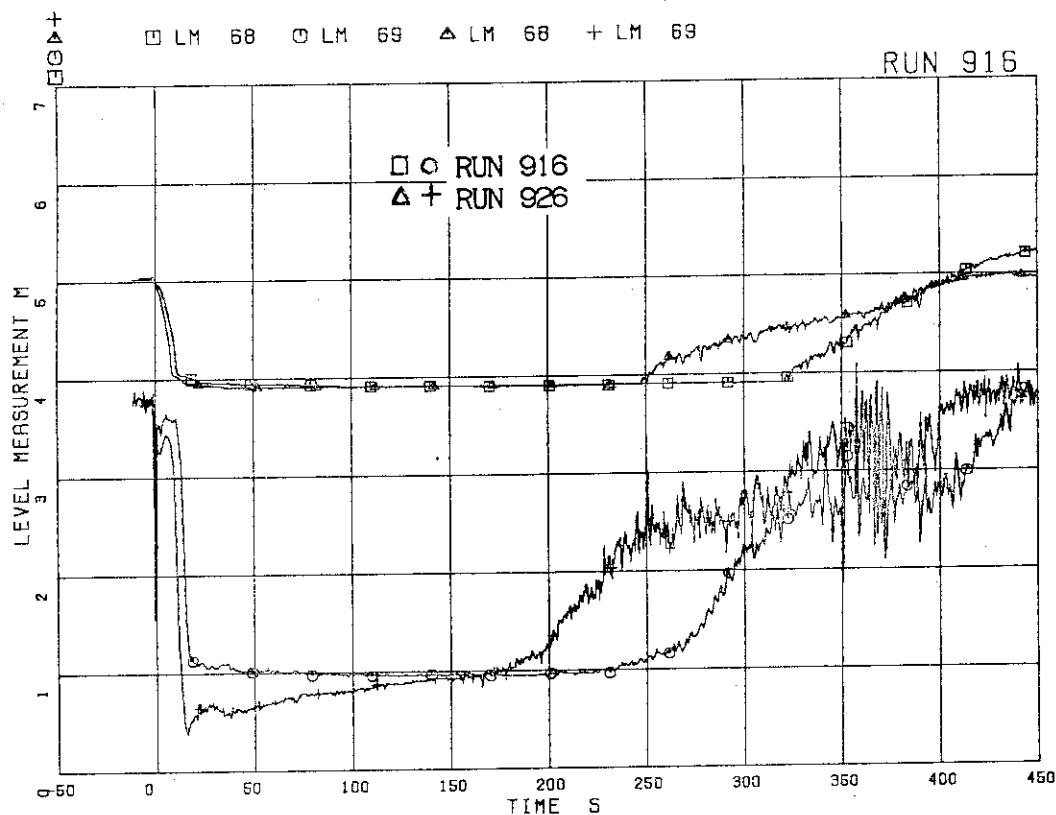


FIG. 6. 3 COLLAPSED LIQUID LEVELS IN DOWNCOMER

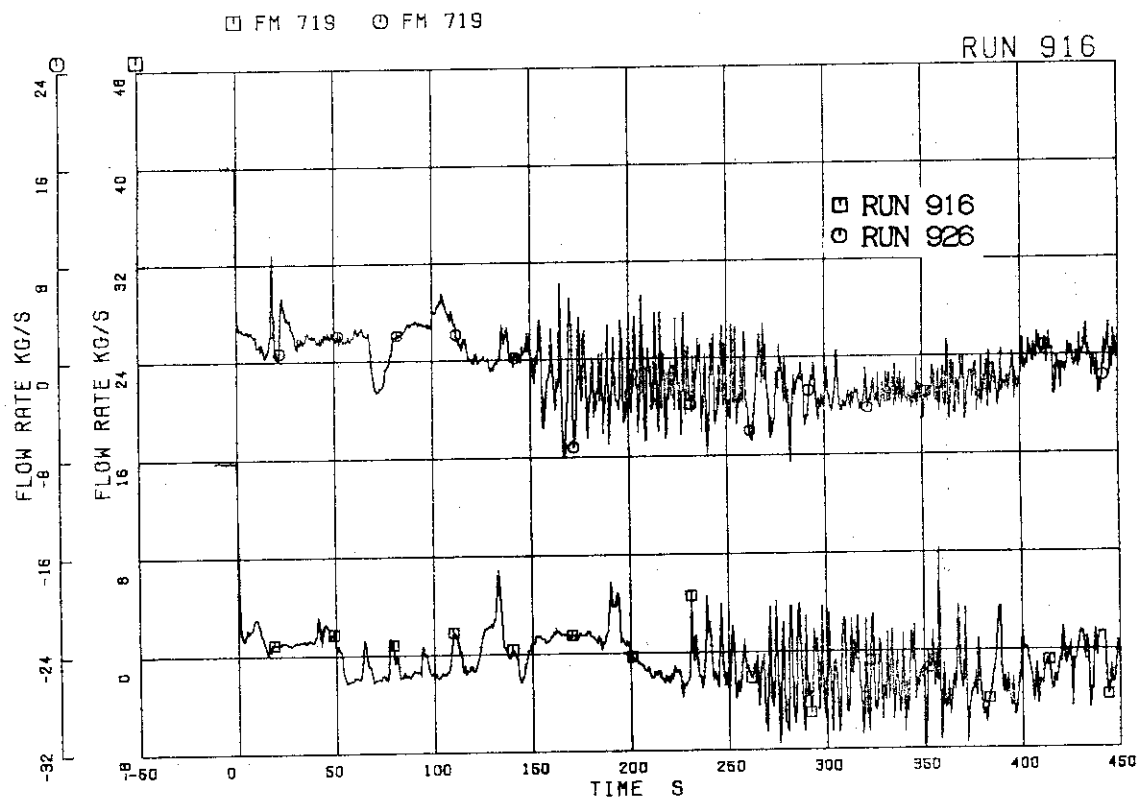


FIG. 6. 4 TOTAL FLOW RATES THROUGH CHANNEL INLET ORIFICES

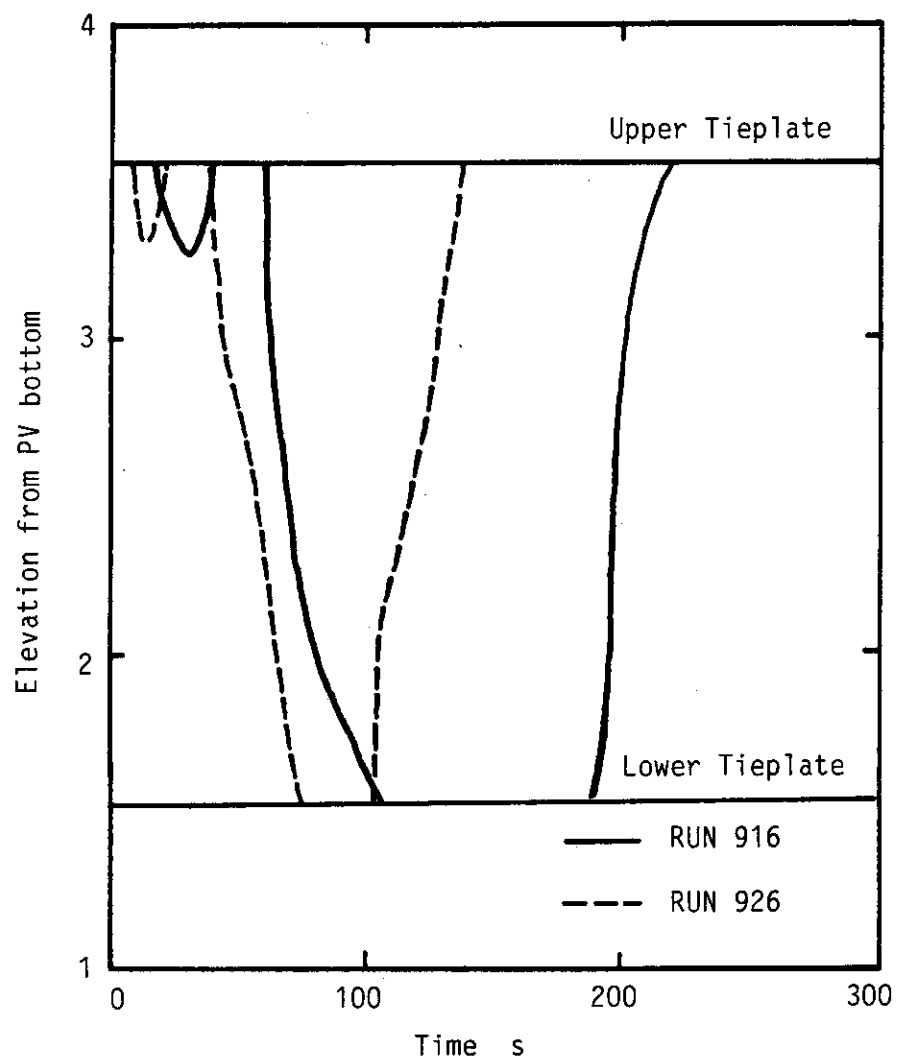


Fig. 6.6 Liquid levels in the core

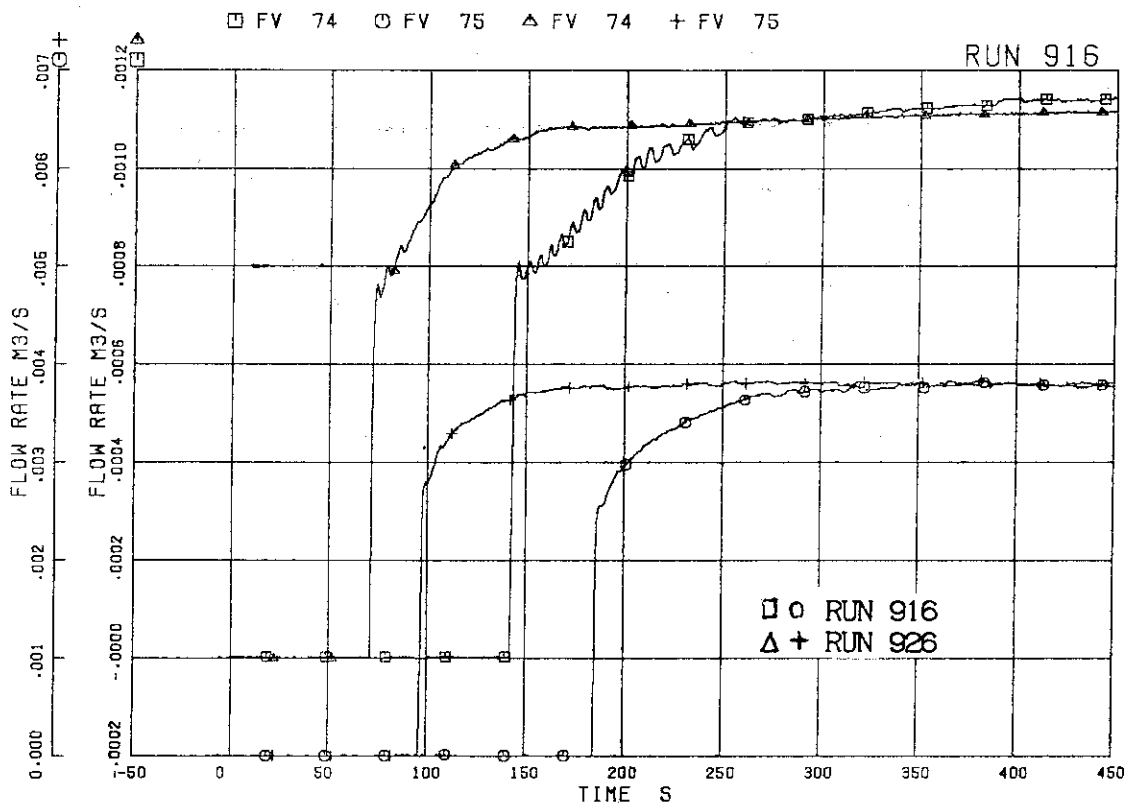


FIG. 6. 5 ECCS FLOW RATES

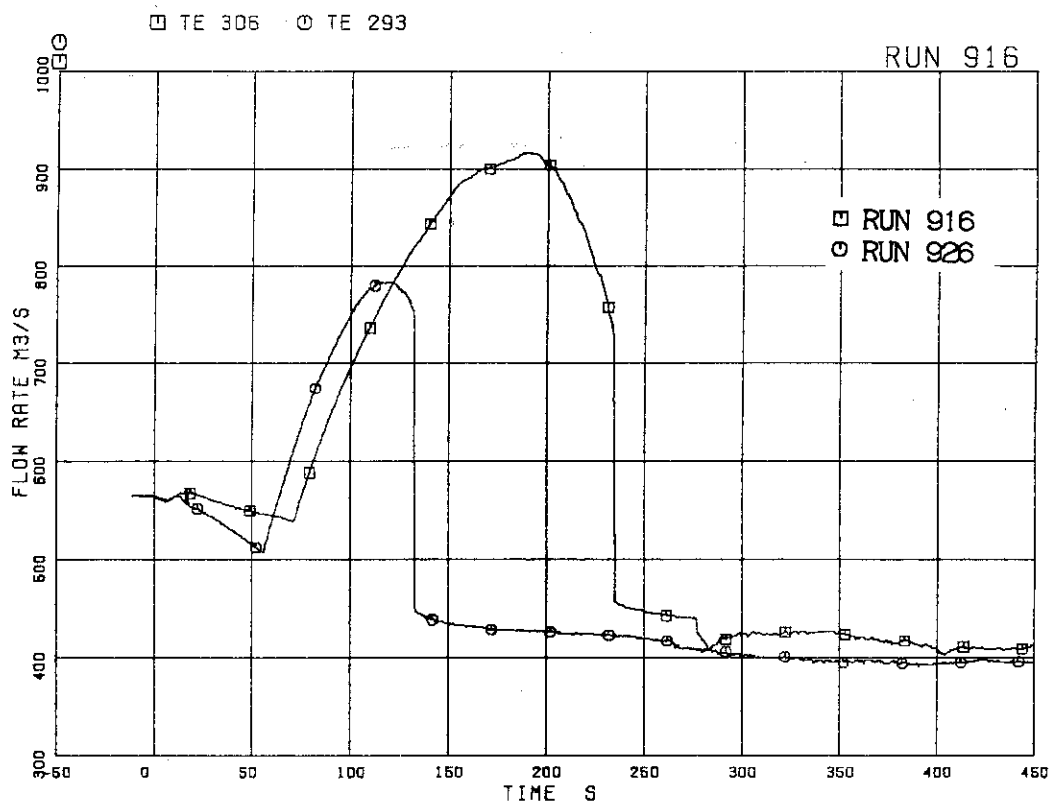


FIG. 6. 7 PEAK CLADDING TEMPERATURES